Assembly and composition of the cellular actin cortex

Miia Bovellan

A thesis submitted to University College London for the degree of
Doctor of Philosophy

London Centre for Nanotechnology
Department of Cell and Developmental Biology
UCL

August, 2012

Declaration

I, Miia Bovellan, confirm that the work presented in this thesis is my own. Where information has been derived from other sources, I confirm that this has been indicated in the thesis.

Acknowledgements

First, I would like to thank my supervisor Dr. Guillaume Charras for his advices and guidance throughout my studies and that he has been so supportive during my PhD.

I would also like to thank all my collaborators, Mate and Ewa in Dresden, Yves and Philippe in Montreal, Antoine and Guillaume in Gif, Dale at the Institute of Child Health, UCL, and Helen and Buzz at LMCB, UCL.

Then, I would like to thank all the past and present members of the Charras lab for being such a great colleagues. Thanks Andrew, Emad, Alex L, Kerry, Dorothy, Loic, Majid, Mario, and Alicia for sharing the lab and coffee breaks with me. Special thanks for Rich for helping me with the ever so cooperative spinning disk microscope. Thanks to Alex B for all the biological and not so scientific discussions. Finally, a special Danke schön for Marco for collaborating with me and teaching me a lot about physics, friendship, and life.

My friends here and abroad also deserve my gratitude as they have motivated me at the times of despair. Special thanks to Ansku and Johanna and finally to Pieta, who has told me many times during these years that it is going to be OK.

I would also like to acknowledge Human Frontier Science Program for the financial support.

Finally, I would like to dedicate this thesis to my mother and thank my aunt Pirjo for her lifelong support, and my husband Aapo, who I love very much, for taking care of me (and our little D), being proud of me, and making me feel loved.

Abstract

The actin cortex is a thin layer of F-actin, actin regulating proteins, and myosin under the cell membrane. It has a fundamental role in cell morphogenesis, motility, mitosis, cytokinesis, and cell shape maintenance. Yet, how the cell cortex forms as well as the protein composition of the cortex remain unknown.

In this study using M2 melanoma cell blebs and metaphase HeLa cells I describe proteins needed for cortex reassembly and reveal the protein composition of the actin cortex. Blebs represent a natural situation in which the membrane is transiently devoid of an actin cortex. Thus the formation of a new actin cortex in the bleb can be studied. Blebs also provide a cell fraction enriched in F-actin cortex, making them an ideal model to study cortex proteomics.

After having shown that no nucleation independent mechanism participate in cortex reassembly in membrane blebs, I discovered by localisation and silencing studies, that formin Diaph1 and the Arp2/3 complex are needed for the cortex nucleation, as both localised to the cortex and depletion of either led to cortical defects. Simultaneous depletion of Diaph1 and the Arp2/3 complex led to disappearance of the cellular cortex, suggesting that together they provide the majority of the F-actin in the cortex. Cortex composition studies of blebs isolated from blebbing cells revealed the presence of many actin binding proteins at the cortex. Localisation and depletion studies revealed that capping, and effective actin turnover are essential for cortical stability and that flightless-I may regulate cortex nucleation together with Rho GTPases.

These findings have important implications for our understanding of cortical properties, which are not only important for cell morphogenesis and shape maintenance, but facilitate tumour growth and dissemination.

Table of Contents

1 INTRODUCTION

Here I present the background related to my research work. This introduction is divided into four sections.

The first part is focused on actin, which is a fundamental protein of the cytoskeleton in cells. Actin biochemistry is presented in detail concentrating on the properties of actin monomers and filaments. Finally a phenomenon called treadmilling of actin filaments is described.

The second part introduces the most important actin structures in non-muscle cells concentrating on lamellipodial and filopodial structures. More in detail I will present what is known about the contractile cell cortex to date, as studying this structure has been the main focus of my PhD work.

Some actin binding proteins are briefly mentioned already in the second part, but the third part is focused in detail on actin regulating proteins. First a group of treadmilling actin binding proteins is presented followed by introducing actin-membrane linker proteins, actin filament bundling proteins, actin filament capping proteins, motor proteins, and scaffold proteins. In the final section actin nucleators needed for filament formation in cells are discussed in depth.

The fourth part describes a phenomenon called membrane blebbing, which occurs due to contraction of the cell cortex. The bleb lifecycle is discussed in detail and in particular what is known about cortex assembly underneath the bleb membrane is presented. Finally examples of cell blebbing in different physiological conditions are described.

1.1 Actin

Actin is one of the most abundant proteins in all eukaryotes. Actins are a family of proteins encoded by a large, highly conserved gene family. Six isoforms of actin, very similar at the amino acid sequence level, exist in vertebrates (Rubenstein, 1990). α_{sk}, α_{ca}, α_{sm}, γ_{sm} -actins are expressed primarily in muscle cells, where they are a main component of a contractile structure called the sarcomere together with the motor protein myosin. β- and γ-actins are co-expressed in non-muscle cells and act as components of the actin cytoskeleton (Alberts, 2002b; Rubenstein, 1990; Sheterline, 1994). Detailed differential roles of β- and γ-actins in non-muscle cells has not yet been revealed, but recent report suggests that β-actin is predominantly involved in stress fibers and cell-cell contacts whereas γ-actin forms cortical and lamellipodial structures in motile cells (Dugina et al., 2009). Interestingly in stationary cells γ-actin is also involved in stress fibers (Dugina et al., 2009).

Actin can exist either in a monomeric (globular actin, G-actin) or in a filamentous (F-actin) form (Fig. 1.1). The actin monomer consists of a single 375 amino acid polypeptide, which folds into two peanut-shaped domains separated by a deep cleft. These two domains can be further divided into four subdomains (Kabsch and Holmes, 1995; Sheterline, 1994). The cleft between the two domains binds a nucleotide, an adenosine triphosphate (ATP) or adenosine diphosphate (ADP). In addition the actin monomer has a high-affinity binding site for a divalent cation (Mg^{2+} or Ca^{2+}) near the binding site of the nucleotide (Kabsch and Holmes, 1995).

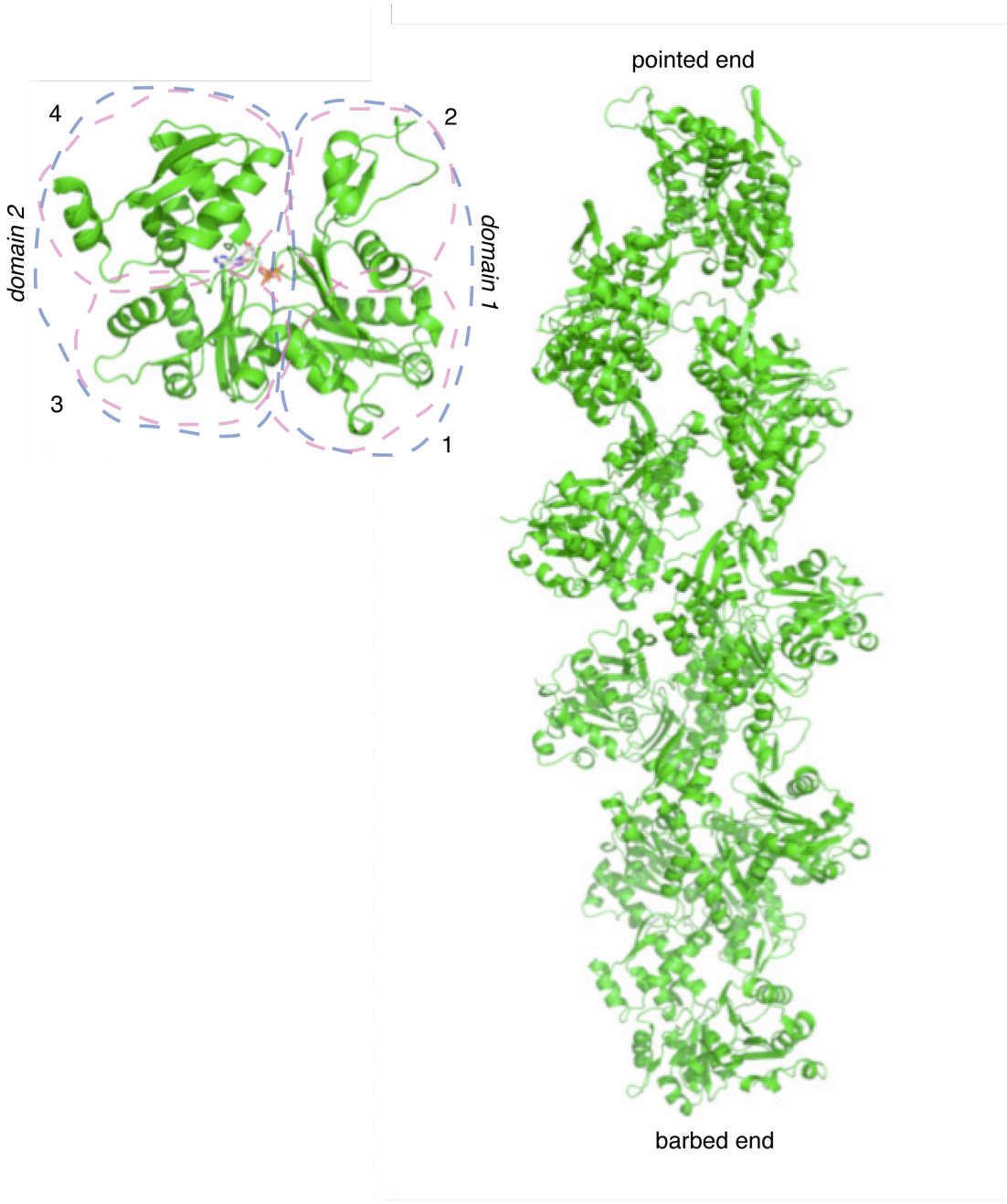

Figure 1.1: Actin monomers and actin filaments are polar structures.

Actin exists in monomeric (left) and filamentous (right) form. The actin monomer folds into two peanut-shaped domains. The two domains (blue dashed line: domain 1 and 2) can be divided into four subdomains (pink dashed line: 1 – 4). The cleft between the two domains binds one nucleotide, ATP or ADP, shown in red and blue. Actin filaments are double-stranded helices. Both actin monomers and filaments are polar structures (Bray, 2001; Kabsch and Holmes, 1995; Sheterline, 1994).

Actin monomers can form into filaments, which are double-stranded helices (Fig. 1.1) where all monomers are oriented in the same direction. In the filament, each actin monomer is in contact with four other actin monomers, although the strongest binding is along the longitudinal axis (Bray, 2001). Actin filaments are polar structures, and thus have two biochemically distinct ends called a pointed end (minus-end) and a barbed end (plus-end). These names were given due to the visualisation of myosin binding pattern on the filament. When the filament is covered with myosin heads, a distinct arrowhead forms pointing towards the minus-end and the tail towards the plus-end, as observed in early electron micrographs (Craig et al., 1985). The nucleotide and cation binding cleft on the monomer points toward the pointed end, and both the amino (N)- and carboxyl (C)- terminal ends of the polypeptide lay on the barbed end.

In vitro actin monomers can polymerise into filaments in buffers of suitable ionic concentrations. *In vitro* polymerisation can be divided into three phases: nucleation, elongation, and steady state. Two actin monomers bind rather weakly to each other, but when a third monomer is added and an actin trimer is formed (nucleation), the structure becomes more stable. This trimer acts as a nucleus (seed) for polymerisation and allows rapid addition of monomers to the growing filament. The assembly of a nucleus is relatively slow, which causes a lag phase during polymerisation from pure G-actin. Cells have overcome the challenge of forming an actin nucleus by synthesising proteins called actin nucleators.

During filament elongation, monomers are rapidly added to the barbed end and slower to the pointed end of the filament. Eventually the system reaches a steady state, in which monomer addition and dissociation are balanced at both filament ends. In steady state the equilibrium concentration of the pool of G-actin is called the critical concentration C_c, which is a measure of the ability of a solution of actin monomers to polymerise (Alberts, 2002a; Sheterline, 1994).

Althought at both filament ends ATP-actin and ADP-actin monomers are able to polymerise and depolymerise, the barbed and the pointed end have different dynamics. At the barbed end ATP-actin monomers polymerise much faster than ADP-actin monomers due to differences in k_{on} rates of ATP- and ADP-actin monomers at the barbed end (Alberts, 2008). In addition, ADP-actin monomers depolymerise at the barbed end faster than ATP-actin due to differences in k_{off} rates of ATP- and ADP-actin monomers at the barbed end (Alberts, 2008). Both ATP- and ADP-actin monomers polymerise and depolymerise slowly at the pointed end.

Each actin monomer catalyses an ATP hydrolysis event shortly after being added to the filament and an ADP-P_i intermediate forms (Fig. 1.2). Release of the γ-phosphate from the intermediate is slow (Blanchoin and Pollard, 1999; Melki et al., 1996) suggesting long actin filaments are rich in ADP-P_i actin. Once the γ-phosphate has dissociated from the actin monomer, ADP-actin forms and thus the oldest part of the filaments, the pointed end, contains mainly ADP-actin (Pollard, 1986).

These events lead to ATP-actin polymerisation at the barbed end and ADP-actin depolymerisation from the pointed end (Alberts, 2008).

Because of the different exchange rates at the pointed and barbed ends, the opposite filament ends have different critical concentrations. C_c for the pointed end is approximately 0.7μM and for the barbed end it is 0.1μM in buffer containing millimolar Mg^{2+} and ATP (Pollard, 1986). This biochemical property of the actin filament enables a phenomenon called treadmilling (Fig. 1.2), where in steady state ATP-actin monomers are added to the barbed end and ADP-actin monomers are dissociated from the pointed end (Alberts, 2002a; Sheterline, 1994).

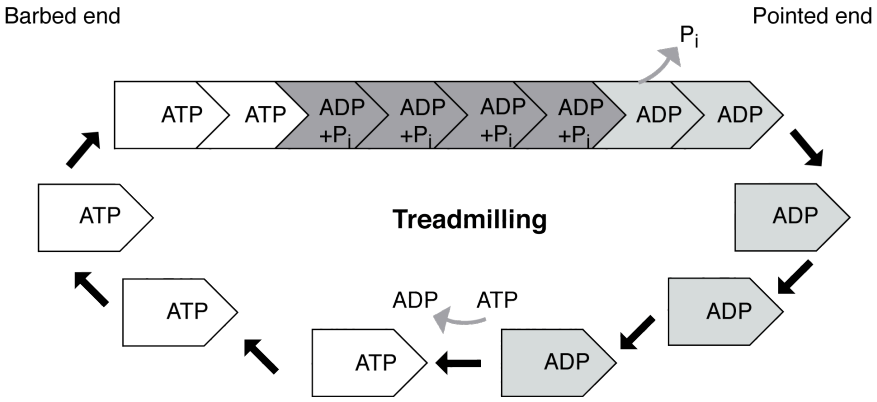

Figure 1.2: Actin filaments undergo treadmilling.
In steady state ATP-actin monomers are added to the barbed end and ADP-actin monomers are depolymerised from the pointed end (Alberts, 2002a; Sheterline, 1994).

1.2 Actin structures in non-muscle cells

In non-muscle cells, the best-characterised functions dependent on actin are cell motility and cytokinesis. First when the cell receives motility-triggering signals, it polarises forming a leading edge and a rear. Protrusions needed for migration are formed at the leading edge of the cell by rapid actin filament barbed end elongation. On 2D substrates these protrusions can be divided into lamellipodia and filopodia structures (Fig. 1.3A-C). The contractions of the lamellum behind the lamellipodium and the acto-myosin cortex at the rear are necessary for detachment of the cell from the substrate to enable forward movement (Fig. 1.3A).

In mitosis the cell rounds up and a rigid cell cortex forms under the cell membrane. At the end of anaphase, when the chromosomes are separated, a contractile ring is assembled equatorially at the cell cortex. This structure will enable cytokinesis. The cortex also has other very important roles in the cell discussed later. Lamellipodial, filopodial, and cell cortex structures are discussed in detail in this chapter. Few actin nucleating and binding proteins are briefly introduced in this section, but they are discussed more in depth later in this thesis.

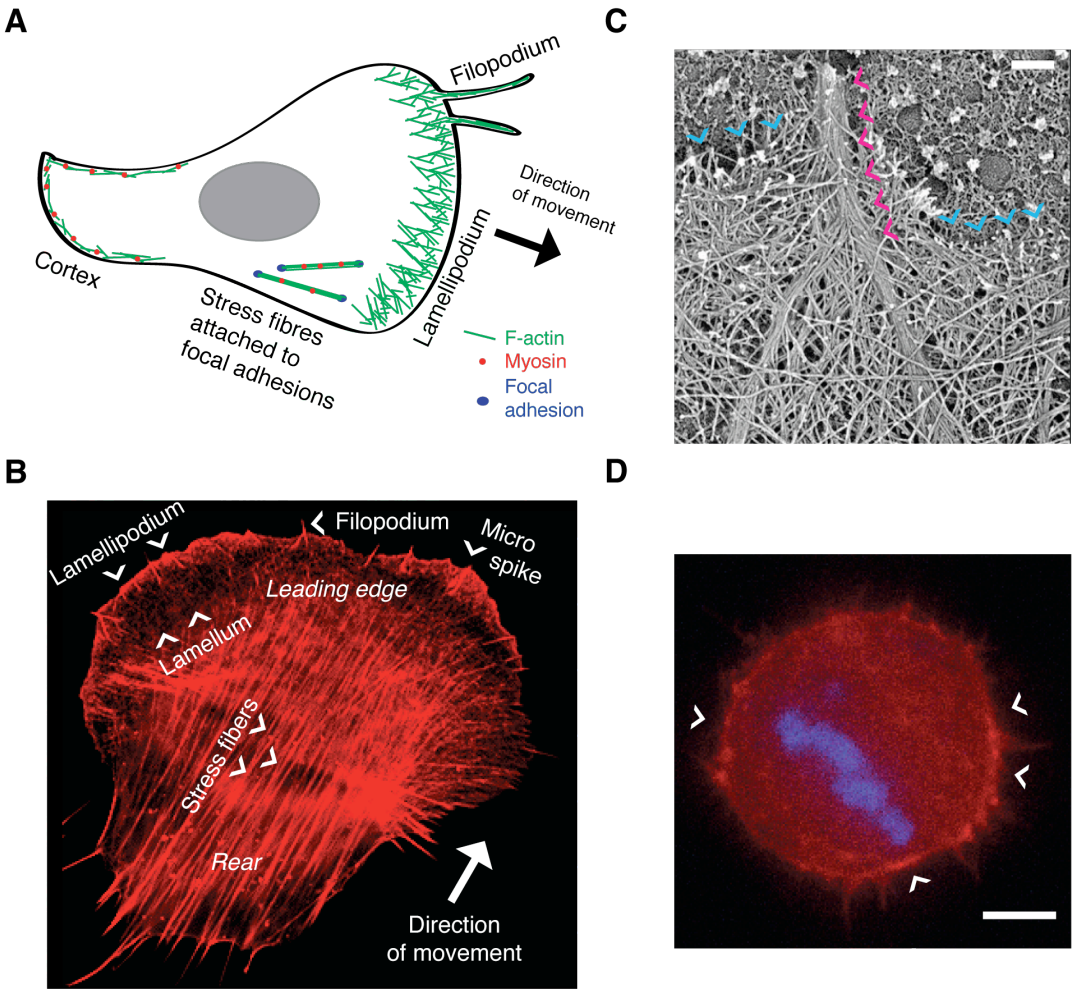
A
Filopodium
Direction of movement
Lamellipodium
Cortex
Stress fibres attached to focal adhesions
F-actin
Myosin
Focal adhesion
C
B
Lamellipodium
Filopodium
Micro spike
Leading edge
Lamellum
Stress fibers
Rear
Direction of movement
D

Figure 1.3: Actin structures in non-muscle cells.

A. A schematic picture of a migrating non-muscle cell showing its actin structures. Rapid actin filament dynamics take place in the lamellipodium at the leading edge of the cell. Filopodia are dynamic spikes formed of actin bundles. Contractile stress fibres are attached to focal adhesions behind the lamellipodium. Actomyosin cortex at the rear together with stress fibres help the cell to contract and detach adhesions when migrating.

B. A fixed primary chick embryo fibroblast with actin stain in red. Microspikes and a filopodium can be seen arising from the lamellipodium. Behind the lamellipodium is the contractile lamellum. Stress fibers, rigid actin bundles, spread vertically between the lamellum and the rear of the cell. Picture is a kind gift from Dr. Louise Cramer.

C. A platinum replica electron micrograph from the leading edge of the cell representing a filopodium (pink arrowheads), which arises from the dense lamellipodial network (blue arrowheads) (Svitkina et al., 2003). Scale bar 0.2µm.

D. Metaphase (chromosomes in blue) HeLa cell stably expressing LifeAct-Ruby (red), a probe for F-actin (Riedl et al., 2008). The actin cortex lies under the cell membrane (arrow heads). Scale bar 5µm.

1.2.1 Lamellipodia

Lamellipodia are thin but dense actin meshworks (Fig. 1.3A, B) that enable movement of the cell by pushing the plasma membrane forward (Mullins et al., 1998b; Svitkina and Borisy, 1999). In the lamellipodium actin filaments are oriented so that the growing barbed ends face toward the leading edge of the cell (Fig. 1.3A) (Small et al., 1994). Behind the lamellipodium is more stable structure called the lamellum, which consists of contractile F-actin bundles and focal adhesions (Geiger, 1983; Mangeat and Burridge, 1984; McKenna et al., 1989; Verkhovsky et al., 1995). Focal adhesions are complex adhesion structures consisting of integrins, zyxin, paxillin, talin, vinculin, and other proteins (Burridge and Connell, 1983; Fath et al., 1989; Geiger et al., 1980; Reinhard et al., 1995; Turner et al., 1990) that keep the cell attached to the substrate. Focal adhesions appear at the transition between the lamellipodium and the lamellum and thus mark the boundary from where the lamellipodium begins (Ponti et al., 2004).

According to the dendritic nucleation model (Pollard et al., 2000) lamellipodia emerge when new actin filaments form in a branched manner. Indeed, the majority of the F-actin in lamellipodia is nucleated by the Arp2/3 complex, which binds to the side of an existing actin filament, nucleates a daughter filament causing the formation of a Y-branch (Amann and Pollard, 2001b; Mullins et al., 1998b), and stays bound at the pointed end of the nascent filament (Mullins et al., 1998b). Arp2/3 complex nucleated filaments elongate until capped by actin filament capping proteins. Because capping proteins are abundant in cells the dendritic nucleation model predicts that branched filaments in lamellipodia are short and thus stiff and able to push the membrane forward (Pollard et al., 2000). Longer linear actin filaments nucleated and elongated by formin proteins also exist in lamellipodia (Gupton et al., 2007; Sarmiento et al., 2008; Yang et al., 2007). The Arp2/3 complex and formins are described later in this thesis together with the other actin

binding proteins necessary for the formation of lamellipodia and other actin structures.

1.2.2 Filopodia

A filopodium, often described as a cell antenna, is a long, thin (0.1-0.3μm thick), and very dynamic protrusion of the cell membrane consisting of parallel bundles of actin filaments, where the barbed ends of the constitutive filaments are orientated towards the tip of the filopodium (Fig. 1.3C) (Pollard and Borisy, 2003; Sheterline, 1994; Welch and Mullins, 2002). The dynamics of growth and shrinkage of the filopodium is controlled by actin polymerisation at the tip of the filopodium and retrograde flow of the actin filament bundle (Mallavarapu and Mitchison, 1999). Filopodia participate in many functions of the cells including motility, adhesion to the substrate, chemotaxis, and neuronal growth-cone pathfinding (Faix and Rottner, 2006; Gupton et al., 2007).

Filopodia are often seen appearing from the lamellipodia (Lewis and Bridgman, 1992; Small and Celis, 1978; Svitkina et al., 2003), where they have been suggested to originate from Arp2/3 complex induced branched network of F-actin (Bu et al., 2009; Johnston et al., 2008). According to the convergent elongation model of filopodia, anti-capper proteins Enabled/vasodilator-stimulated phospho (Ena/VASP) proteins protect the barbed ends of some of the Arp2/3 complex nucleated filaments from capping and maintain their elongation in a synchronized manner alone or together with formins (Svitkina et al., 2003) leading to growth of the filopodium.

However, filopodia independent from the branched network also exist (Takenawa and Suetsugu, 2007). These filopodia are suggested to initiate according to the tip nucleation model (Block et al., 2008; Schirenbeck et al., 2005; Steffen et al., 2006), which predicts that activated formins, in particular

mDia2/Diaph3 (Pellegrin and Mellor, 2005; Yang et al., 2007), cluster locally to the cell membrane, together nucleate new unbranched filaments, and maintain their elongation. After the initiation of the filopodia, actin filaments are bundled in a parallel fashion by fascin (DeRosier and Edds, 1980). To date no consensus on the occurrence of the tip nucleation model in cells has been found, whereas a lot of evidence supports the convergent elongation model (Falet et al., 2002; Gates et al., 2007; Korobova and Svitkina, 2008; Lee et al., 2010).

1.2.3 Actin cortex

The actin cortex is a thin layer of crosslinked actin filaments, actin binding proteins, and myosin under the cell membrane (Bray and White, 1988). The actin cortex plays a fundamental role in many important functions of the cell. First, it enables positioning of the spindle during mitosis through interactions with astral microtubules (Kunda et al., 2008; Lansbergen et al., 2006). During cytokinesis the integrity of the actin cortex appears essential, because disruption of the actin cortex at the pole regions of a dividing cell stalls the progression of the cleavage furrow (O'Connell et al., 2001). In addition, contractions of the cortex during cytokinesis give rise to small oscillations in the cell and perturbations to cortical integrity lead to large uncontrolled whole cell oscillations resulting in aneuploidy (Sedzinski et al., 2011). Second, the cortex enables cells to change shape and resist mechanical forces. The cell membrane is unable to exert extracellular forces or resist shear stresses (Hamill and Martinac, 2001) and therefore cannot alone maintain cell shape or contribute to the change of the shape. Lastly, the actin cortex is important in motility both in 2D and 3D.

In 2D, cells often migrate by forming lamellipodia at their front. At the leading edge in the direction of movement, a lamellipodium extends and pushes the membrane forward (Fig. 1.3A). As the lamellipodium protrudes, a contractile lamellum, situated immediately behind the lamellipodium, is needed for

translocation of the cell body and formation of new adhesions to the substrate (Ridley, 2011). Finally the rear of the cell detaches from the substrate through contractions of the actomyosin cortex (Alberts, 2008).

In 3D matrices lamellipodial migration is rare and the cells often use either mesenchymal, amoeboid, or blebbing modes of migration (Friedl and Brocker, 2000). Polarised cells moving by blebbing are dependent on cortex formation at the leading edge of the cell (Blaser et al., 2006; Pinner and Sahai, 2008; Sahai and Marshall, 2003; Wolf et al., 2003). Blebbing motility is presented more in detail later in this thesis. Finally, it has been shown that, in extracellular matrix gels, cortical contractions help to push the cell nucleus through small constrictions (Lammermann et al., 2008).

Although an important structure in the cell, much less is known about the cell cortex than lamellipodia or filopodia. A lot remains to be revealed of the detailed structure and composition of the cortex, how the cortex assembles, and how it is regulated.

First, at the ultrastructural level, when examined by scanning electron microscopy in detergent extracted cells, the cortex appears as a dense meshwork of actin filaments (Charras et al., 2006). Although the cortex constituents remain largely unknown, localisation and functional studies have revealed that at least some actin binding proteins appear to have a role in the cortex. According to localisation studies the main components in addition to actin at the cortex are actin-membrane linker proteins, actin crosslinking proteins and motor proteins. Indeed, ezrin-radixin-moesin (ERM) proteins localise to the cell membrane and link the actin cortex to the plasma membrane (Bretscher et al., 2002; Charras et al., 2006). In addition it was shown that disruption of ERM-protein functionality leads to defects in membrane-cortex linking in cells (Charras et al., 2006). Cortical actin filaments are crosslinked to one another by actin crosslinking proteins such as α-actinin (Charras et al., 2006). Finally, the contractility of the cortex is

powered by the motor protein myosin II (Charras et al., 2006). Inhibition of myosin II activity by drug blebbistatin has been shown to block contraction of the cortex (Straight et al., 2003) and was reported to change the morphology of hepatic stellate cells suggesting a role in maintaining the cortex (Liu et al., 2010).

Second, to date no consensus exists how the actin cortex assembles. The knowledge on how the actin cortex constitutes relies on few studies that mainly indirectly show an involvement of formin proteins at the cortex assembly (Hannemann et al., 2008). These studies are discussed in depth later in this thesis.

Finally, the regulation of the actin cortex remains largely unknown, but the small GTPase RhoA, presented more in detail later in this introduction, is present at the cell membrane and has been suggested to be the most important regulator of the actin cortex (Charras et al., 2006; Etienne-Manneville and Hall, 2002).

1.3 Actin binding and regulating proteins

In cells both G- and F- actin are regulated by a large group of actin binding and regulating proteins (Fig. 1.4), which are introduced in this part. First, proteins regulating the G-actin pool in cells are presented and are referred to as “treadmilling actin monomer binding proteins”. Second, I present actin filament capping proteins, which block the polymerisation or depolymerisation of the actin filaments depending to which end of the filament they bind. Third, actin-membrane linker proteins are described, which mediate cortical F-actin interactions with the cell membrane. Fourth, I introduce actin filament bundling and crosslinking proteins, which link actin filaments together. Fifth, motor proteins, which power contractility, are presented. Sixth, I present other actin regulating proteins. In the final section of this part I present different actin nucleators in detail.

1.3.1 Treadmilling actin monomer binding proteins

The G-actin pool in cells in maintained by many actin monomer binding proteins. The most abundant of these are β-thymosins, which sequester actin monomers in cells to sustain a pool of G-actin ready to be released for polymerisation when needed (Alberts, 2008). Other important actin monomer binding proteins are profilin and ADF/cofilin presented next.

Profilin

As discussed earlier ATP-actin, instead of ADP-actin, is the preferred form for filament formation. ADP-actin monomers detach from the pointed ends of the filaments and can be reincorporated into filaments after their nucleotide has to be exchanged for ATP. Profilin catalyses this exchange (Mockrin and Korn, 1980) and stays bound until the ATP-actin monomer binds to the barbed end of the filament (Nyman et al., 2002). Indeed, profilin binds exclusively to actin monomers (Lassing and Lindberg, 1985). In addition profilin can interact with its Src homology 3 (SH3) domain to proline-rich motifs of other proteins (Mahoney et al., 1999) including actin nucleators called formins, which are described later, to which profilin supplies ATP-actin monomers for filament elongation.

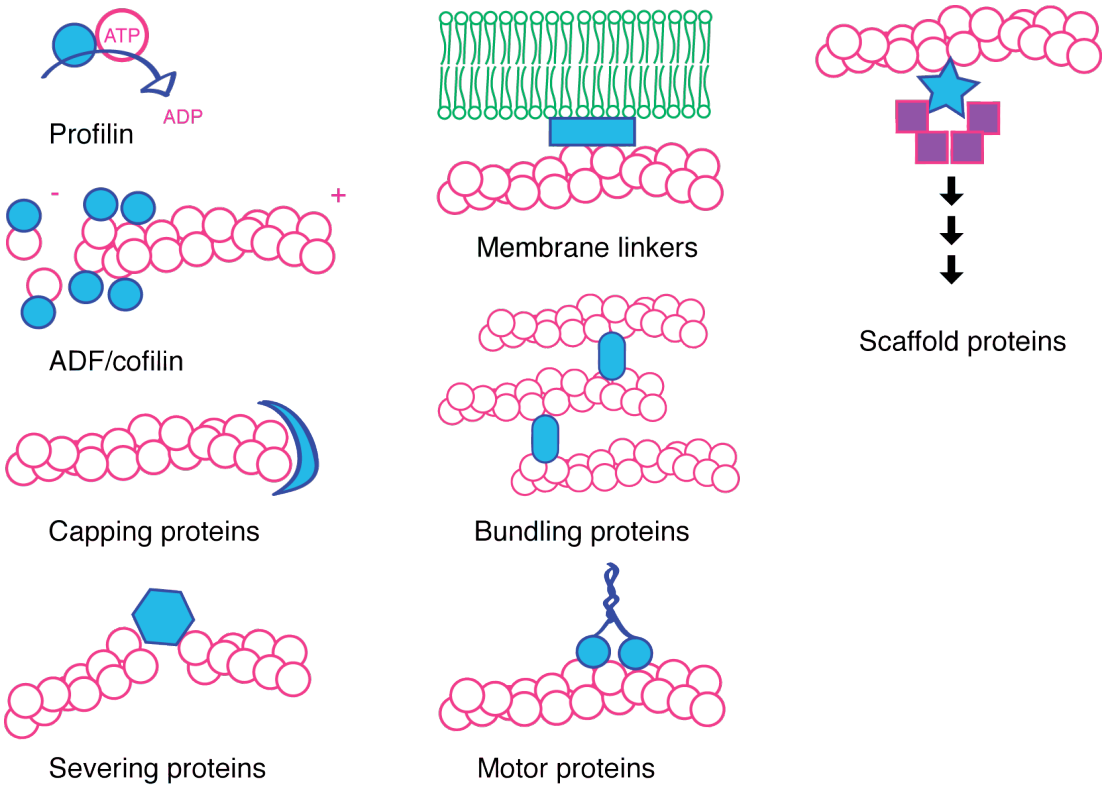

Figure 1.4: Actin binding protein groups.

Schematic pictures of different classes of actin binding proteins. Actin binding proteins profilin and ADF/cofilin are referred as “treadmilling actin monomer binding proteins”, as both are needed for actin turnover in cells. Profilin catalyses the exchange of ADP for ATP in actin monomers. ADF/cofilin depolymerises pointed ends and bind ADP-actin monomers. Capping proteins cap filament ends (barbed or pointed end). Many proteins, including ADF/cofilin, also have filament severing activities. Membrane-linker proteins bind simultaneously membrane lipids or transmembrane proteins and actin. Bundling proteins bind actin filaments to one another and motor proteins travel along actin filaments and generate mechanical forces. Some actin regulating proteins act as scaffold proteins that are proteins, which gather many interaction partners leading to signalling cascades inside the cell. In this thesis they are presented in other actin regulating proteins category.

ADF/cofilin

ADF/cofilins (ADF also known as destrin) bind both monomeric and filamentous actin through distinct binding sites (Lappalainen and Drubin, 1997). ADF/cofilins bind F-actin in a cooperative manner (Bobkov et al., 2006; Hawkins et al., 1993; Hayden et al., 1993) and bind ADP-actin more strongly than ATP-actin (Carlier et al., 1997). Physiologically the most important function of ADF/cofilin is to depolymerise actin filaments from their pointed ends (Carlier et al., 1997) and it is the only actin filament depolymerising protein known to date. ADF/cofilin binding slightly alters the conformation of an actin monomer in the filament (Galkin et al., 2001; McGough et al., 1997), and the thermostability of the filament (McGough and Chiu, 1999). These events ease the release of the monomer from the filament and lead to depolymerisation. In addition to depolymerisation, ADF/cofilins also sever actin filaments (Chan et al., 2000; Maciver et al., 1991; Moriyama et al., 1999), and inhibit nucleotide exchange within the bound monomers (Nishida, 1985). The main regulator of ADF/cofilin is LIM kinase that phosphorylates ADF/cofilin leading to inactivation (Edwards and Gill, 1999). Another important regulator of ADF/cofilin is actin interacting protein 1 (Aip1, WDR1), which enhances the depolymerisation and severing activity of ADF/cofilin (Aizawa et al., 1999; Okada et al., 1999; Rodal et al., 1999).

1.3.2 Actin-membrane linker proteins

Actin-membrane linker proteins link actin structures to the plasma membrane of the cell. Actin-membrane linking is particularly important for actin cortex stability. Many actin-membrane linker proteins are known including spectrin, dystrophin, and utrophin, but only ezrin-radixin-moesin (ERM) proteins, annexins, and filamins are presented in this part.

ERM-proteins

The ezrin-radixin-moesin (ERM) proteins are a family of membrane-associated proteins, which bind actin and thus regulate the cell cortex underneath the plasma membrane (Sato et al., 1992). Inactive ERM-proteins exist in a closed conformation involving a head to tail interaction, which can be released by phosphatidylinositol 4,5- bisphosphate (PIP_2) binding at the plasma membrane (Hirao et al., 1996) and phosphorylation by Rho-associated protein kinase (ROCK) (Matsui et al., 1998; Tran Quang et al., 2000), protein kinase Cα (Ng et al., 2001), or protein kinase Cθ (Pietromonaco et al., 1998; Simons et al., 1998). This leads to active ERM, which one tail binds to the plasma membrane and the other to actin leading to actin-membrane linking (Berryman and Bretscher, 2000; Matsui et al., 1998; Roy et al., 1997; Turunen et al., 1994). In addition to direct phospholipid binding, ERM-proteins also bind membrane proteins including receptor CD44, intracellular adhesion molecule-2 (ICAM-2), and ERM-binding phosphoprotein 50 (Heiska et al., 1998; Reczek and Bretscher, 1998; Tsukita et al., 1994; Yonemura et al., 1998). Interestingly ERM-proteins have been reported to act upstream of Rho GTPase signalling by releasing RhoA from Rho GDP-dissociation inhibitor (RhoGDI), which inhibits nucleotide exchange and hydrolysis activity of RhoA and extracts it from the membrane (Takahashi et al., 1997), suggesting of a regulatory feedback loop between ERM-proteins and RhoA.

Annexins

Annexins are a large family of proteins that bind phospholipids in a Ca^{2+} -dependent manner (Gerke and Moss, 2002). Many families of annexins exist, but only four families, I, II, VI, and VIII, are reported to bind and bundle F-actin (Filipenko and Waisman, 2001; Gerke and Weber, 1984; Glenney et al., 1987; Goebeler et al., 2006; Hayes et al., 2004; Jones et al., 1992; Schlaepfer and Haigler, 1987; Watanabe et al., 1994). Not only phospholipid binding of annexins, but also binding to actin is Ca^{2+}-dependent. Phospholipids at the plasma membrane regulate and recruit annexin to actin

structures leading to membrane-actin linking (Harder et al., 1997; Oliferenko et al., 1999; Rescher et al., 2004). Interestingly it has been reported, that annexin II can inhibit actin polymerisation by capping the barbed end of the filament (Hayes et al., 2006).

Filamins

Filamins proteins are a family of three members A, B, and C that crosslink actin filaments into orthogonal networks (Tseng et al., 2004) and link to the plasma membrane through many membranous binding partners including integrin β (Kiema et al., 2006; Sharma et al., 1995), RhoA (Ohta et al., 1999), and ICAM-1 (Kanters et al., 2008). Functional filamins form homodimers that organise into V-shapes (Tyler et al., 1980), bind to actin through their highly conserved actin binding domains, and create T-, X-, and L- shaped junctions in the F-actin network underlying the plasma membrane (Popowicz et al., 2006). In addition to F-actin crosslinking, filamins also act as scaffolds for signal transduction (Feng and Walsh, 2004).

1.3.3 Actin filament bundling and crosslinking proteins

Bundling proteins link actin filaments parallel to one another thereby generating a bundle of filaments with a higher bending rigidity than individual filaments. In contrast, actin crosslinking proteins link actin filaments at an angle to one another generating a mesh.

Alpha-actinins

Alpha-actinins are a protein family of four members (1-4), which link actin filaments into tight bundles (Maruyama and Ebashi, 1965; Mimura and Asano, 1978). Structurally, monomeric α-actinin appears as a golf club, where the N-terminal 'head' contains a highly conserved actin binding domain with two calponin homology domains, a 'shaft' four spectrin repeats, and the C-terminal 'grip' two EF hand domains (Matsudaira, 1991). When crosslinking two actin filaments together two α-actinin monomers dimerise

through the spectrin repeats and form an anti-parallel homodimer, where conserved actin binding head domains are at either end of the formed rod-like structure (Djinovic-Carugo et al., 1999). Alpha-actinins are a major component of muscle and bundle actin filaments in the Z-disc of sarcomeres (Takahashi and Hattori, 1989). In non-muscle cells, α-actinin localises to the cell-cell contacts, cell-matrix adhesion sites, stress fibers, and to different cellular protrusions including filopodia and membrane blebs (Charras et al., 2006; Otey and Carpen, 2004). In addition to F-actin crosslinking, α-actinins also act as scaffolds for other cytoskeletal and membrane proteins.

Fascin

Fascin is a small globular protein that crosslinks actin filaments into parallel bundles in a monomeric form (Maekawa et al., 1982). Vertebrates express three isoforms (1-3) of fascin, which are composed of four β-trefoil domains (Ponting and Russell, 2000; Sedeh et al., 2010) containing two actin binding sites, which are at the N-terminus overlapping with β-trefoil domain 1 and closer to the C-terminus overlapping with β-trefoil domains 3 and 4 (Cant and Cooley, 1996). Fascin bundles F-actin quite inefficiently and has been suggested to bundle only newly polymerised actin filaments and filaments that have already been bundled loosely together (Kureishy et al., 2002). Fascin is an important actin crosslinker in filopodia together with α-actinin (Svitkina et al., 2003) as it has been reported, that F-actin crosslinked with both, α-actinin and fascin, are stronger and more elastic, than with either bundler alone (Tseng et al., 2002).

1.3.4 Actin filament capping proteins

Actin filament capping proteins bind and block filament ends. Because of preferential polymerisation at the barbed end, capping of the barbed end stalls elongation of the filament. In contrast, capping of the pointed end prevents depolymerisation. Heterodimeric capping protein is presented first in this section followed by gelsolin, a family member of a large gelsolin/villin

superfamily of proteins consisting of gelsolin, villin, adseverin, CapG, advillin, supervillin, and flightless I. Finally twinfilin and tropomodulin are presented.

Heterodimeric capping protein

Heterodimeric capping protein (also known as CapZ) is a ubiquitously expressed, highly conserved protein, which caps the barbed ends of actin filaments (Isenberg et al., 1980) by binding to them with nanomolar affinity (Wear and Cooper, 2004). Heterodimeric capping protein is a heterodimer consisting of α- and β- subunits, and structurally has the shape of a mushroom (Yamashita et al., 2003), with the top surface containing actin binding sites (Wear et al., 2003). When binding the filament, heterodimeric capping protein masks both of the actin monomers at the barbed end of the filament and blocks polymerisation (Yamashita et al., 2003). In cells the concentration of heterodimeric capping protein is comparable to the number of actin filaments (Cooper et al., 1984; Wear et al., 2003), thus capping by the heterodimeric capping protein is tightly regulated. Phosphoinositides inhibit the activity of heterodimeric capping protein (Heiss and Cooper, 1991) but other regulators, direct and indirect, are also known, but are not discussed in this thesis.

Gelsolin

Gelsolin, a member of a large gelsolin/villin superfamily, severs F-actin and caps barbed ends of filaments (Silacci et al., 2004). It is a Ca^{2+}-regulated protein consisting of six gelsolin domains (G1–G6) (McGough et al., 2003; Silacci et al., 2004; Yin and Stossel, 1979). Gelsolin binds to F-actin very fast, but severs the filament slowly (Selden et al., 1998). Once the filament has been severed and two new filaments have formed, gelsolin stays bound at the barbed end of one of the filaments, whereas the barbed end of the other filament remains free of gelsolin (Silacci et al., 2004; Sun et al., 1999) and can elongate, if it is not capped by heterodimeric capping protein. If the capped filament becomes uncapped, both filaments are able to elongate, leading to an increased amount of elongating filaments (Sun et al., 1999).

Indeed, it has been reported that the small GTPase Rac1 releases gelsolin from actin filaments upon chemoattractant stimulation of neutrophils (Sun et al., 2007) suggesting cells have regulatory systems for uncapping.

Twinfilin

Twinfilin was discovered to cap the barbed end of actin filaments, but surprisingly has higher affinity for ADP-actin than ATP-actin (Helfer et al., 2006; Palmgren et al., 2002). It belongs to the ADF-H domain containing protein family together with ADF/cofilin (Palmgren et al., 2002). In addition to capping, twinfilin also binds monomeric actin and acts as an actin sequestering protein (Goode et al., 1998; Vartiainen et al., 2000). Interestingly twinfilin has also been reported to bind but not alter the function of heterodimeric capping protein and this interaction was shown to be essential for correct localisation of twinfilin in yeast (Falck et al., 2004; Kovar et al., 2005; Palmgren et al., 2001). The exact role of twinfilin in mammalian cells remains to be investigated.

Tropomodulin

While heterodimeric capping protein, gelsolin, and twinfilin cap the barbed end of actin filaments, tropomodulin caps the pointed end (Fowler, 1997; Gregorio et al., 1995). In mammals, four isoforms (1-4) of tropomodulin are expressed. Tropomodulins are composed of two functionally distinct parts as the N-terminal part of tropomodulin interacts with tropomyosin (Sung et al., 1992; Sung and Lin, 1994) and the C-terminal part with the pointed end of the filament (Gregorio et al., 1995). Tropomodulins have been extensively studied in muscle cells, but they are also expressed in non-muscle cells (Conley et al., 2001; Cox and Zoghbi, 2000). On its own tropomodulin caps the pointed end weakly, but binding of tropomyosin (discussed more in depth in the next section) along the actin filaments enhances the affinity of tropomodulin for the pointed end (Fowler, 1996; Fowler et al., 2003; Littlefield and Fowler, 1998; Weber et al., 1994; Weber et al., 1999). Recently it has

been suggested that tropomodulin is also able to nucleate actin filaments (Yamashiro et al., 2010).

1.3.5 Motor proteins

Motor proteins, called myosins, 'walk' along actin filaments and when they assemble into bipolar mini-filaments, they can crosslink actin filaments together. Myosins have a directional movement towards the ends of the actin filament; myosin V has been shown to move towards the barbed ends of actin filaments (Nishikawa et al., 2002) while myosin VI moves towards the pointed end (Wells et al., 1999). Only myosins are presented in this section.

Myosins

Myosins are a large superfamily of proteins sharing a globular motor domain, which binds actin filaments and hydrolyses ATP while producing movement (Mermall et al., 1998; Sellers, 2000). Movement of myosin on actin filaments is often described as walking. The myosin motor cycle (Fig. 1.5) (Lymn and Taylor, 1971) begins with a strongly bound state in a nucleotide free state (rigor state). When an ATP nucleotide binds to the motor, it gets released from F-actin (De La Cruz et al., 1999; Holmes et al., 2003; Lymn and Taylor, 1971). ATP hydrolysis activity of myosin is already triggered while still being bound to F-actin (De La Cruz et al., 1999), but only in the detached state the hydrolysis is executed and an ADP+P_i intermediate forms (Lymn and Taylor, 1971). An ADP+P_i bound motor binds actin weakly, but once P_i is released the ADP bound motor becomes strongly bound to actin. Eventually the ADP is also released and the motor returns to a nucleotide free state (Lymn and Taylor, 1971) and the cycle can start over. The myosin motor cycle proposed by Lymn and Taylor as early as 1971 has been proven several times to be correct, but later studies have shown that the cycle is more complex and more ATP and ADP states exist than originally suggested (Bagshaw and Trentham, 1974; Sleep and Hutton, 1980; Whittaker et al., 1995).

Ten classes of myosin are known to date in mammals; I, II, III, V, VI, VII, IX, X, XV, and XVIII (Furusawa et al., 2000; Sellers, 2000). The best-characterised myosin, myosin II, organises first as a dimer and finally as mini filaments through attachment to other myosin II motor dimers via coiled coil heavy chains (Niederman and Pollard, 1975; Svitkina et al., 1995) leading to more complex structures like thick filaments formed in muscle sarcomeres or stress fibers in non-muscle cells. Myosin II heavy chains consist of MYH1, MYH2, MYH3, MYH4, MYH6, MYH7, MYH7B, MYH8, MYH9, MYH10, MYH11, MYH13, MYH14, MYH15, and MYH16 genes in humans and are expressed in muscle and non-muscle cells. Myosins have a variety of functions in cells and tissues, but these roles are not discussed in this thesis.

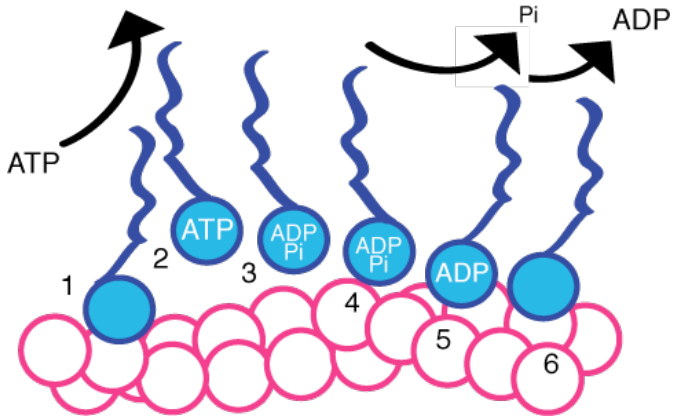

Figure 1.5: Myosin motor cycle.

First the myosin motor is strongly bound to actin in a nucleotide free state (1, rigor state) (Lymn and Taylor, 1971). Binding of an ATP nucleotide to the motor leads to release from F-actin (2) (De La Cruz et al., 1999; Holmes et al., 2003; Lymn and Taylor, 1971). While being detached from F-actin the ATP is hydrolysed to ADP+P_i (3) (Lymn and Taylor, 1971) and the ADP+P_i bound motor binds to F-actin weakly (4). When P_i is released, the ADP bound motor becomes strongly bound to actin (5). Finally, when the ADP is released, the motor returns to a nucleotide free state (6) (Lymn and Taylor, 1971) and the cycle can start over.

1.3.6 Other actin regulating proteins

This section concentrates in describing other actin regulating proteins relevant to this study. These proteins are tropomyosin, drebrin, and IQGAPs, which are presented in the following.

Tropomyosin

Tropomyosins are a large family of α-helical proteins, which first dimerise and then polymerise head-to-tail into long filaments, that bind along F-actin and protect it from severing by gelsolin, villin, or ADF/cofilin (Bernstein and Bamburg, 1982; Burgess et al., 1987; DesMarais et al., 2002). They strengthen pointed end capping by tropomodulin (Fowler, 1996; Fowler et al., 2003; Littlefield and Fowler, 1998; Weber et al., 1994; Weber et al., 1999) and together prevent depolymerisation from the pointed end (Blanchoin et al., 2001). Importantly, tropomyosins also regulate myosins either by activating or inhibiting their ATPase activity (Lehrer and Morris, 1982). In addition, tropomyosins have been reported to inhibit filament bundling and branching by Arp2/3 complex (Blanchoin et al., 2001; Burgess et al., 1987). Lastly it has been proposed that tropomyosin protects actin filaments partially from actin depolymerising drugs latrunculin A and cytochalasin D (Creed et al., 2008). Taken together, these results suggest that tropomyosins stabilise actin filaments. However, although primarily seen in stress fibres and lamella, tropomyosins have also been observed in more dynamic structures like lamellipodia and ruffles (Gupton et al., 2005; Hillberg et al., 2006; Ponti et al., 2004; Schevzov et al., 2005).

Drebrin

Drebrin is a multifunctional F-actin binding protein that brings together many proteins regulating actin dynamics in cells and thus act as a scaffold protein. Drebrin has an N-terminal ADF-H domain and helical/charged motif, but its C-terminal sequences are poorly conserved. Drebrin has many inhibitory effects in actin dynamics as it has been reported to inhibit α-actinin,

tropomyosin (Ishikawa et al., 1994), and myosin binding to actin (Hayashi et al., 1996; Ishikawa et al., 2007). Recently it has been found that drebrin also links F-actin and microtubule networks (Bazellieres et al., 2012).

IQGAPs

IQGAPs are family of multifunctional scaffold proteins, which transmit signals through the mitogen activated (MAP) kinase pathway (Ren et al., 2007; Roy et al., 2005) and bind actin (Bashour et al., 1997). IQGAPs have an N-terminal calponin-homology domain, which binds actin (Stradal et al., 1998) followed by six IQGAP specific repeats, a WW domain, an IQ domain, a G-protein binding domain, and a C-terminal RasGAP sequence. Being scaffold proteins, IQGAPs have many binding partners including small GTPases Rac1 and Cdc42, whose GTPase activity IQGAPs stimulates (Hart et al., 1996; Kuroda et al., 1996). Interestingly, it was reported that IQGAP1 is needed for localisation of formin Diaph1 to the leading edge of migrating cells (Brandt et al., 2007). IQGAPs have been found in many actin structures in cells including adherens junctions, filopodia, and lamellipodia (Bashour et al., 1997; Kuroda et al., 1998; Schmidt et al., 2003) where they participate to many actin functions. These include linking plus ends of microtubules to the actin network together with the cytoplasmic linker protein 170 (CLIP170) (Fukata et al., 2002), F-actin crosslinking, and bundling of actin filaments (Bensenor et al., 2007). Lastly, IQGAP1 has been suggested to stimulate actin nucleation through the Arp2/3 complex (Le Clainche et al., 2007).

1.3.7 Rho GTPases

Rho GTPases are a family of proteins, which regulate many important cellular functions through signalling cascades and belong to the Ras superfamily of small GTPases. In cells, Rho GTPases cycle between inactive GDP bound and active GTP bound states (Boguski and McCormick, 1993) and are regulated by three groups of proteins. First, guanine nucleotide-exchange factors (GEFs) catalyse the exchange of GDP to GTP and thus promote Rho GTPase activity (Schmidt and Hall, 2002). Second, Rho GTPases have a slow intrinsic GTPase activity, which is enhanced by GTPase-activating proteins (GAPs) *in vivo* (Moon and Zheng, 2003) leading to loss of activity. Third, Rho GDP-dissociation inhibitors (GDIs) release Rho GTPases from the membrane, sequester them, inhibit their nucleotide exchange, and GTPase activity (Olofsson, 1999). The most important members of the Rho GTPase family, RhoA, Rac1, and Cdc42, regulate the formation of important F-actin structures, such as stress fibers, lamellipodia, and filopodia, respectively (Nobes and Hall, 1995). Importantly RhoA has been proposed to be the most important regulator of the actin cortex (Charras et al., 2006; Etienne-Manneville and Hall, 2002).

RhoA has two main downstream effectors, ROCK (Ishizaki et al., 1996; Leung et al., 1995; Matsui et al., 1996) and formin Diaph1 (Watanabe et al., 1997). ROCK has two main substrates, which it phosphorylates. First, ROCK inactivates myosin phosphatase and activates myosin light chain by phosphorylation (Amano et al., 1996; Kimura et al., 1996; Uehata et al., 1997) promoting acto-myosin contractility, which is an important property of the cell cortex. Second, ROCK activates LIM kinase, which phosphorylates ADF/cofilin (Maekawa et al., 1999) leading to decreased depolymerisation and severing of F-actin and thus stabilises actin filaments. In addition to myosin phosphatase and LIM kinase, ROCK also phosphorylates and promotes ERM-protein activation (Matsui et al., 1998; Tran Quang et al.,

2000). Formins, including Diaph1, promote formation of linear actin filaments in the cell and are presented in detail in the next part of this thesis.

These data suggest that RhoA has a triple role in the cortex as it can promote contractility, actin polymerisation, and membrane-cortex linking (Fig. 1.6). Interestingly, microinjection of Rho guanine nucleotide dissociation inhibitor α (GDIα), the catalytic domain of p50 Rho GTPase activating protein (GAP), the Rho GTPase-binding domain of rhotekin, or C3 exoenzyme stopped blebbing, a phenomenon dependent on the acto-myosin contractility of the cortex (Charras et al., 2006). In addition RhoA was shown to be required for cortical rigidity and cortical retraction during mitotic rounding (Maddox and Burridge, 2003). Indeed, injection of C3 exoenzyme into mitotic cells led to changes in the cell morphology suggestive of weaker cortex and RhoA was shown to be more active and p190RhoGAP less active in mitotic cells compared to interphase cells (Maddox and Burridge, 2003). These data suggest that active RhoA is needed for functional cortex in interphase and mitotic cells.

In addition to RhoA, other Rho GTPases include RhoB which recruits Diaph1 to endosomes (Fernandez-Borja et al., 2005), RhoC that regulates ADF/cofilin, Fmnl2, and Diaph1 (Bravo-Cordero et al., 2011; Kitzing et al., 2010), and RhoD that recruits formin hDia2C to endosomes (Gasman et al., 2003). Finally the Rho GTPase Rac1 was shown to activate the WAVE complex (Innocenti et al., 2004; Ismail et al., 2009), which in turn activates the Arp2/3 complex (Innocenti et al., 2005; Suetsugu et al., 2003; Yamazaki et al., 2003; Yan et al., 2003) and thus it governs lamellipodia formation.

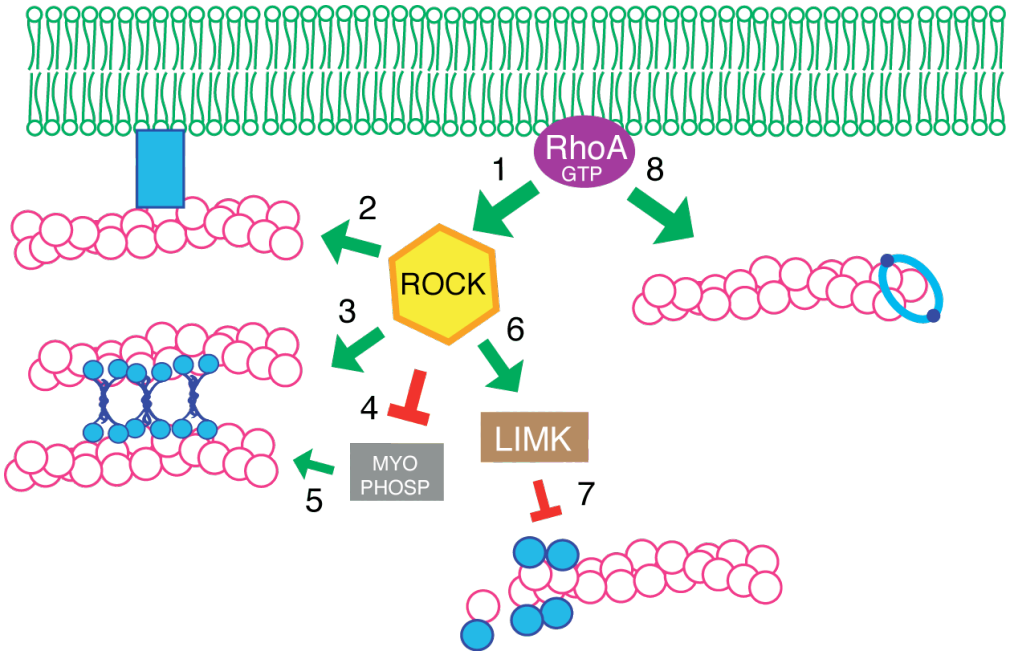

Figure 1.6: Suggested roles for RhoA at the cell cortex.

At the cell cortex RhoA-GTP activates ROCK (1), which promotes membrane-cortex linking through ERM-proteins (2), induces contractility (3, 5) through activating myosin light chains and inactivating myosin phosphatase (4), and inhibits F-actin depolymerisation through activating LIM kinase (6) that phosphorylates ADF/cofilins (7) making them inactive. RhoA-GTP also promotes formin mediated actin polymerisation (8). See main text for details and references.

1.3.8 Actin nucleators

I described earlier that forming an actin seed, needed for actin filament nucleation, is slow, because actin monomers bind rather weakly to each other, but cells have overcome this problem by synthesising proteins called actin nucleators. Six types of actin nucleators are known to date (Fig. 1.7): the Arp2/3 complex together with its nucleation promoting factors, formin family, Spire proteins, Cordon Bleu, JMY, and leiomodin. All are presented in the following.

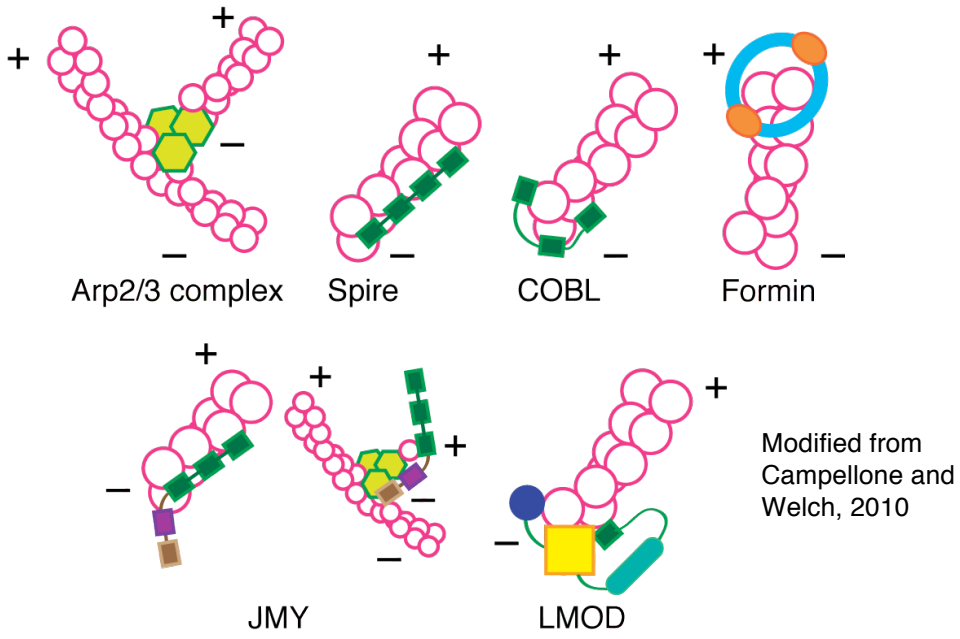

Figure 1.7: Actin nucleators.

The Arp2/3 complex binds to a pre-existing filament and produces branched actin filaments (Pollard et al., 2000). Both Spire and Corbon Bleu (COBL) produce unbranched filaments. The Arp2/3 complex, Spire, and COBL all are bound at the pointed end of the filament. Formins nucleate unbranched filaments like Spire and COBL, but in contrast to the other nucleators, formins stay bound at the barbed end of the filament and speed up elongation (Pruyne et al., 2002; Sagot et al., 2002). JMY has two activities as a nucleator: it nucleates filaments in the same way as Spire and can also activate the Arp2/3 complex (Roadcap and Bear, 2009; Zuchero et al., 2009). Leiomodins (LMODs) also nucleate actin filaments from the pointed end and are muscle specific actin nucleators (Chereau et al., 2008).

1.3.8.1 The Arp2/3 complex

The Arp2/3 complex is a large macromolecule; it is a stable assembly of seven subunits, which are the two actin related proteins (Arp2 and Arp3) described and five actin related protein complexes (ARPC1-5) (Goley and Welch, 2006; Machesky et al., 1994). The Arp2/3 complex nucleates a new actin filament from the side of a pre-existing filament and remains bound at the pointed end of the nascent filament at the branch point (Fig. 1.7). The two Arps in the complex mimic actin monomers and act as a template for the new filament, which after nucleation grows rapidly from its barbed end forming a characteristic 70 degree branch angle between the mother and the daughter filaments (Amann and Pollard, 2001a; Mullins et al., 1998a).

The Arp2/3 complex has only a weak biochemical activity by itself. In the inactive conformation, the complex is open and the Arps are unable to bind an ATP nucleotide. When a nucleation-promoting factor is introduced together with the Arp2/3 complex, its conformation changes to favour binding of an ATP-nucleotide and brings the two Arp subunits close together. These events and binding to the side of a mother actin filament activate the Arp2/3 complex (Pollard, 2007). So far the Arp2/3 complex is the only known protein complex, that enables the formation of branched actin filament networks (Pollard et al., 2000). Proteins regulating the release of the Arp2/3 complex from the actin filaments have been recently characterised. Interestingly, coronin (Cai et al., 2008) and a protein called glia maturation factor (GMF) (Gandhi et al., 2010) were found to participate in dissociating the Arp2/3 complex from the sides of actin filaments leading to de-branching.

The Arp2/3 complex plays an essential role in actin dynamics in cells. In migrating mammalian cells it forms a network of branched actin filaments in the lamellipodium, where the barbed ends of filaments point toward the cell membrane at the cell's leading edge. The growing barbed ends of the filaments push the plasma membrane forward allowing the lamellipodium to

protrude (Goley and Welch, 2006; Mullins et al., 1998a; Welch et al., 1997). In addition, the Arp2/3 complex has been reported to localise to newly formed focal adhesions, suggesting a role as a link between adhesion and protrusion (DeMali et al., 2002). The Arp2/3 complex is not only involved in migration, but also in many other functions and structures of the cell. First, the internalisation step of endocytosis is an Arp2/3 complex -dependent process both in *S. cerevisiae* and mammalian cells (Kaksonen et al., 2003; Kaksonen et al., 2005; Merrifield, 2004; Merrifield et al., 2005). Second, the Arp2/3 complex was reported to interact with E-cadherin, a protein found in cell-cell adhesions, where it is needed for cadherin-based lamellipodia formation, which are essential for extending cadherin-based contacts (Kovacs et al., 2002). Third, the Arp2/3 complex was found to be essential in the formation of phagocytic cup in both Fcγ receptor and complement receptor mediated phagosomes (May et al., 2000). Fourth, the Arp2/3 complex has been suggested to have a role in exocytosis, but its role in this process remains to be thoroughly investigated (Gasman et al., 2004). Fifth, the Arp2/3 complex has been linked to membrane trafficking through initiating actin polymerisation at the Golgi complex (Chen et al., 2004; Fucini et al., 2002; Luna et al., 2002; Matas et al., 2004). Finally, the Arp2/3 complex has been reported to localise to the cortical cap region of meiotic mouse oocytes and inhibition of the Arp2/3 complex by the drug CK666 disrupted the cortical actin cap and cell polarity in these cells (Sun et al., 2011b; Yi et al., 2011).

Because the Arp2/3 complex is involved in so many functions and structures of the cell, its activity and recruitment have to be tightly regulated. Indeed, nucleation promoting factors (NPFs) not only activate the Arp2/3 complex, but also recruit it to the correct locations of the cell. Wiscott-Aldrich syndrome protein (WASP) family proteins and WASP family verprolin homologous protein (WAVE/Scar) family proteins are considered to be the main activators of the Arp2/3 complex. Although these NPFs are diverse in their domain structure, they all contain a VCA domain (class I NPFs), which acts as a platform, where the actin monomer can bind to the Arp2/3 complex and start

the polymerisation of the new daughter filament (Goley and Welch, 2006). Indeed, the WH2 or verprolin (V) domain binds to an actin monomer (Chereau et al., 2005) and the central (C) domain together with the acidic (A) domain mediate binding to the Arp2/3 complex. The C domain also binds to an actin monomer and helps to deliver it to the Arp2/3 complex (Marchand et al., 2001).

WASP is only expressed in haematopoietic cells (Stewart et al., 1996), but N-WASP has been shown to be present in many cell types, although first found expressed predominantly in the brain (Miki et al., 1996). Monomeric N-WASP is involved in many functions of the cell including endocytosis (Table 1.1) (Benesch et al., 2005; Bu et al., 2009; Innocenti et al., 2005; Tsujita et al., 2006). In contrast to N-WASP, active WAVE forms a complex with Sra1, Nap1, Abi1 and Brick1 subunits (Eden et al., 2002; Stovold et al., 2005) and activates the Arp2/3 complex at the lamellipodium tip (Table 1.1) (Innocenti et al., 2005; Suetsugu et al., 2003; Yamazaki et al., 2003; Yan et al., 2003) and cell-cell adhesions (Table 1.1) (Yamazaki et al., 2007). More recently discovered VCA domain containing proteins are the Wiscott-Aldrich syndrome protein and Scar homolog (WASH) and WASP homolog associated with actin, membranes, and microtubules (WHAMM). WASH is evolutionarily conserved and co-localises with actin in filopodia and lamellipodia (Table 1.1) (Linardopoulou et al., 2007). In addition to activation of the Arp2/3 complex WASH was also shown to act downstream of Rho with Spire and the formin Cappuccino in *D. melanogaster* (Liu et al., 2009), further suggesting a link between branched and linear actin networks. WHAMM was shown to localise to *cis*-Golgi (Table 1.1) and, in addition to activation of the Arp2/3 complex, it is able to bind microtubules (Campellone et al., 2008).

Interestingly, class II NPFs do not contain a VCA domain, but activate and stabilise the Arp2/3 complex by other means. Cortactin, a class II NPF, has been reported to inhibit spontaneous dissociation of the Arp2/3 complex from the mother filament by binding to the Arp2/3 complex and stabilising the

branch points (Weaver et al., 2001) and to enhance the N-WASP mediated activation of the Arp2/3 complex (Kowalski et al., 2005; Martinez-Quiles et al., 2004; Tehrani et al., 2007). In migrating cells cortactin localises to the lamellipodia (Table 1.1) (Weed et al., 2000).

Class I NPFs	**Localisation**
N-WASP	Sites of endocytosis
WAVE complex	Lamellipodia, cell-cell adhesions
WASH	Lamellipodia, filopodia
WHAMM	*Cis*-Golgi
Class II NPF	
cortactin	Lamellipodia

Table 1.1: Localisation of nucleation promoting factors in cells.

Localisation of class I and II NPFs in cells are presented. Class I NPFs containing VCA-domain needed for Arp2/3 complex activation are N-WASP, WAVE complex (WAVE, Sra1, Nap1, Abi1 and Brick1), WASH, and WHAMM. Class II NPF cortactin does not contain a VCA domain, but stabilises Arp2/3 complex induced branch points. See main text for details and references.

1.3.8.2 Formins

Formins are actin nucleators that produce unbranched actin filaments and stay attached to the growing barbed end of the filament (Fig. 1.7) (Pruyne et al., 2002; Sagot et al., 2002) preventing barbed end capping and maintaining elongation (Higashida et al., 2004; Zigmond, 2004b). In addition to nucleating and elongating new filaments by themselves, formins can potentially elongate filaments induced by other nucleators like the Arp2/3 complex (Lee et al., 2010).

All formins consist of a highly conserved formin homology 2 (FH2) domain, formin homology 1 (FH1) domain, and more heterogeneous regulatory

domains (Kovar, 2006). The FH2 domain forms a doughnut-shaped homodimer (Lu et al., 2007; Shimada et al., 2004; Xu et al., 2004), which nucleates a new actin filament by capturing two actin monomers and stabilising them as a dimer (Kovar et al., 2003; Li and Higgs, 2003; Pring et al., 2003). Interestingly homodimeric FH2 domains alone are able to nucleate actin filaments *in vitro* (Evangelista et al., 2002; Li and Higgs, 2003; Pruyne et al., 2002; Sagot et al., 2002), however *in vivo* the FH1 domains are needed for efficient elongation. Indeed, the FH1 domain binds profilin with its proline rich motifs (Chang et al., 1997; Watanabe et al., 1997) and delivers ATP-actin monomers to the FH2 domain acting as an accelerator of the nucleation and elongation (Paul and Pollard, 2008; Romero et al., 2004). The number of proline rich motifs in the FH1 domain varies between formins, but the more profilin-actin is bound to a formin, the more efficient its elongation is.

To date 15 formins in eight different protein families have been found in humans (Fig. 1.8). The best-characterised formins belong to the group of Diaphanous related formins (DRFs), but all formins are described in detail later in this section. Many of these formin families share common features in how they are regulated. It is known that at least the Diaphanous (Dia), Formin-related protein in leukocyte (Frl) also known as formin-like protein (Fmnl), Dishevelled-associated activator of morphogenesis (Daam), and FH1 and FH2 domain containing protein (Fhod) families of formins are autoinhibited by interaction between their diaphanous inhibitory domain (DID) and their diaphanous auto-regulatory domain (DAD) and this autoinhibition can be released by binding of small GTPases (for example RhoA) (Fig. 1.9) (Higgs, 2005; Watanabe et al., 1999). Indeed, the small GTPase binding domain overlaps with the DID domain and thus the small GTPase can compete with DAD for binding to the N-terminus of the formin. To date much less is known about the regulation of ‘formins’ (Fmns), delphilin, and inverted formins (INFs).

Dimerisation is important for formin functionality. Not only do the barbed end binding FH2 domains dimerise (Lu et al., 2007; Shimada et al., 2004; Xu et al., 2004), but dimerisation domains and coiled-coil, close to the DID domains, also aid in dimer formation (Romero et al., 2004) leaving FH1 domains free to catch and deliver profilin-actin to the FH2 domains (Fig. 1.9).

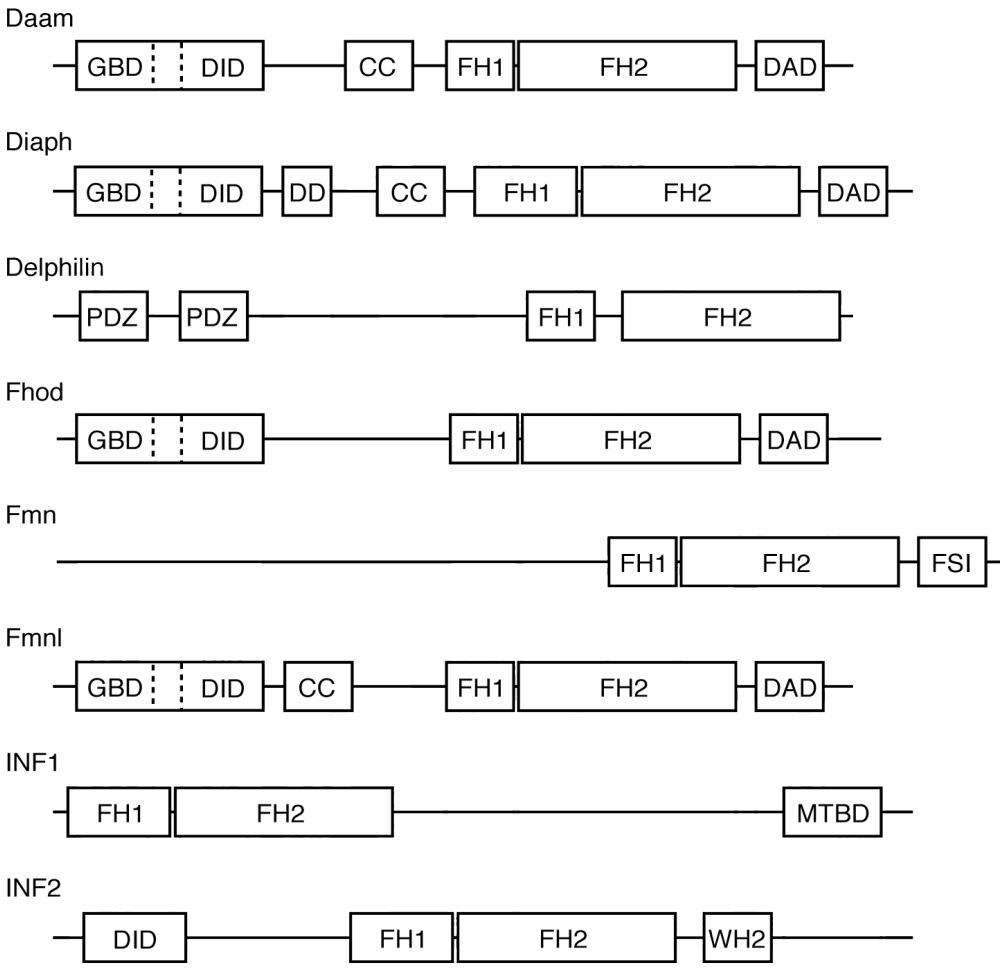

Figure 1.8: Different formins share FH1 and FH2 domains, but have other distinct regulatory domains.

Mammalian formins share conserved FH1 and FH2 domains, whereas the regulatory domains are more heterogeneous. The Daam, Diaph, Fhod and Fmnl groups of formins share the regulatory system through interaction between their diaphanous inhibitory domain (DID) and their diaphanous auto-regulatory domain (DAD). Inverted formin1 (INF1) differs from other formins the most, because is has its FH1 and FH2 domains close to the N-terminus instead of the C-terminus.

GBD=GTPase binding domain, DID=diaphanous inhibitory domain, DD=dimerisation domain CC=coiled coil, FH1=formin homology 1, FH2 =formin homology 2, DAD=diaphanous auto-regulatory domain, FSI=formin-spire interaction domain, PDZ=postsynaptic density protein disc large zona occludens 1 domain, MTBD=microtubule binding domain, WH2=Wasp homology 2 domain

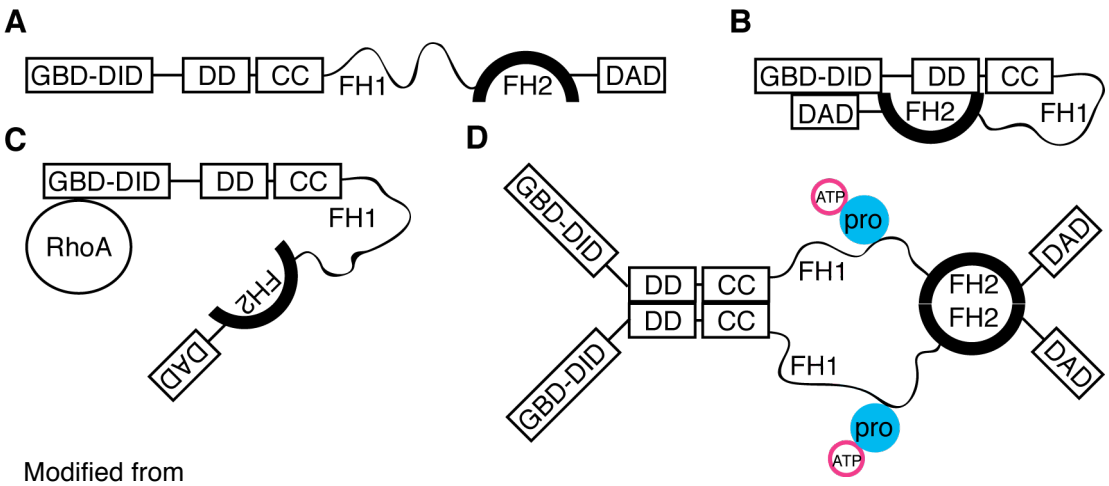

Modified from
Chesarone et al., 2010

Figure 1.9: The structure and regulation of the DRF group of formins.

A. The autoregulatory diaphanous inhibitory domain (DID) overlaps with the GTPase binding domain (GBD), which binds small GTPases like RhoA. The dimerisation (DD) and coiled coil (CC) domains follow GBD-DID. The FH1 domain is flexible and are presented by a ribbon. The FH2 domain will form a doughnut with another FH2 domains once they dimerise. Finally the DAD domain is at the C-terminus.

B. When autoinhibited the C-terminal diaphanous autoregulatory domain (DAD) binds to the N-terminal DID domain masking the FH2 domain needed for nucleation activity (Higgs, 2005).

C. The small GTPase RhoA releases inhibition and activates the formin by binding to the GBD domain.

D. Active formin forms a dimer through binding of their dimerisation, coiled coil, and FH2 domains. Flexible FH1 domains bind profilin-ATP-actin, which are supplied to the dimeric FH2 domain to maintain nucleation and elongation.

How formins stay attached at the barbed end has been under investigation for many years. A recent study showed that formins rotate at the filament tip during elongation (Mizuno et al., 2011) possibly by easing the association to the barbed end. How formins actually place new monomers between themselves and the filament is not yet known. It has been proposed, that the FH2 domain could have two different conformations. In an 'open' state, an actin monomer can be added onto the filament, whereas in a 'closed' state, monomers cannot be added. The idea is that the formin has to have the 'closed' state to be able to stay attached at the barbed end of the filament, while it is not elongating making it equivalent to a capping protein (Pollard, 2007). Hence, formins are often called leaky cappers.

In addition to nucleation, many formins have been reported to bundle actin filaments *in vitro* (Harris and Higgs, 2006) and to bind to microtubules, but this aspect of formins is not discussed in this thesis. Finally, one formin was shown to sever actin filaments *in vitro* (Harris et al., 2004).

Daam proteins

Daam formins were found as binding partners for Dishevelled, a component of the non-canonical Wnt signalling pathway, and therefore were named as Dishevelled associated activators of morphogenesis (Daam) (Habas et al., 2001). The Daam group of formins consists of Daam1 and Daam2 (Higgs and Peterson, 2005). As described Daam formins are autoinhibited through DID-DAD binding and get activated upon Dishevelled binding (Liu et al., 2008). Flightless-I, a gelsolin family protein, was also reported to activate Daam1 both *in vitro* and in cells (Higashi et al., 2010). Daam1 has multiple roles during development. First, Daam1 was reported to be required for planar cell polarity signalling during gastrulation in *X. laevis* (Habas et al., 2001) and second, has been discovered to have a role in endocytosis in developing *D. rerio* (Kida et al., 2007). Third, Daam1 was reported to be essential for heart morphogenesis in mice (Li et al., 2011). In addition Daams are present in developing neuronal tissues (Kida et al., 2004) and are

important in axonal morphogenesis in *D. melanogaster* (Matusek et al., 2008). In mature mammalian cells, Daam1 is needed for centrosome re-orientation during cell motility (Ang et al., 2010) and was also reported to regulate cell growth through microtubule stabilisation in endothelial cells (Ju et al., 2010).

Diaphanous related formin proteins

This group of formins consists of Diaph1 (mDia1), Diaph2 (mDia3), and Diaph3 (mDia2) proteins. The detailed structure and activation of Diaph1 was presented in figure 1.9. RhoA was shown to activate Diaph1 by binding to the GBD domain leading to release of the DID-DAD interaction (Watanabe et al., 1997). In addition to being downstream of RhoA, Diaph1 has interestingly been reported to act upstream of RhoA and promote ROCK1 activation by activating RhoA through leukemia-associated RhoGEF (LARG) (Kitzing et al., 2007). Further, it was also reported, that Flightless-I is able to activate Diaph1 *in vitro* through helping RhoA in releasing the autoinhibitory interaction and enhancing actin polymerisation activity by recruiting actin monomers to the FH1-FH2 domains of Diaph1 (and Daam1) (Higashi et al., 2010).

The three Diaph family formins appear to have specific as well as overlapping functions in cells. First, Diaph1 produces actin filaments for stress fiber formation (Hotulainen and Lappalainen, 2006), is needed for formation of the phagocytic cup (Brandt et al., 2007; Lewkowicz et al., 2008), strengthens cell adhesion junctions (Carramusa et al., 2007; Ryu et al., 2009), and maintains Golgi complex structure (Zilberman et al., 2011). In addition, Diaph1 has been reported to localise to filopodia, where it elongates the filament bundle (Goh et al., 2011b). Finally, Diaph1 has been suggested to have a role in the cell cortex, because it was reported to be necessary for invasion and blebbing motility of MDA-MB-435 cells upon lysophosphatidic acid stimulation (Kitzing et al., 2007).

Second, Diaph2 has been shown to participate in correct chromosome alignment during mitosis, but interestingly its actin nucleation ability was not essential for this process, only its binding to microtubules through end-binding protein 1 (EB1) (Cheng and Mao, 2011). During mitosis Diaph2 is activated by phosphorylation through Aurora B kinase (Guo et al., 2011) leading to Diaph2 mediated stabilisation of kinetochore-microtubule binding (Cheng and Mao, 2011; Guo et al., 2011).

Third, Diaph3, the best-characterised Diaph family formin, is present in lamellipodia (Sarmiento et al., 2008; Yang et al., 2007) and filopodia (Yang et al., 2007). In lamellipodia, Diaph3 nucleates and elongates linear actin filaments and also regulates actin turnover in focal adhesions (Gupton et al., 2007). In filopodia Diaph3 elongates actin filaments maintaining growth and localises strongly to the filopodial tips (Pellegrin and Mellor, 2005; Yang et al., 2007). Interestingly, Diaph3 also participates in the assembly of the contractile ring in dividing cells (Watanabe et al., 2008; Watanabe et al., 2010). Finally, Diaph3 has been suggested to stabilise the cell cortex, because overexpression of diaphanous-interacting protein (DIP) induces blebbing by binding to Diaph3 and inhibiting its activity (Eisenmann et al., 2007a). In addition, recently a specific isoform of Diaph3 was proposed to be essential for cortex formation as depletion of this isoform inhibited blebbing of spreading HeLa cells (Stastna et al., 2011).

Finally, all Diaph proteins are also able to bind microtubules and microtubule binding proteins (Bartolini et al., 2008; Lewkowicz et al., 2008; Wen et al., 2004) and are able to trigger serum response factor (SRF) mediated transcription in cells (Young and Copeland, 2008). *In vitro* Diaph formins have been reported to bundle actin filaments (Harris and Higgs, 2006; Machaidze et al., 2010), suggesting an additional function for these formins.

Delphilin

Delphilin is expressed only in neuronal tissues and was first identified as a protein interacting with the glutamate receptor δ2 (GluRδ2) subunit and localise to the dendritic spines of hippocampal neurons (Miyagi et al., 2002). However, this variant lacked an additional PDZ domain present in the full-length delphilin. The full-length isoform was reported to be present in soma and dendritic shafts (Matsuda et al., 2006). Delphilin does contain FH1 and FH2 domains, but its role in the actin cytoskeleton of neuronal cells remain to be investigated.

Fhod proteins

The formin Fhod1 (also known as FHOS) was first identified as a downstream effector of the small GTPase Rac1 (Westendorf, 2001). However, although downstream of Rac1, the autoinhibition of Fhod1 is released by ROCK that phosphorylates the DAD domain (Takeya et al., 2008). Rac1, instead, appears to be needed for Fhod1 localisation (Gasteier et al., 2005). Activation of Fhod1 leads to stress fiber formation in endothelial cells (Takeya et al., 2008). Interestingly upon overexpression Fhod1 and ROCK1 have been reported to induce blebbing in HeLa cells (Hannemann et al., 2008). The authors suggested that Fhod1 nucleates actin filaments at the cell cortex, because the number of blebs observed after Fhod1 depletion in cells overexpressing a SH4 domain was decreased (Hannemann et al., 2008). Another member of the Fhod group of formins is Fhod3 (also known as Fmnl3), which induces the formation of filopodia in mammalian cells (Harris et al., 2010).

Fmn proteins

The first formin discovered was a mouse formin, encoded by *limb deformity* gene (Mass et al., 1990; Woychik et al., 1990), known today as formin1 (Fmn1). The regulation of Fmns remains to be investigated, as Fmn proteins do not share the DID-DAD interaction observed in DRFs, and do not belong to this superfamily of formins. Fmn1 has been reported to bind microtubules

during interphase (Zhou et al., 2006) and to play a role in focal adhesions and cell spreading, as Fmn1 deficient cells displayed decreased ability to form focal adhesions leading to impaired cell spreading (Dettenhofer et al., 2008). Fmn2 has been reported to associate with asymmetric spindle positioning during meiosis in mouse oocytes (Dumont et al., 2007; Leader et al., 2002). Indeed, it was shown that when the chromosomes and spindle relocate from the center of the oocyte to the cell cortex, Fmn2 localises around the chromosomes and nucleates actin filaments to direct movement (Azoury et al., 2008; Li et al., 2008; Schuh and Ellenberg, 2008). Fmns have also been reported to interact with Spire nucleators (described later) (Pechlivanis et al., 2009).

Fmnl proteins

The first member of the Formin-like (Fmnl) proteins found was formin-related gene in leukocytes 1 or α (Frl1/α, also known as Fmnl1) (Yayoshi-Yamamoto et al., 2000), which is the most studied Fmnl. Other proteins in the Fmnl protein family are Fmnl2 and Fmnl3, the latter is often categorised in the Fhod group, like in this thesis (Fhod3). Like many other formins, Fmnl proteins are also DRFs and have an intramolecular DID-DAD interaction. Fmnl1 appears to be a classical DRF as DID-DAD interaction inhibits its activity and the interaction can be released by small GTPase binding (Cdc42) (Seth et al., 2006). In contrast, DID-DAD binding in Fmnl2 was shown not to inhibit its activity (Vaillant et al., 2008), making the role of the interaction unclear.

Fmnl1 is enriched in macrophages and it has an FH2 domain, which has been reported to nucleate new actin filaments and surprisingly to sever existing filaments *in vitro* (Harris et al., 2004; Yayoshi-Yamamoto et al., 2000). Fmnl1 has been suggested to have many roles in macrophages including cell adhesion modulation, motility, and survival (Yayoshi-Yamamoto et al., 2000), but interestingly it was also revealed that together with the Arp2/3 complex Fmnl1 appears to have a role in the formation of phagocytic

cups in Fcγ receptor mediated phagosomes (Seth et al., 2006). In addition, Fmnl1 is needed for centrosome polarisation upon T-cell activation (Gomez et al., 2007) and participates in podosome formation in macrophages (Mersich et al., 2010). Finally, Fmnl1 has also been linked to cortex stability, because overexpression of constitutively active Fmnl1 induces blebbing independently of ROCK (Han et al., 2009). A specific isoform of Fmnl1, Fmnl1γ was linked to structural maintenance of the Golgi complex and lysosomes through maintaining F-actin content in HeLa cells (Colon-Franco et al., 2010). Fmnl2 has been reported to be up-regulated in tumours of colorectal cancer and has been suggested to have a role in metastasis (Zhu et al., 2008).

INF proteins

INF stands for inverted formin. INF1 is a 'true' inverted formin, because it has the FH1 and FH2 domains close to the N-terminus of the protein instead of the C-terminus like other formins (Fig. 1.8) (Higgs and Peterson, 2005; Katoh, 2004). INF1 was shown to associate with microtubules and stabilise them in Cos1 cells through its C-terminal microtubule binding domain (MTBD) (Young et al., 2008), suggesting INF1 could coordinate microtubule and F-actin networks in cells.

Maybe a bit misleadingly, INF2 is also called inverted formin, even though it has a DID domain close to its N-terminus like other formins, and the FH1 and FH2 domains closer to the centre of the protein (Fig. 1.8) (Higgs and Peterson, 2005). Thus, INF2 is not a true inverted formin like INF1. Additionally, the FH2 domains of INF1 and INF2 are surprisingly different in their sequence further suggesting they should not be placed in the same family of formins.

Interestingly, INF2 has a WASP homology 2 (WH2) domain in its C-terminus, which binds to actin monomers and can accelerate polymerisation (Chhabra and Higgs, 2006). Surprisingly, INF2 has also been shown to accelerate

depolymerisation and to sever F-actin through its WH2 domain (Chhabra and Higgs, 2006). Although INF2 is different from other formins, especially because it contains a WH2 domain (Chhabra and Higgs, 2006), it shares common features with DRFs. The WH2 domain appears to behave like a DAD domain and binds to the DID domain of INF2 (Chhabra and Higgs, 2006). Interestingly the DID-WH2 interaction appears not to affect the polymerisation activity, but inhibits the depolymerisation activity of INF2 (Chhabra et al., 2009). INF2 was found to localise to the endoplasmic reticulum in Swiss 3T3 cells, but its function there is yet to be revealed (Chhabra et al., 2009).

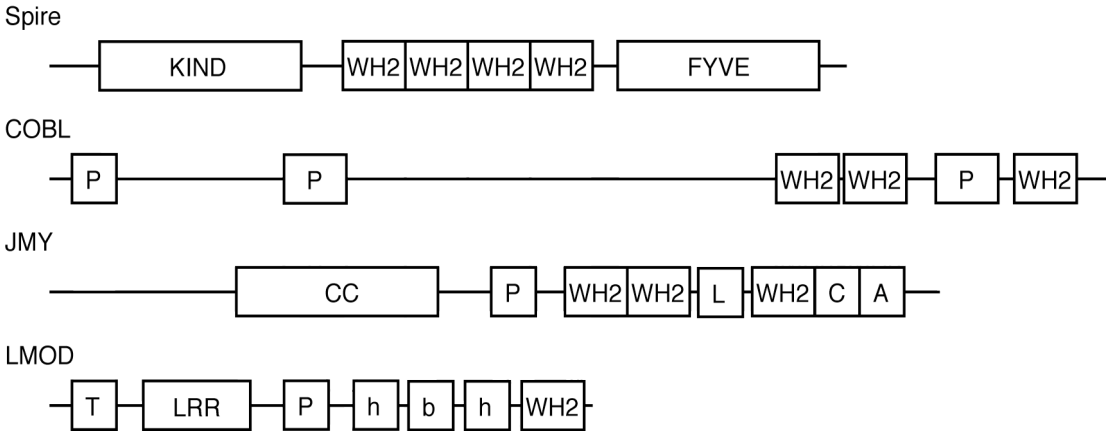

Modified from Campellone and Welch, 2010

Figure 1.10: Spire, Cordon Bleu, JMY, and Leiomodin domain structure. Domains in Spire, Cordon Bleu (COBL), JMY, and Leiomodin (LMOD) are presented. The WH2 domains are crucial for the actin nucleation activity of these proteins. Spire consists of regulatory KIND and FYVE domains and four WH2 domains. Cordon Bleu has conserved polyproline rich regions and three WH2 domains, and the rest of the protein sequence is less conserved. JMY consists of a coiled coil region, a polyproline-rich domain, two WH2 domains, a leucine-rich region and a VCA domain. The VCA domain is needed for Arp2/3 complex activation, which is another function of JMY. Leiomodin, which is a muscle specific nucleator, consists of tropomyosin and actin binding regions, a leucine rich domain, a polyproline rich region, a helix-basic-helix domain, and a WH2 domain.

KIND=kinase non-catalytic C-lobe, WH2=Wasp homology 2, FYVE=Fab1-YOTB-Vac1-EEA1, P=polyproline, CC=coiled coil, L=leucine-rich domain, C=central, A=acidic, T=tropomyosin and actin binding, L or LRR=leucine rich region, h-b-h=helix-basic-helix

1.3.8.3 Spire proteins

Spire nucleators were first found from *D. melanogaster*, where they were shown to nucleate actin filaments by binding to four ATP-actin monomers with their four WH2 domains located in the mid-region of the protein leading to formation a one-stranded actin filament (Fig. 1.7 and 1.10) (Quinlan et al., 2005). Later mammalian Spire1 and Spire2 were identified. Spire produces unbranched filaments, like formins, but in contrast to formins, Spire binds to the pointed end of the filament and protects it from depolymerisation (Quinlan et al., 2005). For efficient nucleation all four WH2 domains are needed, however Spire-mediated nucleation was measured to be slower than nucleation by the Arp2/3 complex (Quinlan et al., 2005). Linkers between the WH2 domains are also important for nucleation as linker L-3 was shown stabilise interactions between two actin monomers during nucleation and to possess weak nucleation activity itself (Quinlan et al., 2005).

It has been confirmed that Spire contributes to actin nucleation, but how it does it remains controversial. Although the presence of a one-stranded 'filament' proposed by Quinlan and colleagues was observed in a X-ray scattering study (Rebowski et al., 2008), detailed biochemical and kinetic studies of human Spire1 suggested that the WH2 domains do not form a one-stranded filament, that initiates polymerisation, but rather form a structure, which is not able to polymerise (Bosch et al., 2007). However, by fine-tuning the *in vitro* conditions, the authors were able to detect actin nucleation activity of the WH2 domains (Bosch et al., 2007). Interestingly it was also observed that Spire1 actually interacts with the barbed end of filaments, inhibits polymerisation, and is able to trigger severing of filaments (Bosch et al., 2007).

In addition to WH2 domains, Spire has two regulatory domains; the kinase non-catalytic C-lobe domain (KIND) in the N-terminus and the Fab1-YOTB-Vac1-EEA1 (FYVE) domain in the C-terminus (Fig. 1.10). Interestingly spires

were reported to interact with formins (Bosch et al., 2007; Rosales-Nieves et al., 2006), and the KIND domain was shown to mediate the interaction with the formin-spire interaction (FSI) domain of Fmn2 and Cappuccino (*D. melanogaster* formin) (Pechlivanis et al., 2009; Quinlan et al., 2007). The effect of this interaction for the nucleation activity of spire and formin remain controversial, as it was shown, that *in vitro* Spire inhibits actin nucleation by Fmn2 and Cappuccino, and enhances its own nucleation activity (Quinlan et al., 2007). However, in *in vitro* bead motility assays (Romero et al., 2004), addition of Spire to mDia1 FH1+FH2 coated beads enhanced the formin mediated motility of beads (Bosch et al., 2007).

Interestingly in *D. melanogaster* oocytes, Spire and Cappucino together localise to the cell cortex (Quinlan et al., 2007; Rosales-Nieves et al., 2006). In contrast, in mammalian cells, Spire localises to endosomes, where it recruits Fmn2 (Quinlan et al., 2007). It has also been suggested that Spire could be involved in membrane trafficking through the Golgi complex, because expression of the C-terminal FYVE domain of Spire is able to inhibit transport from the Golgi to the cell membrane (Kerkhoff et al., 2001). Finally Spire also binds microtubules, suggesting that it links microtubule networks to the actin cytoskeleton (Quinlan et al., 2007; Rosales-Nieves et al., 2006).

1.3.8.4 COBL

Like formins and Spire, Cordon-Bleu (COBL) also produces unbranched filaments and like Spire, COBL stays attached at the pointed end of the filament, but consists of only three WH2 domains (Ahuja et al., 2007) (Fig. 1.7 and 1.10). With these three WH2 domains, which all bind to actin monomers with different affinities and are crucial for the nucleation activity, COBL forms a classical trimeric actin nucleus (Ahuja et al., 2007). The trimer formation is enabled by the linker L-2 between the 2nd and the 3rd WH2 domain, which is long enough to reach around the actin nucleus (Ahuja et al., 2007). Once the actin trimer has been assembled a rapid spontaneous

elongation of the filament takes place (Ahuja et al., 2007). In contrast to Spire, COBL is an efficient nucleator reaching the polymerisation rate of an activated Arp2/3 complex even at low nanomolar G-actin concentrations (Ahuja et al., 2007). Interestingly COBL nucleates F-actin at low G-actin concentration, but in contrast at high G-actin concentration it appears to sever filaments (Ahuja et al., 2007). Although COBL binds to the pointed end of the filament, it does not protect it from depolymerisation (Ahuja et al., 2007). In addition to WH2 domains, COBL also has polyproline rich regions (Fig. 1.10) suggesting binding to profilin, however this binding has not been characterized.

In cells COBL has been shown to have very varied functions. First COBL was found being involved in axis patterning in embryonic stem cells (Gasca et al., 1995). Later COBL was shown to be abundant in neural tissues, especially in the brain, and to localise into actin rich structures in growth cones in hippocampal neurons (Ahuja et al., 2007). Further, COBL was shown to be needed for midbrain development and to influence the number of dendritic branches; when COBL was strongly expressed many axonal branches formed, but in contrast when it was expressed only in low levels less branches appeared (Ahuja et al., 2007). Recently it was shown, that syndapin I recruits COBL to the cell cortex in neurons and that both are needed for dendrite formation (Schwintzer et al., 2011). In addition it was shown that functions of COBL were dependent on the Arp2/3 complex in neurons through syndapin I (Schwintzer et al., 2011), which has been reported to control Arp2/3 complex mediated nucleation (Dharmalingam et al., 2009).

1.3.8.5 JMY

The newest member of the actin nucleator family is p53 cofactor junction-mediating and regulatory protein (JMY). JMY is known to bind p300/cAMP response element-binding (CREB) -binding protein (p300/CBP) and together

they activate p53-dependent transcription (Shikama et al., 1999). Interestingly, JMY was found to have tandem WH2 domains, like Spire, as well as an Arp2/3 complex activation domain VCA, like WASP/WAVE family proteins (Roadcap and Bear, 2009; Zuchero et al., 2009) (Fig. 1.7 and 1.10). In cells JMY predominantly localises to the nucleus, but interestingly in human primary neutrophils it localises to the leading edge of cells and contributes to motility (Roadcap and Bear, 2009; Zuchero et al., 2009). In addition a recent study suggests, that JMY is needed in mouse oocyte for asymmetric division and cytokinesis during maturation events (Sun et al., 2011a). Regulation of the F-actin nucleation and the Arp2/3 complex nucleation promoting factor activity of JMY remains currently unknown.

1.3.8.6 Leiomodins

Leiomodins (LMODs) consist of LMOD1, LMOD2, and LMOD3, which all are expressed specifically in muscle cells (Conley et al., 2001). Interestingly the leiomodin domain structure resembles closely the domain structure of tropomodulin. Both tropomodulins and leiomodins share a leucine-rich region, which binds to actin. However, LMOD2 has an additional polyproline rich region, helices, and a WH2 domain in its C-terminus enabling actin nucleation *in vitro* (Fig. 1.7 and 1.10) (Chereau et al., 2008). In cardiomyocytes LMOD2 localises to sarcomeres, where its silencing leads to perturbed sarcomere assembly, but its overexpression leads to abnormal sarcomere structures (Chereau et al., 2008).

1.4 Membrane blebbing

Blebs are balloon-like protrusions of the cell membrane, which appear and disappear on a minute time-scale. Blebs form when the actomyosin cortex of the cell contracts and increases the pressure inside the cell leading to either detachment of membrane from the cortex or cortex rupture (Charras et al., 2005; Cunningham, 1995; Paluch et al., 2005).

1.4.1 Bleb lifecycle

The bleb lifecycle can be divided into three steps: nucleation, expansion, and retraction (Fig. 1.11 and 1.12). In M2 cells expansion lasts ~10-30 s (Charras et al., 2006) during which cytosol flows from the cell body into the bleb. Initially the bleb is devoid of F-actin when examined by fluorescence microscopy (Fig. 1.11). As expansion slows, an actin cortex reforms under the membrane of the bleb (Fig. 1.11). Retraction lasts ~ 2min (Cunningham, 1995).

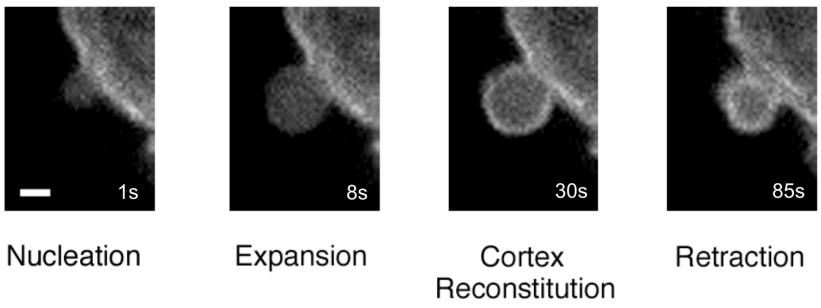

Figure 1.11: The actin cortex in a bleb at different phases of the bleb life cycle.

Blebbing M2 cells were transfected with LifeAct-GFP, a probe for F-actin (Riedl et al., 2008). The bleb life cycle can be subdivided into nucleation, expansion, and retraction phases. During nucleation and expansion (t=0-8s), the bleb is devoid of F-actin. Once expansion slows (t=30s), a cortex reforms and retraction (t=85s) can take place lasting ~2 min. Scale bar 2μm.

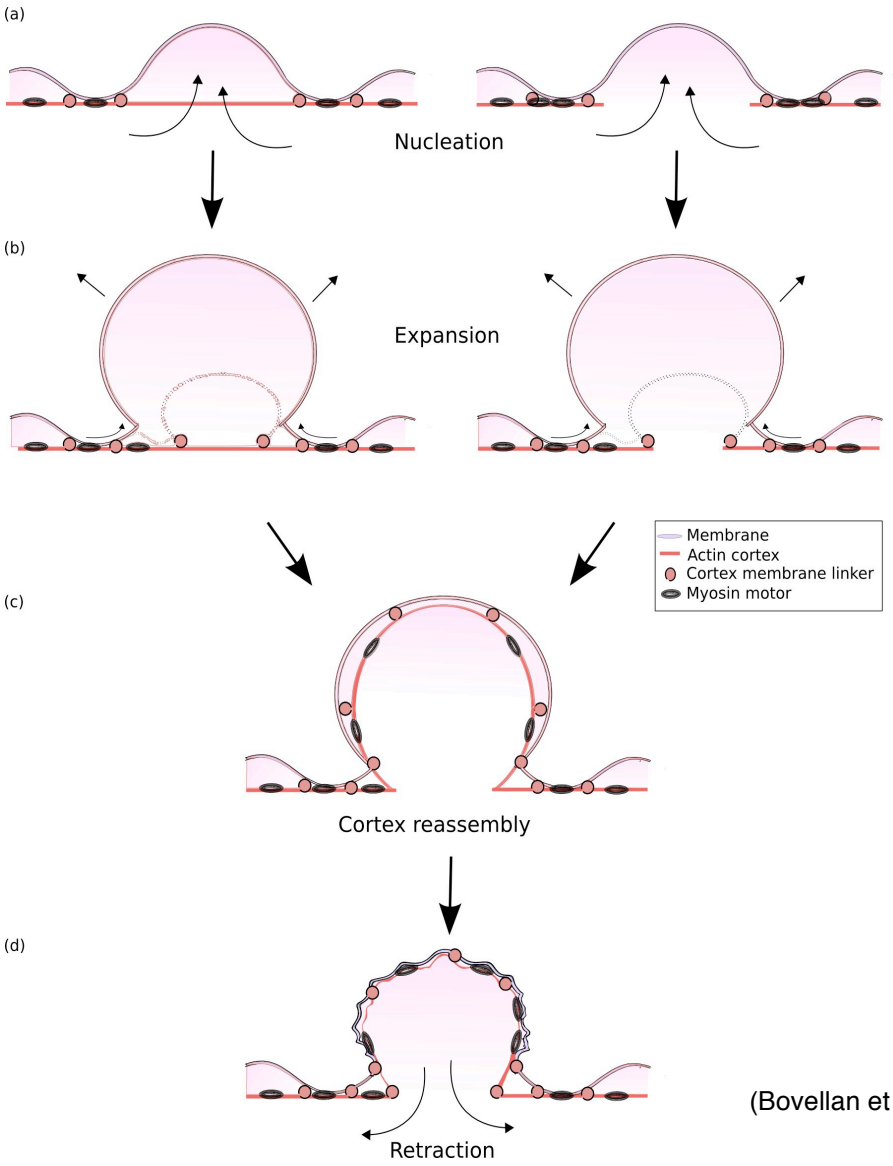

(Bovellan et al., 2010)

Figure 1.12: Schematic diagram of the three phases of blebbing.

(a) High local intracellular pressure (black arrows) tears the membrane from the actin cortex (left) or the actin cortex ruptures and cytosol flows from the cell body (right).

(b) Cytosol pushes the bleb membrane forward and the resulting expansion is accommodated by tearing of the membrane from the actin cortex and by flow of lipids into the bleb membrane through the bleb neck.

(c) When bleb expansion slows down, a new actin cortex reforms.

(d) Recruitment of myosin to the new cortex is followed by bleb retraction, which starts forcing cytosol back into the cell body (black arrows). During this active process, the actin cortex and the membrane crumple.

1.4.1.1 Bleb nucleation

Bleb nucleation is the result of contractions in the actomyosin cortex of the cell (Albrecht-Buehler, 1980). Indeed, inhibition of myosin contractility by treatment with the myosin-II ATPase blocker blebbistatin blocks blebbing (Albrecht-Buehler, 1980; Cheung et al., 2002) and myosin-II null *Dictyostelium* cells are incapable of bleb formation (Langridge and Kay, 2006). Two mechanisms of bleb nucleation have been observed (Fig. 1.12): delamination of the cell membrane from the actin cortex due to a transient increase in intracellular pressure (Charras et al., 2005; Cunningham, 1995) or a rupture of the cellular actin cortex (Paluch et al., 2005). In the first scenario, myosin motor proteins contract at the cortex giving rise to a localised compression of the cytoplasm. As the cytosol cannot flow out of the compressed area, the intracellular pressure increases locally, which can cause the membrane to tear from the actin cortex and nucleate a bleb (Charras et al., 2005; Mitchison et al., 2008). Whether delamination is purely mechanical or facilitated by a biochemical mechanism is unknown. Indeed, the exact location, where a bleb gets nucleated in an area of elevated intracellular pressure could be determined by a locally lower membrane-cortex adhesion. In particular, phosphatidyl-inositol 4,5-bisphosphate (PIP_2) has been proposed to play a role in determining membrane-cortex adhesion, either through regulation of the ERM-protein family of actin-membrane linker proteins or by being chelated by myristoylated alanine-rich C kinase substrate (MARCKS) (Sheetz et al., 2006). Delamination from the actin cortex can be observed in blebbing M2 cells: the actin cortex appears intact during bleb expansion and no fracture of the actin cortex is apparent in fluorescent microscopy images (Charras et al., 2005). In rupture of the actin cortex scenario, myosin contraction leads to fracture of the actin cortex and the cytoplasm flows into the bleb, something that has been observed in L929 cell fragments (Paluch et al., 2005).

1.4.1.2 Bleb expansion

After nucleation, cytosol flows through the bleb neck and pushes the bleb membrane forward (Fig. 1.12). As the bleb expands, its surface area must increase, because lipid membrane cannot be stretched very much (Boal, 2002; Hamill and Martinac, 2001). There are several mechanisms through which surface area increase could proceed. First, if flow of the cytosol is fast enough, tension at the membrane becomes strong enough to break the adhesion between the membrane and the cortex thereby making more surface area available for the bleb to expand. During this process the bleb neck diameter also increases. This has been observed experimentally in M2 cells (Charras et al., 2008). Second, membrane folds can be stored in cells (Hamill and Martinac, 2001). Therefore, bleb surface area increase could simply be the result of unfolding of membrane folds but experimental data suggests, that this alone is insufficient to account for the observed growth of surface area (Charras et al., 2008). Third, if expansion is slow, membrane tension increases only moderately. This causes membrane lipids to flow into the bleb through the bleb neck thereby adding surface area. Lipid flows have been observed in cells during tether extraction (Dai and Sheetz, 1999; Hochmuth and Marcus, 2002), but have yet to be examined during bleb formation. Finally, active membrane trafficking through endo- and exocytosis could regulate the membrane surface area to accommodate changes occurring during bleb expansion (increase in membrane area) or bleb retraction (decrease in membrane area). In support of this, functional endocytic cycle has been shown to be necessary for motility of blebbing *Dictyostelium* cells (Traynor and Kay, 2007). Bleb expansion eventually ceases for one of two reasons: either the local pressure decreases below the threshold needed for expansion and the bleb reaches equilibrium or reassembly of the actin cortex halts the expansion (Tinevez et al., 2009).

1.4.1.3 Actin cortex reconstitution

An actin cortex starts to reform in the bleb once expansion slows down. At the ultrastructural level newly reassembled actin cortex has a cage-like structure (Charras et al., 2006). Reassembly of an actin cortex under the bleb membrane appears to result from the sequential recruitment of membrane-cortex linker proteins, actin, actin bundling proteins, and motor proteins. Indeed, as bleb expansion slows the ERM-protein ezrin is rapidly recruited to the bleb (Charras et al., 2006) to link the forming actin cortex to the membrane (Bretscher et al., 2002). Ezrin is recruited to the membrane independently of actin (Charras et al., 2006). Actin is recruited to blebs after ezrin, followed by recruitment of tropomyosin and the actin crosslinking protein, α-actinin. Finally, myosin is recruited and is concentrated in a few distinct dots along the cortex (Charras et al., 2006).

1.4.1.4 Bleb retraction

The exact mechanism, triggering bleb retraction is unknown. During retraction, the total amount of F-actin and of actin binding proteins do not appear to change significantly, indicating that net actin polymerisation is down-regulated once a continuous rim has been assembled. Myosin II motors drive retraction and were recruited to the bleb during its progress (Charras et al., 2006). During this active process, bleb membrane together with the actin cortex crumples (Fig. 1.12). Once retraction is complete, it is unclear whether the bleb cortex integrates into the cell cortex or whether it is immediately and preferentially depolymerised and replaced by ‘mature’ cortex.

1.4.2 Blebbing in different physiological conditions

Blebs are traditionally mentioned together with apoptosis, but blebbing is observed in a variety of cellular phenomena in 'healthy' cells including cell spreading (Bereiter-Hahn et al., 1990; Pletjushkina et al., 2001), viral infection (Mercer and Helenius, 2008), cell movement (Blaser et al., 2006), and cytokinesis (Boucrot and Kirchhausen, 2007; Burton and Taylor, 1997; Fishkind et al., 1991). In addition blebbing has been observed in embryogenic blastomeres. Of these, blebbing in apoptosis, cytokinesis, motility, and embryonic blastomere blebbing are described more in detail.

Apoptosis

The actual role of blebbing in apoptosis remains unclear. One possibility is that the flows of cytosol inside the cell help to fragment the nucleus and organelles in the apoptotic cell (Mills et al., 1998). Blebbing is not essential for execution of apoptosis as cells can complete apoptosis even when blebbing is inhibited (Nicotera et al., 1999). A more intriguing possibility is that the proteins which once were bound to the membrane of the cell may function as chemoattractants for macrophages to enter the apoptosis site to do the clean up (Segundo et al., 1999).

Cytokinesis

In cells undergoing cytokinesis, blebs tend to form away from the cleavage furrow at the poles of the cell (Boucrot and Kirchhausen, 2007; Burton and Taylor, 1997; Fishkind et al., 1991). Why cells bleb during cytokinesis remains unclear. One possibility is that weakening of the cortex or membrane-cortex attachment (Charras, 2008) plays no obvious role in executing cytokinesis and is just a secondary effect. Another possibility, supported by experimental data, is that blebbing might indeed play an important role in cytokinesis. Indeed correct cortical dynamics at the poles of the dividing cell is essential for executing cytokinesis as it was shown that if the actin cortex is depolymerised due to treatment with the barbed end

capper drug cytochalasin D at the pole region of the dividing cell, the cell is unable to undergo cytokinesis (O'Connell et al., 2001). Blebs might form at the poles of the cell to provide more cortex to cover the growing membrane surface area (Charras, 2008). This newly formed cortex could then flow towards the cleavage furrow (Bray and White, 1988; Wang et al., 1994). Another possibility is that blebbing creates force via polarised blebbing movement to separate the cells from each other (Charras, 2008) or induce sufficient cytoplasmic flow to pull the spindle away from the cleavage furrow as supported by experimental data (Rankin and Wordeman, 2010). Interestingly a recent study showed that during cytokinesis blebs at the poles of the cell stabilize the cell shape by equilibrating the contractile forces of the cortex and thus play as pressure valves (Sedzinski et al., 2011). If the cortex at the poles was perturbed, striking whole cell oscillations were detected leading to cytokinesis failure (Sedzinski et al., 2011).

Motility

Motility by blebbing is important particularly in 3D environments. Various cell types move by polarised blebbing, such as newt blastomeres (Kubota, 1981), Walker carcinosarcoma cells (Fig. 1.12) (Keller, 2000; Sroka et al., 2002), *Dictyostelium* (Langridge and Kay, 2006; Traynor and Kay, 2007; Yoshida et al., 2006), *Fundulus* deep cells (Trinkaus, 1973), *Danio rerio* primordial germ cells (Blaser et al., 2006) as well as neutrophils and tumour cells migrating within 3D-collagen matrices (Friedl et al., 2001; Haston and Shields, 1984; Sahai and Marshall, 2003). Indeed, tumour cells can utilise blebs to squeeze themselves through small empty spaces in extracellular networks (Charras and Paluch, 2008; Fackler and Grosse, 2008) or deform matrices through pushing forces (Charras and Paluch, 2008). In some of the presented cell types, it has been experimentally shown that the cell membrane delaminates from the cortex and expands out from the cell (Blaser et al., 2006; Yoshida et al., 2006), whereas in some tumour cells the delamination of the membrane from the cortex has not been proven yet although the leading edge

morphologically has the appearance of a bleb (Friedl et al., 2001; Haston and Shields, 1984; Sahai and Marshall, 2003).

In motile cells, bleb formation is polarised in comparison to non-motile cells, where blebs form all over the cell surface. When migrating, a new bleb, called a secondary bleb, often forms on top of an existing bleb soon after the cortex has reassembled under the bleb membrane (Fig. 1.13) (Blaser et al., 2006). In motile cells, retraction of the bleb is incomplete or does not occur, but the cell body contracts, and moves in the direction where the bleb was formed. So far motility by blebbing has not been extensively studied and lacks proper characterisation.

Blebbing motility and amoeboid migration have some striking similarities. An actin cortex is attached to the membrane in the amoeba proteus, except where the pseudopodium is growing (Pomorski et al., 2007). The growing pseudopodium alternates periods of growth and cortex reassembly (Pomorski et al., 2007). During growth the membrane is devoid of actin. Tumour cells may utilise amoeboid movement when they no longer express metalloproteinases and move through 3D environments (Friedl et al., 2001; Sahai and Marshall, 2003). The cells squeeze themselves through the network by employing blebs. Once the cortex has regrown under the membrane, a constriction ring forms at the site where the bleb squeezed through. Constriction rings have been observed in neutrophils migrating through collagen gels (Friedl et al., 2001; Haston and Shields, 1984) and in Walker carcinosarcoma cells (Keller and Eggli, 1998).

Embryonic blastomere blebbing

Embryonic blastomere blebbing is morphologically striking, because in these cells only one large bleb is travelling along the cell periphery as a wave and usually circles around the cell many times (Johnson, 1976). This phenomenon is called circus movement. Although these cells seem stationary, it has been proposed that the cells produce circus movements for

net cellular migration needed for morphogenetic rearrangements during embryogenesis (Olson, 1996).

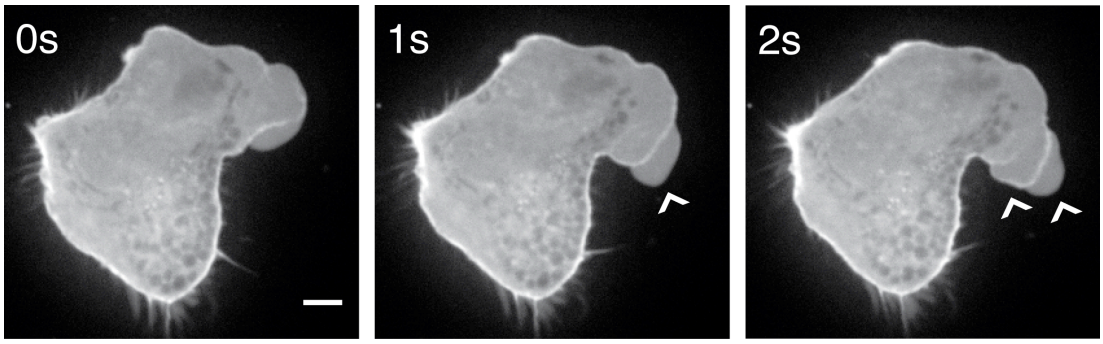

Figure 1.13: Migrating Walker cell forms secondary blebs.

Motile blebbing Walker carcinosarcoma cell stably expressing LifeAct-GFP. The cell has polarised and is migrating by blebbing. Secondary blebs (indicated by arrowheads, t=1-2s) form at the leading edge of the cell. Scale bar 2μm.

1.5 Aims of the thesis

The actin cortex has been shown to be important in many functions of cells. Yet, it has not been characterised carefully. How the cell cortex assembles remains unknown as well as the actin binding proteins needed for maintaining the mechanical integrity of the cortex. All mammalian cells have an actin cortex underlying the plasma membrane. However, in interphase cells, the cortex is very thin and difficult to study by available microscopy methods. In contrast, the cortex is well-defined and visible by fluorecence microscopy during mitosis.

Blebs represent a natural situation in which the membrane is transiently devoid of an actin cortex (Cunningham, 1995) and therefore the formation of a new actin cortex in the bleb can be studied. Blebs also provide a cell fraction enriched in F-actin cortex and are devoid of cell organelles. This makes blebs as an ideal model to study cortex proteomics.

Thus, in this study I use M2 cell blebs and metaphase HeLa cells to study the actin cortex composition and generation. In particular I will investigate how the actin cortex forms and which actin binding proteins associate with the actin cortex. Both of the cell lines used in this study are cancer cell lines of human origin. Cancer cells in general carry multiple mutations and thus are likely to be genetically unstable. To truly assess the generalisation of the results presented in this thesis, the experiments should be verified in primary cells or in other organisms. However, filamin A -deficient M2 cells (Cunningham et al., 1992) provide an advantage to study the reassembly of the actin cortex, because they bleb constitutively for 24-48h after replating and thus cortex reconstitution can be easily followed. Whether or not M2 cells bleb because of filamin A deficiency remains controversial. Both filamin A -deficient M2 cells and clonal cells of M2 that express filamin A at wild type levels bleb after replating, but the latter cell line stops blebbing earlier than the former suggesting filamin A deficiency may play part in blebbing (Cunningham, 1995). However, multiple cell lines with filamin A knockout do not exhibit blebbing (Baldassarre et al., 2009; Feng et al., 2006; Hart et al., 2006). Thus more studies are needed to assess the role of filamin A in membrane blebbing.

In this thesis the two first result chapters concentrate on studying the actin cortex formation. In chapter three, I study the role of actin nucleation independent mechanisms of cortex reassembly and in chapter four I examine in detail the role of actin nucleators in cortex formation. Finally in chapter five I study the composition of the actin cortex and the importance of a few cortex associated proteins for cortical integrity.

2 MATERIALS AND METHODS

2.1 Cell biology techniques

2.1.1 Cell lines used in this study

In my studies I used three cell lines. The majority of the studies were done using blebbing M2 cells, because they have a well-defined actin cortex and blebs can be used as a model to study cortex assembly. The results obtained with M2 cells were verified in prometaphase-metaphase arrested HeLa cells, which also present a well-defined cortex. Finally, I used HL60 actin-GFP neutrophils as a control for treatments that inhibit Arp2/3-mediated actin nucleation and I obtained these from Dr. Wilson, a postdoctoral fellow in the lab.

Blebbing M2 melanoma cells

M2 cells are filamin A-deficient human melanoma cells (Cunningham et al., 1992). They were cultured in MEM with Earle's salts (Sigma), with penicillin /streptomycin, and 10% 80:20 mix of newborn calf serum/fetal calf serum. The cells were split three times a week by aspirating the medium, washing the cells once with phosphate buffered saline (PBS), adding 0.05% trypsin-EDTA (TE) (Gibco) to detach the cells, resuspending the cells with fresh culture medium, and finally centrifuging (1500rpm, 3min, 20°C) the cells to remove traces of TE. Detached pelleted cells were resuspended and re-plated in a new cell culture flask with fresh culture medium and placed into a +37°C incubator with a humidified atmosphere containing 5% CO_2, where cultures were maintained until split again. Previously established M2 cells stably expressing actin-GFP were also used, and were selected with 1µg/ml puromycin (Calbiochem).

Establishing new M2 cell lines

During my studies, I established an M2 cell line stably expressing LifeAct-Ruby and LifeAct-Ruby + Diaph1 shRNA-BFP. LifeAct is a small 17 amino acid peptide, which binds exclusively to F-actin. It was originally extracted

from Abp140 protein in yeast and does not interfere with F-actin dynamics *in vivo* or *in vitro* (Riedl et al., 2008). A stable LifeAct-Ruby M2 cell line was generated to study F-actin dynamics in live cells. Wild type M2 cells were infected overnight at +37°C with MMLV retrovirus carrying LifeAct-Ruby in pLPCX2 vector. To enhance infection efficiency, 8µg/ml polybrene was added together with the viruses. After overnight incubation, the virus solution was discarded and fresh culture medium was added. The cells were grown and selected with 500µg/ml G418 (Calbiochem) for one week, after which sub cloning was performed by plating cells at very low concentration onto a 15cm petri dish with the aim of obtaining colonies derived from single cells. Once colonies were visible by eye, single colonies were isolated with sterilized cloning cones and sterile vacuum grease, and detached with TE. Single colonies were grown in multiwell plates and those with the best phenotypes were amplified and stored in liquid nitrogen. The clone of LifeAct-Ruby M2 cells used in the studies of this thesis had a nice blebby phenotype with mild spikiness.

In addition, an M2 LifeAct-Ruby cell line stably expressing Diaph1 shRNA-BFP was generated by transfection with linearised (by *Ssp*I restriction enzyme, New England Biolabs) Diaph1_08 shRNA-BFP (see 2.1.3 Transfection protocol / shRNA studies). Transfected cells were selected with 500µg/ml G418 (Calbiochem) and 1µg/ml puromycin (Calbiochem) and subcloned as described previously. The clone of LifeAct-Ruby + Diaph1 shRNA-BFP M2 cells used in the studies of this thesis formed very large blebs similar to M2 LifeAct-Ruby cells transiently transfected with Diaph1 shRNA-BFP.

HeLa cells

HeLa cells are cervical cancer cells of human origin (Scherer et al., 1953). Previously established HeLa LifeAct-Ruby cells were cultured in DMEM with Earle's salts (Sigma), with penicillin/streptomycin, and 10% fetal calf serum. Cells were continuously selected with 500µg/ml G418 and were split and

maintained similarly to M2 cells. HeLa cells were arrested in prometaphase by overnight incubation with 100nM Nocodazole (Merck Biosciences) for the localisation studies.

2.1.2 Imaging

All live imaging of M2 and HeLa cells was done in Leibovitz L-15 medium (Invitrogen) supplemented with 10% fetal calf serum. HL60 cells were imaged on fibronectin coated glass coverslips (50µg/ml in PBS, Sigma) in phenol red free RPMI-1640 (PAA) with penicillin/streptomycin, and 10% fetal bovine serum.

Time-lapse microscopy was performed on an inverted confocal microscope (IX81, Olympus) with a spinning disk head (Yokogawa, CSU22). Images were acquired with an Andor iXon camera using 100x or 40x objectives and analysed using Metamorph (Molecular Devices), ImageJ (http://rsbweb.nih.gov/ij/), or Excel (Microsoft) software.

Rhodamine-phalloidin microinjection studies

After 20µg/ml rhodamine-phalloidin (Life technologies) was microinjected into M2 cells, the cells were imaged using 561nm excitation light and collecting emission at 617nm. Pictures were taken every 5s for 60 times with acquisition time of 100ms.

Phalloidin-Qdot microinjection studies

After 1:30 diluted (in microinjection buffer, see 2.1.10) phalloidin-Qdots (Invitrogen, Pierce, Alexis) were microinjected into M2 cells, the cells were imaged using 488nm excitation light and collecting emission at 525nm. Pictures were taken every 300ms for 150 times with acquisition time of 40ms.

p-NN'-phenylenebismaleimide and Alexa-647 labelled dextran microinjection studies

After 0.3mM p-NN'-phenylenebismaleimide (Sigma) together with 0.5µg/ml Alexa-647 labelled dextran (Molecular probes) were microinjected into M2 cells stably expressing LifeAct-Ruby, the cells were imaged using 488nm excitation light and collecting emission at 525nm to study the background fluorescence of pPDM, 561nm excitation light and collecting emission at 617nm to visualise the LifeAct-Ruby, and 640nm excitation light and collecting emission at 685nm to visualise the Alexa-647 labelled dextran. Pictures were taken every 600ms for 150 times with acquisition time of 50-100ms depending on the channel.

Alexa-488 labelled (G- or F-) actin microinjection studies

After 10µM Alexa-488 labelled G-actin or 5µM Alexa-488 labelled stabilised F-actin (both from Dr. Romet-Lemonne) were microinjected into M2 cells, the cells were imaged using 488nm excitation light and collecting emission at 525nm. Pictures were taken every 600ms for 30 times with acquisition time of 50ms (G-actin) or every 600ms for 50 times with acquisition time of 40ms (F-actin).

Localisation and shRNA studies

Fluorescent cells were imaged using 488nm excitation light and collecting emission at 525nm for GFP, 561nm excitation light and collecting emission at 617nm for Ruby, and 405nm excitation light and collecting emission at 447nm for BFP. Pictures were taken every 500ms when imaging single position and every 5s when imaging multiposition. The acquisition time varied from 40ms to 100ms and repeats from 30 to 500 depending on the contruct.

Permeabilisation-fixation localisation studies

Transfected M2 cells stably expressing LifeAct-Ruby were imaged using 488nm excitation light and collecting emission at 525nm for GFP and 561nm excitation light and collecting emission at 617nm for Ruby. Pictures were

taken every 20s for 15 times with acquisition time of 80ms. Multiposition imaging was performed. L-15 FBS imaging solution was replaced with permeabilisation-fixation solution at timepoint 5.

Speckling localisation studies

GFP speckling contruct transfected M2 cells stably expressing LifeAct-Ruby were imaged using 488nm excitation light (with 100% laser power) and collecting emission at 525nm for GFP and 561nm excitation light and collecting emission at 617nm for Ruby. Pictures were taken every 5s for 30 times with the acquisition time of 800ms.

2.1.3 Transfection protocol

Localisation studies

First, M2 cells were detached with TE and plated onto glass coverslips (to 6 well plate) and placed into the incubator for 4h to reattach. Then 100µl of Opti-MEM (Gibco) was mixed with 1µg of cDNA from a miniprep (mix 1). Miniprep cDNA purification was done according to manufacturer's instructions with QIAprep miniprep kit (Qiagen). 3.5µl of Lipofectamine 2000 (Invitrogen) was mixed with 100µl of Opti-MEM (mix 2) by gently tapping the eppendorf tube. Finally, mix 1 and mix 2 were combined by pipetting mix 2 into mix 1, the solution was gently mixed by tapping the tube, and left to incubate at room temperature for 30min. Then the culture medium of M2 cells was discarded and the transfection solution together with 800µl of Opti-MEM was added to the cells. The cells were incubated with the transfection solution in the incubator for 4h. Finally, the transfection solution was replaced with normal culture medium and the cells were imaged the next day.

HeLa cells were detached with TE and plated onto glass coverslips (to 6 well plate). They were also placed in the incubator for 4h to reattach and transfection was carried out similarly to M2 cells except that only 2µl of Lipofectamine 2000 was used for transfection.

shRNA studies

For the gene silencing studies, I used pGIPZ shRNAmir (Open Biosystems) constructs, which contain a fluorophore (GFP or BFP) allowing identification of the transfected cells. Transfection with pGIPZ shRNAmir constructs (see table 2.1) followed the same protocol as for localisation studies with a few differences. First, M2 cells were plated on 6 well plates without glass coverslips. Second, only 0.8µg of DNA (shRNA) from a miniprep together with 2.5µl of Lipofectamine 2000 (Invitrogen) was used for one transfection. Finally, penicillin/streptomycin-free culture medium was used to replace the transfection solution. Culture medium was changed daily to discard dead cells. After 72h transfection, the cells were detached with TE, re-plated onto a glass coverslips, placed into the incubator for 3h to reattach, and finally imaged. The cells needed to be detached and reattach to restart blebbing to obtain a high proportion (>90%) of blebbing cells, as the cells spread and stop blebbing after 24-48h from reattachment.

Construct	Accession	Oligo ID	Sequence: Mature Sense
Non-silencing		RHS4346	
Aip1_03	NM_005112	V2LHS_50263	clone no longer available
Aip1_06	NM_005112	V2LHS_50264	clone no longer available
Aip1_17	NM_005112	V3LHS_393595	AGCAAGGTGGTCACAGTGT
Aip1_19	NM_005112	V3LHS_413548	ACGTTCTTCTGAAAGCTTT
Arp3_1	NM_005721	V2LHS_5786	GAGCTAGTATCTTGGATTA
Arp3_2	NM_005721	V2LHS_198579	CAACCTATCTCAGAAGTTG
Arp3_3	NM_005721	V2LHS_197715	AGTGCAAGAGCTTGTTTAT
CAPZA1_32	NM_006135	V3LHS_355388	TGGAACAAGATACTCAGCT
CAPZA1_89	NM_006135	V3LHS_355389	AGGAGTTTATTAAAATCAT
CAPZA1_91	NM_006135	V3LHS_355391	AGATGTACAGGATTCACTA
CAPZB_13	NM_004930	V2LHS_280836	clone no longer available
CAPZB_14	NM_004930	V2LHS_62217	clone no longer available
CAPZB_31	NM_004930	V3LHS_320774	TGGAGATGGATCAAAGAAG
CAPZB_32	NM_004930	V3LHS_320779	TCGACCTGGTCCCCAGTCT
Cofilin1_16	NM_005507	V2LHS_64316	CTGAGTGAGGACAAGAAGA
Cofilin1_65	NM_005507	V3LHS_342365	AAGGTGTTCAACGACATGA
Cofilin1_69	NM_005507	V3LHS_34236	TGCCTGAGTGAGGACAAGA
Daam1_01	NM_014992	V2LHS_96381	CTACTACTAGATAGAATTA
Daam1_02	NM_014992	V2LHS_229651	CGCTTTCAGACATTAATTA
Daam1_20	NM_014992	V3LHS_339677	TCACTGAACATGACATCCA
Daam1_21	NM_014992	V3LHS_339679	AGAGAGAGACCAATCACAA
Diaph1_08	NM_001079812	V2LHS_43609	CCAATTCTGCTCATAGAAA
Diaph1_10	NM_001079812	V2LHS_43611	GGATTAATTGATCAAATGA
Diaph1_22	NM_001079812	V3LHS_392378	CAGATAGTTCTGCACAAGA
Diaph1_23	NM_001079812	V3LHS_392377	AAGATGTTTCAGATGAACA
Drebrin_28	NM_004395	V3LHS_394371	TGCAGAGGACTTGATGTTC
Drebrin_29	NM_004395	V3LHS_394372	CCGCCTCCTGTGTTCTACA
Drebrin_57	NM_004395	V2LHS_24057	CTGTCCAGGGCTTCAGATA
Fhod1_09	NM_013241	V2LHS_71583	CCTTCAAGCTGGACTATGA
Fhod1_11	NM_013241	V2LHS_71587	CGTGCACCCAGGCTCTCTA
Fhod1_16	NM_013241	V3LHS_313963	AGCGAGAGGAGCATCTACA
Fhod1_18	NM_013241	V3LHS_313962	ACGGTCACCCTCATCAACA
FilaminB_45	NM_001457	V3LHS_351275	TGGTGCAACGAGCACCTCA
FilaminB_47	NM_001457	V3LHS_351274	ACATCATGTGTGACGACGA
FilaminB_85	NM_001457	V2LHS_131785	CTTACATGGTCTCAGTTAA
Fli1_22	NM_002018	V3LHS_386022	ACTGTGGAAGACACACACT
Fli1_24	NM_002018	V3LHS_386024	GCAAGCAGGTTATCAACGA
Fli1_88	NM_002018	V2LHS_113888	GAGCCAACAGTCTGAAGAA
Fmnl1_12	NM_005892	V2LHS_213830	GACGTCCACGTCTGTATTA
Fmnl1_25	NM_005892	V3LHS_309274	AGAACTGGAAAAACAGCTA
Fmnl1_27	NM_005892	V3LHS_309272	AAGCAGACGCTGCTGCACT
Fmnl1_28	NM_005892	V3LHS_309273	AGCAAGGCGACACTCATTG

gelsolin_26	NM_000177	V3LHS_359926	ACGATGCCTTTGTTCTGAA
gelsolin_28	NM_000177	V3LHS_359928	TACATCATTCTGTACAACT
gelsolin_36	NM_000177	V2LHS_82736	ACAGCTACATCATTCTGTA
IQGAP1_05	NM_003870	V3LHS_334310	AGGATGAATTTCCTGAAGA
IQGAP1_07	NM_003870	V3LHS_334306	AGGTTGACTTCACAGAAGA
IQGAP1_09	NM_003870	V2LHS_86781	CTCAATCTCATGGATATCA
Myo1C_31	NM_001080779	V3LHS_338431	AGCGTGCGGACAATAAGCA
Myo1C_33	NM_001080779	V3LHS_338433	TGGCTCGTCGGGAAGATCA
Myo1C_93	NM_004998	V3LHS_326093	AGGAGTAAAGTGTTCATCA
p115RhoGEF_27	NM_004706	V3LHS_317458	ACGAGCTGGAGACAAACTC
p115RhoGEF_30	NM_004706	V3LHS_317457	CCAGATTTTCGACACCTCA
p115RhoGEF_56	NM_004706	V3LHS_317456	CCTATGCTGAGCGAGTTCA
p50RhoGAP_34	NM_004308	V3LHS_310634	CCAAGTCAGATGACTCCAA
p50RhoGAP_35	NM_004308	V3LHS_310635	GGCCTGACCAGCGACAACA
p50RhoGAP_36	NM_004308	V3LHS_401245	AGTGTTCACATTCACACTT
Profilin1_49	NM_005022	V3LHS_366349	CGGTGGTTTGATCAACAAG
Profilin1_50	NM_005022	V3LHS_366350	GGTGGTTTGATCAACAAGA
Profilin1_54	NM_005022	V3LHS_366354	TCAACAAGAAATGTTATGA

Table 2.1: pGIPZ shRNAmir constructs used in this study.

The name of the construct, accession of the targeted gene, manufacturer's oligo ID, and the mature sense sequence of each construct used in the shRNA screens are presented.

2.1.4 Permeabilisation-fixation

Permeabilisation-fixation of transfected cells was performed by replacing L15-FBS with 0.25% glutaraldehyde (Fluka), 0.5% Triton X-100 (Sigma), in cytoskeleton buffer (50mM Imidazole, 50mM KCl, 0.5mM $MgCl_2$, 0.1mM EDTA, 1mM EGTA, pH 6.8) during imaging.

2.1.5 Immunofluorescence sample preparation

For immunofluorescence, cells were fixed with 4% paraformaldehyde (Agar) in PBS at room temperature for 20min. The cells were then washed three times with PBS. Fixed cells were permeabilised for 5min with 0.2% Triton X-100 (Sigma) in PBS and blocked from unspecific antibody binding by incubation with 5% BSA (Sigma) in PBS for 30min at room temperature. Cells

were stained with p34-Arc/ARPC2 (Rabbit) (Millipore) antibody, which was diluted in 1:50 in 1% BSA in PBS. The cells were incubated in a moist, dark chamber with the antibody for 60min at room temperature. Then the cells were washed three times with PBS-BSA and incubated with 1:500 Goat α-rabbit IgG Alexa 488 secondary antibody (Molecular Probes, Invitrogen) and 1:200 tritc-phalloidin (Sigma) in 1% BSA in PBS for 60min at room temperature in a moist, dark chamber. Finally the samples were washed with PBS four times, and mounted with Fluorsave (Calbiochem). For phalloidin stainings, samples were imaged as described previously.

2.1.6 F-actin content analysis by flow cytometry

These samples were prepared together with Dr. Moulding, ICH, UCL. Detached cells from single wells of a 6 well plate were washed in cell culture media, resuspended in 0.5ml PBS alone or with the addition of various combinations of 100µM CK666, 1.25µg/ml CFSE (a cell permeant fixable carboxy-fluorescein cytoplasmic stain (Invitrogen)) or DMSO. After 10min at 37°C, the cells were fixed by addition of 4 volumes of 4% PFA (Agar) and incubated for 20min at room temperature. Then, the cells were washed twice with PBS, the cell cultures were mixed 1:1 (non CFSE and CFSE stained), permeabilised with Perm/Wash (BD Biosciences) and stained with AlexaFluor647-Phalloidin (Invitrogen) as described in (Moulding et al., 2007). This staining protocol allows the concurrent staining with phalloidin of four cell populations that can be distinguished on the basis of the blue fluorescence from the BFP transfection marker (shRNA) and the green fluorescence from CFSE. Concurrent staining removes the variation seen when staining samples separately, allowing for accurate comparison of F-actin content. Dr. Moulding measured the fluorescence on a BD LSRII flow cytometer and analysed the results with Summit software (Dako).

2.1.7 Scanning electron microscopy of actin cytoskeleton

Sample preparation for scanning electron microscopy was optimised and performed together with my supervisor Dr. Charras. The general protocol for sample preparation for scanning electron microscopy is described in (Svitkina and Borisy, 1998), which we followed with minor modifications. Two hours prior to treatment, whole cells were plated onto 13mm glass coverslips. For isolated blebs, preparation took place immediately after attachment to glass coverslips. The coverslips were washed three times with intracellular buffer (for isolated blebs) or L15 without serum (for cells) and transferred to cytoskeleton buffer (50mM Imidazole, 50mM KCl, 0.5mM $MgCl_2$, 0.1mM EDTA, 1mM EGTA, pH 6.8) containing 0.5% Triton-X (Sigma) and 0.25% glutaraldehyde (Fluka) for 5 min. This was followed by a second extraction with 2% Triton-X and 1% CHAPS in cytoskeleton buffer for 5min before washing the coverslips in cytoskeleton buffer three times. The remainder of the protocol was identical to (Svitkina and Borisy, 1998). Briefly, the cells were then dehydrated with serial ethanol dilutions, dried in a critical point dryer, coated with 5-6 nm platinum-palladium and imaged in the department of Cell and Developmental Biology, UCL using the in-lens detector of a JEOL7401 Field Emission Scanning Electron Microscope (JEOL, Tokyo, Japan).

2.1.8 Drug treatments

Cytochalasin D (Calbiochem), a small molecule that promotes actin depolymerisation by capping the fast growing end of actin filaments (Flanagan and Lin, 1980) was used at various concentrations throughout the studies (see chapters 3-5 for details) either to weaken or depolymerise the actin cortex. Latrunculin B (Merck Biosciences), an actin sequestering drug (Coue et al., 1987), was used at a concentration of 750nM to study the actin dynamics of separated blebs. CK666 (Tocris), a small molecule inhibitor against the Arp2/3 complex (Nolen et al., 2009), was used to study the role of

the Arp2/3 complex in the cortex. The protocol utilised for imaging was the following: cells were first imaged for 24 time points at 10s intervals to provide baseline behaviour for comparison, then 100µM CK666 was added and incubated for 3min at room temperature. During this time, the microscope was refocused choosing a plane that cut through the centre of the nucleus. This was necessary because CK666 caused rounding of the cells. After 3min incubation, the cells were imaged for an additional 35 time points.

For all drugs, an amount of DMSO corresponding to the volume the drug was diluted in was used as a vehicle control.

2.1.9 Quantum Dot – phalloidin generation

First 2nmol of Qdot ITK amino- (PEG) quantum dots in 50mM borate buffer pH 8.3 (Invitrogen) were washed by ultrafiltration (100kDa) with 1xPBS pH 7.4. Then the Qdots were transferred into a glass vial, 8µM of crosslinker *Bis*[sulfosuccinimidyl] suberate (BS3) (Pierce) was added, and the Qdot – BS3 solution was incubated 30min at room temperature, gently shaking the tube every 5min. Meanwhile a NAP-5 column (Amersham) was equilibrated with PBS pH 7.4 according to the manufacturer's instructions. Altogether, five complete buffer exchanges were made. After incubation, the Qdots were purified from excess crosslinker by eluting with PBS pH7.4 on the equilibrated NAP-5 column. The coloured eluent was collected into a glass vial containing 80nmol of amino-phalloidin (Alexis). Crosslinker bound Qdots and amino-phalloidin were mixed gently and incubated 2h at room temperature. After the incubation, the Qdot-amino-phalloidin solution was quenched for 15min by adding glycine to final concentration of 50mM. Finally the conjugate was purified from excess phalloidin by ultrafiltration (100kDa) into 50mM borate buffer according to the manufacturer's instructions. The Qdot-phalloidin solution was then filtered with a 0.22µm spin filter (Agilent technologies) and stored at +4ºC.

2.1.10 Microinjections

Microinjections were performed in five separate sets of experiments during this study i) rhodamine-phalloidin microinjections, ii) phalloidin-Qdot microinjections, iii) p-NN'-phenylenebismaleimide and Alexa-647 labelled dextran, iiii) Alexa-488 labelled G-actin microinjections, and iiiii) Alexa-488 labelled stabilised F-actin microinjections.

General protocol for all the microinjections is as follows. The day prior to microinjection, M2 cells were plated onto glass bottom petri dishes (Intracell). For microinjection, borosilicate glass capillaries were pulled using a Sutter P-97 pipette puller (Sutter) to obtain pipettes with a sharp tip of ~0.5µm diameter. Compounds (Table 2.2) were diluted to their final concentrations in microinjection buffer (50mM K-glutamate, 0.5mM $MgCl_2$, pH 7.0) and centrifuged at top speed in a tabletop centrifuge to remove aggregates. Cells were microinjected with a Narishige IM300 microinjector (Narishige) using 0.5psi backpressure. For microinjection, the pipet is brought down to the same focus plane as the cells and placed close to a cell away from the nucleus and the cell edge, but pointing to a thick part of the cytoplasm. To inject, the pipet is brought into contact with the cell, an instant swelling of the cell is observed, and finally the pipet is quickly moved vertically out from the cell. Microinjections were done using a 40x objective. After microinjection, the cells were left to recover for at least 10min. Live cells that had been properly microinjected were identified based on their fluorescence. Timelapse videos of the cells were acquired using a 100× objective.

2.2 Bleb isolation

The bleb isolation protocol was optimised and performed together with my supervisor Dr. Charras. For bleb isolation, cells grown to confluence in T75 tissue culture flasks were exposed to 2ml of medium containing 750nM of the actin depolymerising drug Latrunculin B. Latrunculin-induced blebs were then

shorn off the cell surface by agitation at top speed on a rotary shaker for 15min, the supernatant was collected, and pelleted at 13,000rpm for 5min in a microcentrifuge. The supernatant was removed and blebs were resuspended in 100µl of L15 media. The supernatant was then layered onto a density gradient with steps containing 5%, 12.5%, and 16% Ficoll in L15-FBS. The tubes were then centrifuged at 100,000rpm in an ultracentrifuge for 40min to separate blebs from detached whole cells. After centrifugation, separated blebs concentrated at the 5% - 12.5% interface, while whole cells were pelleted at the bottom of the tube. The collected fraction was then homogenised, blebs were pelleted by centrifugation at maximum speed in a microcentrifuge, and given several washes in L15. Separated blebs were then resuspended in a low calcium (500nM) intracellular buffer (5mM NaCl, 140mM K-Glutamate, 7mM $MgCl_2$, 6.7mM $CaCl_2$, 10.2mM K-EGTA, 20mM K-Hepes, 10mg/ml BSA, pH 7.2) containing an exogenous ATP regeneration system based on creatine kinase hydrolysis of creatine phosphate (Energy mix: 1mM ATP, 1mM UTP, 1mM $MgCl_2$, 10mM creatine phosphate, 1mg/ml creatine phosphokinase). To allow for penetration of ATP into the separated blebs, separated bleb membranes were permeabilised by addition of 50µg/ml Hemolysin A and incubated at room temperature for 30min. For imaging, separated blebs were attached to glass coverslips coated with poly-L-lysine.

To identify proteins present in the detergent insoluable pellet fraction, Dr. Romeo and Dr. Roux at IRIC, Montreal, Canada lysed the purified blebs in RIPA buffer (20mM Tris pH 8, 137mM NaCl, 1% NP-40, 0.1% SDS, 0.5% sodium deoxycholate, 1mM sodium orthovanadate [Na_3VO_4], 1mM phenylmethylsulfonyl fluoride, 5mg/ml of leupeptin, 10mg/ml of pepstatin). After centrifugation (100000rpm, 1h), pellets were resuspended in 2× reducing sample buffer (5× is 60mM Tris-HCl [pH 6.8], 25% glycerol, 2% SDS, 14.4mM 2-mercaptoethanol, and 0.1% bromophenol blue). Following SDS-PAGE, coomassie-stained gel regions were excised and subjected to in-gel trypsin digestion, and finally subjected to mass spectrometry.

2.3 Actin biochemistry

Actin was purified from rabbit muscle (Spudich and Watt, 1971) and labeled with Alexa-488 succinimidyl ester (Molecular Probes, Invitrogen) by Dr. Romet-Lemonne and Dr. Jégou at CNRS, Gif-sur-Yvette, France. The labelled fraction of actin was 49% in my experiments. To polymerise actin filaments, 5µM labelled G-actin was incubated in F-buffer (20mM Tris pH 7.5, 0.2mM DTT, 0.2mM $CaCl_2$, 20mM $MgCl_2$, 10mM ATP, 1M KCl) for 30min at room temperature. A final concentration of 1mM p-NN'-phenylenebis-maleimide (pPDM) (Sigma) was added to actin to form covalent crosslinks between the actin monomers in the filament (Knight and Offer, 1978). Stabilisation by pPDM was allowed to take place for 30min at room temperature. Finally the sample was sonicated thoroughly and stored at 4°C until microinjections were performed. To verify the size of covalently crosslinked filament protomers a 10% SDS-PAGE was run. The 10% SDS-PAGE was done (recipe table 2.3) using Mini Trans-Blot Cell system (Bio-Rad). The sample was loaded into a well formed by a comb. Finally a protein standard marker (ColourPlus prestained protein marker, New England Biolabs) was added. The gel was run in SDS-PAGE running buffer (24mM Tris, 192mM Glycine, 1% SDS). The upper gel was run at 100V and lower gel at 150V until the loading dye had fully travelled through the gel.

10% polyacrylamide lower gel	**5 ml**	**3.75% polyacrylamide upper gel**	**2.5 ml**
30% acrylamide	1.65ml	30 % acrylamide	312.5µl
3M Tris HCl pH 8.8	620µl	3M Tris HCl pH 7.0	104µl
H_2O	2.65ml	H_2O	2.045ml
10% SDS	50µl	10% SDS	25µl
10% ammonium persulfate	25µl	10% ammonium persulfate	25µl
Temed	2.5µl	Temed	2.5µl

Table 2.2: Recipe for 10% SDS-PAGE.

First, the 10% polyacrylamide lower gel is poured between the cleaned glasses and left at room temperature to solidify. Then the packing gel (i.e. the 3.75% upper polyacrylamide gel) is poured on top of the solid lower gel. Finally a comb is placed between the glasses to make wells to the gel.

2.4 Molecular biology methods

2.4.1 Total RNA extraction

Total RNA was extracted from M2 cells by using RNAeasy minikit (Qiagen) following the manufacturer's instructions. RNA was eluted to 30µl of nuclease free water and kept on ice while not used. Total RNA from shRNA transfected cells was sent to Dr. Romeo and Dr. Roux on dry ice for real-time quantitative PCR analysis.

2.4.2 Reverse transcriptase reaction

Total RNA was translated into cDNA by using the SuperScript II system (Invitrogen). The reaction contained 0.5µg of oligo $(dT)_{12-18}$ (Invitrogen), 8µl total extracted RNA (concentration unknown), 0.5mM of dNTP mix (Invitrogen), and RNase free water. The mixture was placed at +65°C for 5min, then on ice to cool down and finally spun down in microcentrifuge. Then, 1x first strand buffer (50mM Tris-HCl, pH 8.3, 75mM KCl, 3mM $MgCl_2$, Invitrogen) was added together with 10mM DTT (Invitrogen), the mixture was mixed by tapping the tube gently, and placed at +42°C, for 2min. Finally, 200U of SuperScript II enzyme was added, the solution was mixed by pipetting up and down and incubated at +42°C, for 50min. All incubations were done in an Eppendorf Mastercycler PCR machine.

2.4.3 PCR

I carried out the cloning of constructs described here. Other constructs used during my studies were available already in the laboratory, were received as gifts from other research groups, or cloned by other members of the laboratory.

A DNA fragment corresponding to the full-length protein of interest cDNA was amplified from I.M.A.G.E. full-length cDNA clones purchased from Source Bioscience or from a M2 cDNA library. The cDNA clones used are presented in table 2.4. For cloning Diaph1 domains, a vector containing full-length Diaph1 was used as a template. Standard polymerase chain reaction (PCR) reaction mixture contained 70ng of miniprep DNA or 2µl of reaction mixture from reverse transcription, 1xThermopol buffer (20mM Tris-HCl, 10mM $(NH_4)_2SO_4$, 10mM KCl, 2mM $MgSO_4$, 0.1% Triton X-100 pH 8.8, New England Biolabs), 0.5µM of both end primers (table 2.5), 1mM of dNTP mix (Invitrogen), and 2U of Vent DNA polymerase (New England Biolabs). The standard PCR amplification program used was: 1min 30s pre-denaturing at

+95°C, 40 cycles of [30s +95°C (denaturation), 45s annealing at ~3°C below the lowest melting temperature of the primer pair, 1min/kb elongation +72°C] and finally extension at +72°C for 15min and cool down at +4°C.

Gene	Gene ID	I.M.A.G.E. ID	Restriction sites		Other template
Diaph1	23002	40125808	*XhoI*	*KpnI*	
Diaph1 GBD			*XhoI*	*KpnI*	Diaph1-GFP template
Diaph1 GBD+FH3			*XhoI*	*KpnI*	Diaph1-GFP template
Diaph1 FH1+FH2			*XhoI*	*KpnI*	Diaph1-GFP template
Diaph1 DAD			*XhoI*	*KpnI*	Diaph1-GFP template
CA-Diaph1			*XhoI*	*KpnI*	Diaph1-GFP template
Diaph3	81624	4830888	*EcoRI*	*ApaI*	
Fmnl1	752	4343469	*HindIII*	*BamHI*	
INF1	229474	8860651	*SalI*	*KpnI*	
INF2	64423	4053416	*HindIII*	*BamHI*	
Aip1	9948		*HindIII*	*BamHI*	M2 cell cDNA

Table 2.3: Genes cloned into GFP vector in this study.

The gene name and Gene ID of the genes cloned in this study are presented. If I.M.A.G.E clones were used then the I.M.A.G.E ID is provided. Restriction sites created for given gene are presented. If I.M.A.G.E clones (Source Bioscience) were not used, other templates are provided.

Phusion high fidelity DNA polymerase was also used. The standard PCR reaction mixture contained 70ng of miniprep DNA, 1x GC buffer for Phusion containing 7.5 mM $MgCl_2$ (Finnzymes), 0.5µM of both end primers (table 2.5), 1mM of dNTP mix (Invitrogen), and 1U of Phusion DNA polymerase (Finnzymes). The standard PCR amplification program used was: 3min pre-denaturing at +98°C, 40 cycles of [40s +98°C (denaturation), 45s annealing at ~3°C below the lowest melting temperature of the primer pair, 30s/kb +72°C] and finally extension at +72°C for 10min and cool down at +4°C.

In all cases, an Eppendorf Mastercycler PCR machine was used for PCR cycles and reaction products were analyzed by agarose gel electrophoresis (described later). DNA was purified from the gel by using a QIAquick Gel extraction Kit (Qiagen) according to the manufacturer's instructions, and finally eluted into 30µl of milli Q-water or 10µl of milli Q-water if using MinElute column (Qiagen).

Name	Description	Sequence	Pol
MB1101	Diaph1 *XhoI* 5 C1N1	GCCTCGAGGAGTGAACCGGGACATGGAGCC	P
MB1102	Diaph1 *KpnI* 3 C1N1	GGGGTACCCCGCTTGCACGGCCAACCAACTC	P
MB1103	GTP Diaph1 *KpnI* 3 C1N1	GCGGTACCCCTAGAATACAAAGAGCAGAAAG	P
MB1104	GTPFH3 Diaph1 *KpnI* 3 C1N1	GCGGTACCCCCTTTGTCTTATCAATCATTTG	P
MB1105	FH1FH2 Diaph1 *XhoI* 5 C1	GCCTCGAGGAGTCTGGGGATGCTACCATCCC	P
MB1106	FH1FH2 Diaph1 *KpnI* 3 C1	GCGGTACCCTCCTTGACTGCTTGCAAAAA	P
MB1107	DAD Diaph1 *XhoI* 5 C1	GCCTCGAGCGGGCGATGAGACAGGTGTGATG	P
MB1108	DAD Diaph1 *KpnI* 3 C1	GCGGTACCCCGTCGGAATGCTGCCCCTGA	P
MB1034	Diaph3 *EcoRI* 5 C2	GCGAATTCATGAGTGAGGAGAGGAGCCTTTC	V
MB1035	Diaph3 *ApaI* 3 C2	GCGGGCCCTAAATACGGTTTATTACCATGG	V
MB1039	FMNL1 *HindIII* 5 C3	GGAAGCTTATGCCACTCTTGAACTGGGTG	V
MB1040	FMNL1 *BamHI* 3 C3	GCGGATCCCTACAGCGAGACTTCGGAGG	V
MB1007	INF1 5' *NheI* N1	GCGCTAGCTGTATGCATGTTATGAATTGT	V
MB1008	INF1 3' *AgeI* N1	GCACCGGTGCCTTCCGTAAGGGATTGAGGA	V
MB1041	INF2 *HindIII* 5 C3	GCAAGCTTATGTCGGTGAAGGAGGGCGC	V
MB1042	INF2 *BamHI* 3 C3	GGGGATCCCCGCAGGCGAGCCAGGACGTC	V
MB0903	Aip1 *HindIII* C2 5'	GCAAGCTTATGCCGTACGAGATCAAGAA	V
MB0904	Aip1 *BamHI* C2 3'	GCGGATCCCCTCAGTAGGTGATTGTCCA	V

Table 2.4: Primers used in this study.

First the name of the primer used is presented. Then the gene and specific restriction site of the primer, and whether the primer is a sense or antisense primer (5´or 3´) are presented in the description column. The 5' to 3' sequence of the primer is presented in the sequence column and finally the DNA polymerase used in PCR is described in Pol column (P=Phusion, V=Vent).

2.4.4 Digestion

The purified PCR product and pEGFP-C or pEGFP-N vectors were digested with the appropriate restriction enzymes (table 2.4). All the restriction enzymes used were purchased from New England Biolabs. The digestion reaction mixture contained the appropriate 1x NEB buffer (New England Biolabs), 1x BSA, PCR product / vector (separately), and 40U of each restriction enzyme. Reactions were incubated at +37°C for 4h. DNA-loading buffer (GelPilot loading dye, Qiagen) was added to the samples, which were loaded onto a 0.5-1.5% agarose gel for electrophoresis. Digested DNA samples were cut with a clean, sharp scalpel from the gel under UV-light. If

multiple DNA bands were detected, a band corresponding to the size of the PCR product of interest was excised from the gel. The PCR product was purified with the MinElute Gel Extraction Kit (Qiagen) and the vector with QIAquick Gel Extraction Kit (Qiagen). Both were eluted into milli-Q water.

For experiments where shRNA silencing was to be used in cell lines stably expressing GFP tagged constructs, I replaced the GFP in the pGIPZ shRNAmir constructs with a BFP by using *Sna*BI and *Bsr*GI sites. BFP was obtained from a previously established pGIPZ Arp3 shRNAmir BFP construct (a kind gift of Dr. Moulding).

2.4.5 Agarose gel electrophoresis

Agarose gels were made by adding agarose (1% = 1g/100ml) (Sigma) to TBE buffer (0.1M Tris, 0.1M boric acid, 2.5mM EDTA), boiling until the agarose was fully dissolved into the buffer, cooling them down to +37°C, and pouring them into the gel tray. Finally a few microliters of ethidium bromide was added into the liquid gel, the gel was mixed, a comb was placed to form wells, and the gel was left to solidify at room temperature for ~30min. After the gel had solidified, it was placed into Mini Sub cell GT electrophoresis device (Bio-Rad) with TBE buffer and finally the comb was removed. Then samples with 1x agarose gel loading dye (GelPilot loading dye, Qiagen) were loaded onto the gel together with a standard marker (1kb DNA ladder or 100bp DNA ladder, New England Biolabs) to determine the size of the products run into the gel. The gel was run for 60-80min, at 69V, at room temperature with a Mini Sub Cell GT power supply from Bio-Rad. Finally the gel was photographed under UV light in GenoPlex Chemi (VWR) cabinet to determine the sizes of the products.

2.4.6 Ligation

The concentrations of the digested insert DNA and vector were determined from the agarose gel picture by comparing the band intensities with one another. For the ligation reaction, approximately three times higher molar concentration of insert-DNA was used compared to vector-DNA. A control reaction was made without insert-DNA. The ligation reaction mixture contained: the vector and insert in correct concentrations, T4 DNA ligase buffer (50mM Tris-HCl, 10mM $MgCl_2$, 1mM ATP, 10mM dithiothreitol pH 7.5, New England Biolabs), and 40U T4 DNA ligase (New England Biolabs). The reactions were incubated at +4°C overnight.

2.4.7 Transformation and plasmid selection

Ligation products were introduced by chemical transformation into chemically competent *Escherichia coli* DH5α bacterial cells. For transformation 10µl of ligation reaction after overnight incubation at +4°C or 100ng of miniprep DNA was added to 50µl of bacteria, which were thawed slowly on ice. The ligation reaction or DNA was incubated with the bacteria for 25min on ice, then a heat shock in a +42°C water bath was performed (35s), after which the bacteria were placed on ice for 2min. Then 500µl of room temperature Luria-Bertani (LB) medium was added to the bacteria, which were then incubated with vigorous shaking at +37°C for 1h. Then, the bacteria were centrifuged at room temperature for 5min at 4500rpm. After centrifugation, the bacteria were resuspended in 100µl and plated on LB-agar plates (25g/l of bactoagar in LB medium) containing 50mg/l of kanamycin or 100mg/l of ampicillin. The bacteria were evenly distributed throughout the plate with the help of sterile glass beads. When amplifying plasmid no centrifugation was carried out, but 100µl of culture was plated on an LB-agar plate containing the appropriate antibiotic.

After incubation at +37°C overnight, the number of colonies was estimated. The amount of colonies was compared to the amount of colonies on control plates to determine if the cloning had succeeded. If the cloning plate contained more colonies than the control plate, a few (6-10) isolated colonies were selected from the cloning plate and inoculated into a tube containing 4ml of LB-medium and 50µg/ml of kanamycin or 100µg/ml of ampicillin. When plasmids were amplified the plates contained hundreds of colonies and a streak of bacteria was transferred into culture. The bacteria were cultured with vigorous shaking at +37°C overnight. The next morning the cells were collected by centrifugation (5min, 4500rpm, room temperature, microcentrifuge). The plasmid DNA was isolated using a QIAprep Miniprep Kit (Qiagen) and eluted in 40µl of milli-Q water.

To study if the plasmid DNA contained the insert, 5µl of the plasmid DNA was used for test digestions using the same enzymes as previously were used. The digested plasmids were then analyzed by agarose gel electrophoresis. One of the positive clones that contained an insert with the correct size was sequenced in the DNA sequencing laboratory at the Gene Service, UCL to verify that the sequence was correct.

2.5 Image processing, analysis, and statistics

In this chapter I present all the quantification, analysis, statistics, and database searches carried out in this thesis.

2.5.1 shRNA screen analysis

To quantify the results from the shRNA screen, I categorised cells transfected with targeting or non-silencing shRNA constructs as having normal, large, or small blebs. Transfected cells were identified on the basis of their expression of a fluorescent protein present on the pGIPZ vector. The effect of targeting shRNAs on cellular phenotype was assessed by

comparing the experimentally observed number of cells in each category to that expected for control cells using Chi-square tests. Results were deemed significant for $p<0.01$.

2.5.2 Quantification of protein accumulation upon bleb retraction in M2 cells

To quantify protein accumulation during bleb retraction, I measured the intensity of actin, CA-Diaph1, CAAX, and Diaph1 GBD+FH3 at the bleb apex at the beginning and at the end of retraction. Background fluorescence was subtracted and the data was normalised to the intensity at the onset of retraction. At least 11 blebs were analysed per construct. The average intensity and standard deviation from each series was calculated. For statistical analysis, t-tests were performed and results were deemed significant for $p<0.01$.

2.5.3 Quantification of bleb area to cell body area ratio in M2 cells

To quantify the Diaph1 shRNA phenotype, I measured the cell body area, which appeared smaller than in control cells, and bleb area, which appeared larger than in control cells. First, using Metamorph software (Molecular Devices), I created a time projection of 3min long movies of cells expressing either non-silencing shRNA (n= 66 cells) or Diaph1 shRNA (n= 97 cells). Then, I manually segmented the cell body by drawing a line along the cortex. By thresholding the image based on fluorescence intensity, I was able to separate the cell from its background and, using the manual segmentation of the cell body, I was able to segment the cell into cell body (area inwards from the cortex) and blebs (area outward from the cortex). The number of pixels in each area was determined and a ratio of bleb area to cell body area was calculated. From each category, the average ratio and standard deviation were calculated and t-tests performed to assess statistical significance. Results were deemed significant for $p<0.01$.

2.5.4 Quantification of cortical actin fluorescence in M2 cells

To assess loss of cortical actin induced by CK666 treatment or DMSO, I measured the average intensity of the cortex and the cytoplasm pre- and post-treatment. The intensity of the cytoplasm was measured in three different sites of the cell body excluding the nucleus and the cortical fluorescence on an area right underneath the cell membrane. The average ratio and standard deviation were calculated prior to and after treatment and t-tests were performed to assess statistical significance.

2.5.5 Localisation of actin cortex regrowth in blebs

M2 LifeAct-Ruby cells were imaged for 4min at 200ms intervals and fluorescence intensity was measured along the periphery of blebs after the end of expansion. To do this, I drew a region along the fully expanded bleb perimeter in Metamorph and the fluorescence intensity was monitored until a fully formed cortex was observed (this took on average 40s). Kymographs of the intensity changes were created and these were displayed in pseudocolours to aid determination of sites of cortex regrowth. In the pseudocolour images, cold colours represented low intensities and warm colours high intensities. Altogether 20 blebs were analysed, and one kymograph is presented later in this thesis.

Kymographs of quantum dot-phalloidin microinjected cells were generated similarly to M2 LifeAct-Ruby cells. Altogether 10 blebs were analysed, and one kymograph is presented later in this thesis.

2.5.6 Protein abundance index

In the mass spectrometry studies we calculated the protein abundance index (PAI) to adjust for differences between proteins in the number of observable peptides because enzymatic digestion of a large protein results in a high

number of peptides and digestion of a small protein results in a low number of peptides (Rappsilber et al., 2002). PAI was calculated by dividing the number of observed peptides by the protein molecular weight (kDa).

2.5.7 The appearance of Daam1 and Fhod1 compared to actin

M2 LifeAct-Ruby cells transfected with Daam1-GFP or Fhod1-GFP were imaged for 4min at 500ms intervals. Using Metamorph software (Molecular Devices), the fluorescence intensity was first followed in the Ruby channel to determine in which frame a visible F-actin rim appeared in the bleb. This frame was set as time zero. Then, the GFP channel was followed to determine when Daam1 or Fhod1 appeared in the bleb.

2.5.8 Localisation of filamin B, drebrin, and IQGAP1 in blebs

M2 cells transfected with filamin B-GFP were imaged for 4min at 400ms intervals and fluorescence intensity was measured along a line drawn through the diameter of a growing bleb using Metamorph software (Molecular Devices). Kymographs of the intensity changes were created to follow the recruitment of filamin B to the bleb membrane.

M2 LifeAct-Ruby cells transfected with drebrin-GFP, IQGAP1-GFP, or CA-Diaph1-GFP were imaged for 2min 30s at 1s intervals and fluorescence intensity was measured along a line drawn through the diameter of a growing bleb using Metamorph software (Molecular Devices). Two-colour kymographs of the intensity changes were created to follow the recruitment of LifeAct-Ruby and drebrin-GFP, IQGAP1-GFP, or CA-Diaph1-GFP to the bleb membrane.

2.5.9 String database searches

String database (Szklarczyk et al., 2011) searches were effected at http://string-db.org/ to study known and predicted protein interactions. Results are presented according to confidence and were obtained with the following prediction methods: neighbourhood, gene fusion, co-occurrence, co-expression, experiments, databases, and textmining with medium confidence (0.400), and with no more than 10 interactors shown.

3 ACTIVE ACTIN NUCLEATION IS NEEDED FOR CORTEX REGROWTH

3.1 Introduction

Bleb membranes are devoid of filamentous actin during nucleation and expansion, but when expansion slows an actin cortex reassembles (Charras et al., 2006; Cunningham, 1995) and therefore blebs are an ideal model to study actin cortex reassembly. How the actin cortex reassembles in blebs and cells remains unknown.

I propose four possible models for actin cortex regrowth in blebs. First, elongation of the cell cortex at the base of the bleb could eventually reassemble a cortex under the bleb membrane and no specific signaling would be needed (Fig. 3.1A). In dividing cells, the half time of the actin cortex turn over is 45±11s (Murthy and Wadsworth, 2005) and in interphase M2 cells 14.1±1s (see Fig. 4.9). Both are comparable to the time-scale for bleb expansion (10-30s) and therefore invasion of the cell cortex from the sides of the bleb could occur.

Second, small actin seeds from the existing cell cortex, undetectable by light microscopy, could persist under the bleb membrane, elongate, and reform the cortex (Fig. 3.1B).

Third, actin seeds could flow with the cytosol into the bleb during expansion and bind to actin-membranelinker proteins, which are necessary to keep actin at the membrane. It was shown that ERM-proteins are recruited to the bleb membrane before actin to link the forming cortex to the membrane (Charras et al., 2006). Therefore small actin seeds could become captured by ERM-proteins and lead to cortex reassembly by rapid actin filament elongation (Fig. 3.1C).

Fourth, an unknown actin nucleator or various nucleators could polymerise filaments *de novo* under the bleb membrane (Fig. 3.1D). Interestingly many studies have linked various formins to cortex maintenance (Eisenmann et al.,

2007; Han et al., 2009; Hannemann et al., 2008; Kitzing et al., 2007; Stastna et al., 2011).

The aim of this chapter is to study which mechanisms of actin cortex regrowth are needed for cortex assembly in membrane blebs. The models do not necessarily exclude one another as for example actin nucleators could assist in cortex elongation even if invasion, bound filaments, or flow of actin seed mechanisms participate in cortex reassembly. First the invasion model is investigated followed by the bound filaments model and the flow of actin seeds model. Aspects of the nucleation model are discussed in the next chapter of this thesis.

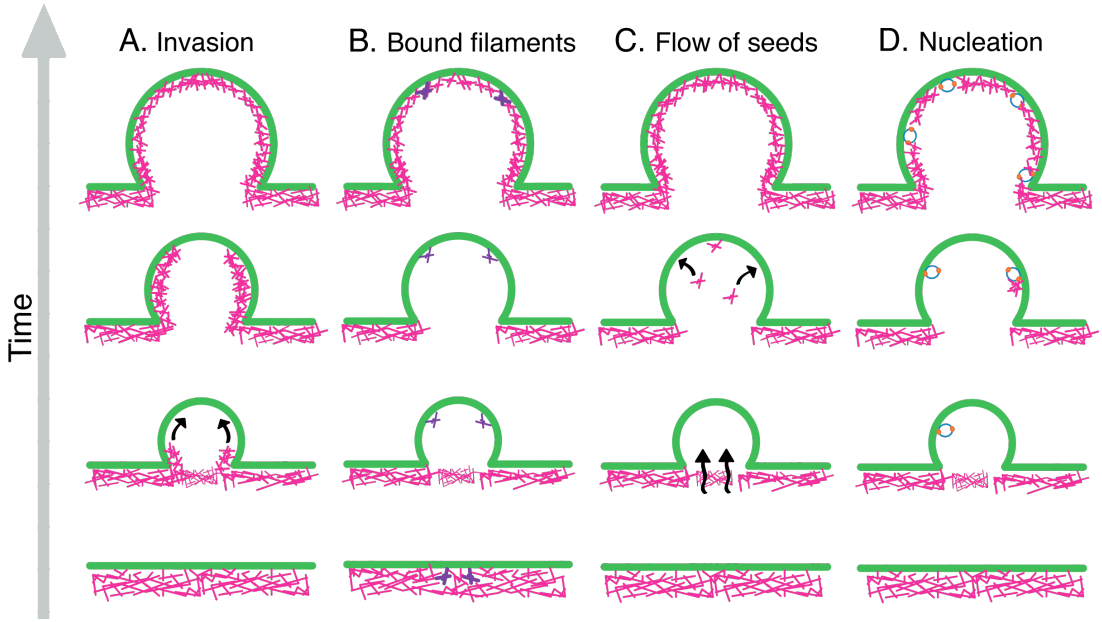

Figure 3.1: Schematic models of how the actin cortex could reassemble in blebs.

A. The elongation of the existing cell cortex could eventually invade the bleb by growing from the sides of the bleb.

B. Cortex fragments bound to actin-membranelinker proteins could persist under the bleb membrane during expansion and be elongated to recreate a cortex.

C. Actin seeds could flow with the cytosol to the bleb during expansion and be captured by the ERM-proteins at the membrane during late expansion, elongate and reconstitute a cortex.

D. Active F-actin nucleation by actin nucleators could be needed for *de novo* cortex reassembly.

3.2 Invasion model

According to the invasion model, the cortex underneath the bleb membrane would reappear when the existing cortex at the base of the bleb invades the bleb. Such invasion would mean that the cortex appears first at the sides of the bleb before reaching the tip of the bleb.

To study this mechanism of cortex regrowth, I carried out rapid time-lapse imaging (frame every 200ms) of M2 cells stably expressing LifeAct-Ruby, a probe, which binds to actin filaments. To analyse carefully where F-actin appears first in blebs, I followed the recruitment of LifeAct in a region along the fully expanded bleb perimeter until the beginning of retraction. Visually no recruitment of F-actin starting from the sides of the bleb could be observed (Fig. 3.2A, 10 out of 10 cells examined).

To further analyse the intensity increase over the bleb perimeter, I created kymographs presenting intensity change over time. The kymographs were created over an area of approximately eight pixels around the bleb membrane, but areas at the base of the bleb were not included, because signal from the existing cortex at the base of the bleb could disturb visualisation (Fig. 3.2B). Recording of the kymograph was started when the bleb was visually fully expanded and ended when the bleb started to retract. I displayed the kymographs in pseudocolours, where cold colours represent low intensities and hot colours high intensities. From the kymographs, I could detect at which locations on the bleb perimeter the cortex appeared first. Results from the kymographs were consistent with the visual observation and indicated that no invasion of the cell cortex from the sides of the bleb could be observed. Instead, the kymographs show, that the cortex grows from random locations under the bleb membrane (Fig. 3.2C one representative kymograph of 20 acquired). I analysed two blebs per cell from 10 cells, a total of 20 blebs.

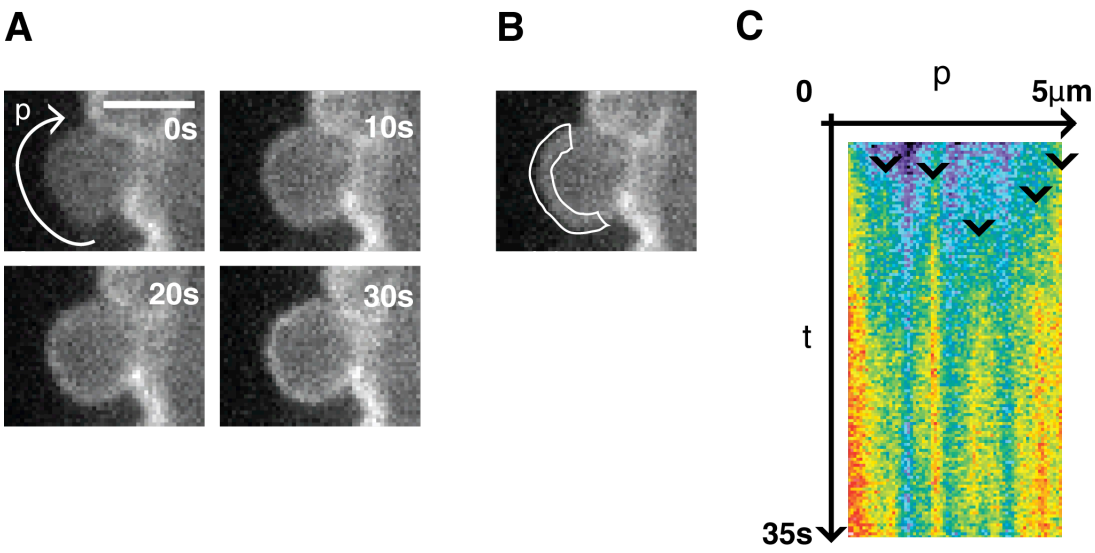

Figure 3.2: Actin cortex starts to regrow from random locations under the bleb membrane.

A. Cortex regrowth during the lifecycle of a bleb in an M2 cell stably expressing LifeAct-Ruby probe was investigated by following intensity change over the bleb perimeter (p, arrow). Timings are given in sec. Scale bar 3µm.

B. An example of the bleb perimeter area from where the kymographs were recorded.

C. Kymograph of the bleb perimeter from A. Recording of the kymograph was started when the bleb was fully expanded and stopped when retraction began. Time is shown on the y-axis and the bleb perimeter on the x-axis. Cold colours represent low intensities and hot colours high intensities. The kymograph reveals that the cortex starts to assemble from random positions (arrowheads) along the bleb membrane suggesting that existing cell cortex does not invade the bleb (n=20 blebs). The fluorescence intensity of the cortex increases over time suggesting actin recruitment continues until retraction starts.

However, because I excluded the base of the bleb from the kymographs, some invasion of the existing cortex could occur into the bleb at the timescales similar to the regrowth rate of F-actin at random locations at the bleb membrane. Despite of this possibility, the data supports that invasion of the existing cell cortex to the bleb is not the main mechanism of actin cortex regrowth in blebs, but rather the cortex reappears under the bleb membrane at random positions along the bleb perimeter. The data also suggest that the bleb cortex strengthens prior to retraction as more actin is recruited to the cortex.

If the cell cortex invaded the bleb, the bleb morphology would likely differ from what is observed. As described the cell cortex would first reach the sides of the bleb. Therefore for a moment the sides of the bleb would get more mechanical support than the tip of the bleb. This should lead to more frequent secondary bleb formation, when a bleb forms on top of an existing bleb. Cells migrating by blebbing often form secondary blebs and thus this kind of cortex reassembly could be favorable for motile cells (see Fig. 1.13, Keller and Eggli, 1998). Whether or not invasion of cell cortex occurs in blebs of motile blebbing cells remains to be investigated. Second, aberrant bleb retraction morphologies would likely occur if invasion was taking place, because actin binding proteins, including myosin II, would first get recruited to the sides of the bleb. This could lead to situation where the sides of the bleb start retracting earlier than the tip of the bleb, potentially causing morphologies different from the quasi-spherically morphology we generally observe.

3.3 Bound filaments model

The bound filaments mechanism of actin cortex reassembly into blebs suggests that small actin filaments stay tethered under the bleb membrane from the onset of bleb formation. Studied by following recruitment of actin-GFP or LifeAct-Ruby to the bleb membrane, blebs appear to be devoid of F-actin during expansion. However, the actin filaments could be so small that their signal is too weak to be detectable with conventional light microscopy. To overcome this problem we decided to functionalise quantum dots with phalloidin and microinject them into blebbing cells.

We used phalloidin because it is a toxin that stabilizes actin filaments by binding to the junction between actin subunits in the filament (Cooper, 1987; Steinmetz et al., 1998) and thus can be used to detect even small actin filaments in the cell. Phalloidin itself is not fluorescent and therefore to detect a strong signal from it, we decided to use quantum dots (Qdots). Qdots are roughly protein-sized fluorophores made of semiconductor material, are bright, blink irregularly (in sec timescales), have a long lifetime, and can be conjugated with other compounds (Michalet et al., 2005) including phalloidin. Quantum yield, which measures the efficiency of the fluorescence process, of Qdots is 90% making them brighter fluorophores than EGFP with quantum yield of 60% (Michalet et al., 2005). Because the Qdots are so bright, I expected that short acquicition times (40ms) and moderate laser power (45%) were sufficient to detect even single Qdots with the spinning disk microscope.

The size of one pixel and thus ability of the spinning disk microscope to differentiate between objects is 133x133nm when imaging with with 100x objective. One Qdot is 15-20nm in diameter (Invitrogen) and thus multiple Qdots can be detected as one pixel. However, to differentiate whether or not a single Qdot is observed, blinking of the Qdots can be exploited. Indeed, blinking is observed with one Qdot, but when many Qdots blink in a non-

synchronised manner, blinking can no longer be detected (Michalet et al., 2005). During my studies I did not analyse if I was observing one or clusters of Qdots at the bleb membrane, but I did observe many blinking Qdots during my studies as described later in this chapter.

Taken together, due to the brightness and blinking of Qdots, one single phalloidin-Qdot at the cell membrane can be detected suggesting this method is sensitive enough to detect if actin seeds stay bound at the cell membrane during expansion.

First, I verified that phalloidin does not interfere with blebbing by microinjecting fluorescent rhodamine-phalloidin into M2 cells at the same concentration as phalloidin used in phalloidin-Qdots microinjections. With 20µg/ml rhodamine-phalloidin the cells still blebbed and the blebs were able to retract (n=6 blebs) (Fig. 3.3A), suggesting that the amount of phalloidin used in the phalloidin-Qdots microinjections should not interfere with blebbing and actin recruitment to the bleb membrane.

Once introduced into the cell by microinjection, phalloidin can bind even small actin filaments and we can detect binding events by following the phalloidin-Qdots. When the Qdots are not bound to F-actin and diffuse in the cytoplasm, only a background signal is detected because diffusion is many-fold faster than image acquisition. Conversely, when the phalloidin-Qdot bind to F-actin, a single, bright, stationary quantum dot can be detected.

When I microinjected phalloidin-Qdots into blebbing cells I observed that Qdots diffused freely in the cytoplasm constituting background fluorescence (Fig. 3.3B). I also observed that phalloidin-Qdots penetrated into the blebs from the onset of blebbing, indicating that the phalloidin-Qdots were not sieved by the cell cortex at the base of the blebs. In blebbing cells phalloidin-Qdots bound to the actin cortex and accumulated to the bleb membrane

before retraction (Fig. 3.3B and 3.4 upper row) mirroring all aspects of actin dynamics observed with GFP-actin and rhodamine-phalloidin.

To visually detect when stationary Qdots appeared during bleb lifetime, I generated time-projections of the expansion and retraction phases for each bleb. To understand when the Qdots were bound to the membrane during the bleb lifetime, I reasoned that in time projection images, the trajectory of Qdots bound to the membrane should appear as streaks of fluorescence. I analysed 5 blebs each from 15 different cells, a total of 75 blebs. I detected no bound phalloidin-Qdots during expansion (n=0 out of 75 blebs examined); whereas, during retraction, many stripes representing phalloidin-Qdot trajectories were observed (n=75 out of 75 blebs examined, Fig. 3.4, lower row arrows).

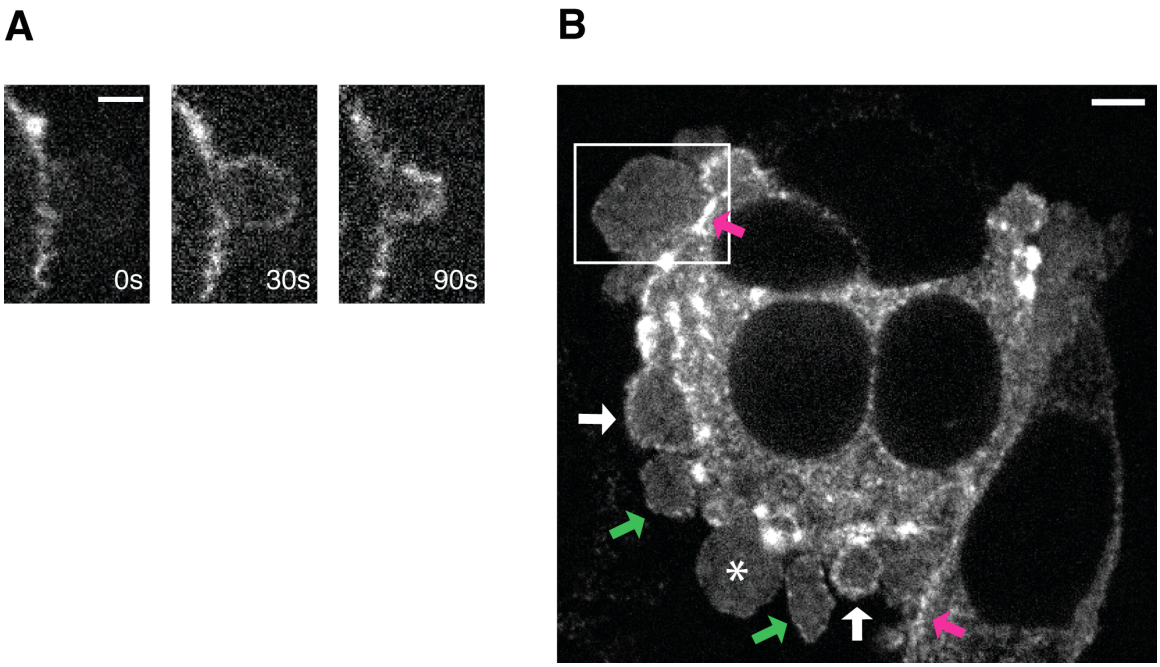

Figure 3.3: Phalloidin does not interfere blebbing and is functional in live cells.

A. Blebbing M2 cells were microinjected with 20µg/ml rhodamine-phalloidin. Phalloidin did not interfere with blebbing; blebs were able expand (t=0s), to reform a cortex (t=30s), and retract (t=90s). Timings are given in sec. Scale bar 3µm.

B. M2 cells were microinjected with quantum dots crosslinked to phalloidin. Phalloidin-Qdots freely diffused in the cytoplasm and penetrated into the blebs (white star). Phalloidin-Qdots appeared at the membrane when expansion slowed (green arrows). When retraction took place (white arrows) the signal from the quantum dots was the strongest suggesting the presence of a high concentration of F-actin under the bleb membrane. The quantum dots also localised to the cell cortex (pink arrows). The bleb in the white box is presented in the next figure. Scale bar 5µm.

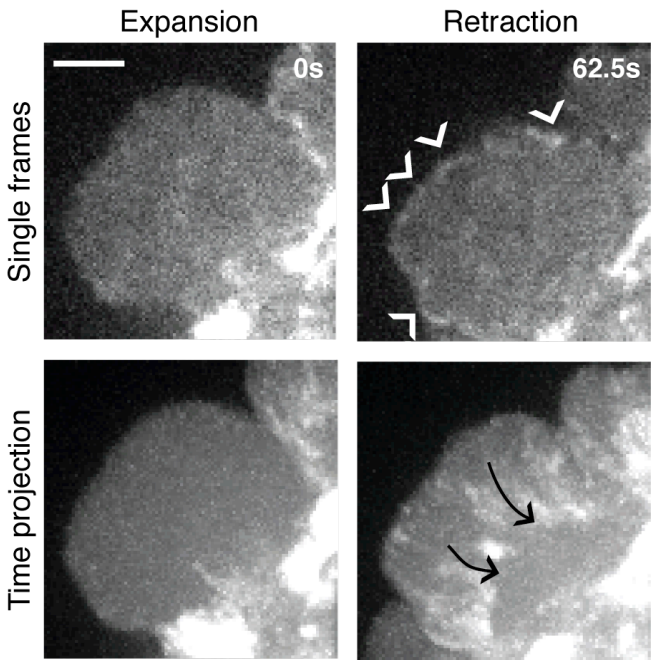

Figure 3.4: Actin cortex reconstitution is not due to cortex fragments remaining under the bleb membrane during expansion.

Representative phalloidin-Qdot localisation in a bleb during expansion and retraction. Bound phalloidin-Qdots were visible at the bleb membrane during retraction (upper row, 62.5s, arrowheads), but not during expansion (upper row, 0s). Lower row images show a projection of all the time frames during the expansion and retraction phases of a bleb. Trajectories of Qdots bound to the membrane appear as stripes in the time projections. No stripes were detected during expansion (0 out of 75 blebs analysed). In contrast during retraction many stripes were detected (indicated with arrows on lower row, 75 out of 75 blebs analysed) suggesting that actin filaments are bound to the membrane only during retraction. Timings are given in sec. Scale bar 3µm.

Because the phalloidin-Qdots compounds appeared at bleb membrane only during retraction, I concluded that no cortex fragments persist under the bleb membrane during expansion invalidating the bound filaments model of cortex reassembly.

A few clues from the literature also suggest that no actin seeds stay bound under the bleb membrane during expansion. It has been shown that during expansion the bleb is devoid of ERM-protein ezrin (and moesin) (Charras et al., 2006). This suggests that at least ERM-proteins cannot be responsible for tethering actin seeds under the bleb membrane during expansion. However, ERM-proteins are not the only cortex-membrane linker proteins found in blebs. Filamins or annexins could also tether the actin seeds to the bleb membrane and both proteins are present in blebs (see chapter 5). Although filamin B localises to the bleb throughout the bleb lifetime (see chapter 5) its affinity for actin has been reported to be relatively weak (Sawyer et al., 2009). Therefore it would be unlikely that filamin alone could keep the actin filaments tethered to the membrane from the onset of bleb growth. Taken together the phalloidin-Qdot experiments together with clues from the literature strongly suggest that no actin seeds stay bound under the bleb membrane during expansion.

Interestingly, phalloidin-Qdot microinjections also suggest that no invasion of the cell cortex into the bleb occur either because recruitment of Qdots did not occur at the sides first, supporting the results from the cortex invasion studies. To verify this observation, I followed intensity changes along the bleb perimeter of fully expanded blebs until the beginning of retraction. From the kymographs I detected that phalloidin-Qdots appear in random locations under the bleb membrane (Fig. 3.5 one kymograph of 10 presented), supporting the invalidity of the invasion model.

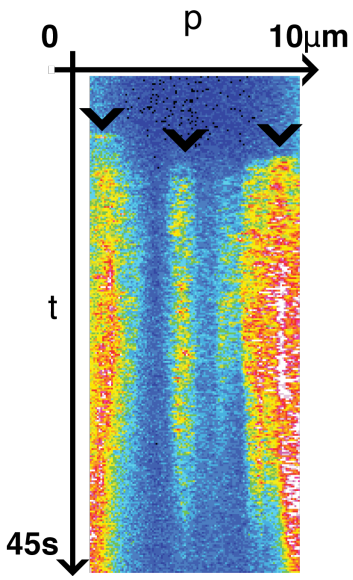

Figure 3.5: Phalloidin-Qdots appear in random locations under the bleb membrane.

Kymograph of the bleb perimeter from a phalloidin-Qdot microinjected cell. Recording of the kymograph was started when the bleb was fully expanded and stopped when retraction begun. Time is shown on the y-axis and the bleb perimeter on the x-axis. Cold colours represent low intensities and hot colours high intensities. The kymograph reveals that phalloidin-Qdots appear in random positions (arrowheads) along the bleb membrane suggesting invasion does not occur (n=10 blebs).

3.4 Flow of actin seeds model

According to the flow of actin seeds model cortex regrowth in blebs would arise from elongation of small actin seeds that get captured by actin-membrane linkers proteins present at the membrane during late expansion. To study this mechanism I followed the localisation of fluorescent, stabilised, exogenous F-actin seeds in blebbing cells after microinjection.

To generate these fluorescent exogenous F-actin seeds, I first polymerised Alexa-488 labelled actin *in vitro.* However, when introduced into the cell these filaments might get depolymerised by the machinery regulating actin dynamics in the cell. To prevent depolymerisation of the actin seeds in the cell, I crosslinked the filament protomers to one another covalently with p-NN'-phenylenebismaleimide (pPDM) (Knight and Offer, 1978) that creates stabilised regions to the filament that act as caps. Stabilisation with pPDM does not interfere F-actin dynamics (other than depolymerisation) as it has been shown, that *in vitro* pPDM-crosslinked actin filaments can elongate and bind actin regulating proteins including gelsolin and myosin (Doi, 1992; Gilbert and Frieden, 1983; Kim et al., 2002; Knight and Offer, 1978; Knight and Offer, 1980; Mockrin and Korn, 1983). However, pPDM crosslinked protomers act as caps that block or slow depolymerisation.

First to verify that pPDM does not impede blebbing and is not autofluorescent, I microinjected pPDM together with Alexa-647 labelled dextran into blebbing cells stably expressing LifeAct-Ruby. I detected the microinjected cells with the Alexa-647 dye and followed the actin cortex dynamics with LifeAct-Ruby and observed that blebs expanded, reassembled actin cortex, and were able to retract. I found that pPDM is not autofluorescent when excited with 488nm light and thus fluorescent, stabilised, exogenous F-actin seeds can be imaged with 488nm wavelength light without background fluorescence from pPDM.

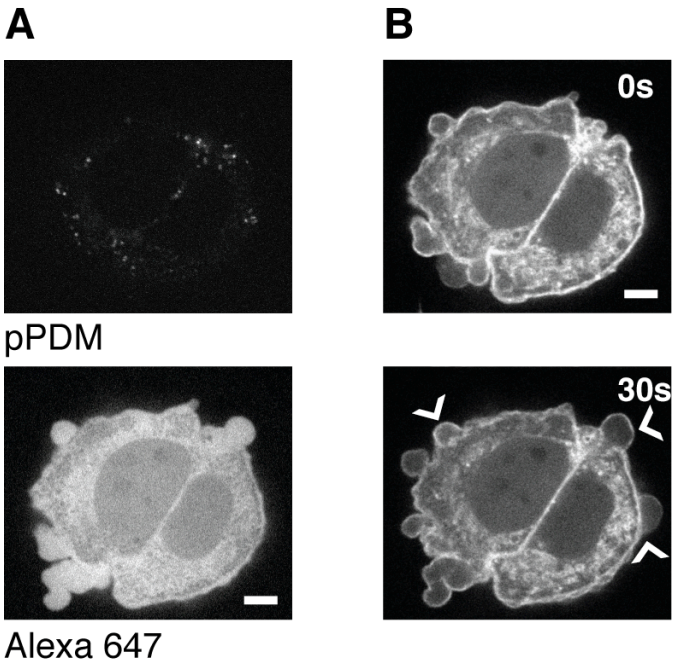

Figure 3.6: pPDM is not autofluorescent and does not interfere with blebbing.

A. Blebbing M2 cells stably expressing LifeAct-Ruby were microinjected with pPDM together with Alexa-647 labelled dextran. pPDM is not autofluorescent when excited at 488nm and collecting emission at 525nm (pPDM). Microinjected cells were observed by following the Alexa-647 dye exciting at 647nm and collecting emission at 670nm (Alexa 647). Scale bar 5µm.

B. Same cells as in A imaged in the Ruby channel (excitation at 568nm and emission 600nm) to visualise the F-actin dynamics using LifeAct. Blebs were seen forming, expanding, and retracting (0s, 30s, arrow heads). No perturbations in actin cortex assembly were detected. Scale bar 5µm.

After producing fluorescent, pPDM-stabilised F-actin I sonicated the sample to diminish the average size of actin filaments. To assess the size of crosslinked protomer modules I ran a sample on an SDS-PAGE gel.

Normally actin filaments cannot be seen on SDS-PAGE because of denaturation of actin by SDS, but pPDM crosslinks protomers in the filament covalently to one another crosslinked protomers cannot be denaturated and can thus be visualised in the gel (Fig. 3.6A). I observed many oligomers of different sizes in the gel (Fig. 3.6B arrowheads) confirming that some of the protomers in the sample were crosslinked and thus stabilised and resistant to depolymerisation.

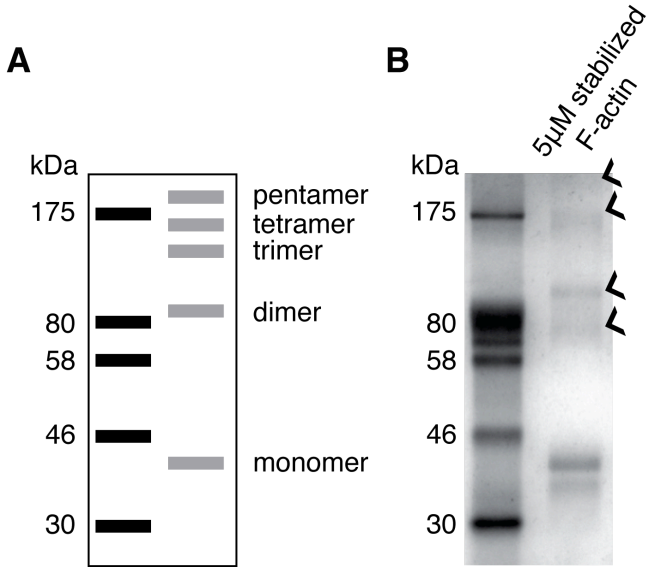

Figure 3.7: Determination of crosslinked oligomer size after pPDM stabilisation.

A. Cartoon of the oligomer sizes and how they should appear in SDS-PAGE gel. The molecular weight of an actin monomer is 42kDa. Thus dimers should appear at 84kDa, trimers at 126kDa, tetramers at 168kDa, and pentamers at 210kDa.
B. Stabilized filaments (indicated as 5µM stabilized F-actin) were run into a SDS-PAGE. Covalently crosslinked F-actin seeds of many sizes were detected (indicated by arrowheads).

To determine the functionality of the G-actin used in the assay, I microinjected a high concentration (10μM) of Alexa-488 labelled G-actin into the blebbing cells. Fluorescent actin incorporated into the actin cortex of cells and blebs (n=12 cells, Fig. 3.7A) indicating the Alexa-488 labelled actin was functional and able to participate to cellular actin dynamics. Finally, to study if small actin seeds get recruited to cortical structures and get captured by proteins at the bleb membrane, I microinjected the Alexa-488 labelled, stabilised, exogenous F-actin seeds into the blebbing cells (Fig. 3.7B). In contrast to the cortical localisation of exogenous monomeric actin, the F-actin seeds remained diffuse and never concentrated at the cell cortex or other actin structures in the cells (n=44 out of 44 cells examined, Fig. 3.7B).

Previously Sanders and Wang have shown that exogenous F-actin seeds play no or little role in actin dynamics when microinjected into cells and suggested that this occurs because of sequestration of G-actin in the cell (Sanders and Wang, 1990). Indeed the cell has to tightly control its actin dynamics, especially polymerisation, because uncontrolled F-actin elongation might lead to dramatic changes in the cytoskeleton. In cells polymerisation is not only controlled by actin sequestration but also by barbed end capping.

Taken together, my data and results obtained by Sanders and Wang (Sanders and Wang, 1990) suggest that exogenous actin seeds fail to participate in actin dynamics and localise to actin structures in cells, suggesting the invalidatation of the flow of actin seeds model. However, limitation of this assay is that although the stabilised actin seeds have been found to be functional *in vitro*, their functionality in cells remains unknown.

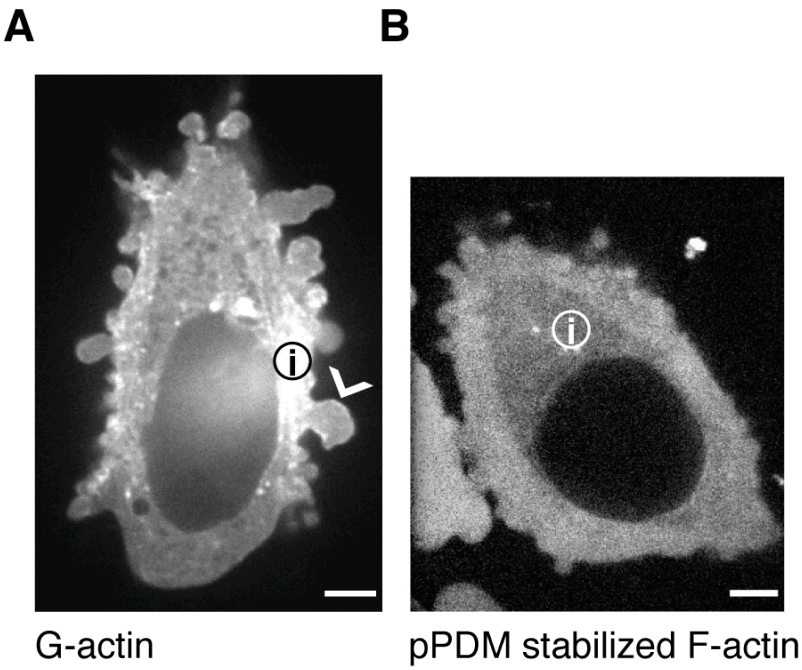

Figure 3.8: Fluorescent G-actin incorporates into the cortex but stabilised F-actin seeds remain diffuse in blebbing cells.

In both images the site of microinjection is indicated with i and scale bars are 5µm.

A. 10µM Alexa-488 labelled G-actin was microinjected into blebbing M2 cells. Fluorescent G-actin incorporated into the cell cortex both in the cell body and in blebs (arrowhead).
B. 5µM Alexa-488 labelled pPDM stabilized F-actin seeds were microinjected into blebbing M2 cells. These actin seeds remained diffuse and did not incorporate into actin structures in the cells.

3.5 Conclusions

Four possible models of actin cortex regrowth were presented; 1) the invasion model, where existing cell cortex elongates and invade the bleb, 2) the bound filaments model, where F-actin seeds stay bound to the membrane during expansion and elongate, 3) the flow of actin seeds model, where F-actin seeds flow into the bleb during expansion and are captured by membrane-cortex linker proteins at the membrane and finally elongate, and 4) the nucleation model, where active actin nucleation is needed for cortex assembly.

First, I studied the invasion model and showed that the cortex starts to reappear at random locations along the bleb membrane, suggesting the cell cortex at the base of the bleb does not invade the bleb. Second, I investigated the bound filaments model and showed that actin filaments are only present at the bleb membrane when expansion slows in blebbing M2 cells. Results from the phalloidin-Qdot microinjections also suggest that invasion does not occur, because no earlier accumulation of actin filaments was noted at the sides of the bleb compared to the tip of the bleb.

Finally, I studied the flow of actin seeds model and learned that pre-polymerised, fluorescent, stabilized actin seeds do not localise to the actin cortex in cells or in blebs suggesting they do not participate in cortical actin dynamics. In addition, others have shown that microinjected exogenous F-actin seeds stay diffuse and do not induce actin polymerisation in cells (Sanders and Wang, 1990). However, the functionality of the stabilised actin seeds in cells remains unknown.

Taken together, these results suggest that the first three modes of actin assembly do not appear to be the main mechanisms of actin cortex regrowth in blebs. Finally, the nucleation model remains to be investigated and is the topic of the following chapter.

4 FORMIN DIAPH1 AND THE ARP2/3 COMPLEX ARE NECESSARY TO FORM THE ACTIN CORTEX

4.1 Introduction

Because I found that no nucleation-independent mechanisms contributed to reconstitution of the actin cortex, I examined the role of *de novo* actin nucleation in cortex reassembly. Indeed, actin nucleators are essential for other actin structures, like lamellipodia, filopodia, and stress fibers. In lamellipodia, the Arp2/3 complex induces formation of a branched network that pushes the plasma membrane forward (Amann and Pollard, 2001; Mullins et al., 1998; Svitkina and Borisy, 1999). Filopodia, often arising from the lamellipodium, are elongated with Diaph3/mDia2 localised at their tips (Pellegrin and Mellor, 2005; Yang et al., 2007). Formins also participate in stress fiber formation as Diaph1 and Fhod1 both have been shown to nucleate them (Gasteier et al., 2005; Hotulainen and Lappalainen, 2006; Watanabe et al., 1999).

Although studies exist, there is little consensus about the nucleators needed for cortex assembly. When studying the cortex maintenance and assembly blebbing is often used as a marker of cortical instability (Charras et al., 2008). First, it has been proposed that diaphanous-related formin Fhod1 is responsible for cortex nucleation on the basis of a decrease in the number of blebs observed after Fhod1 depletion in HeLa cells overexpressing a SH4 domain (Hannemann et al., 2008). Formin Fmnl1 was linked to cortex stability, because overexpression of constitutively active Fmnl1 induces blebbing independently of ROCK (Han et al., 2009). Further, Diaph family formins have been linked to induction of blebbing and cortex maintenance. Diaph3 has been suggested to have a role in the cortex, because overexpression of diaphanous-interacting protein (DIP) induces blebbing through specific inhibition of Diaph3 (Eisenmann et al., 2007). In contrast, depletion of Diaph3 was recently reported to efficiently reduce blebbing in spreading HeLa cells and it was therefore concluded that it is a novel regulator of membrane blebbing (Stastna et al., 2011). Diaph1 has been suggested to have a role in the cell cortex, because it appears to be

necessary for invasion and blebbing motility of MDA-MB-435 cells upon lysophosphatidic acid (LPA) stimulation (Kitzing et al., 2007). In addition in *D. melanogaster* embryos Diaphanous was shown to be required for proper cortical organisation during cellularisation (Afshar et al., 2000). However, earlier localisation studies suggested that Diaph1 is not present in blebs of M2 cells (Charras et al., 2006). Interestingly, the Arp2/3 complex was been reported to localise to the cortical area of polarised meiotic mouse oocytes suggesting a possible role in cortex assembly (Sun et al., 2011; Yi et al., 2011). In blebbing M2 cells, the localisation of Arp2/3 complex appeared cytoplasmic (Charras et al., 2006) and was therefore suggested not to participate in cortex assembly. In summary little clarity exists.

These previous studies concentrated on investigating changes in cortex stability, but none examined the actual involvement of the identified actin nucleators in cortex nucleation. In addition in all of these studies, when perturbing the nucleator under investigation, the cells appeared to still retain a substantial proportion of the actin cortex suggesting that multiple nucleators may be needed for cortex assembly.

The aim of this chapter is to determine which actin nucleators are needed for *de novo* cortex assembly. We used natural and induced cell blebs to study nucleation of the actin cortex and used a combination of proteomics, gene silencing, and imaging approaches to reveal a role for two actin nucleators at the cell cortex.

4.2 Multiple actin nucleators localise to the cell cortex

Because the cortex is an important structure in all cells we reasoned that nucleators needed for cortex assembly should be expressed in multiple cell lines. Therefore we investigated cortex reassembly in two cell lines: M2 cells, because they display a visible cortex throughout the cell cycle, bleb, and thus need to reassemble cortex continuously, and mitotic HeLa cells, because they have a rigid cortex during metaphase.

First, we investigated the expression of all actin nucleators that are expressed in humans (both cell lines are of human origin) with the exception of those nucleators that are expressed only in specific tissues (e.g. delphilin only in nervous system). To study the expression of the Arp2/3 complex, Spire proteins, and 12 formin family proteins by quantitative real-time PCR we established a collaboration with Dr. Yves Romeo and Dr. Philippe Roux, IRIC, Montreal. We learned that the Arp2/3 complex proteins ACTR2 and ACTR3, as well as Spire1, Spire2, and seven formins (Daam1, Diaph1, Diaph3, Fhod1, Fmnl1, INF1, and INF2) were expressed in both cell lines (Fig. 4.1). Formins Fhod3 and Diaph2 were only expressed in M2 cells but not in HeLa cells, while Daam2, Fmn1 and Fmn2 were not detected in either cell line.

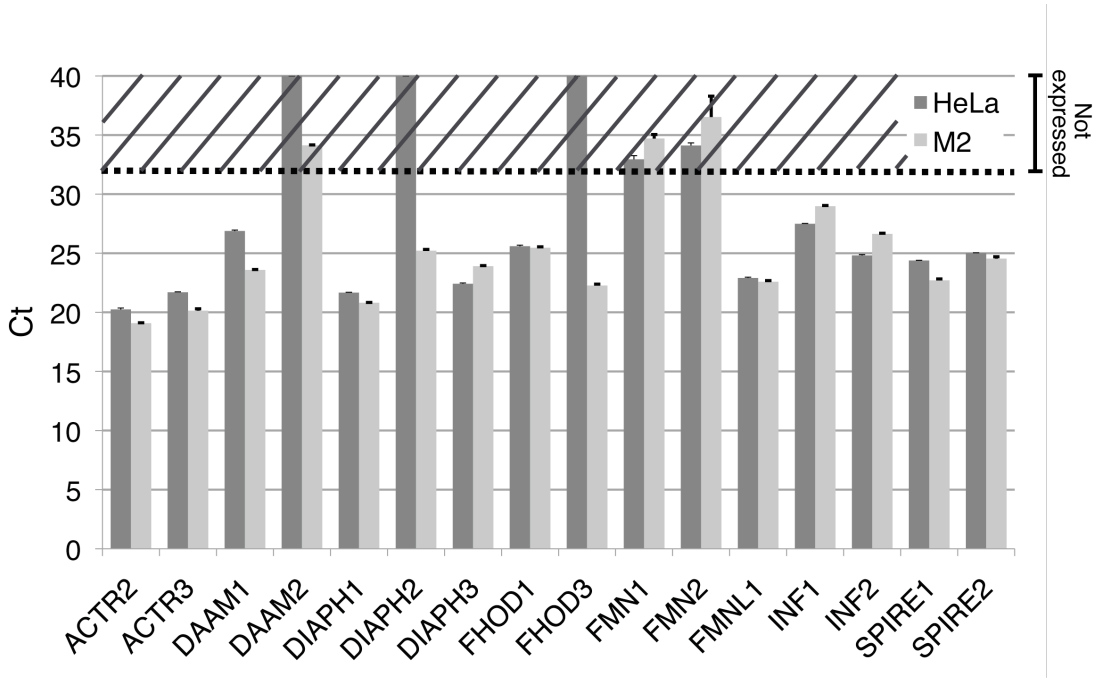

Figure 4.1: Multiple actin nucleators are expressed in M2 and HeLa cells.

Using quantitative real-time PCR we found that mRNA of the Arp2/3 complex (ACTR2 and ACTR3), Spire1 and Spire2, and seven formin family proteins (Daam1, Diaph1, Diaph3, Fhod1, Fmnl1, INF1, and INF2) were expressed in M2 (light grey columns) and HeLa (dark grey columns) cells. The data is normalised to the expression of glyceraldehyde 3-phosphate dehydrogenase (GADPH). The graph shows the number of PCR cycles (Ct) needed to obtain detectable transcript levels. We considered that genes were not transcribed if signal was detected after more than 32 cycles (dashed line). Error bars indicate SD.

Having narrowed down the possible candidates for cortex nucleation, I next performed an imaging screen to study, which actin nucleators localise to the actin cortex. In this screen I concentrated only on the expressed nucleators, but decided to exclude the Spire proteins, because of the absence of Fmn2, an interaction partner of Spire proteins necessary for elongation of Spire-induced actin seeds (Pechlivanis et al., 2009; Quinlan et al., 2007). In addition, Spire proteins have been shown to have role in internal cell organelles, endosomes and Golgi apparatus (Kerkhoff et al., 2001; Quinlan et al., 2007) suggesting that Spire proteins are not likely to play a significant role in cortical actin nucleation. For the screen we tagged Daam1, Diaph1, Diaph3, Fhod1, Fmnl1, INF1, INF2, and three subunits of the Arp2/3 complex (ACTR3, ARPC1, and ARPC5) with GFP and I followed their localisation in M2 cells stably expressing the F-actin reporter LifeAct-Ruby.

First, I observed that formins Daam1 and Fhod1 localised to the cortex (or membrane) in cell body and in blebs. Daam1 was present at the cell membrane throughout the bleb lifetime (Fig. 4.2A) and thus appeared before actin (Fig. 4.3, -3.5s±1.76s compared to actin, n=14 blebs). Visually no fluorescence enrichment was detected towards the end of retraction unlike with F-actin, that appears enriched in the blebs after retraction (Fig. 4.2A, 'R') suggesting Daam1 might be bound mainly to the membrane and only weakly to the cortex. Fhod1 localised to the cortical structures in the cell body but appeared in the cortex in blebs only during late retraction (Fig. 4.2B and Fig. 4.3, 17.4s±4.81s compared to actin, n=14 blebs). However both formins localised to the correct area in blebbing cells making them candidates for cortical cortex nucleation.

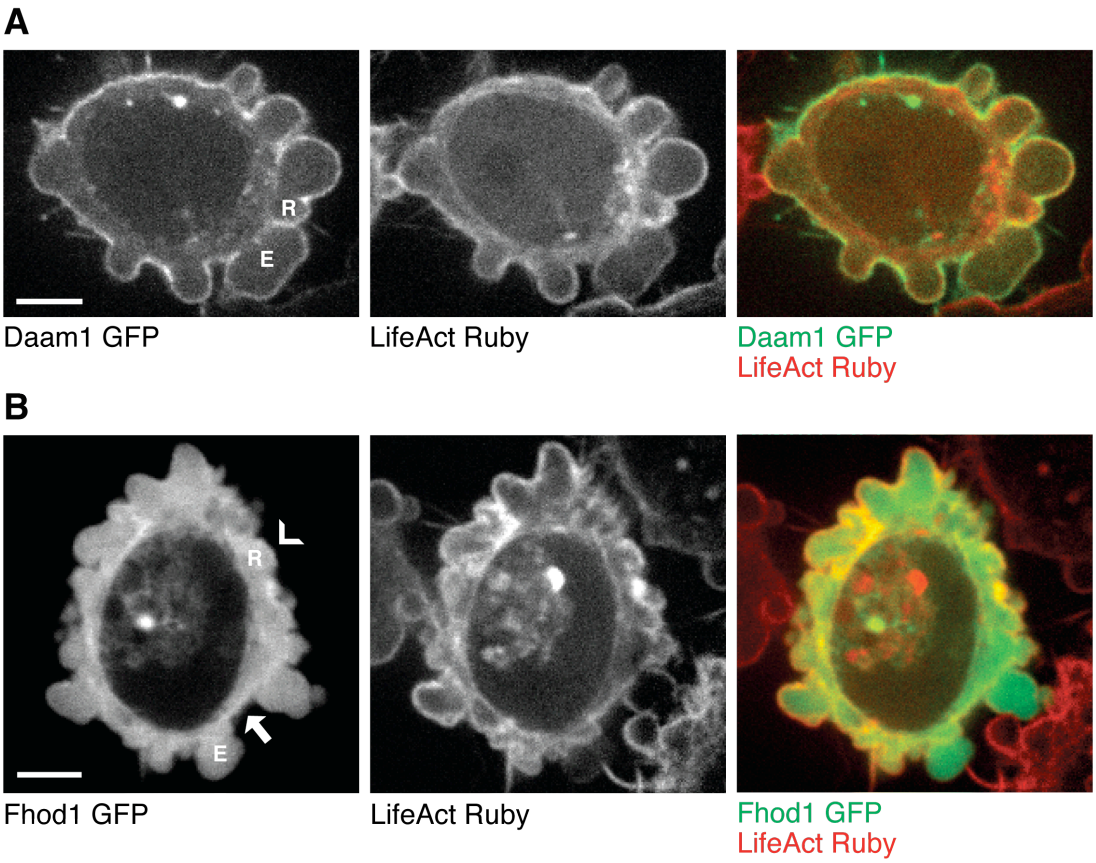

Figure 4.2: Daam1 and Fhod1 localise to the cell membrane in M2 cells.

In images 'E' indicates an expanding bleb and 'R' retracting bleb. Scale bars 5µm.

A. Localisation of Daam1-GFP in M2 cells stably expressing LifeAct-Ruby. Daam1 localises to the cell membrane and appears to be present there throughout the bleb lifetime. In the retracting bleb, R, enrichment of F-actin can be detected in the LifeAct-Ruby channel but visually no enrichment of Daam1-GFP can be observed towards the end of retraction.

B. Localisation of Fhod1-GFP in M2 cells stably expressing LifeAct-Ruby. Fhod1 appears to be present at the cell cortex (arrow) and enriched in retracting blebs (R, arrowhead). A high cytoplasmic fraction of Fhod1-GFP can also be seen.

Formins INF1, also called as FHDC1, and Diaph3 localise to other structures than the cortex in M2 cells. INF1 localised subcortically and never appeared in blebs in M2 cells (Fig. 4.4A), consistent with reports that it links microtubules to F-actin structures in NIH3T3 cells (Young et al., 2008). Diaph3 has been reported to localise to tips of filopodia (Pellegrin and Mellor, 2005; Yang et al., 2007). Consistent with this, in M2 cells Diaph3 localised strongly to the tips of filopodia but never appeared in blebs (Fig. 4.4B). The remaining nucleators (subunits of the Arp2/3 complex, Diaph1, Fmnl1, and INF2) appeared cytoplasmic when tagged with GFP and overexpressed in M2 cells.

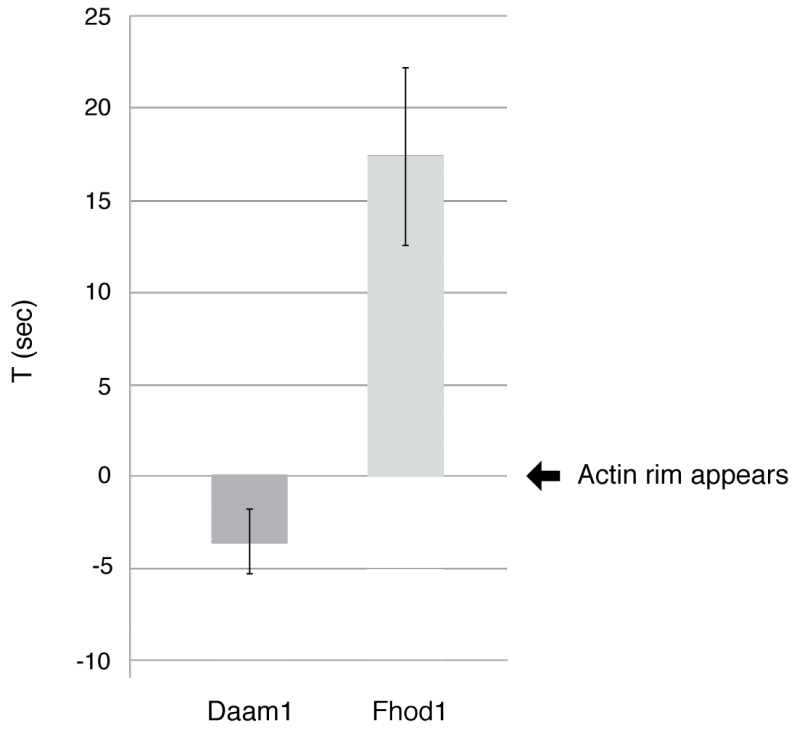

Figure 4.3: Time of appearance of Daam1 and Fhod1 compared to actin.

The graph shows the time of appearance of Daam1-GFP and Fhod1-GFP compared to actin. In the graph, the actin rim appears to the bleb at timepoint 0sec. Daam1 localises to the bleb membrane throughout the bleb lifetime and thus is present there before an actin rim appears. Fhod1 appears in the bleb only after an actin rim appeared. Error bars indicate SD.

The cytoplasmic localisation of GFP-tagged proteins could first be due to a high bound/unbound ratio. Indeed, if only a small amount of the protein is bound at the cortex or other structure at any given time, the unbound fraction of the GFP-tagged protein could lead to strong background fluorescence hindering the observation of the bound protein. In addition, the cell may prefer using endogenous protein for its structures instead of the GFP-tagged protein. Second, the protein of interest might stay inactive under imaging conditions. Finally, the GFP tag might interfere the protein function.

To overcome the problem of bound/unbound ratio simultaneous permeabilisation-fixation was carried out. In this approach, the unbound fraction is removed by permeabilisation, whereas the bound fraction can be visualised, because it is stabilised by fixation.

Then, to detect proteins that are tightly regulated (possibly high unbound fraction) and mostly remain in an inactive state when overexpressed in cells, the localisation can potentially be revealed by single molecule speckle microscopy. In this method, GFP-tagged proteins are expressed from a vector where the majority of the cytomegalovirus (CMV) gene promoter has been deleted leading to very low expression levels of the GFP-tagged protein (Watanabe and Mitchison, 2002). Thus the background fluorescence remains low, and the bound GFP-tagged proteins, speckles, can be detected using high laser power and long acquisition time. Indeed, as described in the previous chapter the quantum yield of EGFP is much lower and the lifetime much shorter due to bleaching than of bright, long-lasting Qdots and thus maximum laser power (100%) and very long acquisition times (500-800ms) need to be used for speckle imaging. In the cell the unbound GFP-tagged proteins emit background fluorescence when diffusing in the cytoplasm. Once the GFP-tagged protein binds to F-actin or to the membrane a single speckle can be detected. As described the pixel size of the spinning disk microscope, when imaging with 100x objective, is 133x133nm. Like single Qdot, also one GFP-tagged protein is smaller than 133nm in diameter and

thus one pixel can contain multiple GFP-tagged proteins. During my studies I did not analyse if I was observing one or clusters of GFP-tagged proteins at the bleb membrane, but I could have measured relative amounts of GFP molecules by comparing intensities between different speckles. Indeed, if all the speckles have equal intensity levels it is likely that one speckle represents one GFP molecule. Conversely, differences in intensity levels between different speckles could give clues of relative numbers of GFP molecules.

Finally, in the case of GFP tag interfering with the protein function, live imaging approaches are impossible but instead localisation may be revealed with immunostaining in fixed cells. Immunostaining reveals the localisation of endogenous protein in cells making it an attractive imaging approach. However, with immunostaining the imaging is limited to fixed cells and thus dynamics of the protein of interest is not easily followed. In addition, availability of good antibodies might be problematic.

INF2 tagged with GFP appeared cytoplasmic in M2 cells but, when I performed a simultaneous permeabilisation-fixation of the transfected cells, I observed that INF2 localised to the endoplasmic reticulum (Fig. 4.4C) consistent with a previous report (Chhabra et al., 2009). The localisation of other nucleators still remained cytoplasmic. Taken together the data suggest that Diaph3, INF1, and INF2 are not involved in cortex formation because they localise to other structures than the actin cortex.

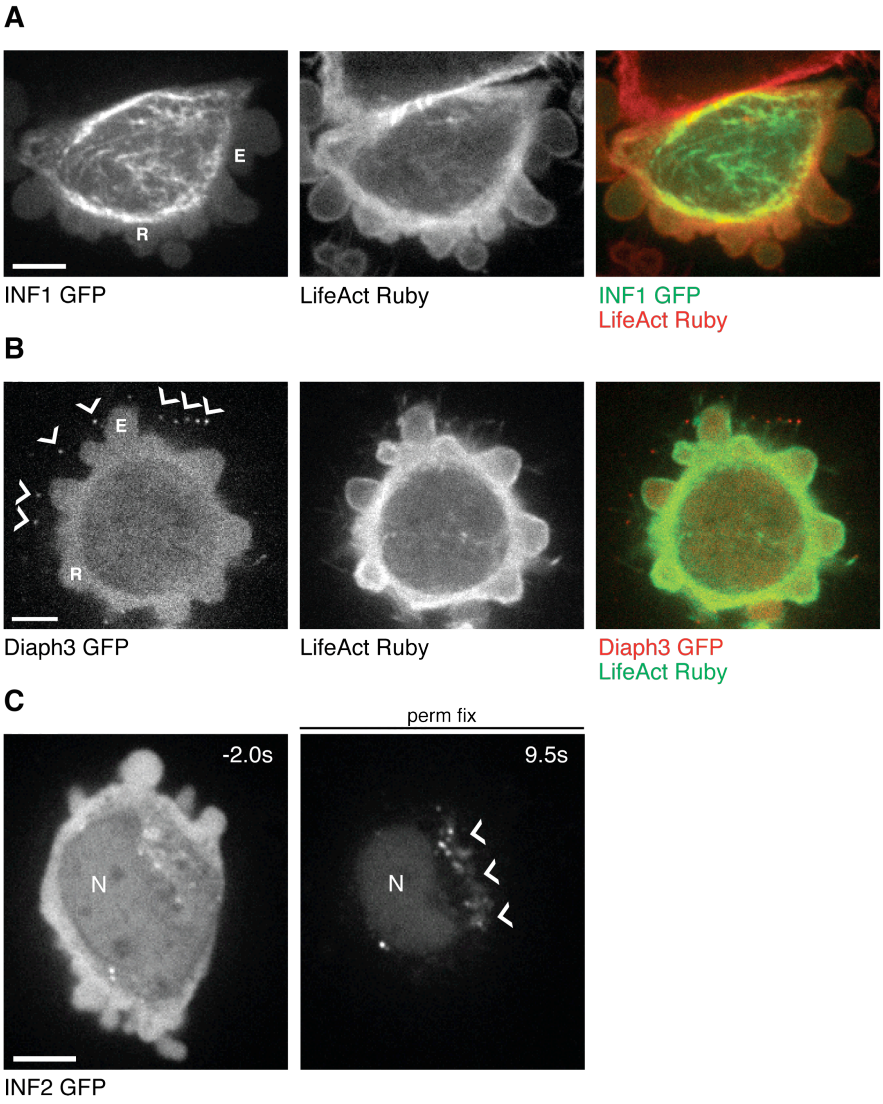

Figure 4.4: INF1, Diaph3, and INF2 localise to other structures than the actin cortex.

In images 'E' indicates an expanding bleb and 'R' retracting bleb. Scale bars 5µm.

A. Subcortical localisation of INF1-GFP in M2 cells stably expressing LifeAct-Ruby.

B. Filopodial tip localisation of Diaph3-GFP (arrowheads) in M2 cells stably expressing LifeAct-Ruby.

C. After simultaneous permeabisation-fixation (performed at timepoint 0.00s) INF2-GFP localises to the endoplasmic reticulum (arrowheads, N represents nucleus). Timings are in sec.

To reveal the localisation of the Arp2/3 complex (subunits ACTR3, ARPC1, and ARPC5), Diaph1, and Fmnl1, we expressed them in speckle amounts in M2 cells. Upon imaging the background signal consists of diffuse, unbound proteins and appears dim. The bound proteins, instead, appear as bright spots. Interestingly I observed that Diaph1 speckles concentrated in retracting blebs and co-localised there with F-actin (Fig. 4.5A arrowheads, Movie 1). The other proteins still remained cytoplasmic and no speckles were observed. To further characterize the localisation of the Arp2/3 complex, I carried out immunostaining of the M2 cells with ARPC2 antibody and found that the Arp2/3 complex also localised to the actin cortex (Fig. 4.5B).

Taken together formins Daam1, Fhod1, and Diaph1 together with the Arp2/3 complex localise to the cortical area in M2 cells, whereas INF1, INF2, and Diaph3 localised to other structures (summarised in table 4.1). Interestingly only speckle imaging revealed the localisation of Diaph1 at the cortex. Indeed, it was surprising that no indication of the cortical localisation of Diaph1 was detected with permeabilisation-fixation method. However, the chemical fixation appeared to weaken the signal from the GFP quite considerably which cannot be only explained by the loss of unbound fluorescent molecules due to permeabilisation. Thus, if only a small fraction of Diaph1-GFP is cortex bound, the signal from those molecules upon fixation may not be strong enough to meet the sensitivity of the microscope.

For further investigation we reasoned that nucleators that localised to incorrect structures were presumably not involved in cortex assembly. The cytoplasmic localisation observed with Fmnl1 could be due to the GFP tag interfering with the protein function and therefore I decided not to exclude it from further investigation. Hence, although the localisation of Fmnl1 could not be revealed it was included for further studies together with Daam1, Fhod1, Diaph1, and the Arp2/3 complex.

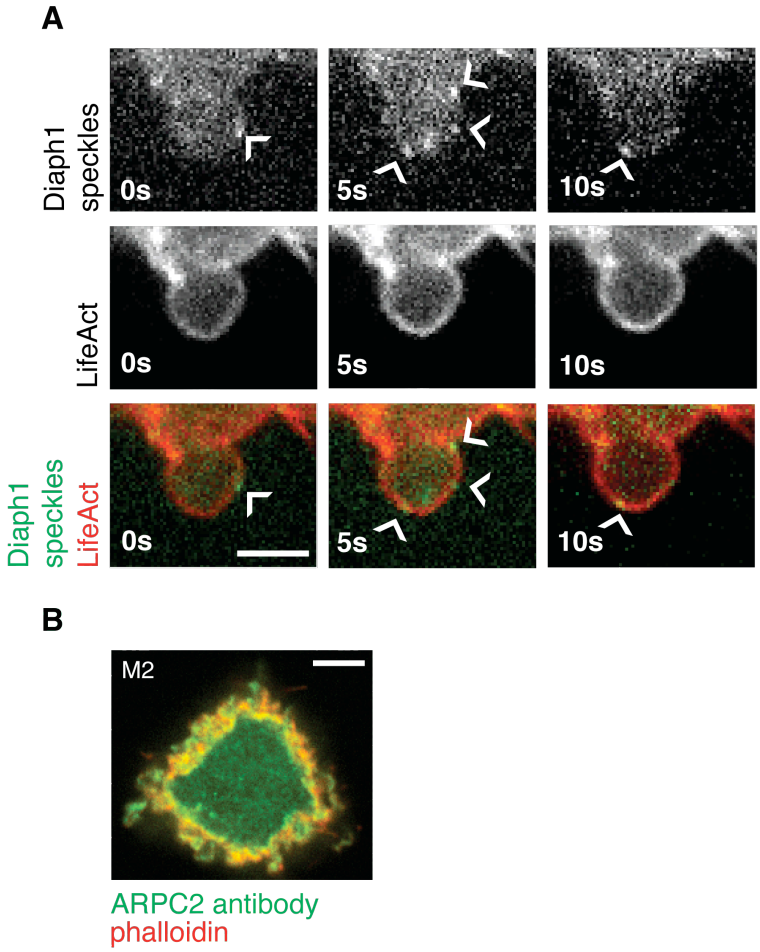

Figure 4.5: Diaph1 and the Arp2/3 complex localise to the cell cortex.

A. Single molecule imaging of full-length EGFP-Diaph1 (green) in M2 cells stably expressing LifeAct-Ruby (red). Diaph1 speckles localise to the cortex of cell blebs. Speckles appear as bright spots and are indicated with arrowheads. Timings are given in sec. Scale bar 3µm.

B. Immunostaining of the ARPC2 subunit of the Arp2/3 complex in an M2 cell. ARPC2 co-localises with phalloidin at the cell cortex. Scale bar 5µm.

	GFP-tagging	Permeabilisation -fixation	Speckle microscopy	Immunostaining
Daam1	**membranous**	-	-	-
Fhod1	**cortical**	-	-	-
Diaph3	**filopodia**	-	-	-
INF1	**subcortical**	-	-	-
INF2	cytoplasmic	**endoplasmic reticulum**	-	-
Diaph1	cytoplasmic	no localisation	**cortical**	-
Fmnl1	cytoplasmic	no localisation	cytoplasmic	-
ACTR3	cytoplasmic	no localisation	cytoplasmic	-
ARPC1	cytoplasmic	no localisation	cytoplasmic	-
ARPC5	cytoplasmic	no localisation	cytoplasmic	-
ARPC2	**-**	-	-	**cortical**

Table 4.1: Localisation of expressed actin nucleators in M2 cells.

Localisation studies by GFP-tagging, simultaneous permeabilisation-fixation, speckle microscopy, or immunostaining revealed that Daam1, Fhod1, Diaph1, and the Arp2/3 complex localise to the cortical area in M2 cells. Diaph3, INF1, and INF2 localised to other structures than the cortex. Localisation of Fmnl1 could not be determined.

4.3 Formin Diaph1 contributes to stability of the actin cortex

Having narrowed down the possible candidates for cortex nucleation using the localisation screen, I performed a mini screen by silencing individually Daam1, Fhod1, Diaph1, Fmnl1, and the Arp2/3 complex (ACTR3).

Some studies already exist on disrupting these nucleators either by RNA interference (RNAi) or mutation in cells or model organisms. First, the role of Daam1 has especially been investigated during morphogenesis. In developing chick embryos silencing Daam1 led to defective signalling of PDZ-RhoGEF, which is downstream of Daam1, causing disruption of the polarised acto-myosin contraction of neural plate cells and the failure of the neural tube closure (Nishimura et al., 2012). In addition, in developing Daam1 mutant *M. musculus* the F-actin organisation in the cardiac sarcomeres was disrupted leading to disruption of heart development (Li et al., 2011). Further, in *X. laevis* Daam1 depletion led to failure of gastrulation due to defects in planar cell polarity signalling (Habas et al., 2001). In Daam mutant *D. melanogaster* the F-actin organisation was disrupted in parallel actin cables of tracheal cells (Matusek et al., 2006). In mature mammalian cells, Daam1 depletion led to inhibition of centrosome re-orientation during cell motility (Ang et al., 2010).

Second, the role of mammalian formin Fhod1 in cells or *M. musculus* has not yet been thoroughly studied. However, it was shown by silencing methods that Fhod1 is needed for stress fiber formation (Takeya et al., 2008).

Third, several studies exist in depleting mammalian Diaph1. Aging Diaph1 knockout mice develop myeloproliferative defects in bone marrow and blood (Peng et al., 2007), which are mainly caused by problems in T-cell activation and function (Eisenmann et al., 2007). In cellular level Diaph1 depletion has been reported to lead to decreased content of stress fibers (Echarri et al., 2012; Hotulainen and Lappalainen, 2006), decreased Rif-mediated filopodial

protrusion (Goh et al., 2012), and to inhibition of blebbing motility (Kitzing et al., 2007).

Further, developing *D. melanogaster* Diaphanous (Diaph) mutant embryos have been shown to have defects in cellularisation, suggesting a crucial role for Diaph in membrane invagination (Afshar et al., 2000). In addition, Diaph mutant *D. melanogaster* has been reported to suffer from cytokinesis defects leading to for example multinuclei spermatids and polypoid follicle cells (Castrillon and Wasserman, 1994). Studies in Diaph depleted *D. melanogaster* cells revealed that these defects were caused by failure in forming a contractile ring during cytokinesis (Afshar et al., 2000; Giansanti et al., 1998).

Fourth, the role of mammalian formin Fmnl1 in cells or *M. musculus* has not yet been thoroughly studied. However, it was shown that depletion of Fmnl1 in cultured cells leads to impaired cell adhesion (Mersich et al., 2010), increased F-actin content, and fragmentation of the Golgi complex (Colon-Franco et al., 2010).

Finally, the Arp2/3 complex is conserved across species. Both in *S. cerevisiae* and *S. pombe* deletion of the genes encoding the Arp2/3 subunits leads to lethality or major growth defects (Morrell et al., 1999; Winter et al., 1997). Developing *D. melanogaster* embryos defective in the Arp2/3 complex functionality have disruptions in multiple structures including in the blastoderm and eye and do not reach adulthood (Hudson and Cooley, 2002; Zallen et al., 2002). Depletion of the Arp2/3 complex in developing *C. elegans* leads to disruption of ventral closure and results also in lethality (Sawa et al., 2003). In cultured HeLa cells Arp2/3 depletion by RNAi also leads to death (Harborth et al., 2001).

From the available gene silencing methods, we found that using pGIPZ shRNA constructs was the most attractive approach because the vector co-

expresses a fluorophore (GFP or BFP) together with the shRNA and therefore detection of cells that have been transfected is easy. In addition pGIPZ shRNA constructs can be used to produce stable cell lines that can be selected with puromycin.

The main challenge in performing the shRNA miniscreen was to determine what phenotypic changes would be expected when a nucleator responsible for cortex assembly is depleted. We envisaged two possible phenotypes: i) if a nucleator involved in cortex assembly is silenced, the actin cortex should be depleted in F-actin and therefore weaker leading to larger blebs, ii) alternatively, changes in the microstructural organisation of actin in the cell cortex could lead to disruption of myosin contractility and therefore lead to smaller blebs. If the cortex is completely lost or contraction is completely prevented, the most dramatic phenotype that could occur would be a complete cessation of blebbing or cell death. First, to determine the phenotypic changes to expect when the cells have a weaker cortex, I treated the blebbing cells with a low dose of cytochalasin D (40nM), a drug that stops elongation by binding to the barbed ends of actin filaments (Flanagan and Lin, 1980). After few minutes in the presence of the drug, the cells reached a new steady state and formed very large blebs, which were still able to reassemble a cortex and retract (Fig. 4.6A). Thus large blebs can be expected when cortical actin is reduced for example due to nucleation depletion. Second, it has been reported that perturbation of cortical contractility by myosin inhibition leads to formation of small blebs (Charras et al., 2008). Hence, if the cortical F-actin meshwork topology has changed and myosin contractility is disrupted a small bleb phenotype can be expected. These observations advised me to concentrate on the bleb size when analyzing the phenotype of knockdown cells and confirmed that blebs are good reporters of cortical perturbations.

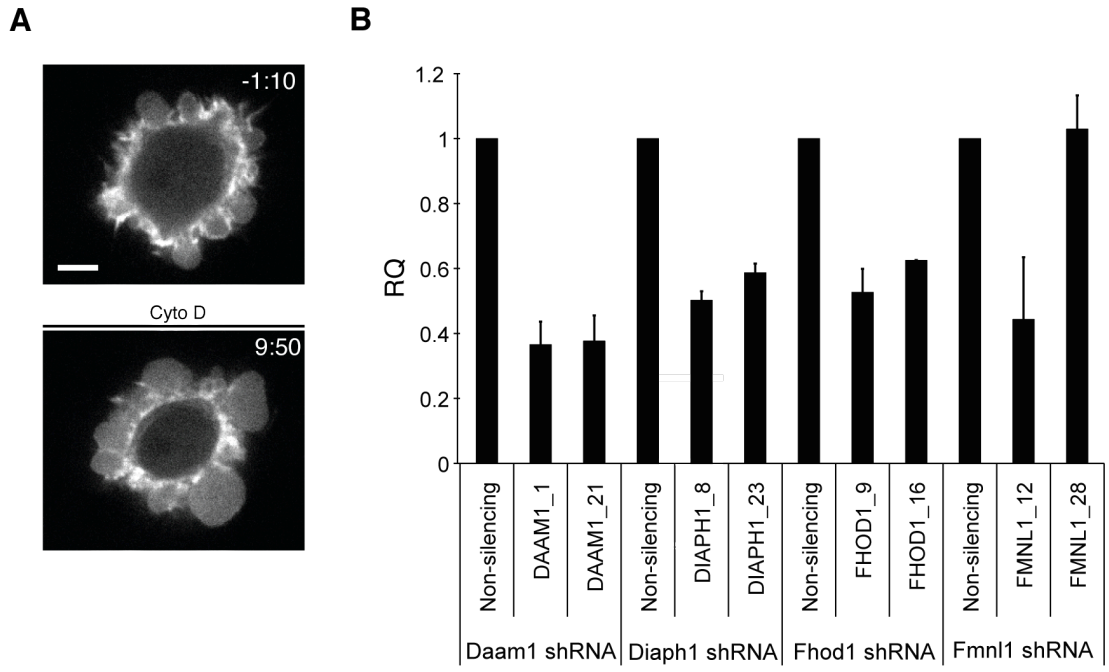

Figure 4.6: Controls for the shRNA mini-screen.

A. Cytochalasin treatment of M2 blebbing cells stably expressing actin-GFP. 40nM cytochalasin D was added at timepoint 0:00. Time is given as min:sec. After treatment cells displayed large blebs suggesting a weaker cortex. Scale bar 5µm.

B. mRNA abundance measured by quantitative real-time PCR in M2 cells after 72h of transfection with shRNA constructs. Graph shows gene expression levels relative to control non-silencing shRNA construct (RQ). Abundance was normalised to GAPDH mRNA levels. Differences were significant if relative mRNA abundance (RQ) was reduced by at least 40%.

In the shRNA screen, I used a minimum of three separate shRNA constructs for each nucleator and as a negative control, non-silencing shRNA. For each nucleator (two shRNAs for each nucleator) we first verified by quantitative real-time PCR (carried out by Dr. Romeo and Dr. Roux) that the target mRNA levels were reduced after 72h of transfection (Fig. 4.6B). The total RNA was purified from a mixed population of silenced (transfected) and non-silenced

(non-transfected) cells. Therefore we were satisfied if higher than 40% reduction in mRNA level was detected and found, that all the shRNAs caused significant reductions in mRNA level of their target genes with the exception of Fmnl1_08 shRNA (Fig. 4.6B).

In the analysis, I grouped together all the separate shRNA constructs for each nucleator, because visually no significant differences between shRNA constructs were detected, and categorised the transfected cells according their bleb size into large, normal sized, or small bleb categories. I compared the distribution of cells in these categories with non-silencing shRNA after normalising the number of cells to the control. Finally, I calculated the significance of changes in distribution compared to non-silencing control (Table 4.2) with a chi-test and found, that transfection with shRNAs targeting Fhod1 or Fmnl1 led to no detectable changes in bleb size compared to non-silencing control (Table 4.2). shRNAs targeting Daam1 led to a significant increase in cells displaying normal sized blebs ($p<0.01$, Table 4.2), suggesting some other role in the cortex or cell membrane than actin nucleation. Interestingly, actin nucleation activity of the FH2 domain of Daam1 has been shown to be weak (Lu et al., 2007) further suggesting that Daam1 does not act as a nucleator in the cell cortex. Although the main function of formins in the cell appears to be actin nucleation, some formins have been shown to bundle or sever actin filaments *in vitro* (Harris and Higgs, 2006; Harris et al., 2004), however such activities have not yet been confirmed in cells. Future studies are needed to determine if for example Daam1 could carry out some of these alternative functions in cells.

PHENOTYPE	Observed (number of cells in each category)	Expected number of cells in each category based on control	P – VALUE (CHITEST)
	CONTROL (non-silencing shRNA)		
Normal	51		
Large blebs	11		
Small blebs	7		
	DAAM1 shRNA		
Normal	126	96.8	3.7×10^{-8}
Large blebs	1	20.9	
Small blebs	4	13.3	
	DIAPH1 shRNA		
Normal	37	48	4.3×10^{-7}
Large blebs	26	10.4	
Small blebs	2	6.6	
	FHOD1 shRNA		
Normal	34	28.8	0.13
Large blebs	2	6.2	
Small blebs	3	4.0	
	FMNL1 shRNA		
Normal	22	19.2	0.07
Large blebs	0	4.1	
Small blebs	4	2.6	

Table 4.2: Significance of the phenotypes in the shRNA screen

Cells transfected with the shRNA construct of interest (separate shRNAs grouped together for the analysis) were categorized as having normal blebs, displaying large blebs, and displaying small blebs. For each targeting shRNA construct, observed distributions were compared to expected numbers based on the categorization observed in non-silencing shRNA controls using a chi-square test. Differences were considered significant for $p<0.01$.

Transfection with shRNAs targeting the ACTR3 subunit of the Arp2/3 complex led to high cell-death rate consistent with reports by others (Goley and Welch, 2006; Harborth et al., 2001) and the results are therefore not included in Table 4.2. High cell death rate was detected as early as 24h after transfection suggesting the Arp2/3 complex is essential for cell survival even on relatively short timescales. Although extensively studied in lamellipodia during migration, the Arp2/3 complex is involved in many functions of the cell including endocytosis and membrane trafficking (Kaksonen et al., 2003; Kaksonen et al., 2005; Merrifield, 2004; Merrifield et al., 2005; Chen et al., 2004; Fucini et al., 2002; Luna et al., 2002; Matas et al., 2004) and is therefore likely to be essential for cell survival.

Finally, cells expressing shRNAs targeting Diaph1 displayed very large blebs that were still able to reform a cortex and retract. This phenotype resembled that seen with low dose cytochalasin D treatment suggesting the cortex was weaker in Diaph1 depleted cells (Table 4.2, $p<0.01$, Fig 4.7A, Movies 2 and 3). Large blebs led to a reduction in cell body area in Diaph1 depleted cells compared to non-silencing control and the phenotype was observed with a penetrance of ~40%. Importantly, the large bleb phenotype was observed with four out of the four shRNAs targeting Diaph1. To quantitatively characterize the Diaph1 silencing phenotype, I compared bleb size in cells expressing Diaph1 targeting shRNA to non-silencing shRNA by measuring the ratio of the area of blebs to the area of the cell body. Thus, I first produced time-projected images of 3min movies of Diaph1 shRNA or non-silencing shRNA transfected cells. Then the cell body area was marked manually in the time-projected images by following the position of the cortex and finally the image was thresholded to enable the calculation of the number of pixels in the bleb and cell body area (Fig. 4.7B). The ratio of bleb versus cell body surface area was calculated from the amount of pixels in the bleb area (pixels outside of the marked cortex) and cell body (pixels inside of the marked cortex) (Fig. 4.7B). Cells expressing Diaph1 shRNA had significantly larger bleb/cell body area ratios when compared to cells expressing non-

silencing shRNA (n=97 and 66 respectively, p<0.01, Fig. 4.7C) and this was two-fold larger when we restricted our analyses to cells with a visibly larger bleb phenotype (n=40 out of 97 cells).

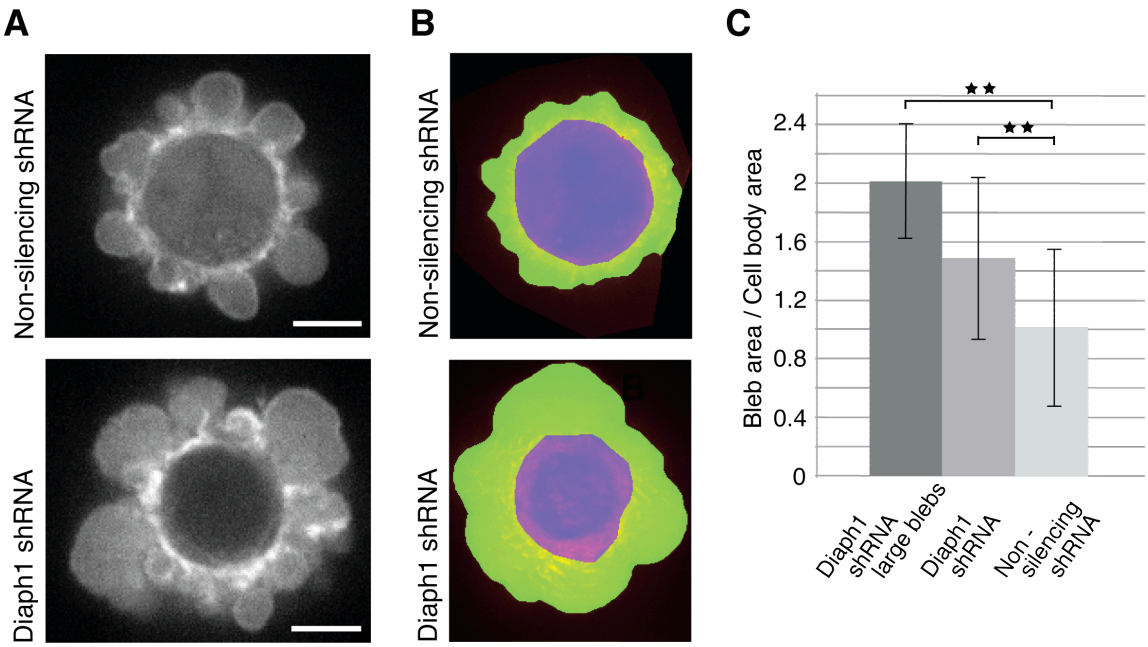

Figure 4.7: Silencing Diaph1 in M2 cells leads to formation of large blebs.

A. Live confocal microscopy images of M2 cells stably expressing actin-GFP. One cell is transfected with non-silencing shRNA and the other with shRNA targeting Diaph1. Cells expressing Diaph1 shRNA form very large blebs. Scale bar 5µm.

B. Time-projected images of Diaph1 shRNA or non-silencing shRNA transfected cells were thresholded for quantification. In the analysis the area outside the cell cortex (green) was called the bleb area and the area inside the cell cortex (purple) was called the cell body area.

C. Ratio of bleb area to cell body area in control and Diaph1 shRNA cells. Quantification of the Diaph1 phenotype revealed that on average the bleb area of the Diaph1 depleted cells was twice as large as in the control cells. Data are derived from: Diaph1 shRNA large bleb phenotype n=40 cells, Diaph1 shRNA n=97 cells, non-silencing n=66 cells. Error bars indicate SD (**p < 0.01).

Reduced Diaph1 protein levels after 72h of transfection were confirmed by Western blotting (carried out by our collaborators Dr. Mate Biro and Dr. Ewa Paluch, MPI, Dresden) (Fig 4.8A). To gain further information on the Diaph1 depleted cells, I generated a stable clonal line expressing Diaph1 shRNA selecting cells with a large bleb phenotype. To verify that the large bleb phenotype was caused by Diaph1 depletion alone, we also examined possible changes in the expression of mRNA of other nucleators in the Diaph1 shRNA stable cell line. We found that the cell line had 90% lower Diaph1 mRNA levels compared to control, but no significant change in mRNA levels of other nucleators (carried out by our collaborators Dr. Romeo and Dr. Roux) (Fig 4.8B) suggesting that Diaph1 depletion alone was causing the large bleb phenotype. In addition Western blotting (carried out by our collaborators Dr. Biro and Dr. Paluch) of the Diaph1 shRNA stable cell line showed a significant reduction in Diaph1 protein levels (Fig 4.8C).

Taken together our results show that Diaph1 contributes to cortex maintenance, because Diaph1 depletion leads to the formation of large blebs, suggesting a weaker cortex. In addition the data suggest that formins Daam1, Fhod1, and Fmnl1 do not participate in F-actin nucleation at the cortex.

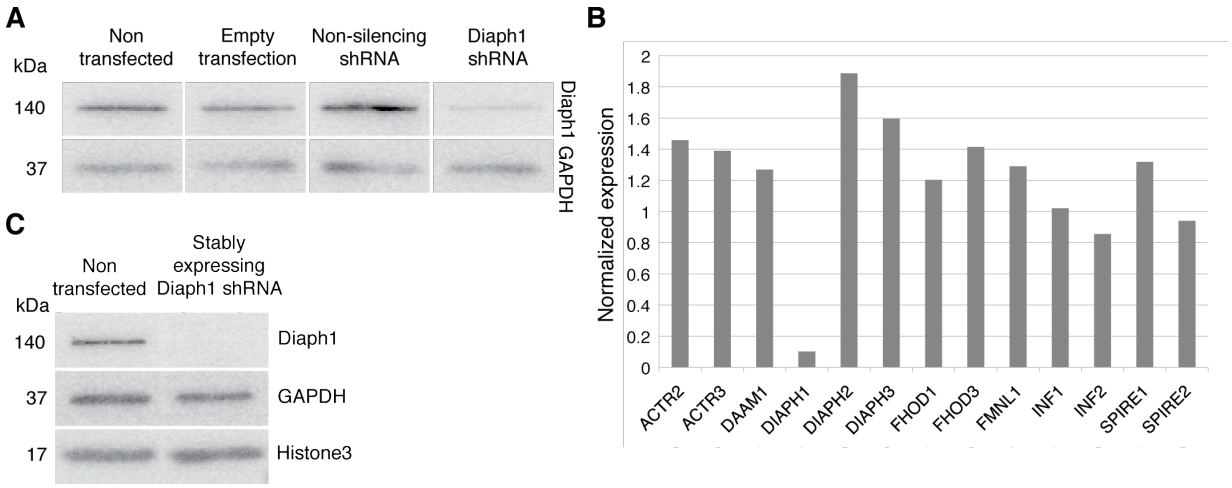

Figure 4.8: Diaph1 protein and mRNA levels were reduced after silencing with shRNA.

A. Immunoblot of M2 cells that are not transfected, have been transfected with no plasmid, transiently transfected with non-silencing shRNA, or with Diaph1 shRNA probed with anti-Diaph1 and anti-GAPDH. Cells were prepared for blotting 72 hours after transfections. Reduced Diaph1 protein levels were detected in cells transfected with Diaph1 shRNA but not in other conditions.

B. mRNA abundance in M2 cells stably expressing Diaph1 shRNA. The graph shows gene expression levels relative to the control shRNA construct. Abundance was normalised to GAPDH mRNA levels. Differences were considered significant if relative mRNA abundance was reduced by at least 40% or increased by at least 100%. No difference in mRNA expression of other nucleators other than Diaph1 was detected.

C. Immunoblot of non-transfected M2 cells and M2 cells stably expressing Diaph1 shRNA probed with anti-Diaph1, anti-GADPH, and anti-Histone3. Diaph1 protein levels in M2 cells stably expressing Diaph1 shRNA are significantly reduced compared to non-transfected controls.

4.3.1 Formin Diaph1 is tightly bound to actin in the cortex and appears to be recruited to the membrane independently of F-actin

I was only able to reveal the cortical localisation of full length Diaph1-GFP with speckling microscopy suggesting that Diaph1 is tightly regulated in the cells. To gain deeper understanding of recruitment and function of Diaph1 at the cortex, I carried out a domain analysis of Diaph1. The N-terminus of Diaph1 is composed of a GTPase binding domain and an FH3 domain, which both overlap with a diaphanous inhibitory domain (DID) (Fig. 4.9A). The FH3 domain contains a central coiled coil motif and amino acids needed for dimerisation of Diaph1 (Campellone and Welch, 2010). The FH3 is followed by the FH1 domain responsible for providing profilin-actin to the FH2 domain. The FH2 domain binds to the barbed end of actin filaments and is needed for the nucleation and elongation activity of the formin. Finally, the diaphanous autoinhibitory domain (DAD) is located close to the C-terminus of the protein (Fig. 4.9A). Diaph1 is regulated by an intramolecular interaction between the DID and the DAD domain (Watanabe et al., 1999) leading to a closed conformation, where the FH2 domain is masked and the formin is inactive. Upon RhoA binding to the GTPase domain, DID-DAD binding is released and Diaph1 becomes active (Watanabe et al., 1999).

First, we asked if the cytoplasmic localisation of overexpressed Diaph1-GFP was due to protein being in mainly inactive conformation. To study this I cloned Diaph1ΔDAD-GFP thereby releasing the DID-DAD interaction leading to constitutively active (CA) form of Diaph1 (Watanabe et al., 1999) (Fig. 4.9A). CA-Diaph1 lacked cytoplasmic localisation and localised strongly to the cell membrane (Fig. 4.9B, Movie 4), suggesting that Diaph1 is indeed tightly regulated in cells. CA-Diaph1 localised to the membrane at all stages of bleb lifecycle including nucleation and expansion when no F-actin is present in the bleb suggesting its recruitment is independent of F-actin (Fig. 4.9B, time point 0s). Next I asked if actin was involved in Diaph1 recruitment to the membrane and treated CA-Diaph1 transfected cells with doses of cytochalasin D (5μM) sufficient to disrupt the whole cortex. Cytochalasin D

treatment did not alter CA-Diaph1 localisation (Fig. 4.9C) suggesting that Diaph1 is recruited to the membrane independently of actin, consistent with a nucleation role.

Finally I asked which domains of Diaph1 are necessary for membranous localisation. To answer this, I followed the localisation of GBD (aa 1-260), GBD+FH3 (aa 1-464), FH1+FH2 (aa 583-1141), and DAD (aa 1183-1203) domains of Diaph1. The GBD domain alone displayed only weak localisation to the membrane (Fig. 4.9D), whereas GBD+FH3 was sufficient for membranous localisation of Diaph1 (Fig. 4.9E), consistent with previous report (Copeland et al., 2007). Both the FH1+FH2 and the DAD domains displayed only cytoplasmic localisation. Interestingly, overexpressing FH1+FH2 did not induce formation of detectable actin filaments in the cytoplasm, possibly due to lack of a dimerisation domain.

Previously it has been shown a point mutation at the GBD domain, leading to defective RhoA binding of mDia1 (Diaph1 in *M. musculus*), caused only a partial loss of N-terminal mDia1 from the cell membrane (Seth et al., 2006) suggesting RhoA independent mechanisms for membrane targeting. Recently it was shown that mDia1 can directly bind to the lipids at the cell membrane (Ramalingam et al., 2010). It was shown that at the very N-terminus of mDia1 is a basic domain (aa 1-60) that contains two clusters of positively charged residues, which can bind to phosphatidylserine and PIP_2 at the cell membrane (Ramalingam et al., 2010). Further, not only the N-terminal regions but also residues at the C-terminus of mDia1 were shown to bind PIP_2. This interaction appeared to inhibit the activity of mDia1 and thus it was proposed that the formin stays active only while the C-terminus stays free from the membrane, suggesting a regulatory mechanism for mDia1 elongation (Ramalingam et al., 2010).

When formins elongate actin filaments, they stay bound to the barbed ends (Pruyne et al., 2002; Sagot et al., 2002). We found that the CA-Diaph1

localised to the bleb membrane even when no F-actin was visible and thus we asked if CA-Diaph1 was bound to the actin cortex once it had reassembled. During bleb retraction, the fluorescence intensity of GFP-actin increases due to concentration of F-actin over a smaller area (Charras et al., 2008). If CA-Diaph1 was strongly bound to the cortex, similar enrichment to actin should be detected, whereas if it was only membrane bound, only weak enrichment should be observed due to lipids flowing in the plane of the membrane during retraction. Therefore I compared fluorescence intensities at the bleb cortex at the beginning and end of retraction of actin, CA-Diaph1, GBD+FH3 (that lacks an actin binding domain), and a membrane targeted GFP (GFP-CAAX). I observed that both actin and CA-Diaph1 displayed a strong enrichment after bleb retraction (+75% and +65% respectively, n=12 cells) and thus was much greater than either GBD+FH3 or CAAX (both +20%, n=11 cells) (Fig. 4.10A).

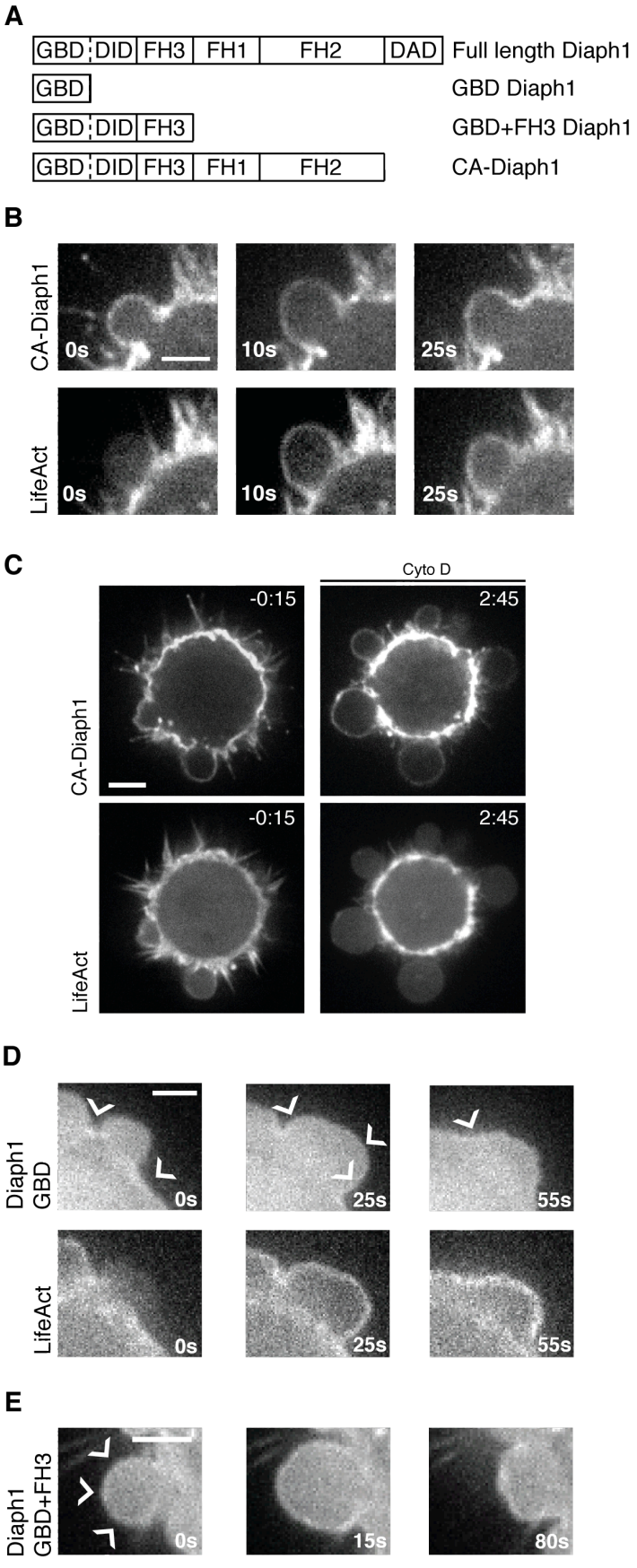
A
GBD
DID
FH3
FH1
FH2
DAD
Full length Diaph1
GBD Diaph1
GBD+FH3 Diaph1
CA-Diaph1
B
CA-Diaph1
LifeAct
0s
10s
25s
C
Cyto D
-0:15
2:45
CA-Diaph1
LifeAct
D
Diaph1 GBD
LifeAct
0s
25s
55s
E
Diaph1 GBD+FH3
0s
15s
80s

Figure 4.9: Localisation of Diaph1 domains in M2 cells.

In all images, times are given in sec and scale bars are 3µm, except in C where time is give in min:sec and scale bar is 5µm.

A. Full length Diaph1 consists of a GTPase binding domain (GBD), a diaphanous inhibitory domain (DID), Formin homology -3, -1, and -2 domains (FH3, FH1, FH2), and a diaphanous autoinhibitory domain (DAD). Domains used in localisation studies are presented (GBD and GBD+FH3 Diaph1). CA-Diaph1 lacks the DAD domain leading to constitutively active Diaph1.
B. Constitutively active Diaph1 localises to the cell membrane throughout the bleb lifetime even during nucleation and expansion when no F-actin is visible in the bleb (time point 0s). Compare LifeAct channel and CA-Diaph1 channel at 0s.
C. CA-Diaph1 localises to the bleb membrane upon cytochalasin D treatment even when no actin gets recruited to the blebs. 5µM cytochalasin D was added at time point 0:00.
D. GTPase binding domain (GBD) of Diaph1 displays only weak localisation to the membrane (arrowheads).
E. GTPase binding domain together with FH3 domain localises to the cell membrane (arrowheads) throughout the bleb lifetime.

To verify my results and get an independent confirmation that CA-Diaph1 binds to the cortex, a fluorescence recovery after photobleaching (FRAP) analysis on CA-Diaph1, actin, and the GBD+FH3 domain was carried out together with Marco Fritzsche, a fellow PhD student in the lab. We reasoned that if CA-Diaph1 is bound to the actin cortex the turnover rate of CA-Diaph1 should be significantly slower than that of the GBD+FH3 domain, which lacks an actin binding domain, but similar to actin. The average half-time of fluorescence recovery for CA-Diaph1 ($t_{1/2}$=13.6±2s, n=14 cells) was on average four-fold longer than for membrane bound GBD+FH3 ($t_{1/2}$=3.5±1.2s, n=15 cells, $p<0.01$ compared to CA-Diaph1) but comparable to actin ($t_{1/2}$=14.1±1s, n=25 cells, p=0.87) (Fig. 4.10B). The immobile fraction for CA-Diaph1 was significantly larger than for GBD+FH3 (Fig. 4.10C) suggesting CA-Diaph1 is bound to the actin cortex and detaches from it slowly.

Finally, having shown localisation of full length Diaph1 speckles, CA-Diaph1, and the Arp2/3 complex in M2 cells, I verified their localisation in metaphase arrested HeLa cells. Consistent with my results in M2 cells, Diaph1 speckles (Fig. 4.11A) and CA-Diaph1 (Fig. 4.11B, arrows) localised to the actin cortex in HeLa cells. Interestingly live imaging methods did not reveal the cortical localisation of the Arp2/3 complex in M2 cells, but in live metaphase HeLa cells ARPC1-GFP localises to the actin cortex (Fig. 4.11C).

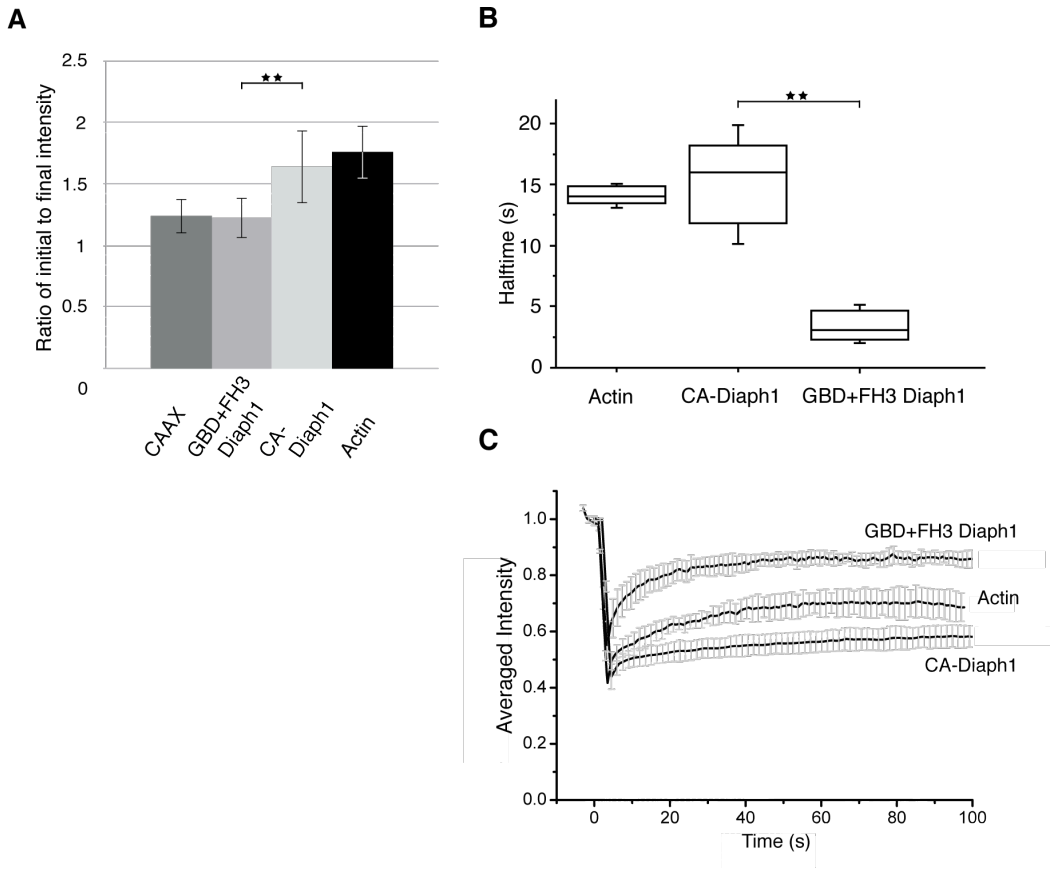

Figure 4.10: Diaph1 binds to the actin cortex.

A. Fluorescence intensity enrichment of GFP-tagged CAAX motif, Diaph1 GBD+FH3, CA-Diaph1, and actin at the bleb cortex during retraction. The ratio of initial to final intensity was computed as mean fluorescence intensity at the end of retraction divided by mean fluorescence intensity at the onset of retraction (**p=<0.01).

B. Half-times of fluorescence recovery after photobleaching (FRAP) for GFP-tagged actin, CA-Diaph1 and Diaph1 GBD+FH3 domain at the cortex of M2 cells. Data are plotted as box plots and derived from multiple cells (actin n=25, CA-Diaph1 n=14, GBD+FH3 n=15). Bars indicate the maximum and minimum measurements (**p= < 0.01).

C. Average fluorescence recovery curves after photobleaching for GFP-actin, GFP-CA-Diaph1 and GFP-GBD+FH3 domain at the cortex of M2 cells. Graphs are averaged over 25, 14, and 15 cells respectively.

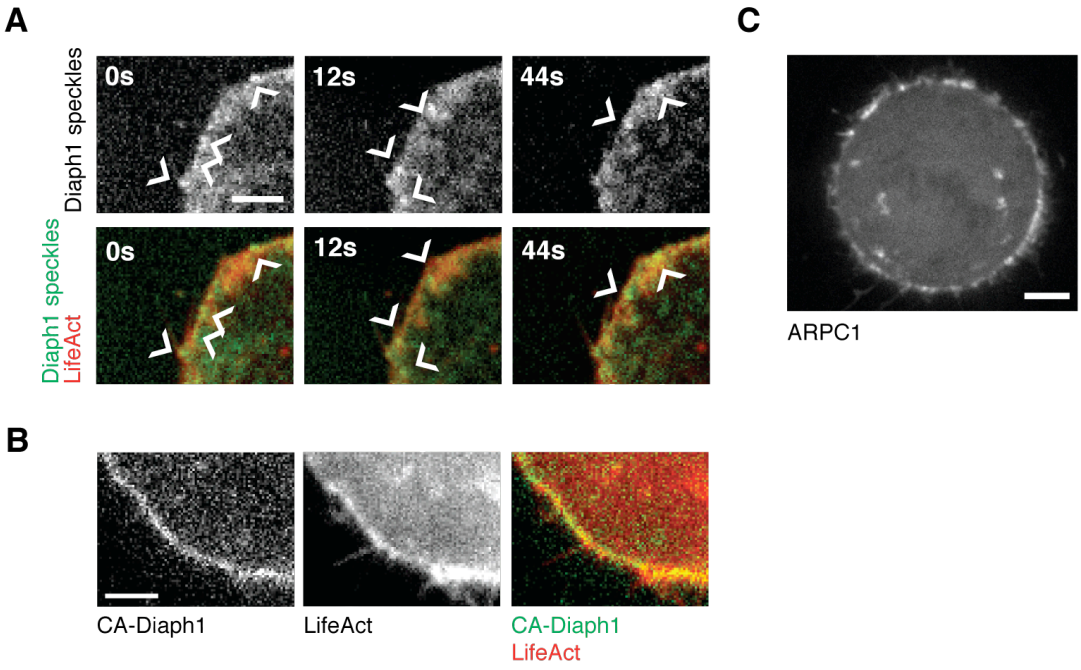

Figure 4.11: Diaph1 localises to the cell cortex in metaphase HeLa cells.

A. Single molecule imaging of full-length Diaph1-GFP (green) in metaphase arrested HeLa cells stably expressing LifeAct-Ruby (red). Diaph1 speckles localise to the cell cortex. Speckles are indicated with arrowheads. Scale bar 3µm.

B. Localisation of CA-Diaph1-GFP (green) in HeLa cells stably expressing LifeAct-Ruby (red). CA-Diaph1 localises to the cell cortex of metaphase HeLa cells. Scale bar 3µm.

C. Localisation of ARPC1-GFP in HeLa cells. ARPC1 localises to the cell cortex of live metaphase HeLa cells. Scale bar 5µm.

Taken together, our data show that Diaph1 is recruited to the cell membrane independently of F-actin and binds to the cellular actin cortex. Diaph1 activity appears to be tightly regulated because localisation of full length Diaph1 was only observed when utilizing single molecule imaging techniques, suggesting that only a small portion of endogenous Diaph1 is bound to the cortex at any given time. What pathways regulate Diaph1 at the cortex remain to be thoroughly investigated. Interestingly RhoA is has been shown to release the autoinhibition of Diaph1 (Lammers et al., 2005; Otomo et al., 2005). In addition RhoA is present on bleb membranes (Charras et al., 2006) and in metaphase HeLa cortex (Nishimura and Yonemura, 2006). Finally, the domain analysis of Diaph1 revealed that GBD+FH3 domain was sufficient to target Diaph1 to the cell membrane. These data suggest that RhoA may indeed be the main regulator of Diaph1 at the cortex. However RhoC might also participate in Diaph1 activation at the cortex as RhoC has been shown to bind Diaph1 (Rose et al., 2005) and is associated with the cortex (see chapter 5).

4.4 Formin Diaph1 and the Arp2/3 complex are components of the actin cortex

Although a clear cortical weakening phenotype was observed in Diaph1 knockdown cells, the cells still retained a visible cortex and blebs were able to retract, suggesting that other actin nucleators may play a role in cortex maintenance. To identify other proteins involved and confirm the importance of Diaph1, we undertook a proteomic analysis of the cell cortex.

The main challenge in performing the proteomic analysis was isolating a cell fraction enriched in actin cortex and we reasoned that as blebs reassemble a cortex and appear devoid of cell organelles, they could act as a cortex rich fraction for proteomic analyses. Hence, we optimised a protocol to isolate blebs from whole cells. When blebbing cells are exposed to high concentration of actin depolymerising drugs, such as cytochalasin D or latrunculin B, they form very large and fragile blebs that cannot retract

(Charras et al., 2006). When exposed to fluid shear stresses by shaking, these blebs pinch off from the cells. By scaling up this approach, large amounts of separated blebs can be obtained and purified by ultracentrifugation on a Ficoll gradient. After centrifugation and washing, the blebs were exposed to the bacterial toxin Hemolysin A to create membrane pores large enough to allow entry of exogenous ATP and ions but small enough to prevent protein leakage. This protocol allowed us to purify blebs that formed a well-defined actin cortex (Fig. 4.12A) ultrastructurally similar to whole cell cortices when studied with scanning electron microscopy (Fig. 4.12B). Isolated bleb cortices were sensitive to actin depolymerising drugs (cytochalasin and latrunculin, Fig. 4.12C) indicating that actin filaments were turning over. We concluded that isolated blebs did indeed represent a good model for cortex proteomics.

To study the proteomics of the cortex, we collaborated with Dr. Romeo and Dr. Roux to carry out mass spectrometry analysis on the separated blebs. Analysis of the detergent insoluble fraction of isolated blebs (i.e the actin cortex) revealed the presence of only two nucleators associated with the actin cortex: the formin Diaph1 and the Arp2/3 complex (Table 4.3).

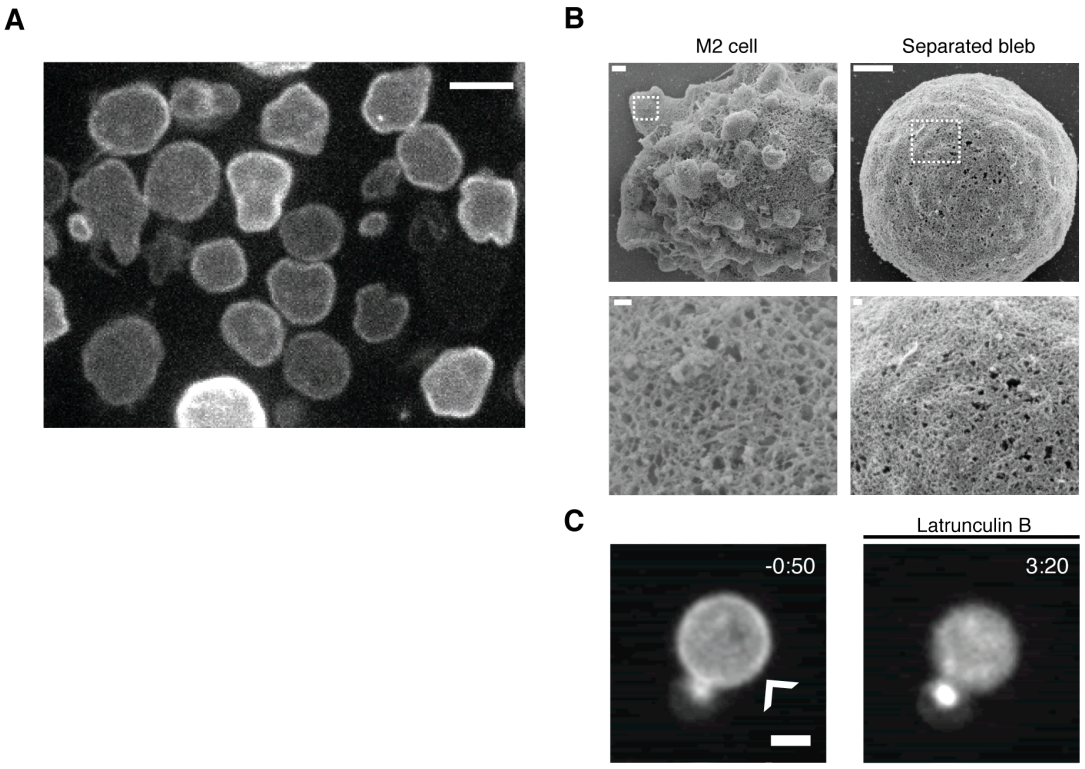

Figure 4.12: A dynamic actin cortex forms in separated blebs and is similar to the cell cortex.

A. Blebs separated from blebbing M2 cells stably expressing LifeAct-Ruby after purification. Scale bar 5µm.

B. Scanning electron microscopy (SEM) image of M2 cell cortex (left) and separated bleb (right). Lower row images are magnified from the boxed areas in the upper row images. Cell cortex and separated bleb cortex appear similar. Scale bars on upper row=1µm and on lower row=100nm.

C. Separated bleb from an M2 cell stably expressing LifeAct-Ruby treated with 750 nM latrunculin B (added at time point 0:00). Prior to latrunculin treatment, a well-defined actin cortex was present (arrowhead), it then disappears upon latrunculin B treatment (time point 3:20). Times are given as min:sec. Scale bar 3µm.

	Protein	Accession no	kDa	Average no. of peptides	PAI
Arp2/3 complex	**ACTR2**	**P61160**	**44.7**	**16.4**	**36.65**
	ACTR3	**P61158**	**47.3**	**15.0**	**31.61**
	ARPC1	**Q92747**	**41.5**	**5.8**	**13.88**
	ARPC2	**O15144**	**34.4**	**14.9**	**43.33**
	ARPC3	**O15145**	**20.5**	**8.2**	**40.19**
	ARPC4	**P59998**	**19.7**	**2.9**	**14.50**
	ARPC5	**O15511**	**16.3**	**7.1**	**36.65**
	DIAPH1	**O60610**	**140.0**	**19.2**	**43.82**
WAVE complex	ABI1	Q8IZPO	55.0	2.1	3.90
	BRCK1	Q8WUW1	8.7	0.0	0.00
	NAP1	**Q9Y2A7**	**12.9**	**12.4**	**95.98**
	SRA1	**Q7L576**	**14.5**	**19.2**	**132.35**
	WAVE2	Q9Y6W5	54.3	2.8	5.17
	Cortactin	**Q14247**	**61.5**	**12.2**	**19.82**
	DAAM1	Q9Y4D1	123.4	0.0	0.00
	DIAPH3	Q9NSV4	136.9	0.0	0.00
	FHOD1	Q9Y613	126.6	0.0	0.00
	FMNL1	O95466	121.9	0.2	0.14
	INF1	Q9C0D6	124.8	0.0	0.00
	INF2	Q27J81	135.6	0.0	0.00
	SPIRE1	Q08AE8	85.6	0.0	0.00
	SPIRE2	Q8WWL2	79.7	0.0	0.00

Table 4.3: Diaph1, the Arp2/3 complex, and the Arp2/3 complex activators WAVE complex and cortactin are components of the cortex.

Actin nucleators and nucleation promoting factors found in the detergent insoluble fraction of separated blebs. All subunits of the Arp2/3 complex and Diaph1 were found to associate with the cortex together with two subunits of the WAVE complex (NAP1 and SRA1) and cortactin, which are Arp2/3 complex nucleation promoting factors. Subunits of the same complex and protein isoforms are grouped together. Peptide numbers are averaged over three separate experiments. Protein names in bold indicate proteins detected with high certainty. Protein Abundance Index (PAI) was calculated based on spectral count as follows: PAI = spectral count/MW, where MW corresponds to the protein molecular weight (kDa), which was used to adjust for differences between proteins in the number of observable peptides.

All seven subunits of the Arp2/3 complex were identified along with nucleation promoting factors cortactin and the Wave complex (Table 4.3, subunits SRA1 and NAP1) (Gautreau et al., 2004; Uruno et al., 2001), consistent with reports that silencing subunits of the WAVE complex gives rise to blebbing, reflective of a weakened actin cortex (Derivery et al., 2008).

4.5 The Arp2/3 complex also participates in the actin cortex assembly

Having been unable to study the phenotypic changes (other than cell death) in M2 cells upon Arp2/3 complex depletion by shRNA, I decided to perturb the Arp2/3 complex by acute treatment with the small molecule inhibitor of Arp3 CK666 (Nolen et al., 2009). First, I tested the ability of CK666 to inhibit lamellipodium formation, a well-characterised Arp2/3 complex -dependent structure. In differentiated HL60 neutrophils, I observed rapid loss of lamellipodia in 70% of cells upon drug addition (t=90s, n=18 cells, Fig 4.13, Movie 5).

In 52% of M2 cells inhibition of the Arp2/3 complex by CK666 led to formation of smaller blebs than in control cells (Fig. 4.14A and B, Movie 6), consistent with the second phenotype we envisaged for cortical nucleator depletion. In a further 26% of CK666 treated M2 cells, formation of broad bean-shaped blebs, rather than quasi-spherical blebs, was observed (Fig. 4.14A and C, Movie 7) also suggesting a perturbation of the cortex consistent with cortical weakening. Other phenotypes (10% of treated cells) included cells that stopped blebbing or displayed less blebs than normally (Fig. 4.14A) also consistent with loss of contractility. Finally in only 14% of M2 cells, no phenotypic changes were detected upon CK666 treatment (Fig. 4.14A). In summary, in 78% of CK666 treated blebbing cells phenotypic changes were observed consistent with perturbation of cortex function.

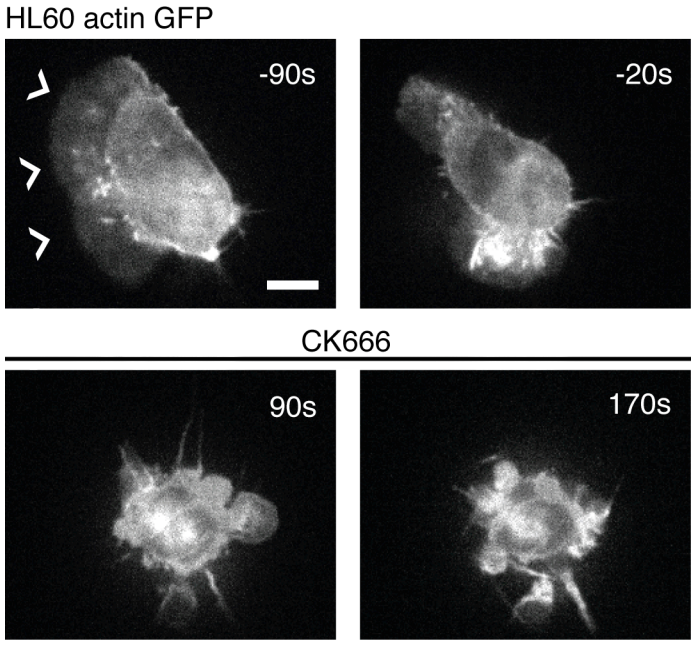

Figure 4.13: CK666 disrupts lamellipodium formation in HL60 neutrophils.

HL60 cells stably expressing actin-GFP were treated with CK666. The drug was added at time point 0s. Prior to CK666 addition (-90s and -20s) HL60 cells migrated by forming lamellipodia (-90s arrow heads) on fibronectin coated coverslips in the presence of fMLP chemoattractant. Upon drug addition (100µM), lamellipodial formation was disrupted (90s and 170s). Times are given in sec. Scale bar 5µm.

A common feature of all phenotypes was a loss of cortical actin fluorescence intensity and a concomitant increase in cytoplasmic fluorescence in cells expressing actin-GFP. In images of cells expressing actin-GFP, cortical actin fluorescence results both from actin-GFP bound in the filaments within the cortex and free monomeric actin-GFP diffusing through the cortex. Hence, normalised cortical F-actin fluorescence can be estimated as $f=(F_{cortex}-F_{cytoplasm})/F_{cytoplasm}$ with F_{cortex} and $F_{cytoplasm}$ the mean fluorescence intensities of the cortex and cytoplasm respectively. Treatment of cells with CK666 led to a 64% decrease in normalised cortical actin fluorescence ($f_{DMSO}=1.3\pm0.2$, $f_{CK666}=1.1\pm0.1$, $p<0.01$, $n=30$ cells for each, Fig. 4.14D). Taken together, these observations suggest that the Arp2/3 complex is also involved in actin cortex nucleation.

In addition to Diaph1 our localisation, proteomic analysis, and drug treatments also revealed the presence of the Arp2/3 complex together with nucleation promoting factors WAVE and cortactin at the cortex. Arp2/3 complex knockdown was lethal upon shRNA treatment, but acute inhibition of the Arp2/3 complex by CK666 led to significant loss of cortical actin, suggesting that a substantial proportion of the cortex is nucleated by the Arp2/3 complex.

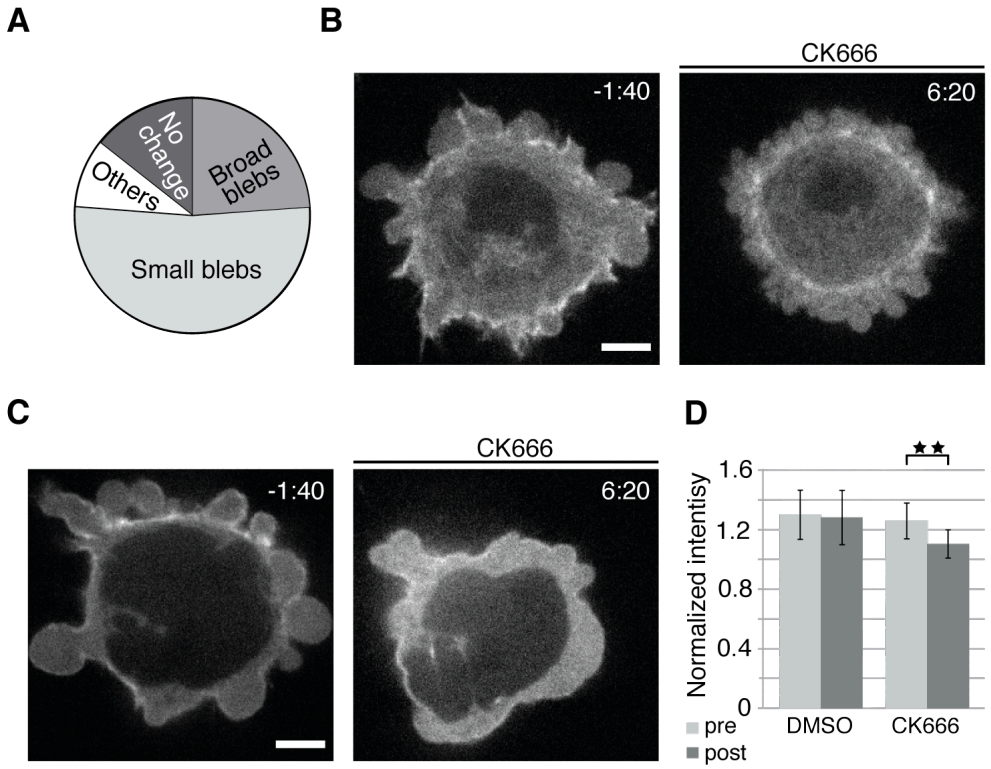

Figure 4.14: Treatment with CK666 led to loss of cortical F-actin in M2 cells.

A. Distribution of phenotypes after CK666 treatment in M2 cells. 'Others' include cells that stopped blebbing or formed less blebs than normally.

B. Small bleb phenotype in M2 cells stably expressing actin-GFP. 100µM CK666 was added at time point 0:00. Time is given in min:sec. Intensity scales were kept constant between images. See Movie 6.

C. Broad bean shaped bleb phenotype in M2 cells stably expressing actin-GFP. 100µM CK666 was added at time point 0:00. Time is given in min:sec. Intensity scales were kept constant between images. See Movie 7.

D. Ratio of average cortex fluorescence intensity to average cytoplasmic fluorescence intensity in M2 cells stably expressing actin-GFP pre and post treatment with DMSO or 100µM CK666. A significant change in the fluorescence ratio was detected with CK666. Data are derived from 30 cells for each experiment. Error bars indicate SD (**p= < 0.01).

4.6 Together the formin Diaph1 and the Arp2/3 complex are necessary to form the actin cortex

Considering that depletion of either the Arp2/3 complex or Diaph1 led to cortical defects, I asked if together they accounted for the majority of cellular cortical F-actin. When I depleted both nucleators simultaneously by exposing Diaph1 shRNA cells to CK666, I observed gross morphological defects consistent with near complete loss of cortical actin. Prior to addition of the drug, cells still retained a clear actin cortex along the cell body (Fig. 4.15A, arrow heads, t=-30s, Movie 8) and reformed cortex under the membrane of blebs. Following addition of CK666, cells lost their shape, displayed global oscillations, and retained only a few discernible foci of submembranous actin (Fig. 4.15A, t=4.40-7.00, Movie 9). Occasionally the nucleus appeared to be expelled from the cell body in a large bulge (Fig. 4.15A, t=6.00). In some cells, the remaining cortex aggregated to one side of the cell with no visible cortex on the other side and in others, cortex was lost entirely. Phenotypes with loss of visible cortex were called 'collapse' and this was observed in 34% of the Diaph1 shRNA cells treated with CK666 (Fig. 4.15B). A further 30% of cells displayed broad bean shaped blebs (Fig. 4.15B). Together 64% of all the Diaph1 shRNA cells treated with CK666 suffered from extensive cortical defects. Some CK666 treated Diaph1 shRNA cells displayed small blebs (26%) and the rest of the cells (10%) had either uncategorized phenotypic changes or no change in phenotype. Quantification of the ratio of cortical actin fluorescence intensity to cytoplasmic intensity revealed that nearly all cortical actin was lost with ratios approaching one after treatment (Fig. 4.15C, $[F_{cortex}/F_{cytoplasm}]_{CK666}$ = 1.06±0.13, $p<0.01$, n= 30 cells, DMSO: $[F_{cortex}/ F_{cytoplasm}]_{Control}$ = 1.19±0.22, n= 30 cells) down from 1.3 in control cells.

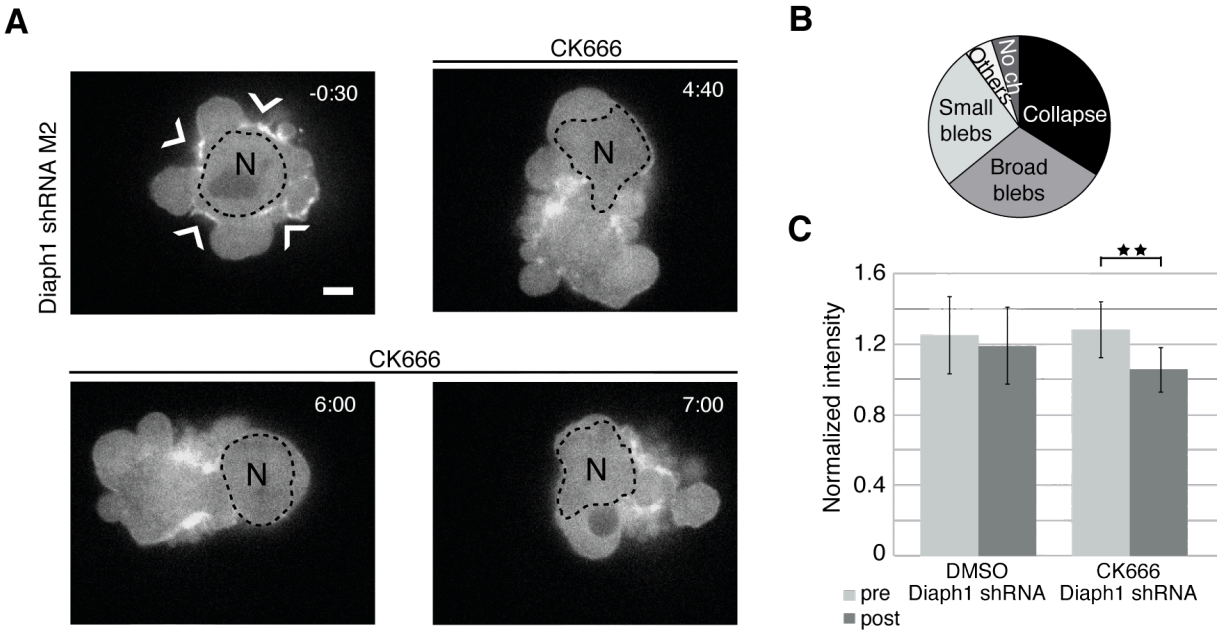

Figure 4.15: Diaph1 and Arp2/3 complex depletion together lead to cortical collapse and loss of cortex in M2 cells.

A. Treatment with CK666 in Diaph1 depleted M2 cell stably expressing actin-GFP leads to cortical collapse. Prior to drug addition cells still have a visible cortex (time -0:30, arrowheads). 100µM CK666 was added at time point 0:00 (min:sec). After drug addition cells displayed global oscillations and had lost nearly all cortex. The nucleus (N) is outlined with a dashed line. Scale bar 5µm.

B. Distribution of phenotypes after CK666 treatment in M2 cells transfected with Diaph1 shRNA stably expressing actin-GFP. Phenotype in A was categorised as a 'collapse' phenotype. Other phenotypes were seen also with CK666 alone (see Fig. 4.14).

C. Ratio of average cortex fluorescence intensity to average cytoplasmic fluorescence intensity in M2 cells stably expressing GFP-actin treated with DMSO or 100 µM CK666. The fluorescence intensity of cortex was nearly the same than the fluorescence intensity of cytoplasm after CK666 treatment (ratio close to 1). Data are derived from 30 cells for each experiment. Error bars indicate SD (**$p<0.01$).

4.6.1 Diaph1 and the Arp2/3 complex are needed for maintaining the F-actin content in the cortex

To gain further understanding of what fraction of cellular F-actin was contributed by each nucleator, we established a collaboration with Dr. Dale Moulding and Prof. Adrian Thrasher, ICH, UCL to measure the total cellular F-actin mass by flow cytometry of AlexaFluor647-phalloidin stained M2 cells in the presence or absence of Diaph1 and Arp2/3 complex (Fig. 4.16A, values and statistical comparisons are summarised in 4.16B). To be able to compare the F-actin content of depleted and control cells accurately, concurrent AlexaFluor647-phalloidin staining was carried out to remove the variation seen when samples are stained separately. To differentiate the depleted and control cells from one another, the control cells were stained with CFSE, a cell permeant fixable carboxyfluorescein cytoplasmic stain, prior to fixation.

Diaph1 depletion alone led to a 7.3±3.7% decrease in F-actin content and Arp2/3 complex inhibition alone to a 17.2±0.6% decrease ($p<0.05$ and $p<0.01$ respectively compared to control). When we depleted both nucleators simultaneously, cellular F-actin mass decreased by 27.7±4.1% ($p<0.01$), which was not very different from the addition of their individual effects (-24.5±4.3%). Consistent with this, actin depletion concomitant upon CK666 treatment was not significantly different in wild type cells compared to Diaph1 depleted cells ($p>0.05$) and actin depletion resulting from Diaph1 silencing was not significantly different in DMSO versus CK666 treated cells ($p>0.05$). Finally, expression of CA-Diaph1 led to a significant increase in total cellular F-actin mass (15.6±2.3%, $p<0.01$). Dr. Moulding carried out the flow cytometry measurements and did the statistical calculations.

A

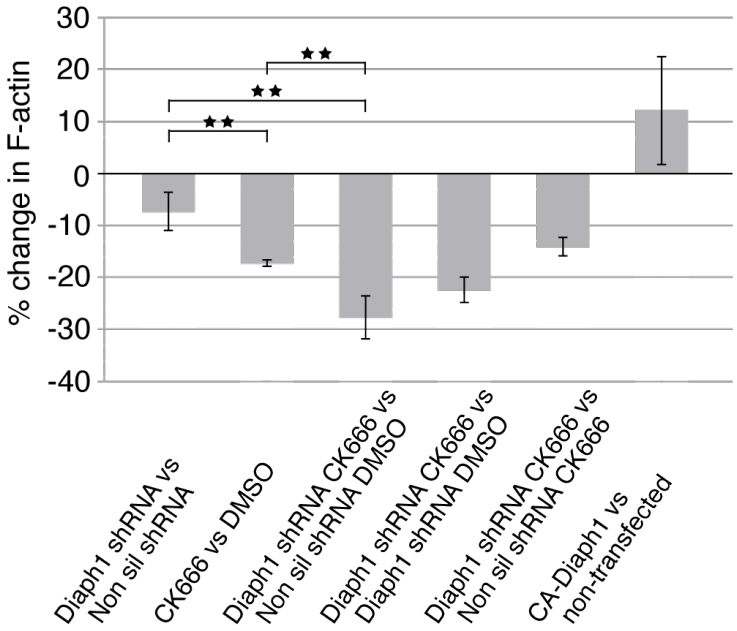

B

	TREATMENT	CHANGE IN F-ACTIN	P COMPARED TO 0	TREATMENT COMPARISON
1	Diaph1 shRNA **vs** Non-silencing shRNA	-7.3±3.7%	<0.05	1 vs 2: p<0.01 1 vs 3: p<0.01 1 vs 5: NS
2	CK666 **vs** DMSO	-17.2±0.6%	<0.001	2 vs 3: p<0.01 2 vs 4: NS
3	Diaph1 shRNA CK666 **vs** Non-silencing shRNA DMSO	-27.6±4.1%	<0.001	
4	Diaph1 shRNA CK666 **vs** Diaph1 shRNA DMSO	-22.32±2.5%	<0.001	2 vs 4 : NS
5	Diaph1 shRNA CK666 **vs** Non-silencing shRNA CK666	-14.0±1.8%	<0.001	1 vs 5 : NS
6	CA-Diaph1 **vs** Wild type cells	+12.1±10.4%	<0.001	

Figure 4.16: Diaph1 and Arp2/3 complex depletion decreases F-actin content in M2 cells.

A. Relative change in total cellular F-actin in M2 cells measured by flow cytometry resulting from treatments targeting Diaph1 and the Arp2/3 complex. Diaph1 and the Arp2/3 complex depletion led to decrease in F-actin fluorescence and CA-Diaph1 to an increase in F-actin content. All changes were significant compared to controls. Differences between treatments were examined using a one-way ANOVA with Bonferroni post-test. Errors bars indicate SD (**$p < 0.01$).
B. The changes in F-actin fluorescence intensity are averages from 3 independent experiments examining at least 5000 cells for each condition measured by flow cytometry. Statistical differences of the average change in F-actin fluorescence intensity were compared to 0 with a one-way ANOVA with Bonferroni post-test. Statistical differences between populations were calculated with a one-way ANOVA with Bonferroni post-test.

If one nucleator was upstream of the other, we would expect depletion of the upstream nucleator to contribute to the F-actin content approximately the same amount than the combined depletion of both nucleators. In contrast, if the nucleators act independently their effect on the F-actin content should be additive. When both nucleators were depleted simultaneously the decrease in F-actin mass was not very different from the addition of their individual effects, suggesting the nucleators act independently.

These results suggest that together Diaph1 and the Arp2/3 complex provide the majority of the F-actin cortex in blebbing melanoma cells and are necessary for cell shape maintenance. Interestingly, rapid loss of the actin cortex upon Diaph1 and Arp2/3 complex depletion suggests that, at homeostasis, cortex turnover is dependent on constant nucleation of new filaments and not just on treadmilling of pre-existing filaments.

4.6.2 Depletion of Diaph1 or the Arp2/3 complex leads to perturbation of actin cortex regrowth

To quantitatively study the role of Diaph1 and the Arp2/3 complex in metaphase cortex in HeLa cells we established collaboration with Dr. Mate Biro and Dr. Ewa Paluch, MPI, Dresden. They have developed a method where they induce a formation of a single bleb by laser ablation of the actin cortex of metaphase HeLa cell (Tinevez et al., 2009). The cortical site for laser ablation was always chosen perpendicular to the aligned chromosome plane in the cell (Tinevez et al., 2009). When the bleb had formed the rate of regrowth of the actin cortex was quantified by following F-actin fluorescence intensity under the bleb membrane using automated image segmentation algorithms (Fig. 4.17A).

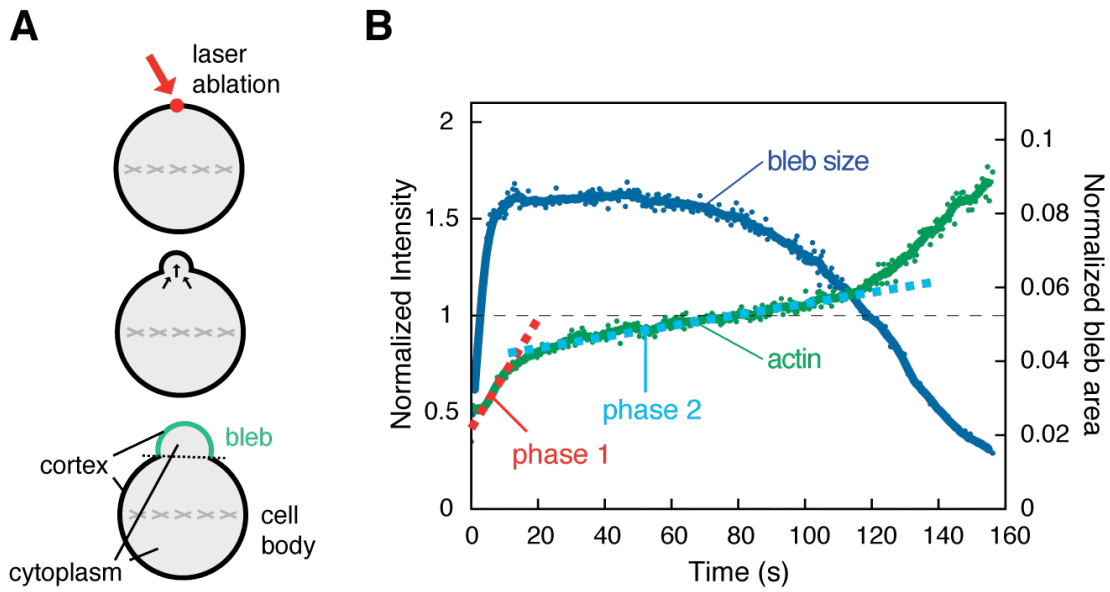

Figure 4.17: Actin regrowth was studied in induced blebs of metaphase HeLa cells.

A. Blebs are induced in metaphase HeLa cells by laser ablation of the cortex at the spot marked by an arrow. Laser ablation was performed perpendicular to the aligned chromosome plane of the cell. Automated image analysis is used to segment the cell into cytoplasm, cell body cortex, and bleb cortex and allows precise measurement of the evolution of fluorescence intensity in these regions over time.

B. Representative actin regrowth rate curve as a function of time after ablation in blebs normalised to the average intensity of fluorescence in the cortex (green). The evolution of bleb area with time is plotted in blue. Initial regrowth rates measuring F-actin fluorescence intensity after ablation are linear with time. During phase 1 (red dashed line) a rapid accumulation of actin was observed and during phase 2 (turquoise dashed line) a slower one was observed. Laser ablation takes place at t=0s.

In HeLa cells actin cortex accumulation started immediately after bleb induction and displayed two distinct phases: a rapid accumulation until the end of bleb growth, then a slower accumulation until the start of retraction (Sedzinski et al., 2011). In both regimes, accumulation was linear with time and could therefore be quantified by an accumulation rate. We reasoned that the first rate should depend strongly on nucleation because there is initially no F-actin under the cell membrane at the onset of growth; whereas accumulation in the second phase may contain significant contributions from elongation of pre-existing filaments (Fig. 4.17B).

The laser ablation experiments revealed that in Diaph1 depleted metaphase HeLa cells, where the actin accumulation is due primarily to Arp2/3 complex ($v_{Arp2/3}$), initial cortex accumulation was two-fold slower than in cells transfected with non-silencing shRNA ($v_{Arp2/3} \sim v_{Diaph1shRNA}=0.96\pm0.6\%.s^{-1}$, n=17 cells, $v_{Non\text{-}silencing\ shRNA}=1.8\pm0.5\%.s^{-1}$, n=10 cells, $p<0.01$, Fig. 4.18A). In contrast in CK666 treated (Arp2/3 complex depleted) metaphase HeLa cells, where the actin accumulation is due to Diaph1 (v_{Diaph1}), initial cortex accumulation was two-fold faster than in cells treated with DMSO ($v_{Diaph1} \sim v_{CK666}=3\pm1\%.s^{-1}$, n=14 cells, $v_{DMSO}=1.6\pm0.5\%.s^{-1}$, n=9 cells, $p<0.01$, Fig. 4.18B). Diaph1 depletion was confirmed with Western blotting and a significant decrease in Diaph1 protein levels was detected (Fig. 4.18C). Taken together accumulation of Diaph1 nucleated and elongated F-actin in the metaphase cortex is ~4-fold faster than that nucleated by the Arp2/3 complex. This is consistent with measurements where it was shown that formins elongate filaments many-fold faster compared to spontaneous elongation *in vitro* (Romero et al., 2004). In controls, the accumulation rate was intermediate between Diaph1 and Arp2/3 complex nucleated actin suggesting that cortex regrowth results from the combined action of Diaph1 and the Arp2/3 complex.

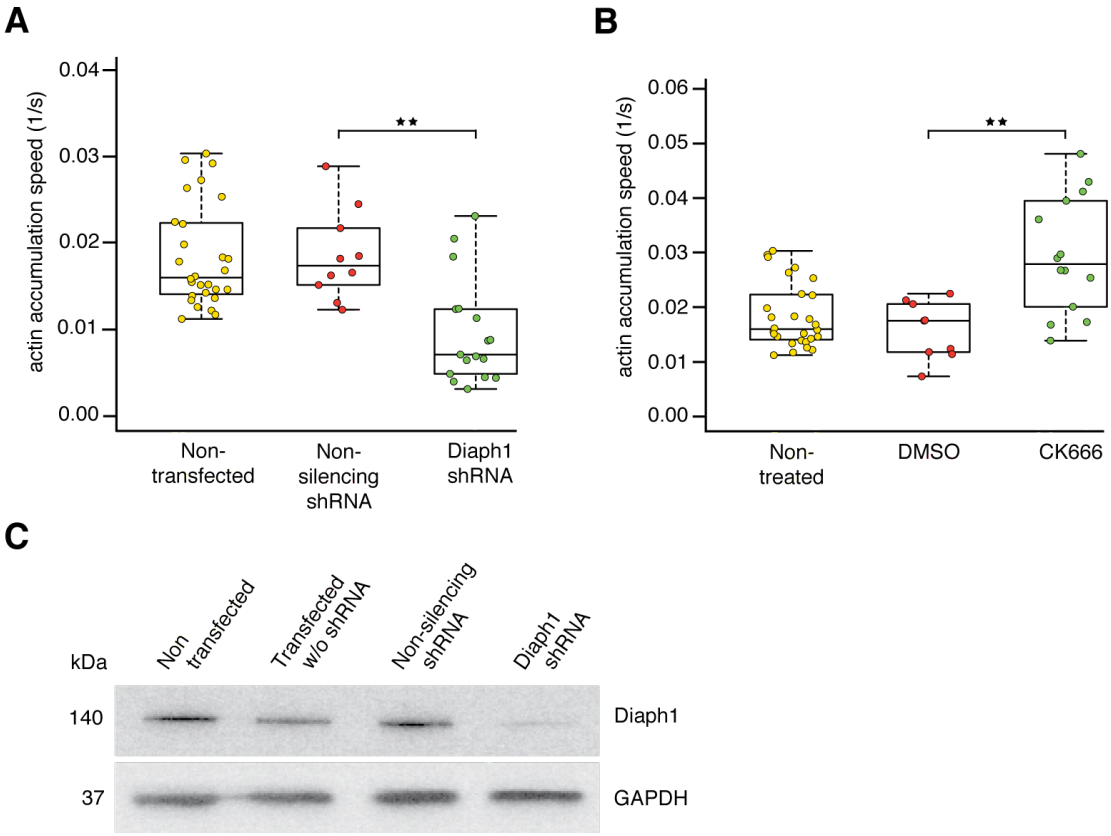
A
actin accumulation speed (1/s)
0.04
0.03
0.02
0.01
0.00
**
Non-transfected
Non-silencing shRNA
Diaph1 shRNA
B
actin accumulation speed (1/s)
0.06
0.05
0.04
0.03
0.02
0.01
0.00
**
Non-treated
DMSO
CK666
C
kDa
Non transfected
Transfected w/o shRNA
Non-silencing shRNA
Diaph1 shRNA
140
Diaph1
37
GAPDH

Figure 4.18: Disruption of Diaph1 or the Arp2/3 complex changes actin cortex regrowth rates in HeLa cells.

A. Actin cortex accumulation rate in non-transfected control cells, cells transfected with non-silencing shRNA or Diaph1 shRNA. Data are plotted as box-whisker plots and derived from multiple cells: non-treated control n=28 cells, non-silencing shRNA n=10 cells, Diaph1 shRNA n=17 cells. Whiskers indicate minimum and maximum actin accumulation rates. Data points are overlaid (**p= < 0.01).
B. Actin cortex accumulation rate in non-treated control, DMSO, or CK666 treated metaphase HeLa cells. Data are derived from non-treated control n=28 cells, DMSO control n=9 cells, CK666 n=14 cells. Whiskers indicate minimum and maximum actin accumulation rates. Data points are overlaid (**p= < 0.01).
C. Western blot showing Diaph1 protein levels compared to GAPDH in non-transfected HeLa cells, HeLa cells transfected without shRNA, with non-silencing shRNA, and with Diaph1 shRNA. A significant decrease in Diaph1 protein level was detected in cells 72h after transfection with Diaph1 shRNA.

One of the most intriguing questions on the presence of Diaph1 and Arp2/3 complex at the cortex is whether the nucleators act independently or cooperatively. Indeed, recently, several studies have revealed cooperative action of pointed-end nucleators and formins like Spire proteins and formin 2 (Quinlan et al., 2007). If Diaph1 and the Arp2/3 complex acted cooperatively at the cortex, two different mechanisms would be possible. First, Diaph1 could elongate new daughter filaments nucleated by the Arp2/3 complex (Fig. 4.19A) or second, Arp2/3 complex nucleation could be activated by binding to the side of a mother filament, which was generated by Diaph1 (Fig. 4.19B).

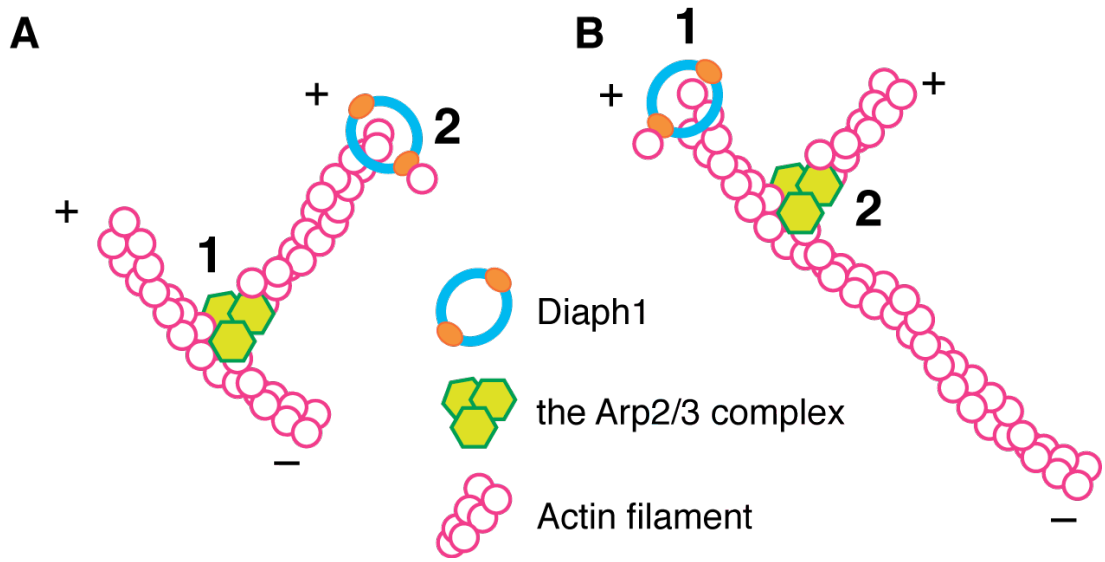

Figure 4.19: Co-operativity of Diaph1 and the Arp2/3 complex.

A. The Arp2/3 complex induces formation of a branch, which Diaph1 then elongates.
B. Diaph1 nucleates and elongates a filament that could acts as a mother filament for the Arp2/3 complex leading to new branch formation.

However our experiments suggest that Diaph1 and the Arp2/3 complex act independently in the cortex. First, when we depleted each nucleator separately, the cells still had a functional cortex although perturbations were detected, but upon simultaneous depletion the majority of the cortex was lost. If one nucleator was upstream of another, depletion of the upstream nucleator should have also led to loss of cortex. Second, our flow cytometry assay on loss of F-actin content upon Diaph1 or Arp2/3 complex depletion showed that when both nucleators were depleted simultaneously the decrease in F-actin mass was not very different from the addition of their individual effects, further suggesting the nucleators act independently. Finally, actin accumulation rate in blebs induced in metaphase HeLa cells showed that Diaph1 knockdown slowed and Arp2/3 complex inhibition accelerated actin accumulation suggesting that each nucleator contributes independently with different elongation rates to the cortex reassembly.

4.7 Conclusions

Having shown in chapter 3 that nucleation independent mechanisms do not contribute to the actin cortex reassembly, I started investigating which actin nucleators are involved in *de novo* cortex nucleation. Being an important structure in all cells I chose to study the cortex reassembly in two cell lines displaying a well defined cortex: blebbing M2 cells and metaphase HeLa cells. First we found that many actin nucleators are expressed in both cell lines. To narrow down the possible candidates, I did an imaging screen that revealed that from the expressed nucleators only Daam1, Fhod1, Diaph1, and the Arp2/3 complex localised to the cell cortex, whereas other nucleators localised either to incorrect organelles or their localisation was cytoplasmic (Fmnl1). Interestingly from the expressed nucleators, Fhod1 had been suggested to nucleate the cortex in HeLa cells (Hannemann et al., 2008), Fmnl1 has been reported to regulate cortex stability (Han et al., 2009), and Diaph1 was shown to be needed for invasion and blebbing motility of MDA-MB-435 cells (Kitzing et al., 2007).

Silencing Diaph1 in M2 cells led to formation of large blebs, possibly because of weaker cortex. Depletion of Arp2/3 complex by inhibitor CK666 (Nolen et al., 2009) revealed a loss of cortical fluorescence intensity in M2 cells. In addition proteomic studies on cortex rich separated blebs were carried out to investigate which nucleators associate with the cortex. Together these studies revealed that only Diaph1 and the Arp2/3 complex are bound at the cortex and are needed for cortex maintenance. Further characterization in M2 cells showed that, when both Diaph1 and the Arp2/3 complex are disrupted, the cell cortex is lost suggesting that these two nucleators are needed for cortex nucleation and maintenance.

Measurements of total F-actin mass in M2 cells by flow cytometry confirmed that when Diaph1 or the Arp2/3 complex are depleted the total F-actin content in M2 cells decreases. In contrast expression of constitutively active Diaph1 led to an increase in the total F-actin content. When both nucleators were depleted simultaneously, no significant potentiating effect from their combined individual effects was observed, suggesting the nucleators act independently.

Finally, we studied the effect of depleting Diaph1 or the Arp2/3 complex on the cortex regrowth rate in induced blebs of metaphase arrested HeLa cells. We observed that when Diaph1 was silenced leading to F-actin being nucleated mainly by the Arp2/3 complex, the cortex regrowth rate was slowed. In contrast, when the Arp2/3 complex was inhibited leading to F-actin being nucleated mainly by Diaph1, the cortex regrowth rate was accelerated. This suggested that cortex regrowth results from the combined action of Diaph1 and the Arp2/3 complex.

Taken together our data suggest, that Diaph1 and the Arp2/3 complex act independently to generate the cellular actin cortex. Thus the actin cortex is potentially composed of two subpopulations of filaments; one population nucleated by the Arp2/3 complex, where the barbed ends of filaments are

free, and another nucleated and elongated by Diaph1, that stays bound at the barbed ends of the filaments. How the cortex is regulated, and if the filament populations are functionally different remain to be studied. A few aspects of the cortex regulation and overall cortex composition are presented in the next chapter.

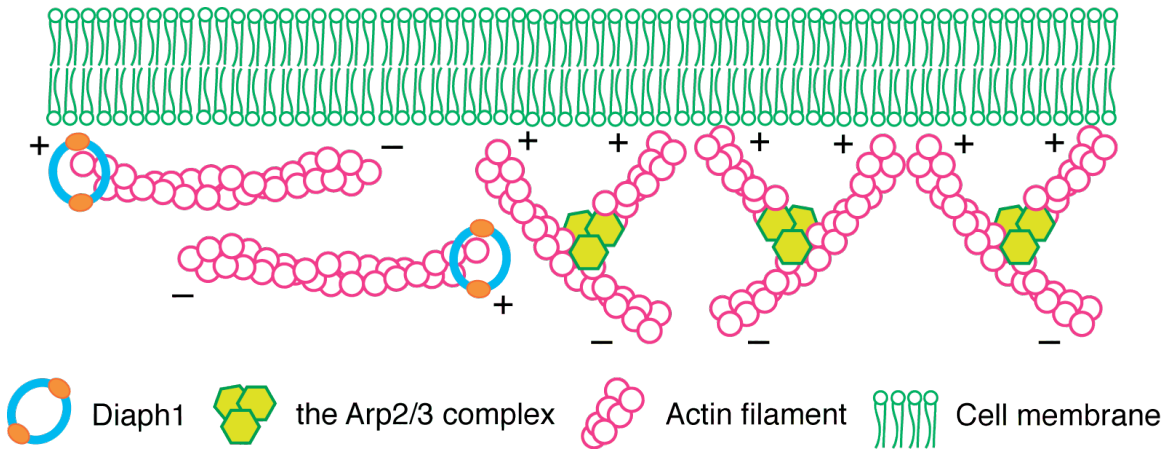

Figure 4.20: Diaph1 and the Arp2/3 complex act independently at the cortex.

The actin cortex may be composed of two subpopulations of filaments. One population is nucleated by the Arp2/3 complex and the other by Diaph1. The Arp2/3 complex nucleated filaments have free barbed ends whereas the filaments that are nucleated and elongated by Diaph1 are capped at the barbed end.

5 CORTEX COMPOSITION

5.1 Introduction

The contractile cortex is rich in F-actin, actin regulating proteins, and myosin II (Bray and White, 1988), but the overall protein composition of the cortex remains largely unknown. To date the most detailed analysis of the cortex composition was done by studying localisation and recruitment of GFP-tagged actin binding proteins to the bleb cortex in M2 cells (Charras et al., 2006). The proteins, which localised to the bleb cortex belonged to the group cortex-membrane linker proteins (ezrin, moesin, and annexin II), actin filament crosslinkers (α-actinin, filamin B, fimbrin), and proteins needed for contractility (myosin II, myosin I, and tropomyosin) together with the small GTPase RhoA (Charras et al., 2006). In addition, spectrin network associated proteins (spectrin, adducin, ankyrin B), the actin branch remodelling protein coronin 3, the pointed end capper tropomodulin, and the scaffold protein anillin were found to localise to the bleb cortex (Charras et al., 2006). In contrast, the F-actin bundling protein fascin, the filament elongation factor VASP, and the barbed end capper heterodimeric capping protein appeared cytoplasmic in blebbing cells (Charras et al., 2006).

While investigating which actin nucleators are needed for cortex reassembly in membrane blebs, we developed a method to separate blebs from whole cells. After isolation these blebs were prepared for mass spectrometry analysis, which revealed proteins present in the actin cortex. Hence, we not only verified that Diaph1 and the Arp2/3 complex were associated with the cortex, but revealed the whole protein composition of the cortex. To demonstrate, that the separated blebs were suitable model for studying the cortex, we showed that their actin cortex was formed of actin filaments undergoing dynamic turnover, but no thorough analysis of the presence of cell organelles was carried out nor was it shown that the separated blebs were indeed enriched in F-actin compared to whole cells.

In addition to the proteic composition of the cortex, only little is known about the regulation of the cortex. It has been shown that RhoA is an important regulator of cortical actin dynamics (Charras et al., 2006; Etienne-Manneville and Hall, 2002), but to date the role of other small GTPases, Rho GTPase regulators GEFs, GAPs, and GDIs, or other regulatory proteins at the cortex have not been thorougly studied. As a consequence detailed regulation of the cortex nucleation remains to be elucidated.

Interestingly, recently the protein composition of isolated focal adhesions was revealed (Kuo et al., 2011). The authors exploited the sensitivity of focal adhesions to tension by looking for changes in focal adhesion protein abundance in response to drugs changing myosin II activity (Kuo et al., 2011). Thus we reasoned that, as dynamic actin filaments are sensitive to drugs altering polymerisation, these drugs could be used to reveal what proteins are associated with F-actin of the separated blebs. Indeed, to determine which actin regulating proteins were strongly bound to the actin structures in isolated blebs, we treated the separated blebs with cytochalasin D, a drug that blocks the growing barbed ends of actin filaments, and followed the change in protein abundance of the cortex.

The aim of this chapter is to verify that the separated blebs are a good model for studying the cell cortex, to reveal the protein composition of the cortex, to show which actin binding proteins are strongly bound to the cortex, and to study the cortex regulation. Finally the role of different actin binding proteins present at the bleb fraction is studied by localisation and gene silencing methods.

5.2 F-actin is enriched in the bleb fraction

Previously we had shown that the separated blebs reassemble a well-defined actin cortex, which was ultrastructurally similar to whole cell cortices and that they were sensitive to actin depolymerising drugs, indicating that the actin filaments in their cortex were dynamic and turning over (chapter 4, Fig. 4.11). To further establish that the separated blebs are a good model for the proteomic screen of the cortex, we studied if they were: i) depleted in cell organelles, like the mitochondria, the nucleus, and intracellular membrane structures, ii) or enriched in actin.

First, our collaborators Dr. Romeo and Dr. Roux studied by immunoblotting the presence of nuclear components (Ki67 and histone 3), mitochondrial voltage-dependent anion channel (VDAC), intracellular membrane organelles (GM130 for Golgi complex and calnexin for endoplasmic reticulum), and β-actin in whole cell and bleb fraction extracts (Fig. 5.1). Comparison between whole cells and bleb fraction revealed that whole cells expectedly contained a lot of nuclear material but, in contrast, bleb fraction displayed only a weak signal for the nuclear components Ki67 and histone 3 (Fig. 5.1). Likewise with mitochondrial marker VDAC, whole cells displayed a strong signal and bleb fraction a weak one (Fig. 5.1). In contrast, signal from the Golgi complex and the endoplasmic reticulum (ER) was stronger in bleb fraction than whole cells (Fig. 5.1, GM130, calnexin). Finally, the bleb fraction showed a clear enrichment in β-actin compared to whole cells (Fig. 5.1, beta actin).

Taken together these data indicate that compared to whole cells, the bleb fraction was depleted in nuclei and mitochondria and enriched in intracellular membrane organelles and most importantly in β-actin. Visually the majority of the F-actin in isolated blebs is cortical (Fig. 4.11A) and the actin filaments in the isolated blebs are dynamic (Fig. 4.11C). These results together with data presented in this section suggest that the purified bleb fraction is a good

model for studying the protein composition of the actin cortex, but contains contaminants from other cell organelles.

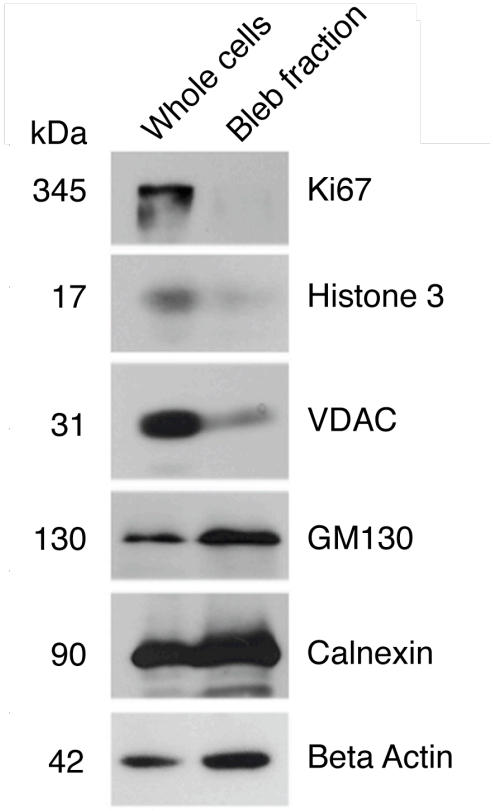

Figure 5.1: Bleb fraction is depleted in nuclei and mitochondria, but enriched in intracellular membrane structures and actin compared to whole cells.

The presence of the nuclear components Ki67 and histone3, the mitochondrial marker VDAC, the Golgi complex marker GM130, the endoplasmic reticulum bound protein calnexin, and β-actin was studied by immunoblotting in whole cell and bleb fraction extracts. In bleb fraction, a clear decrease in nuclear and mitochondrial signal was detected compared to whole cells. In contrast, the bleb fraction displayed a stronger signal for endoplasmic reticulum, Golgi complex, and β-actin than the whole cells.

The unexpected enrichment of bleb fraction in Golgi complex and ER proteins could be due to flow of intracellular membrane structures along with cytosol into the blebs at the onset of bleb growth. It is possible that in normal conditions when the cortex at the base of the bleb is intact, it prevents the cell organelles from entering the bleb. However, during the bleb purification process, the majority of the actin cortex is depleted by the actin sequestering drug latrunculin B. Hence, sieving no longer occurs and leads to the entry of cell organelles into the blebs. Mitochondria and in particular the nucleus are large organelles and possibly therefore do not enter the blebs. In contrast, intracellular membrane structures are widespread throughout the cytoplasm and deform easily, and thus upon latrunculin B treatment can enter into the blebs. In addition, cell organelles may be cofractionated with the blebs during ultracentrifugation when whole cells are separated from blebs in a Ficoll gradient. Indeed the bleb isolation protocol is adapted from assays used to isolate membranes for biochemistry (Boone et al., 1969; Fujiki et al., 1982; Lund et al., 2009).

Next, Dr. Romeo and Dr. Roux ran samples of whole cells and bleb fraction on an SDS-PAGE gel to study differences in protein content between the two total protein extracts. Although similarities in protein composition were apparent, the bleb fraction showed enrichment or depletion in several distinct regions compared to whole cells (Fig. 5.2A). In bleb fraction, a particularly strong enrichment of proteins was detected at ~170kDa, 70kDa, and 42kDa (Fig. 5.2A R1-3), which are molecular weights close to myosin II heavy chain (~200 kDa) and actin (42kDa). Mass spectrometry analysis was carried out by concentrating only on the most abundant proteins in each region. This revealed a two-fold enrichment in myosins and spectrin at ~170kDa (Fig. 5.2B) in bleb fraction compared to whole cells. Interestingly at 70kDa (Fig. 5.2B), a two-fold enrichment of heat shock proteins was observed in bleb fraction compared to whole cells, and finally at 42kDa (Fig. 5.2B) a 26% enrichment of actin isoforms and a two-fold enrichment of signalling molecules were observed.

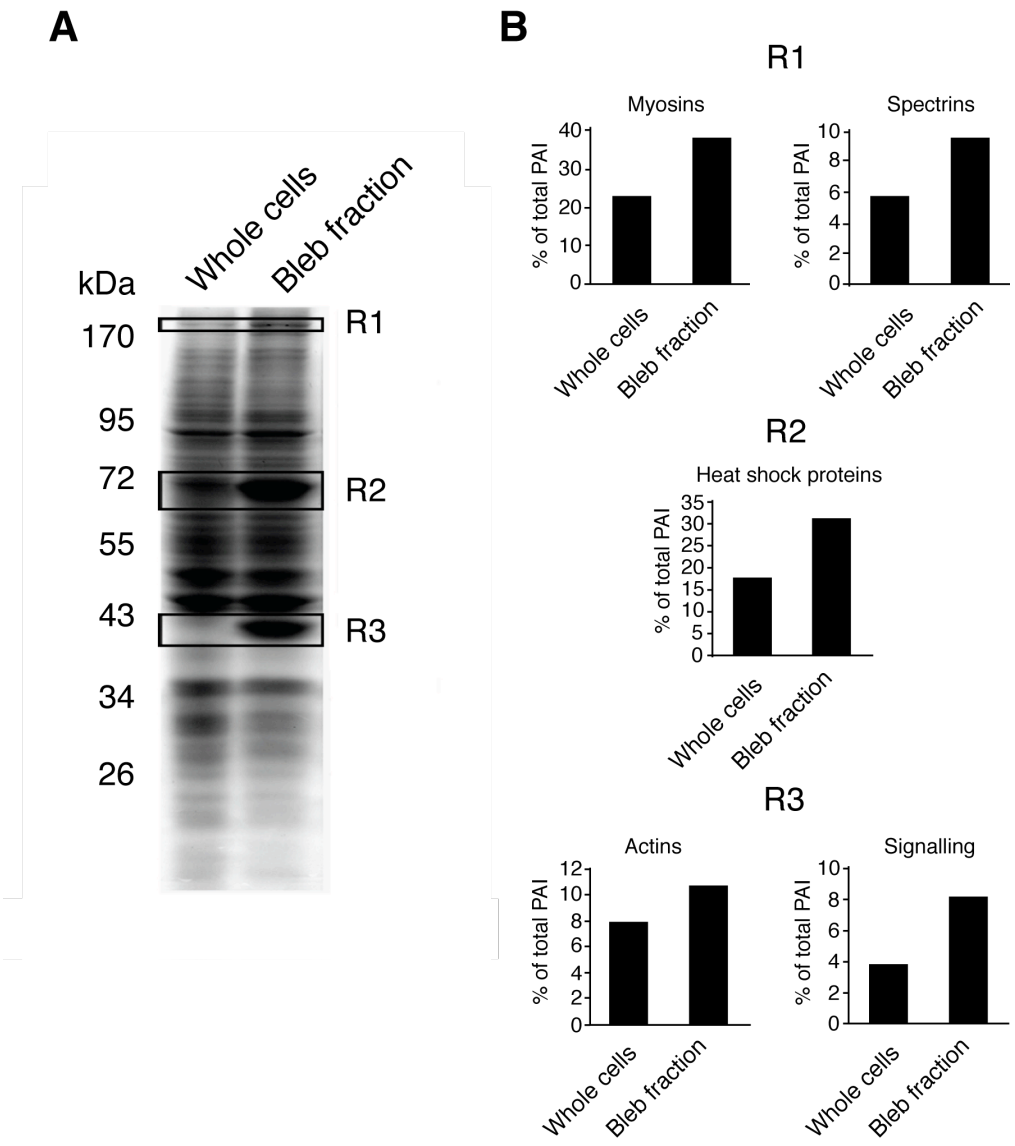

Figure 5.2: Cytoskeletal proteins, heat shock proteins, and signalling proteins are enriched in bleb fraction.

A. Total protein extracts of whole cells and bleb fraction were run onto an SDS-PAGE gel and stained with coomassie blue. Three regions (R1-3 ~170kDa, 70kDa, and 42kDa, respectively) visibly enriched in protein content in bleb fraction compared to whole cells were chosen for further analysis.

B. An enrichment of myosins and spectrins was observed at R1, heat shock proteins at R2, and actins and signalling proteins at R3 in bleb fraction compared to whole cells. The y-axes display the protein abundance index (PAI) in percent of the total peptides identified in the region.

Our data show that the bleb fraction is enriched in actin and depleted in nuclear and mitochondrial components, but contain intracellular membrane organelles and heat shock proteins. In particular the bleb fraction was enriched in proteins of the actin cortex including actins, myosins, and spectrin.

The Golgi complex and ER both bind actin (di Campli et al., 1999; Kachar and Reese, 1988). Thus if an actin binding protein is found at the mass spectrometry analysis of the bleb fraction, it is not necessarily a cortex bound protein, but can be Golgi complex or ER bound. Indeed, further studies, including localisation and RNAi studies, are needed to assess whether or not a protein found in the mass spectrometry analysis has a role at the cortex. However, if a particular actin binding protein is not found in the bleb fraction, it is unlikely to participate in cortical actin dynamics (or in Golgi or ER actin dynamics).

These data together suggest that the purified blebs are a cell fraction enriched in cortical actin, but also contains actin bound to the Golgi complex and ER. By carefully analysing of the F-actin pellet of the purified blebs together with further studies of the pellet bound actin binding proteins, the bleb fraction can be used as a model to study the actin cortex composition.

5.3 Proteomic analysis of the bleb fraction

After having shown that despite of Golgi complex and ER contamination, the bleb fraction can be used as a model for studying the actin cortex, I studied the composition of the pellet fraction of the purified blebs by mass spectrometry analysis in collaboration with Dr. Romeo and Dr. Roux. We reasoned that after detergent extraction and ultracentrifugation of the bleb fraction, the cytosolic, unbound proteins and membrane fraction of the blebs remain in the supernatant due to the usage of detergents, whereas actin and actin bound proteins stay in the pellet fraction. Therefore, I undertook a

careful analysis of the detergent insoluble fraction of the purified blebs referred as pellet later in the text.

I analysed the proteins detected from one mass spectrometry run and found that there were 3185 proteins (isoforms not grouped) present in the pellet fraction. To increase the certainty that the protein was present in the pellet I excluded proteins, which displayed less than four peptides resulting in restricting my analysis to 1044 proteins. These proteins I manually classified according to their biological function into the following categories: nuclear proteins, cytoskeletal proteins, protein synthesis, biosynthetic pathways, protein regulation, membrane trafficking, proteasome, signalling, heat shock proteins, small GTPases, cell cycle, protein folding, mitochondrial proteins, cell-cell adhesion proteins, and miscellaneous (Fig. 5.3).

Surprisingly the largest group of proteins found in the bleb fraction was nuclear proteins (Fig. 5.3), in apparent contradiction with the studies by immunoblotting. However, if even a small portion of the bleb fraction contained nuclear material, it might result in detection of a high number of nuclear proteins because of the high protein content of the nucleus. The second largest group was cytoskeletal proteins consisting of actin and actin binding proteins (52%), tubulin and microtubule binding proteins (34%), and proteins from other cytoskeletal structures like intermediate filaments, spectrins and septins (14%). The large fraction of cytoskeletal proteins observed was expected given that our assay was designed to enrich for cortical proteins. The third largest group consisted of proteins needed for translation including ribosomal proteins and proteins regulating translation consistent with ER enrichment in the bleb fraction. Proteins forming part of the biosynthetic pathway, protein regulation (kinases, phosphatases etc), and membrane trafficking categories were also observed in the bleb fraction in relatively high numbers. In addition, proteasome proteins were observed in the pellet of bleb fraction. Some signalling proteins were observed together

with heat shock proteins consistent with the initial mass spectrometry studies of a band on coomassie stained SDS-PAGE gel (Fig. 5.2).

Finally, many small GTPases and their regulators (GEFs, GAPs, GDIs), discussed later in this chapter, were also associated with the pellet in the bleb fraction providing clues to the cortex regulation. A miscellaneous group consisted mainly of proteins that have not yet been characterized. The categories with the smallest number of proteins were cell cycle regulation, protein folding (chaperones other than heat shock proteins), mitochondrial, cell-cell adhesion proteins.

In conclusion, the detergent insoluble fraction of the purified blebs contained proteins from many functional categories including nuclear proteins, and proteins needed for protein synthesis, biosynthetic pathways, protein regulation, and membrane trafficking. Most importantly, the pellet fraction contained many cytoskeletal proteins of which actin and actin regulating proteins were the most abundant. However, the presence of many proteins not expected to have a role in or bind to the actin cortex suggests that some proteins may bind Golgi complex, ER, or bind unspecifically to the pellet. Thus, a careful analysis of the actin binding proteins in the pellet fraction is required to assess whether or not they are integral components of the actin cortex. However, first the actin regulating proteins found in the pellet of bleb fraction are presented.

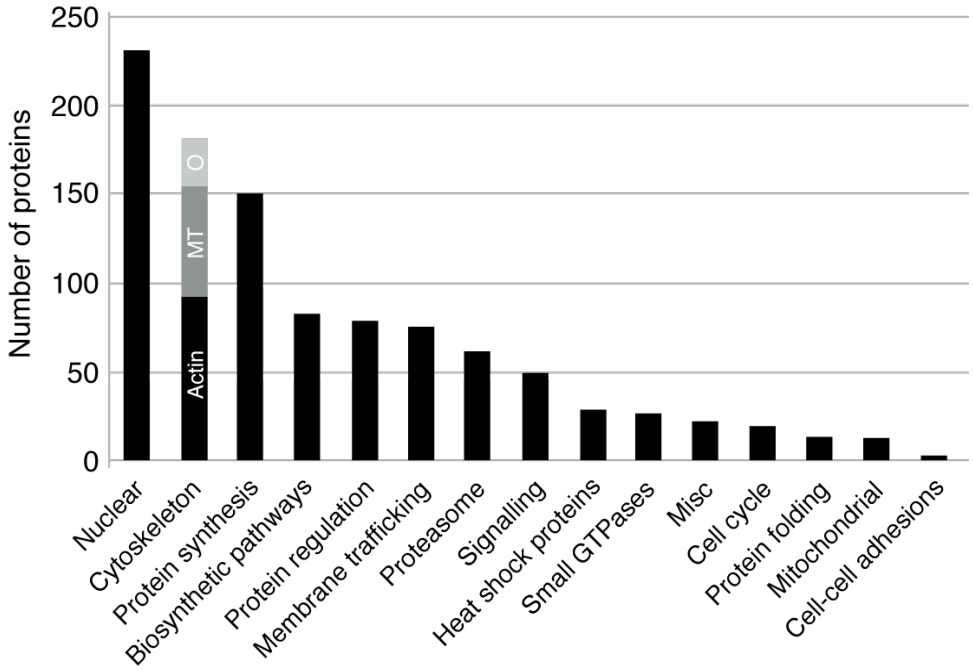

Figure 5.3: Protein categories found in the pellet fraction of the bleb fraction.

Proteins in the pellet of the bleb fraction that displayed four or more peptides in the mass spectrometry results were subdivided into 15 categories. The categories going from the most represented to the least represented were: nuclear proteins, cytoskeletal proteins, protein synthesis, biosynthetic pathways, protein regulation, membrane trafficking, proteasome, signalling, heat shock proteins, small GTPases, miscellaneous (Misc), cell cycle, protein folding, mitochondrial proteins, and cell-cell adhesion proteins. The cytoskeletal protein category was subdivided into actin and actin binding proteins (Actin, 52%), tubulin and microtubule binding proteins (MT, 34%), and others like spectrins and septins (O, 14%). The y-axis displays the number of proteins detected in each category.

5.4 Actin binding proteins present at the bleb fraction

After having manually categorised the cytoskeletal proteins, further analysis of the actin binding group revealed the presence of 93 actin binding proteins including different actin isoforms. These I manually classified into the following categories: F-actin nucleators (8.7%), actin isoforms (7.6%), filament capping proteins (15.2%), proteins regulating actin or actin binding proteins (14.1%), F-actin crosslinking proteins (10.9%), proteins needed for actin turnover (6.5%), proteins linking actin to the plasma membrane (7.4%), motor proteins needed for contractility (17.4%), actin binding scaffold proteins needed for signal transduction (7.6%), and focal adhesion proteins (4.3%) (Fig. 5.4). Some of the actin regulating proteins have multiple functionalities, and therefore cleanly separating them into one category or another is not always possible. However, my aim was to categorise the proteins according to their reported main function.

Figure 5.4: Actin binding proteins found in the detergent insoluble fraction of purified blebs.

Actin binding proteins were categorised into nucleator, actin, capping, regulatory, crosslinking, turnover, membrane linking, motor, scaffold, and focal adhesion protein groups. The actin group consists of the different actin isoforms identified. The category with the most proteins was the motor protein group, which included different myosin isoforms.

To reveal how abundant different actin binding proteins were in the pellet, I calculated the protein abundance index (PAI) by dividing the number of peptides found in the mass spectrometry run by the protein molecular weight for each protein (Table 5.1) (Rappsilber et al., 2002). PAI allows us to normalise the peptide count to the protein weight, which is necessary because enzymatic digestion of a large protein results in high number of peptides, whereas digestion of a small protein results in low number of peptides (Rappsilber et al., 2002). For proteins identified with less than four peptides in the detergent insoluble fraction, I chose a cutoff of PAI>9 to qualify them for further analysis. With this parameter, no additional actin binding proteins were found. In the following paragraphs, I list what proteins were found in each category.

Nucleators and their regulators

This group consisted of the Arp2/3 complex (all seven subunits), Diaph1, the WAVE complex (subunits NAP1 and SRA1), and cortactin as described in the previous chapter (Table 4.3, Table 5.1, nucleators and nucleation regulation). Coronin, a protein thought to play a role in dissociating the Arp2/3 complex from branch points (Cai et al., 2008) and potentiating ADF/cofilin mediated depolymerisation (Cai et al., 2007; Kueh et al., 2008), was also found associated to the pellet (Table 5.1, nucleation regulation). Previously coronin has been shown to localise to the cell cortex in M2 cells (Charras et al., 2006) and suggesting that Arp2/3 complex induced branch remodeling by coronin could occur in the cortex.

Actin isoforms

Surprisingly three actin isoforms were found associated with the pellet fraction, although α-actin has been suggested to be mainly muscle specific (Table 5.1, actin isoforms). According to PAI the most abundant protein found in the pellet fraction was γ-actin, though β-actin was also abundant.

Membrane linkers

The ERM-protein ezrin was shown to appear under the bleb membrane prior to and independently from actin (Charras et al., 2006) to link the forming cortex to the membrane. In addition another ERM-protein, moesin, was reported to localise to the bleb membrane (Charras et al., 2006). Consistent with this, moesin and especially ezrin were found to be abundant at the pellet (Table 5.1, membrane linkers). The third ERM-protein, radixin, was present, though in lower abundance.

Filamin B, which crosslinks actin filaments creating T-, X-, and L- shaped junctions under the plasma membrane (Popowicz et al., 2006), was found associated with the bleb fraction. Interestingly blebbing M2 cells have been shown to be filamin A-deficient (Cunningham et al., 1992) and were suggested to bleb constitutively because of decreased membrane-cortex adhesion due to filamin A deficiency (Cunningham et al., 1992; Dai and Sheetz, 1999). Thus, the role of filamins in the cortex is intriguing and the role of filamin B is further studied later in this thesis. Finally, actin-membrane linker protein utrophin was found in the pellet fraction.

Actin crosslinkers

It is known that the cell cortex is a crosslinked F-actin structure and therefore we were expecting to find many actin crosslinkers associated with the bleb fraction (Table 5.1, actin crosslinkers). First, α-actinin isoforms (2-4) were found to be abundant in the pellet. Interestingly α-actinin-2 and -3 have been shown to be muscle-specific (Beggs et al., 1992), whereas α-actinin-1 and -4 are widely expressed. Thus, given that M2 cells are not muscle cells, the presence of α-actinin-2, and -3 was surprising. The role of α-actinin-1 at the cortex has been previously characterized (Charras et al., 2006). Thus, the presence of α-actinin-1 at the pellet was not suprising. The presence of α-actinin-4 was surprising but only because this isoform has not widely been studied.

In addition, the association of fascin was surprising as it has been suggested to bundle actin filaments in filopodia (DeRosier and Edds, 1980) and displayed cytoplasmic localisation in blebbing M2 cells (Charras et al., 2006). However fascin was not as abundant in the cell cortex as α-actinin-1 or α-actinin-4 (fascin PAI 9.2 versus α-actinin-1 PAI 109.7 and α-actinin-4 PAI 107.9) suggesting that it may have a minor role at the cortex, might be present for potential filopodia formation, or may simply be a contaminant.

Finally, annexins were abundant in the pellet. Surprisingly, even though they have been suggested to have a role not only in actin crosslinking but also in actin-membrane linking (Harder et al., 1997; Oliferenko et al., 1999; Rescher et al., 2004), upon GFP-tagging annexin II displayed a cytoplasmic localisation in blebbing cells (Charras et al., 2006). However, it has been reported that the activity of annexins is tightly regulated by Ca^{2+} (Gerke and Weber, 1984; Glenney et al., 1987), possibly leading to a high unbound/ bound ratio of the GFP-tagged annexins in cells.

Capping proteins

Many capping proteins were found to be associated with the pellet (Table 5.1, capping proteins). The barbed end cappers twinfilin, gelsolin and heterodimeric capping protein (CapZ) were identified in the bleb fraction. In addition to barbed end cappers, pointed end cappers tropomodulin and emerin were associated with the pellet. Given that emerin has been reported to be bound to nuclear membranes (Holaska et al., 2004), its presence in the pellet may be due to nuclear contamination of the bleb fraction. Because gelsolin and especially the heterodimeric capping protein were abundant in the pellet and barbed end capping has been shown to be essential for motility (Cunningham et al., 1991; Hug et al., 1995; Sun et al., 1995), the potential role of heterodimeric capping protein and gelsolin are studied more in detail in the cortex later in this thesis.

Turnover proteins

Proteins regulating F-actin turnover were also found in the pellet fraction (Table 5.1, turnover proteins). F-actin depolymerising (Carlier et al., 1997) and severing (Chan et al., 2000; Maciver et al., 1991; Moriyama et al., 1999) protein ADF/cofilin was found associated at the bleb fraction. Indeed all known ADF/cofilin isoforms in humans, cofilin-1, cofilin-2, and destrin (also known as ADF) were present suggesting pointed-end depolymerisation and severing of actin filaments could take place in the cortex. In addition, profilin, which catalyses the exchange of ADP to ATP on actin monomer (Mockrin and Korn, 1980), was found to be abundant in the pellet. This was not surprising given that Diaph1 nucleates actin in the cortex and profilin is known to deliver ATP-actin monomers to formins (Paul and Pollard, 2008; Romero et al., 2004). To reveal the role of depolymerisation and severing, as well as to study if efficient actin turnover is needed for cortical integrity, the role of cofilin and profilin in the cell cortex is studied more in detail later in this thesis. Finally adenylyl cyclase-associated protein 1 (CAP1), a bifunctional protein, which has been reported to co-operate with ADF/cofilin and recycle actin and ADF/cofilin leading to rapid actin turnover (Moriyama and Yahara, 2002), was found at the pellet.

Myosin motors

The largest group of proteins present at the pellet was myosin isoforms (Table 5.1, myosin motors) presumably because they are needed to generate contractility in the cortex. Myosin II localises to the bleb cortex after actin has assembled, but its localisation differs from other actin binding proteins as myosin regulatory light chain (MRLC) and myosin heavy chain localise in a dot-like manner in the bleb cortex and not as a continuous rim as other actin binding proteins (Charras et al., 2006). Multiple myosin isoforms were identified at the pellet fraction, including myosin-I, -V, -VI, -XI, and XVIII. However, the most abundant myosin isoforms was myosin-II, as the PAI of its heavy chains was high (MYH9 PAI 38.4 and MYH10 PAI 45.0). Given that myosin-II is considered to be the main myosin isoform in non-muscle cells

(Alberts, 2002) and it localises to the actin cortex (Charras et al., 2006), its presence was not surprising. Although less studied than myosin-II, monomeric myosin-Is are also found in most eukaryotic cells, where they not only bind to actin, but also to the plasma membrane (Barylko et al., 2000; Hokanson and Ostap, 2006). Interestingly myosin-IC was also an abundant (PAI 24.6) myosin motor in the pellet and has been shown to localise to the cell cortex (Charras et al., 2006). Thus, its role in the cortex maintenance is studied more in detail later in this thesis.

Regulatory proteins

Many actin regulating proteins were found associated with the pellet (Table 5.1, regulatory proteins). First, multiple isoforms of tropomyosins, which strengthen the pointed end capping of tropomodulin (Fowler, 1996; Fowler et al., 2003; Littlefield and Fowler, 1998; Weber et al., 1994; Weber et al., 1999) and regulate myosins (Lehrer and Morris, 1982) were present in the pellet.

Second, flightless I (Fli1), a member of the gelsolin family (Campbell et al., 1993) and a possible activator of Diaph1 (Higashi et al., 2010) was found associated with the bleb fraction. Its potential role in the actin cortex is discussed more in depth later in this thesis.

Third, the master regulator ROCK1, which promotes contractility (Amano et al., 1996; Kimura et al., 1996; Uehata et al., 1997) and ERM-protein activation (Matsui et al., 1998; Tran Quang et al., 2000) as well as indirectly inhibits the activity of ADF/cofilin through LIM-kinase (Maekawa et al., 1999) was found to be associated with the pellet. The presence of ROCK1 was not surprising, given that it has been previously shown to be essential for bleb formation (Coleman et al., 2001; Mills et al., 1998) and to localise to the cell cortex (Pinner and Sahai, 2008).

Fourth, LIM-kinase, which inactives ADF/cofilin (Edwards and Gill, 1999), was found present at the cortex. Finally, Aip1 (WDR1), which in contrast to

LIM-kinase enhances the depolymerisation and severing activity of ADF/cofilin (Aizawa et al., 1999; Okada et al., 1999; Rodal et al., 1999) and caps filament barbed ends in ADF/cofilin dependent manner (Okada et al., 2002) was found to be associated with the pellet. Interestingly the presence of both, LIM-kinase and Aip1, suggests that depolymerisation and severing may be tightly regulated in the cortex. The role of activation of depolymerisation and severing and barbed end capping by Aip1 is especially interesting. Thus, its role in the cortex is studied more in detail later in this thesis.

In addition a few potential, less characterised, regulators (Table 5.1, potential regulators) were present in the pellet. However they were not abundant and their role is not discussed further in this thesis.

Other actin regulating proteins

Other actin regulating proteins included proteins that have multiple binding partners or were not categorised to other groups (Table 5.1, other actin regulating proteins). The most abundant of these was drebrin, which has been reported to inhibit α-actinin, tropomyosin (Ishikawa et al., 1994), and myosin binding to actin (Hayashi et al., 1996; Ishikawa et al., 2007). In addition, IQGAPs (1-3) were also present at the pellet. Interestingly IQGAP1 was reported to be needed for localisation of Diaph1 at the leading edge of migrating cells (Brandt et al., 2007) as well as to stimulate the Arp2/3 complex induced nucleation (Le Clainche et al., 2007). Hence, the role of drebrin and IQGAP1 in the cell cortex is studied in detail later in this thesis.

Focal adhesion proteins

Finally, focal adhesion proteins talin, vinculin, and zyxin were found in the pellet fraction (Table 5.1, focal adhesion proteins). To date the localisation of focal adhesion proteins has not been studied in blebbing M2 cells, however their presence in blebs is surprising given that blebs are dynamic, expand often away from the substrate, and do not appear to attach anywhere.

Interestingly talin-1 appeared to be abundant in the pellet (PAI 32.6), but being part of complex focal adhesion structures, it has multiple binding partners suggesting that talin-1 and other focal adhesion proteins found in the pellet fraction are contaminants. However, further studies are needed to verify this.

Nucleators		kDa	Peptides	PAI
IPI00005160	ARPC1 Actin-related protein 2/3 complex subunit 1	40.9	5	12.2
IPI00028091	ACTR3 Actin-related protein 3	47.3	7	14.8
IPI00550234	ARPC5 Actin-related protein 2/3 complex subunit 5	16.3	4	24.5
IPI00005159	ACTR2 Actin-related protein 2	44.7	11	24.6
IPI00005162	ARPC3 Actin-related protein 2/3 complex subunit 3	20.5	6	29.3
IPI00554811	TTLL3;ARPC4 Actin-related protein 2/3 complex subunit 4	19.7	7	35.5
IPI00005161	ARPC2 Actin-related protein 2/3 complex subunit 2	34.3	15	43.7
IPI00852685	DIAPH1 Diaphanous1	14.1	19	134.8
Nucleation regulators				
IPI00867509	CORO1C Coronin-1C	58.9	4	6.8
IPI00029601	CTTN Cortactin	61.5	17	27.6
IPI00719600	CYFIP2 Cytoplasmic FMR1-interacting protein 2 (SRA1)	14.5	8	55.2
IPI00031982	NCKAP1 Nck-associated protein 1 (NAP1)	12.8	8	62.5
Actin isoforms				
IPI00003627	ACTL6A Isoform 1 of Actin-like protein 6A	47	5	10.6
IPI00008603	ACTA2 Actin; alpha smooth muscle	41.9	21	50.1
IPI00021428	ACTA1 Actin; alpha skeletal muscle	42	36	85.7
IPI00021439	ACTB Actin; beta cytoplasmic	41.7	56	134.3
IPI00021440	ACTG1 Actin; gamma cytoplasmic	41.8	75	179.4
Membrane linkers				
IPI00009329	UTRN Utrophin	394.2	18	4.6
IPI00017367	RDX Radixin	71	7	9.9
IPI00219365	MSN Moesin	67.7	10	14.8
IPI00746388	EZR Ezrin	69.2	16	23.1
IPI00289334	FLNB Filamin-B	27.8	38	136.7
Actin crosslinkers				
IPI00002459	ANXA6 Annexin 6	75.2	4	5.3
IPI00163187	FSCN1 Fascin1	54.4	5	9.2
IPI00019884	ACTN2 Alpha-actinin-2	103.7	18	17.4
IPI00032137	ACTN3 Alpha-actinin-3	103.1	19	18.4
IPI00550363	TAGLN2 Transgelin-2	22.3	5	22.4
IPI00329801	ANXA5 Annexin A5	35.9	10	27.9
PI00418169	ANXA2 Annexin A2	40.3	23	57.1
IPI00013808	ACTN4 Alpha-actinin-4	104.7	113	107.9
IPI00013508	ACTN1 Alpha-actinin-1	103	113	109.7
Capping proteins				
IPI00550917	TWF2 Twinfilin-2	39.5	4	10.1
IPI00646773	GSN Gelsolin	80.6	12	14.9
IPI00005087	TMOD3 Tropomodulin-3	39.5	7	17.7
IPI00032003	EMD Emerin	28.9	7	24.2
IPI00005969	CAPZA1 F-actin-capping protein subunit alpha-1	32.9	17	51.7
IPI00026182	CAPZA2 F-actin-capping protein subunit alpha-2	32.9	18	54.7
IPI00218782	CAPZB F-actin capping protein subunit beta	37.4	23	61.5

Turnover proteins		kDa	Peptides	PAI
IPI00008274	CAP1 Adenylyl cyclase-associated protein 1	51.8	13	25.1
IPI00413344	CFL2 Cofilin-2	18.7	5	26.7
IPI00473014	DSTN Destrin (ADF)	18.4	5	27.2
IPI00012011	CFL1 Cofilin-1	18.4	10	54.3
IPI00216691	PFN1 Profilin-1	15	10	66.7
Myosin motors				
IPI00760846	MYO18A Myosin-XVIIIa	232.9	4	1.7
IPI00336047	MYO9B Myosin-Ixb	243.4	6	2.5
IPI00414980	MYO1B Myosin-Ib	124.8	7	5.6
IPI00873959	MYO5A Myosin Va	212.1	14	6.6
PI00743857	MYH11 smooth muscle myosin heavy chain 11	227.9	15	6.6
IPI00844172	MYO6 Myosin VI	144.9	13	9.0
IPI00243742	MYL3 myosin light chain 3, alkali, ventricular, skeletal, slow	21.9	5	22.8
IPI00607818	MYH14 nonmuscle myosin II heavy chain 14	231.8	54	23.3
IPI00216070	MYL1 myosin light chain 1, alkali, skeletal, fast	21.1	5	23.7
IPI00010418	MYO1C Myosin-Ic	117.8	29	24.6
IPI00019502	MYH9 nonmuscle myosin II heavy chain-A	226.3	87	38.4
IPI00397526	MYH10 nonmuscle myosin II heavy chain-B	228.8	103	45.0
IPI00335168	MYL6B myosin light chain 6B, alkali, smooth muscle and non-muscle	16.9	15	88.8
IPI00033494	MRLC2 myosin regulatory light chain 2	19.7	15	76.1
Regulators				
IPI00022542	ROCK1 Rho-associated protein kinase 1	158	6	3.8
IPI00008918	LIMA1 LIM kinase1	85.1	5	5.9
IPI00031023	FLII flightless-1	144.6	10	6.9
IPI00000230	TPM1 tropomyosin 1	32.6	5	15.3
IPI00218820	TPM2 Tropomyosin 2	28.6	5	17.5
IPI00010779	TPM4 Tropomyosin 4	28.5	7	24.6
IPI00746165	WDR1 WD repeat-containing protein 1 (Aip1)	66.1	24	36.3
IPI00643370	TPM3 Tropomyosin 3	18.6	30	161.3
Potential regulators				
IPI00549766	FAM40A Isoform 1 of Protein FAM40A	95.5	5	5.2
IPI00007935	PDLIM5 PDZ and LIM domain protein 5	63.9	4	6.3
IPI00014399	FHL3 Four and a half LIM domains protein 3	31.1	4	12.9

Other actin regulating proteins		kDa	Peptides	PAI
IPI00023283	TTN Titin	3803.4	4	0.1
IPI00328905	IQGAP3	184.4	7	3.8
IPI00871709	IQGAP2	180	18	10.0
IPI00009342	IQGAP1	189.1	66	34.9
IPI00003406	DBN1 Isoform 1 of Drebrin	71.3	56	78.5
Focal adhesion proteins				
IPI00219299	TLN2 Talin-2	271.3	9	3.3
IPI00291175	VCL Vinculin	116.6	7	6.0
IPI00020513	ZYX Zyxin	67.2	8	11.9
IPI00298994	TLN1 Talin-1	269.6	88	32.6

Table 5.1: Actin isoforms and actin binding proteins associated with the pellet.

Actin binding proteins were classified into nucleators, nucleation regulators, actin isoforms, membrane linkers, actin crosslinkers, capping proteins, turnover proteins, myosin motors, regulators, potential regulators, other actin regulating proteins, and focal adhesion proteins categories. International protein index (IPI) number, protein description, molecular weight in kDa, number of peptides in one run, and protein abundance index (number of peptides / protein molecular weight) are presented in the table. In each category proteins are presented from least abundant to most abundant according to PAI.

5.4.1 Multiple small GTPases and GTPase regulators are associated with the bleb fraction

Small GTPases are enzymes, which hydrolyse guanosine triphosphate (GTP) and regulate many functions of the cell. Small GTPases are regulated by GTPase activating proteins (GAPs), guanine nucleotide exchange factors (GEFs), and guanosine nucleotide dissociation inhibitors (GDIs), as described previously in the introduction of this thesis. Interestingly mass spectrometry analysis of the insoluable pellet of bleb fraction revealed that many small GTPases and their regulators were associated with the pellet.

Indeed, all together 11 small GTPase proteins were found to be present in the pellet together with six GAPs and eight GEFs (Table 5.2). Rab GTPases are a large group of Ras-related GTPases that regulate many functions of the cell including membrane trafficking (Novick and Zerial, 1997) and vesicle movement along actin filaments (Pruyne et al., 1998; Schott et al., 1999). RhoGTPases, instead, have been shown to regulate the actin cytoskeleton. Indeed, RhoA has been suggested to be the master regulator of the cortex (Charras et al., 2006; Etienne-Manneville and Hall, 2002) and was shown to be present at the bleb membrane throughout the bleb lifetime (Charras et al., 2006), suggesting of cortex association.

First many Rab GTPases were found at the pellet. Given that to date the Rab GTPases have not been shown to regulate the actin cortex together with their role in trafficking and vesicle movement, the cortical presence of Rab GTPases was surprising. However, because the bleb fraction contained intracellular membrane organelles, Rab GTPases associated with the pellet may be contaminants from these structures.

As RhoA has previously been shown to regulate the cortex (Charras et al., 2006; Etienne-Manneville and Hall, 2002), the presence of Rho GTPases in the pellet was not surprising. Consistent with previous studies, RhoA was abundant in the pellet (Table 5.2, PAI=50.7), but RhoC (PAI=22.8), RhoG (PAI=23.6), and Rac1 (PAI=28) were also present. RhoC association to the pellet is especially interesting, as it has been suggested to regulate ADF/cofilin, Fmnl2, and Diaph1 (Bravo-Cordero et al., 2011; Kitzing et al., 2010), suggesting that it might be an important regulator of cortical actin dynamics. Furthermore, functions previously attributed to RhoA may also result from RhoC activity. Indeed, most commonly used inhibitors of RhoA also inhibit RhoC (C3 exoenzyme and rhotekin binding domain) and thus results from previous studies (Charras et al., 2006) cannot truly differentiate between RhoA and RhoC. Therefore, more studies are needed to thoroughly understand the respective roles of RhoA and RhoC at the cortex. Rac1 has

been shown to activate the WAVE complex (Innocenti et al., 2004; Ismail et al., 2009), which in turn activates the Arp2/3 complex (Innocenti et al., 2005; Suetsugu et al., 2003; Yamazaki et al., 2003; Yan et al., 2003). Because WAVE complex activation by Rac1 is usually linked to lamellipodial formation, the presence of Rac1 at the pellet was unexpected.

Rho GTPase GAPs ARHGAP1 (p50RhoGAP) and RACGAP1 were present at the pellet (Table 5.2, GAPs in bold characters). Indeed, their presence was not surprising given that ARHGAP1 has been shown to inactivate RhoA (Lancaster et al., 1994), whereas RACGAP1 inactivates Rac1 (Toure et al., 1998). Being a RhoA regulator, the role of ARHGAP1 at the cortex is studied more in detail later in this thesis.

Further, Rho GTPase GEFs TRIO, PLEKHG2, ARHGEF7, DOCK7, and ARHGEF1 (p115 RhoGEF) associate with the pellet (Table 5.2, GEFs in bold characters). TRIO has been shown to activate both RhoA and Rac1 (Bellanger et al., 1998; Debant et al., 1996), but because TRIO was not abundant (Table 5.2, PAI=2.9, below our cutoff for reliable detection) in the pellet, it is unlikely to play a role. Other RhoA or Rac1 activators ARHGEF1 (Hart et al., 1998) (Table 5.2, PAI=10.1) and ARHGEF7 (Hsu et al., 2010) (Table 5.2, PAI=10.7) respectively, were several fold more abundant and thus more likely to be important regulators of GTPase activity in the cortex. PLEKHG2 (Ueda et al., 2008) and DOCK7 (Yamauchi et al., 2008) have been shown to stimulate two different Rho GTPases, Rac1 and Cdc42, but of these only Rac1 is present at the pellet. Being the most abundant RhoA activator, the role of ARHGEF1 in the cortex regulation is investigated by depletion studies later in this thesis.

Small GTPases		kDa	Peptides	PAI	Target
IPI00012451	GNB4 Guanine nucleotide-binding protein subunit beta-4	37.5	5	13.3	Unknown
IPI00291928	RAB14 Ras-related protein Rab-14	23.8	5	21	Golgi transport
IPI00016339	RAB5C Ras-related protein Rab-5C	23.4	5	21.4	Receptor trafficking
IPI00008964	RAB1B Ras-related protein Rab-1B	22.1	5	22.6	ER to Golgi transport
IPI00027434	**RHOC**	**21.9**	**5**	**22.8**	**Cofilin, Fmnl2, and Diaph1**
IPI00017342	RHOG	21.2	5	23.6	Phago- and endocytosis
IPI00023526	RAB6A Ras-related protein Rab-6A	23.5	6	25.5	Golgi transport
IPI00016513	RAB10 Ras-related protein Rab-10	22.5	6	26.7	Membrane trafficking
IPI00010271	**RAC1**	**21.4**	**6**	**28**	**WAVE complex**
IPI00005719	RAB1A Ras-related protein Rab-1A	22.6	7	31	Endocytic vesicle transport
IPI00020436	RAB11B Ras-related protein Rab-11B	24.4	8	32.8	Receptor trafficking
IPI00478231	**RHOA**	**21.7**	**11**	**50.7**	**ROCK and Diaph1**
GAPs					
IPI00016702	RABGAP1 Rab GTPase-activating protein 1	121.6	4	3.3	Rab6
IPI00554590	RAB3GAP2 Rab3 GTPase-activating protein 2	155.8	8	5.1	Rab3
IPI00020567	**ARHGAP1 Rho-GTPase-activating protein 1 (p50RhoGAP)**	**52.7**	**5**	**9.5**	**RhoA**
IPI00012442	G3BP1 Ras GTPase-activating protein-binding protein 1	52.1	5	9.6	Ras proteins
IPI00292753	GAPVD1 GTPase-activating protein and VPS9 domain-containing protein 1	166	17	10.2	Rab31
PI00794613	TBC1D15 TBC1 domain family member 15	77.3	9	11.6	Rab7
IPI00152946	**RACGAP1 Rac GTPaseactivating protein 1**	**70.9**	**10**	**14.1**	**Rac1**
GEFs					
IPI00002186	ARFGEF2 Brefeldin A-inhibited guanine nucleotide-exchange protein 2	201.9	4	2	ARF1, ARF5, and ARF6
IPI00657953	**TRIO triple functional domain**	**346.6**	**10**	**2.9**	**Rac1 and RhoA**
IPI00303373	**PLEKHG2 Pleckstrin homology domain-containing family G member 2**	**147.8**	**6**	**4.1**	**Rac1 and Cdc42**
IPI00183572	**DOCK7 Dedicator of cytokinesis protein 7**	**241.2**	**18**	**7.5**	**Rac1 and Cdc42**
IPI00746360	RIC8A I Synembryn-A	59.5	6	10.1	GNAI1, GNAO1 and GNAQ
IPI00339379	**ARHGEF1 Rho guanine nucleotide exchange factor 1 (p115RhoGEF)**	**98.7**	**10**	**10.1**	**RhoA**
IPI00449907	**ARHGEF7 Rho guanine nucleotide exchange factor 7**	**84.4**	**9**	**10.7**	**Rac1**
Other interactors					
IPI00171230	ERC1 ELKS/RAB6-interacting/CAST family member 1	113.8	4	3.5	Rab6
IPI00293009	RABEP1 Rab GTPase-binding effector protein 1	99.2	4	4	RABGEF1 -> Rab5A

Table 5.2: Small GTPases, their regulators, and interaction partners at the pellet.

Many small GTPases called Rab proteins together with Rho GTPases were found associated with the pellet. In addition, many GTPase activating proteins (GAPs) and guanine nucleotide exchange factors (GEFs) were found. GAPs and GEFs related to Rho and Rac regulation are in bold characters. International protein index (IPI) number, protein description, molecular weight in kDa, number of peptides in one run, and protein abundance index (number of peptides / protein molecular weight) are presented in the table. In each category proteins are presented from least abundant to most abundant according to PAI.

5.4.2 Changes in the pellet association of actin regulating proteins upon cytochalasin D treatment

Dynamic actin filaments are sensitive to drugs altering polymerisation. One of these drugs is cytochalasin D, which caps the growing barbed ends of actin filaments (Cooper, 1987) leading to disassembly of filaments that do not have a capped pointed end to prevent depolymerisation. Filaments with a protected pointed end (tropomodulin or Arp2/3 complex bound) will remain as static filaments until the pointed end capper is released or cytochalasin D is washed out. Finally, if the cytochalasin D concentration is low enough, a small fraction of barbed ends stay free from the drug and keep polymerising.

We reasoned that cytochalasin D could be used to investigate which proteins of the bleb fraction are potentially integral components of the cortex and which ones are contaminants that are pelleted non-specifically. Indeed, in M2 cells, when actin is depolymerised, many proteins lose their cortical localisation and become cytoplasmic (Charras et al., 2006). Similarly, I expect that upon depolymerisation of actin filaments in bleb fraction, proteins associated with the pellet and dependent upon actin for their localisation will shift to the supernatant. However, actin depolymerising drugs function

through disrupting the turnover of filaments. Therefore, if filaments are not turning over or turn over slowly due to stabilisation, actin depolymerising drugs will not depolymerise these filaments and protected filaments will be enriched in the pellet. I expect to find proteins that cap pointed ends or protect filaments from depolymerisation in this category. Finally, if no change in the abundance of a protein in the pellet is observed upon cytochalasin D treatment, then I expect the protein to be unspecifically sedimented upon centrifugation and thus be a contaminant or to be only transiently associated with the pellet (e.g. regulatory proteins). However, even if a particular actin binding protein appears to be strongly bound to the pellet according to these studies, its role at the cortex has to be further assessed because of potential contamination of Golgi complex and ER bound actin.

It is known, that in response to high doses (5µM) of cytochalasin D, actin recruitment to the cortex is terminated (Charras et al., 2006). Such an effect was too dramatic as we wanted to obtain a decrease in the filament mass in the bleb fraction but not a complete loss of the cortex. Thus, to retain a fraction of the filaments at the cortex, but to obtain a clear decrease in the filament mass we chose to treat the bleb fraction with 2.5µM of cytochalasin D. Treament with cytochalasin D and the mass spectrometry were carried out by Dr. Romeo and Dr. Roux.

Previously the recruitment of some actin regulating proteins upon cytochalasin D treatment has been studied. It was shown, that α-actinin, coronin 3, and myosin II are recruited to the bleb cortex after actin and were not observed in blebs after 5µM cytochalasin D treatment (Charras et al., 2006). In contrast, ERM-proteins ezrin and moesin appear in the bleb membrane before actin and were not affected by cytochalasin D treatment, suggesting that the recruitment of ERM-proteins is independent from actin (Charras et al., 2006). Indeed, proteins whose cortical localisation is actin independent might not be as severely affected by cytochalasin D treatment as proteins, whose localisation depends on actin. Thus, we have to carefully consider based on the potential role of the protein at the cortex whether or

not the protein is a contaminant, if no change or only a small decrease or increase is observed after the cytochalasin D treatment.

First, as a negative control I followed the peptide shift of tubulin isoforms and vimentin (constituents of microtubules and intermediate filaments respectively) between the pellet of control and cytochalasin D treated bleb fraction, as microtubules and vimentin have been reported to be insensitive to cytochalasin D (Dentler and Adams, 1992; Kumar et al., 2007). I observed that no greater than -20% decrease of tubulins or vimentin occurred upon cytochalasin D treatment (controls Table 5.3, with the exception of -63% with tubulin beta2B chain). Thus, I chose 20% change upon cytochalasin D treatments as my threshold for the analysis and concluded that proteins that varied less than ±20% (marked with blue in Table 5.3) after cytochalasin D treatment compared to control did not show a significant change. Those proteins that increased more than 20% (marked with green in Table 5.3) or decreased more than -20% (marked with red in Table 5.3) were likely to be truly pellet associated proteins.

With 2.5µM of cytochalasin D, the majority of the barbed ends of the filaments in the pellet should have been blocked and the filament mass should have decreased. Thus I reasoned, that an overall decrease in actin binding proteins in the pellet of bleb fraction after the cytochalasin D treatment should be observed. Consistent with this reasoning cytochalasin D treatment led to significantly decreased pellet association in 60% of the actin regulating proteins (marked with red in Table 5.3). Further, only in 7% of the actin regulating proteins the binding to the pellet fraction did increase due to cytochalasin D treatment (marked with green in Table 5.3) and finally in 30% of the actin regulating proteins in the pellet fraction displayed no significant change in pellet association due to cytochalasin D treatment (marked with blue in Table 5.3).

Nucleators and their regulators

As cytochalasin D blocks the barbed end of the filaments, I reasoned that proteins involved in the filament barbed end dynamics should be affected more dramatically than pointed end-associated proteins because they compete for the same binding site. Consistent with this, pellet association of the barbed end bound formin Diaph1 decreased substantially (-47%). Interestingly, there was a high degree of variability in the change in pellet association of the different subunits of the Arp2/3 complex upon cytochalasin treatment. Those subunits that bind to the mother filament (Goley and Welch, 2006) were not significantly affected (ARPC1, ARPC2, and ARPC4 all ±20% and ARPC5 -25%, Table 5.3, nucleators) but the pellet association of Arp3 which is bound to the daughter filament (Goley and Welch, 2006) increased significantly (+43%, Table 5.3, nucleators) suggesting the Arp2/3 complex may stabilise the filament by remaining bound to the pointed end of daughter filaments preventing their depolymerisation. The pellet association of the Arp2/3 complex activators (Table 5.3, nucleation regulation) the WAVE complex (NAP1 -25% and SRA1 0%) and cortactin (-24%) were hardly affected by the cytochalasin D treatment perhaps because they are predominantly membrane-bound and only transiently and indirectly associated with actin. In contrast, coronin-1C association with the pellet was dramatically affected by cytochalasin (-75%), suggestive of strong actin binding, which might indeed signify that branch remodelling by coronin occurs in the cortex, but would need to be investigated more in detail.

Actin isoforms

Inhibiting filament elongation had variable effects on the different actin isoforms (Table 5.3, actin isoforms). The association of α- and γ-actin to the pellet decreased (-48% and -40% respectively), but a substantial increase was observed with β-actin (+52%). One possible explanation to this surprising effect could be that a large portion of β-actin filaments have capped pointed ends or are protected from depolymerisation, therefore enriching them in the pellet after cytochalasin treatment. Consistent with this

hypothesis, a recent report suggests that β-actin is predominantly involved in stress fibers and cell-cell contacts whereas γ-actin forms cortical and lamellipodial structures in motile cells (Dugina et al., 2009). Similar to contractile structures within cells, the contractile actin network within the cortex may be stabilised against depolymerisation by actin binding proteins such as tropomyosins, tropomodulin, and caldesmon (Tojkander et al., 2012). Speculating further, in the cortex, β-actin and γ-actin may therefore be involved in different networks. Indeed, it has been suggested that several different types of actin networks may exist within the cell optimised for specific functions, with different mechanical and dynamic properties (Michelot and Drubin, 2011). However, the potential differential roles of β-actin and γ-actin are controversial and remain to be investigated in the cortex.

Membrane linkers

All actin cortex-membrane linker proteins lost association with actin upon cytochalasin D treatment (Table 5.3, membrane linkers) consistent with the decreased filament mass and suggesting that all cortex-membrane linker proteins are strongly associated with actin in the pellet. Initially, I expected that there would be no change or only a small decrease in the association of ERM-proteins upon cytochalasin D treatment is observed because ERM-proteins are recruited to the bleb membrane independently of actin (Charras et al., 2006). However, all ERM-proteins decreased significantly and in similar proportions with one another upon cytochalasin D treatment (ezrin -38%, radixin -30%, moesin -29%), suggesting that ERM-proteins are tightly bound to F-actin and that actin independent recruitment to the bleb did not affect to the result of the assay. Filamin B was affected more than ERM-proteins and lost association with actin (-47%). Finally the most dramatic loss of pellet association was with utrophin, which decreased by -89% upon cytochalasin D treatment. To date the role of utrophin as an actin-membrane linker in non-muscle cells have not been studied, but may be interesting to characterise in the view of these results.

Actin crosslinkers

Association of α-actinin with the pellet was quite dramatically decreased upon cytochalasin D treatment (-69% – -39%), consistent with decreased filament mass (Table 5.3, actin crosslinkers). Surprisingly, a concomitant increase in the association of fascin with the pellet was observed. The main function of fascin has been shown to be filament bundling in filopodia (Svitkina et al., 2003), but interestingly a recent study suggested that fascin might impede the activity of ADF/cofilin in filopodia (Breitsprecher et al., 2011). Indeed, such a protective mechanism against depolymerisation in the cortex upon cytochalasin D treatment would be favourable to retain cortical filaments. However it is also possible that fascin is simply a contaminant in the pellet. Thus, futher analysis is needed to verify if fascin has a role in the cortex. Finally no significant change in annexin association to the pellet between control and cytochalasin D treated isolated blebs was observed (0 – +10%), suggesting annexins are not strongly associated with actin.

Capping proteins

Both barbed and pointed end cappers were present at the pellet (Table 5.3, capping proteins) and a significant loss of all the capping proteins from the pellet was observed after cytochalasin treatment regardless of the capper being barbed or pointed end associated protein (CapZ <-38%, gelsolin -100%, tropomodulin-3 -43%). Interestingly it has been proposed, that cytochalasin D and barbed end capping proteins compete for barbed end binding (Wakatsuki et al., 2001). Thus, if cytochalasin D is unable to replace heterodimeric capping protein at the barbed end, slow dissociation of heterodimeric capping protein from the barbed end (recovery $t_{1/2}$=30min *in vitro* (Schafer et al., 1996)) might contribute to incomplete loss of capping proteins. In contrast, gelsolin, also a barbed end capper (Silacci et al., 2004; Sun et al., 1999), was completely lost from the pellet after cytochalasin D treatment. Twinfilin, whose capping activity of the pointed end is less characterized, showed a minor increase in the association to the pellet after cytochalasin D treatment (+25%), however the increase was hardly

significant. Emerin showed no change to control upon cytochalasin D treatment, suggesting that it might indeed be a contaminant. Finally, tropomodulin-3 was partly lost (-43%) from the cortex due to cytochalasin D treatment. Being a pointed end capper (Fowler, 1997; Gregorio et al., 1995), it is not directly affected by barbed end capping, but probably loses pellet association due to decreased filament mass.

Turnover proteins

In general proteins participating in actin turnover were not significantly affected by cytochalasin treatment (Table 5.3, turnover, ADF/cofilins and profilin-1 ±20% change), which was expected as ADF/cofilins and profilin both maintain the G-actin pool in cells. Interestingly an increase (+46%) in the association of CAP1, an ADF/cofilin co-operator and actin recycler (Moriyama and Yahara, 2002), to the pellet was observed upon cytochalasin D treatment, suggesting a possible increase in actin recycling due to filament depolymerisation and disappearance.

Myosin motors

All myosin motors lost association with the pellet upon cytochalasin treatment (Table 5.3, myosin motors, -27% – -100%) consistent with the decreased filament mass. This suggests that all myosin motor isoforms are strongly associated with actin.

Regulatory proteins

Pellet association of proteins regulating actin binding proteins was very randomly affected by the cytochalasin D treatment (Table 5.3, regulatory proteins). Indeed, flightless-I and ROCK1 were not significantly affected (+20% and +17% respectively), suggesting that they are probably not strongly actin bound, but bound to the proteins they regulate prior to their interaction with the cortex. Indeed flightless-I possibly binds Diaph1 (Higashi et al., 2010), whereas ROCK1 has multiple binding partners. The ADF/cofilin

binding regulator LIM-kinase and Aip1 lost association with actin upon cytochalasin D treatment (-100% and -25% respectively).

Tropomyosins protect actin filaments from severing by gelsolin, villin, or ADF/cofilin (Bernstein and Bamburg, 1982; Burgess et al., 1987; DesMarais et al., 2002) and strengthen pointed end capping by tropomodulin (Fowler, 1996; Fowler et al., 2003; Littlefield and Fowler, 1998; Weber et al., 1994; Weber et al., 1999) suggestive that the association of tropomyosins with actin should increase upon cytochalasin D treatment. However, interestingly tropomyosin isoforms were very randomly affected (tropomyosin-1 +40%, tropomyosin-2 -100%, tropomyosin-3 +7%, tropomyosin-4 +29%) suggestive of differences in actin binding affinity or differential functions in cells between isoforms. Indeed, different isoforms of tropomyosins have been found in different structures of cells. Tropomyosin-1 and -2 have been shown to participate in vesicle movement (Hegmann et al., 1989) and tropomyosin-3 and -5 in mitochondria and lysosome movement (Pelham et al., 1996). Further, tropomyosin-1, -2, -4, and -5 all have been shown to localise to leading edge of motile cells (Hillberg et al., 2006), but interestingly only tropomyosin-2 and -3 have been shown to participate in stress fiber formation (Gimona et al., 1996). In the context of the actin cortex it remains to be investigated which tropomyosin isoforms participate in cortical dynamics.

Other actin regulating proteins

Consistent with the decreased filament mass, the pellet association of drebrin and IQGAPs were decreased after cytochalasin D treatment (Table 5.3, other actin regulating proteins, drebrin -52%, IQGAP1-3 -17% – -100%). Interestingly IQGAP2 was the most affected (-100%) suggesting strong binding to actin.

Focal adhesion proteins

Association of focal adhesion proteins with the pellet was not dramatically affected by the cytochalasin D treatment (Table 5.3, focal adhesion proteins,

-29% – +11%), suggesting they are possibly contaminants. However, a clear reduction (-50%) in the association of zyxin with the pellet fraction upon cytochalasin D treatment was observed. Although mainly studied in focal adhesions, a recent study showed that zyxin mediates actin-membrane linking in cell-cell junctions (Sperry et al., 2010), suggesting that zyxin might have a role in the cell cortex, however another possibility is that zyxin gets co-purified with the actin structures and does not participate in cortical dynamics.

Negative controls		Control	CytoD	CytoD change %	PAI
IPI00180675	TUBA1A Tubulin alpha1A chain	99	79	-20	
IPI00387144	TUBA1B Tubulin alpha1B chain	126	106	-16	
IPI00218343	TUBA1C Tubulin alpha1C chain	107	86	-20	
IPI00011654	TUBB Tubulin beta chain	143	134	-6	
IPI00006510	TUBB1 Tubulin beta1 chain	17	16	-6	
IPI00013475	TUBB2A Tubulin beta2A chain	53	62	17	
IPI00031370	TUBB2B Tubulin beta2B chain	113	42	-63	
IPI00007752	TUBB2C Tubulin beta2C chain	133	124	-7	
IPI00418471	VIM Vimentin	117	112	-4	
Nucleators					
IPI00005160	ARPC1 Actin-related protein 2/3 complex subunit 1	5	6	20	12.2
IPI00028091	ACTR3 Actin-related protein 3	7	10	43	14.8
IPI00550234	ARPC5 Actin-related protein 2/3 complex subunit 5	4	3	-25	24.5
IPI00005159	ACTR2 Actin-related protein 2	11	11	0	24.6
IPI00005162	ARPC3 Actin-related protein 2/3 complex subunit 3	6	7	17	29.3
IPI00554811	TTLL3;ARPC4 Actin-related protein 2/3 complex subunit 4	7	7	0	35.5
IPI00005161	ARPC2 Actin-related protein 2/3 complex subunit 2	15	12	-20	43.7
IPI00852685	DIAPH1 Diaphanous1	19	10	-47	134.8
Nucleation regulators					
IPI00867509	CORO1C Coronin-1C	4	1	-75	6.8
IPI00029601	CTTN Cortactin	17	13	-24	27.6
IPI00719600	CYFIP2 Cytoplasmic FMR1-interacting protein 2 (SRA1)	8	8	0	55.2
IPI00031982	NCKAP1 Nck-associated protein 1 (NAP1)	8	6	-25	62.5
Actin isoforms					
IPI00003627	ACTL6A Isoform 1 of Actin-like protein 6A	5	6	20	10.6
IPI00008603	ACTA2 Actin; alpha smooth muscle	21	11	-48	50.1
IPI00021428	ACTA1 Actin; alpha skeletal muscle	36	34	-6	85.7
IPI00021439	ACTB Actin; beta cytoplasmic	56	85	52	134.3
IPI00021440	ACTG1 Actin; gamma cytoplasmic	75	45	-40	179.4
Membrane linkers					
IPI00009329	UTRN Utrophin	18	2	-89	4.6
IPI00017367	RDX Radixin	7	5	-29	9.9
IPI00219365	MSN Moesin	10	7	-30	14.8
IPI00746388	EZR Ezrin	16	10	-38	23.1
IPI00289334	FLNB Filamin-B	38	20	-47	136.7

Actin crosslinkers		Control	CytoD	CytoD change %	PAI
IPI00002459	ANXA6 Annexin 6	4	4	0	5.3
IPI00163187	FSCN1 Fascin1	5	15	200	9.2
IPI00019884	ACTN2 Alpha-actinin-2	18	11	-39	17.4
IPI00032137	ACTN3 Alpha-actinin-3	19	7	-63	18.4
IPI00550363	TAGLN2 Transgelin-2	5	3	-40	22.4
IPI00329801	ANXA5 Annexin A5	10	11	10	27.9
PI00418169	ANXA2 Annexin A2	23	24	4	57.1
IPI00013808	ACTN4 Alpha-actinin-4	113	57	-50	107.9
IPI00013508	ACTN1 Alpha-actinin-1	113	50	-56	109.7
Capping proteins					
IPI00550917	TWF2 Twinfilin-2	4	5	25	10.1
IPI00646773	GSN Gelsolin	12	0	-100	14.9
IPI00005087	TMOD3 Tropomodulin-3	7	4	-43	17.7
IPI00032003	EMD Emerin	7	7	0	24.2
IPI00005969	CAPZA1 F-actin-capping protein subunit alpha-1	17	7	-59	51.7
IPI00026182	CAPZA2 F-actin-capping protein subunit alpha-2	18	3	-83	54.7
IPI00218782	CAPZB F-actin capping protein subunit beta	23	14	-39	61.5
Turnover proteins					
IPI00008274	CAP1 Adenylyl cyclase-associated protein 1	13	19	46	25.1
IPI00413344	CFL2 Cofilin-2	5	6	20	26.7
IPI00473014	DSTN Destrin (ADF)	5	4	-20	27.2
IPI00012011	CFL1 Cofilin-1	10	12	20	54.3
IPI00216691	PFN1 Profilin-1	10	8	-20	66.7
Myosin motors					
IPI00760846	MYO18A Myosin-XVIIIa	4	0	-100	1.7
IPI00336047	MYO9B Myosin-Ixb	6	3	-50	2.5
IPI00414980	MYO1B Myosin-Ib	7	3	-57	5.6
IPI00873959	MYO5A Myosin Va	14	7	-50	6.6
PI00743857	MYH11 smooth muscle myosin heavy chain 11	15	11	-27	6.6
IPI00844172	MYO6 Myosin VI	13	0	-100	9.0
IPI00243742	MYL3 myosin light chain 3, alkali, ventricular, skeletal, slow	5	2	-60	22.8
IPI00607818	MYH14 nonmuscle myosin II heavy chain 14	54	0	-100	23.3
IPI00216070	MYL1 myosin light chain 1, alkali, skeletal, fast	5	0	-100	23.7
IPI00010418	MYO1C Myosin-Ic	29	12	-59	24.6
IPI00019502	MYH9 nonmuscle myosin II heavy chain-A	87	75	-14	38.4
IPI00397526	MYH10 nonmuscle myosin II heavy chain-B	103	72	-30	45.0
IPI00335168	MYL6B myosin light chain 6B, alkali, smooth muscle and non-muscle	15	10	-33	88.8
IPI00033494	MRLC2 myosin regulatory light chain 2	15	0	-100	76.1

Regulators		Control	CytoD	CytoD change %	PAI
IPI00022542	ROCK1 Rho-associated protein kinase 1	6	7	17	3.8
IPI00008918	LIMA1 LIM kinase1	5	0	-100	5.9
IPI00031023	FLII flightless-1	10	12	20	6.9
IPI00000230	TPM1 tropomyosin 1	5	7	40	15.3
IPI00218820	TPM2 Tropomyosin 2	5	0	-100	17.5
IPI00010779	TPM4 Tropomyosin 4	7	9	29	24.6
IPI00746165	WDR1 WD repeat-containing protein 1 (Aip1)	24	18	-25	36.3
IPI00643370	TPM3 Tropomyosin 3	30	32	7	161.3
Potential regulators					
IPI00549766	FAM40A Isoform 1 of Protein FAM40A	5	1	-80	5.2
IPI00007935	PDLIM5 PDZ and LIM domain protein 5	4	3	-25	6.3
IPI00014399	FHL3 Four and a half LIM domains protein 3	4	3	-25	12.9
Other actin regulating proteins					
IPI00023283	TTN Titin	4	3	-25	0.1
IPI00328905	IQGAP3	7	5	-29	3.8
IPI00871709	IQGAP2	18	0	-100	10.0
IPI00009342	IQGAP1	66	55	-17	34.9
IPI00003406	DBN1 Drebrin	56	27	-52	78.5
Focal adhesion proteins					
IPI00219299	TLN2 Talin-2	9	10	11	3.3
IPI00291175	VCL Vinculin	7	5	-29	6.0
IPI00020513	ZYX Zyxin	8	4	-50	11.9
IPI00298994	TLN1 Talin-1	88	82	-7	32.6

Table 5.3: Changes in actin isoforms and actin binding proteins upon cytochalasin D treatment.

The changes in actin binding protein association to the pellet were studied after cytochalasin D treatment. The amount of peptides in control and after cytochalasin D (CytoD) treatment is presented together with the percentage decrease or increase caused by the cytochalasin treatment compared to control (CytoD change %). Proteins that decreased more than -20% were marked with red, increased more than 20% with green, and no change with blue. Protein abundance index (number of peptides / protein molecular weight) is also presented in the table. In each category proteins are presented from least abundant to most abundant according to PAI.

5.5 Several actin regulating proteins are necessary for cell cortex maintenance

Next, I decided to study the role of a set of interesting pellet associated actin binding proteins that may have a role at the cortex by localisation and depletion studies. Which proteins and why they were interesting to study in the context of the cell cortex are presented next together with what is known about their localisation in cells and what effects their depletion led to in other cells.

First, I was interested in the role of barbed end capping, filament severing, and depolymerisation in the cortex. Heterodimeric capping protein, consisting of CapZA and CapZB domains (Fig. 5.5), efficiently caps the barbed ends of filaments (Isenberg et al., 1980). In the lamellipodium heterodimeric capping protein was found to localise very near to the leading edge and its depletion led to loss of lamellipodia (Iwasa and Mullins, 2007). Interestingly, studies indicate that the loss of heterodimeric capping protein leads to mislocalisation and loss of the Arp2/3 complex activity (Iwasa and Mullins, 2007; Mejillano et al., 2004). The reason for this still remains to be fully investigated, but it appears that controlling filament length is essential for lamellipodia maintenance (Bear et al., 2002; Iwasa and Mullins, 2007; Mogilner and Oster, 1996). I included heterodimeric capping protein for further studies, because I was interested in understanding if controlled filament length by barbed end capping was also needed in the cortex. Interestingly heterodimeric capping protein was abundant and strongly associated with the pellet according to the mass spectrometry studies, suggesting that barbed end capping might be important for cortical integrity.

Gelsolin, which consists of six gelsolin repeats (Fig. 5.5), caps and severs F-actin (Silacci et al., 2004). Gelsolin has not been extensively studied in cells, but it has been reported to localise to stress fibers (Dissmann and Hinssen, 1994) and cadherin based adhesions (Chan et al., 2004) in fibroblasts. Indeed, knockdown of gelsolin led to reduction in E-cadherin in cell-cell

junctions (Tanaka et al., 2006), suggesting a role in maintaining cell-cell adhesions. Interestingly we found that gelsolin associates with the pellet and is expressed in blebbing cells according to qPCR studies (Fig. 5.6). Although gelsolin was not abundant in the pellet, it appeared to be strongly bound to actin. Because gelsolin is potentially involved in severing of the cortex, I wanted to study if it is needed for cortex maintenance.

ADF/cofilin depolymerises (Carlier et al., 1997) and severs (Chan et al., 2000; Maciver et al., 1991; Moriyama et al., 1999) F-actin. In motile cells depolymerisation appears to take place at the junction between lamellipodium and lamellum where cofilin-1 localises in most cell types (Svitkina and Borisy, 1999). Silencing cofilin led to problems in cell spreading (Iwasa and Mullins, 2007; Rogers et al., 2003), but those cells that succeeded in spreading displayed normal gross morphologies (Iwasa and Mullins, 2007). However, a detailed analysis revealed that cofilin depletion led to an increase in F-actin content in the cells (Iwasa and Mullins, 2007) indicating impaired depolymerisation. Further, actin-GFP speckles moved slower in cofilin depleted cells compared to control and led to extended lamellipodia (Iwasa and Mullins, 2007), suggesting slower actin turnover upon cofilin depletion. Interestingly from the ADF/cofilin isoforms, cofilin-1 (Fig. 5.5) was the most abundant isoform in M2 cells according to the qPCR results (Fig. 5.6) and was abundant in the pellet. Thus, I included cofilin-1 for the localisation and depletion studies to investigate if efficient depolymerisation and severing by cofilin-1 is necessary for correct cortical actin dynamics.

Aip1 (WDR1), consisting of multiple WD40 repeats (Fig. 5.5), enhances the depolymerisation and severing activity of ADF/cofilin (Aizawa et al., 1999; Okada et al., 1999; Rodal et al., 1999) and caps the barbed end of severed filaments in a cofilin-dependent manner (Okada et al., 2002). Consistent with its interaction with ADF/cofilin, Aip1 colocalises with cofilin at the lamellipodium of XTC cells (Tsuji et al., 2009). Silencing studies revealed that

in mitotic HeLa cells depletion of Aip1 led to abnormal F-actin accumulation at the contractile ring (Kato et al., 2008). In addition, in motile Jurkat cells, Aip1 silencing led to formation of multiple lamellipodia, whereas in control cells only one lamellipodium was observed (Kato et al., 2008), suggestive of disrupted polarisation. Aip1 was included in the localisation and depletion studies, because we found that Aip1 is expressed in M2 cells (Fig. 5.6) as well as abundant and strongly bound to actin according to the mass spectrometry studies. Thus, it may be an important positive regulator of ADF/cofilin activity and participate in barbed end capping in the cortex. In addition, clues from the literature suggest that Aip1 may be important for cortical integrity as it was reported that Aip1 knockdown HeLa cells occasionally bleb (Kato et al., 2008).

Second, in addition to understanding the role of barbed end capping, filament severing, and depolymerisation at the cortex, I wanted to study cortex nucleation and cortex homeostasis. Profilin (Fig. 5.5) catalyses the exchange of ADP for ATP in actin monomers (Mockrin and Korn, 1980) and delivers ATP-actin monomers to formins (Chang et al., 1997; Watanabe et al., 1997). In motile cells, profilin localises to the lamellipodium and lamellum (Buss et al., 1992). Interestingly, the effect of profilin-1 depletion in cell motility depends on the cell type: in some cell lines profilin depletion inhibits migration, whereas in others it seems to promote it (Bae et al., 2009; Ding et al., 2009; Ding et al., 2006; Janke et al., 2000). Although the main function of profilin-1 is arguably nucleotide exchange on actin monomers, profilin also interacts with membranes (Hartwig et al., 1989) and has been suggested to dock other proteins to the membrane-cytosol interface by a mechanism that requires phospholipid binding (Bae et al., 2009), suggesting that in different cell types the lack of membrane binding and protein docking may result in different outcomes. I was interested in profilin-1 because it was associated with the pellet and might be important for Diaph1 mediated actin nucleation and elongation.

Flightless-I is a gelsolin family protein (Campbell et al., 1993) consisting of gelsolin and leucine rich repeats (Fig. 5.5), suggesting that it might have severing activity like gelsolin. Indeed flightless-I homolog in *C. elegans* has been reported to sever F-actin (Goshima et al., 1999). In Swiss 3T3 cells flightless-I was shown to localise to membrane ruffles as well as to colocalise with microtubules (Davy et al., 2001). Interestingly recently flightless-I was shown *in vitro* to co-activate Diaph1 together with RhoA (Higashi et al., 2010). Thus, although flightless-I was not abundant or strongly bound to the actin pellet, it may be a potential Diaph1 regulator and was included in the localisation and depletion studies.

The small GTPase RhoA is present at the cell cortex in M2 cells (Charras et al., 2006) and cytokinetic cells (Nishimura and Yonemura, 2006). Interestingly RhoA has been proposed to be the most important regulator of the cortex (Charras et al., 2006; Etienne-Manneville and Hall, 2002) as it activates ERM-proteins (Fukata et al., 1998; Kotani et al., 1997; Matsui et al., 1998; Matsui et al., 1999; Shaw et al., 1998), formins (Higashida et al., 2004), and myosin II (Totsukawa et al., 2000), which are all present at the cortex. Most importantly microinjection of Rho guanine nucleotide dissociation inhibitor α (GDIα), the catalytic domain of p50Rho GTPase activating protein (GAP), the RhoGTPase-binding domain of rhotekin, or C3 exoenzyme stopped blebbing in M2 cells (Charras et al., 2006). Thus, I wanted to study the role of RhoA regulators in the cell cortex maintenance. The only RhoA specific regulators found associated with the pellet were p115RhoGEF and p50RhoGAP (Fig. 5.5). With these regulators, I was especially interested in revealing, whether their silencing perturbs cortical integrity or not and thus included them in the shRNA screen.

M2 cells have been shown to be filamin A-deficient (Cunningham et al., 1992) and it was hypothesised that this led to decreased membrane-cortex adhesion and thus to blebbing (Cunningham et al., 1992; Dai and Sheetz, 1999). Vertebrates express three filamin isoforms A, B and C, of which

filamin A and filamin B are ubiquitously expressed, whereas filamin C is muscle specific (Stossel et al., 2001; van der Flier and Sonnenberg, 2001). All filamins are very homologous through their sequence that consists of calponin homology domains and multiple filamin repeats (Fig. 5.5). Thus, it is not surprising that they have overlapping functions. Indeed, both filamin A and filamin B localise to stress fibers and to the cell cortex (Sheen et al., 2002). Interestingly all filamins were expressed in M2 cells (Fig. 5.6), but only filamin B was observed to be abundant and strongly associated with pellet. To assess the role of filamin B in cortex maintenance and especially to reveal if its overexpression can rescue M2 cell blebbing, I included it for further examination.

Third, I wanted to study the motor proteins in M2 cells a bit further. The role of myosin-II has been extensively studied in non-muscle cells and myosin IIA and IIB were found to be abundant and strongly bound to the pellet. However, myosin-IC was also strongly expressed in M2 cells (Fig. 5.6), abundant, and strongly associated with actin. Myosin-Is have been shown to localise to the cell membrane (Bose et al., 2002; Ruppert et al., 1995) and thus may be involved in cortex-membrane linking. Myo1C consists not only of myosin head and tail domains, but also contains IQ-repeats found in IQGAPs (Fig. 5.5), suggesting other functions in addition to force generation. Therefore I decided to study its role in the cortex.

Finally, I also wanted to understand more of the role of two actin regulating proteins, drebrin and IQGAP1, that were both abundant in the pellet. Interestingly, drebrin that contains an ADF-H domain like ADF/cofilin (Fig. 5.5), inhibits α-actinin, tropomyosin (Ishikawa et al., 1994), and myosin binding to actin (Hayashi et al., 1996; Ishikawa et al., 2007). Drebrin has been reported to localise to the apical membrane in epithelial cells (Keon et al., 2000) and to the leading edge of motile cells (Peitsch et al., 2001). In addition drebrin also localised to cell-cell contacts (Peitsch et al., 1999), which were disrupted upon drebrin depletion (Butkevich et al., 2004). Drebrin

not only was abundant in the actin pellet, but also appeared strongly bound and because it could be involved either in regulating contractility or actin crosslinking, both important features of the cortex, it was included for further studies.

Interestingly IQGAP1, consisting of calponin homology domain, IQ repeats, and RasGAP domains (Fig. 5.5), was shown to be needed for localisation of Diaph1 at the leading edge of migrating cells (Brandt et al., 2007) and to stimulate Arp2/3 complex induced nucleation (Le Clainche et al., 2007). In addition, IQGAP1 has been shown to localise to the exocyst-septin complex (Rittmeyer et al., 2008), to cell-cell contacts (Noritake et al., 2004), and to the leading edge of motile Vero cells (Watanabe et al., 2004). Upon IQGAP1 depletion polarised migration of Vero cells was disrupted (Watanabe et al., 2004). I found IQGAP1 interesting to study further as it may regulate cortex nucleation through both Diaph1 and the Arp2/3 complex.

I carried out localisation and depletion studies with the proteins described. First, I performed a localisation screen by tagging the proteins with GFP and followed their localisation in blebbing M2 cells stably expressing LifeAct-Ruby. If a high unbound fraction of the protein was expected, I carried out a simultaneous permeabilisation-fixation. Second, I performed a silencing screen using at least three separate shRNA constructs for each gene and a negative control, non-silencing shRNA. After 72h of transfection with the shRNAs, the cells were replated to obtain vigorous blebbing and imaged once the cells had attached (4h) to glass coverslips.

Verification of target mRNA level reduction after 72h transfection by quantitative real-time PCR or immunoblotting have not been carried out at the time of submission of this thesis but are in progress. In addition, it is in progress to quantify the results from the shRNA screen by classifying the shRNA transfected cells (GFP as a marker for transfected cells) into large blebs, small blebs, normal sized blebs, and no blebs categories with the help

of Cell Profiler and Cell Profiler Analyst, which are cell image analysis programs designed for quantification of phenotypes.

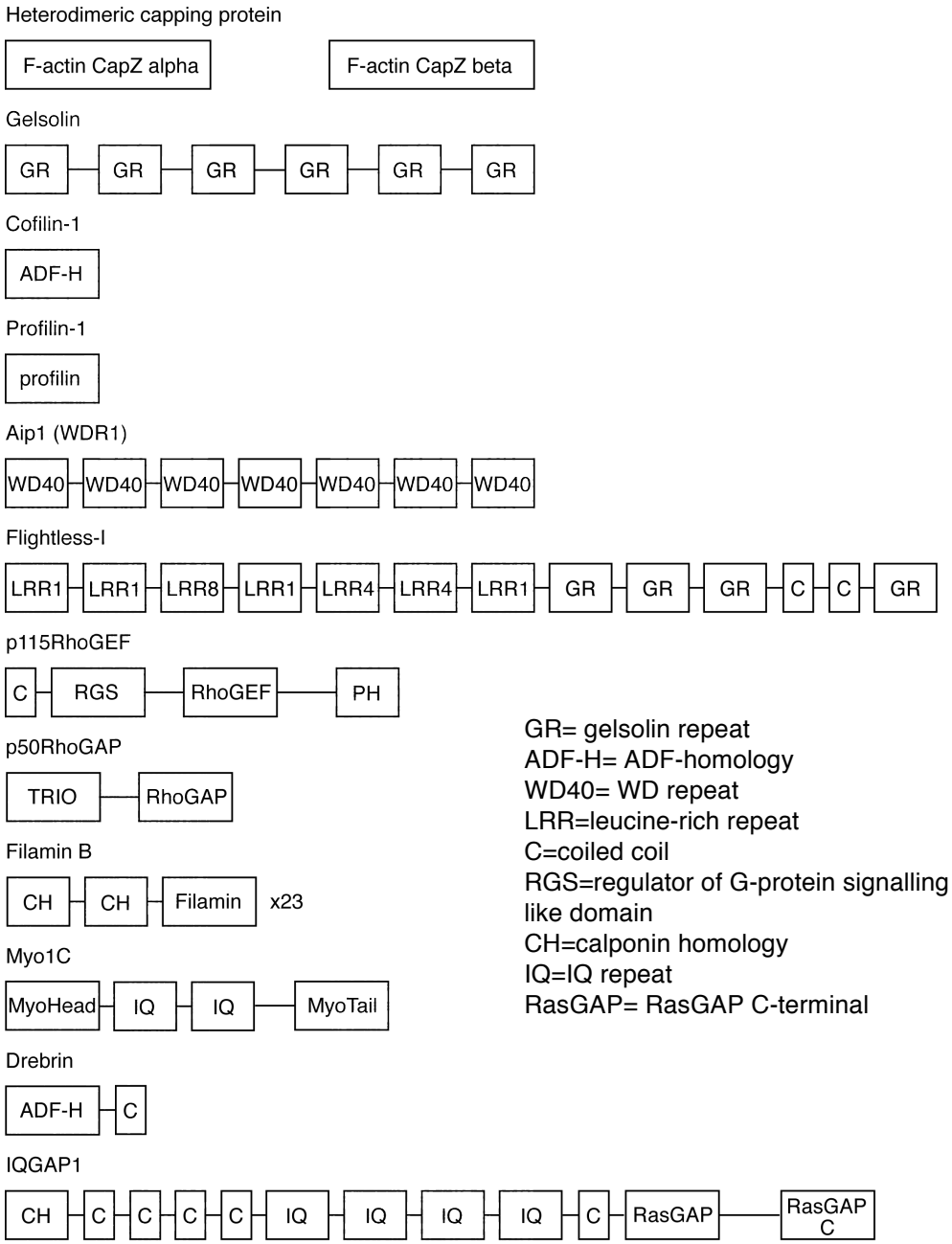

Figure 5.5: Pellet associated proteins chosen for the localisation and silencing screen.

The domain structure of the subset of proteins, studied more in detail. These included proteins involved in actin filament capping, turnover, cortex regulation, membrane linking, and contractility.

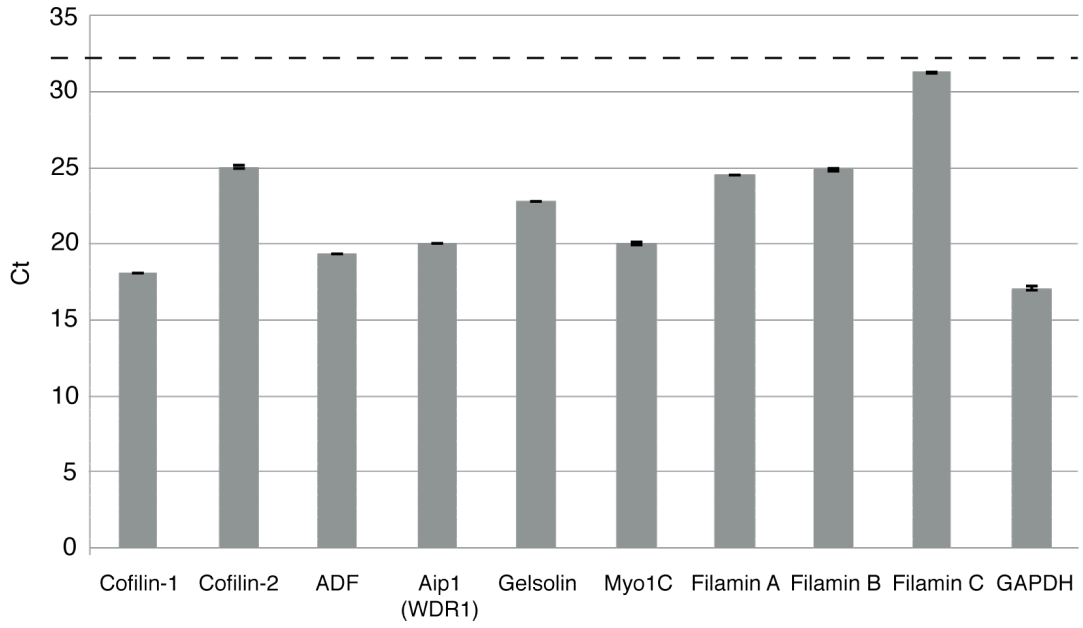

Figure 5.6: Multiple actin regulating proteins are expressed in M2 cells.

Using quantitative real-time PCR (performed by Dr. Romeo and Dr. Roux) we found that mRNA of cofilin-1, cofilin-2, ADF, Aip1, gelsolin, Myo1C, filamin A, filamin B, and filamin C were expressed in M2 cells confirming the mass spectrometry results. The data is normalised to the expression of GADPH. From ADF/cofilin isoforms cofilin-1 and from filamin isoforms filamin A and B are expressed the most. Graph shows number of PCR cycles (Ct) needed to obtain detectable transcript levels. We considered that genes were not transcribed if signal was detected after more than 32 cycles (dashed line). Error bars indicate SD.

5.5.1 Actin filament barbed end capping and efficient F-actin turnover are needed for cortical integrity

To assess the importance of barbed end capping, severing, and effective actin turnover in the cortex homeostasis I decided to evaluate the role of CapZ, gelsolin, profilin-1, cofilin-1, and Aip1 in cortical actin dynamics.

First, I investigated the localisation of GFP-tagged gelsolin, profilin-1, cofilin-1, and Aip1 in M2 cells and observed only cytoplasmic localisation. GFP-tagged heterodimeric capping protein displayed only cytoplasmic localisation in M2 cells consistent with previous report (Charras et al., 2006). Cytoplasmic localisation of these proteins may be due to high bound/unbound ratio of the GFP-tagged protein or GFP interfering with the protein function, and thus does not reveal whether or not the protein participates in cortical actin dynamics.

Next, I depleted gelsolin, profilin-1, cofilin-1, Aip1, and heterodimeric capping protein by targeted shRNAs. In my shRNA screen depletion of gelsolin, profilin-1, or cofilin-1 led to no detectable phenotype, however a minor increase in cell death rate upon cofilin-1 depletion was detected.

First, this suggests that filament severing by gelsolin is not essential for cortex integrity. Second, I expected to observe large blebs in profilin-1 depleted cells due to impaired Diaph1 nucleation. However, profilin-1 depletion failed to give a large-bleb phenotype consistent with perturbation of Diaph1 mediated nucleation and elongation. Interestingly, profilin depletion decreased the initial cortex accumulation rate (phase 1, see Fig. 4.17) in induced blebs in HeLa cells by ~30% suggesting that it does play a role in polymerisation (Biro et al., 2011 manuscript under review). Finally, I expected to observe filament accumulation as a result of cofilin-1 depletion in M2 cells as previously observed in other cell lines (Iwasa and Mullins, 2007). However, cofilin-1 depletion did not cause cortical defects, which may be due to redundancy in function of cofilin-1, cofilin-2, and ADF, all expressed and

associated with the pellet fraction. Thus all ADF/cofilin family members should be depleted simultaneously to study the role of depolymerisation. In addition, further characterization could be studied by overexpressing LIM-kinase in blebbing cells, as this should lead to inactive ADF/cofilin. However, to verify if any F-actin accumulation occurred in cofilin-1 depleted cells, the total F-actin content should be measured by phalloidin stainings described in chapter 4.5.1.

Interestingly depletion of CapZB or CapZA1, subunits of the heterodimeric capping protein, led to formation of larger blebs (Fig. 5.6B and C) than in cells transfected with non-silencing shRNA (Fig. 5.6A), suggesting that barbed end capping is needed for correct cortex homeostasis. The large bleb phenotype was observed with three out of four shRNAs targeting CapZB and two out of the three shRNAs targeting CapZA1. When barbed end capping is disrupted by silencing heterodimeric capping protein, the filaments should on average grow longer as their barbed ends should stay free. Longer filaments could lead to enhanced contractility, because of more binding sites for myosins and thus to formation of large blebs. To assess if the large bleb phenotype was due to increased contractility as reasoned, a phospho myosin staining could be carried out on CapZB or CapZA1 depleted cells and control cells to assess if CapZ depleted cells have more active myosin.

Finally, when I silenced Aip1 with targeted shRNAs, I again observed the formation of larger blebs (Fig. 5.6D) than in cells transfected with non-targeted shRNA (Fig. 5.6A), consistent with cortical defects observed in Aip1 knockdown HeLa cells (Kato et al., 2008). The large bleb phenotype was observed with all four shRNAs targeting Aip1. First, in the context of being an important regulator of ADF/cofilin, the large bleb phenotype could be caused by defective depolymerisation, because all ADF/cofilin family members may be affected by Aip1 silencing. Hence, more or longer actin filaments should accumulate in the cell. Visually no abnormal accumulation of LifeAct probe to the cortex (or other actin structures) was detected. However LifeAct is not

suitable marker for filament mass, and thus phalloidin stainings for assessing the F-actin mass in Aip1 depleted cells should be carried out as described in chapter 4.5.1.

Second, as Aip1 also caps the barbed ends of filaments, a similar phenotype to silencing the heterodimeric capping protein is logical and suggests that indeed capping of the ADF/cofilin severed filaments appears important for cortex maintenance.

In summary barbed end capping by heterodimeric capping protein and Aip1 appear to be important for cortical integrity, but the reason for this remains to be investigated.

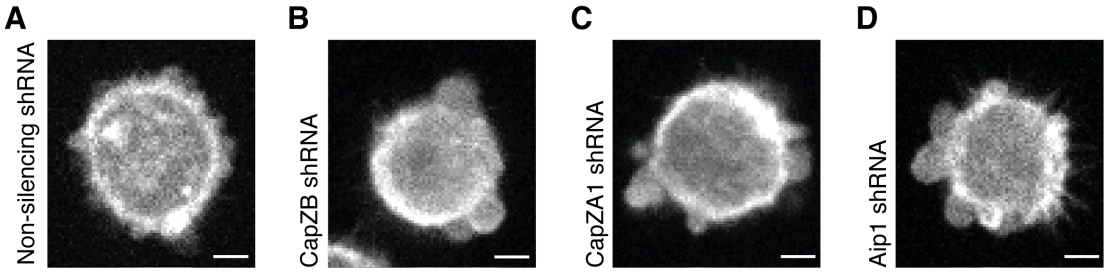

Figure 5.7: Silencing of heterodimeric capping protein and Aip1 lead to formation of large blebs.

All images are live confocal microscopy images of M2 cells stably expressing LifeAct-Ruby and transfected with either non-silencing shRNA (A), shRNAs targeting the CapZB subunit (B) and the CapZA1 subunit (C) of the hetorodimeric capping protein or Aip1 (D). Cells transfected with CapZB, CapZA1 or Aip1 shRNAs formed significantly larger blebs than cells transfected with non-silencing shRNA. All images were acquired with 40x magnification. Scale bars 5µm.

5.5.2 Membrane–cortex linker protein filamin B, motor Myo1C, and scaffold proteins drebrin and IQGAP1 localise to cell cortex, but are not essential for cortex maintenance

Next I studied the importance of filamin B, the motor protein Myo1C, and the scaffold proteins drebrin and IQGAP1 for actin cortex homeostasis.

As expected GFP-tagged filamin B localised to the cell membrane in M2 cells (Fig. 5.8A). Interestingly overexpression of filamin B did not fully rescue M2 cell blebbing, but the blebs did appear smaller than in wild type cells. In addition, the cells displayed elongated morphologies with few blebs instead of a rounded shape with many blebs (Fig. 5.8A). Finally, in contrast to ezrin, which is transiently absent from blebs during expansion but gets recruited to the membrane prior to actin (Charras et al., 2006), filamin B appeared to localise to the cell membrane throughout the bleb lifetime (Fig. 5.8A white arrowhead for growing bleb and red arrowhead for retracting bleb). Indeed, when I visualised its localisation during the bleb lifetime on kymographs, this confirmed my observation (Fig. 5.9A). Considering that overexpression of filamin B could have rescued filamin A-deficiency due to isoform similarity, the results suggest that filamin deficiency alone may not explain why M2 cells bleb.

I expected that filamin B depletion should lead to more severe blebbing phenotype in M2 cells because decreased membrane-cortex adhesion due to filamin A-deficiency has been suggested to cause blebbing in M2 cells (Cunningham et al., 1992; Dai and Sheetz, 1999). However, no abnormal phenotype was detected upon filamin B depletion with shRNAs, perhaps suggesting that filamin A and B may have differential roles in M2 cells or pointing to a less important role than generally thought for filamins in membrane-cortex adhesion.

Next I verified that Myo1C localises to the cell cortex in M2 cells as described previously (Charras et al., 2006) and then depleted it with targeted shRNAs in blebbing cells.

If Myo1C is important for cortical contractility, its depletion should result either in cells that do not form blebs, because inhibition of myosin-IIA mediated contractility by drug blebbistatin blocks blebbing (Straight et al., 2003) or in formation of small blebs because of decreased intracellular pressure. In contrast, if Myo1C participates mainly in membrane-cortex linking, its silencing should lead to decreased membrane-cortex adhesion leading to formation of large blebs and in the appearance of secondary blebs.

Despite its cortical localisation and abundance, depletion of Myo1C with shRNA led to no detectable phenotype suggesting a minor role in contractility, membrane-cortex adhesion, or membrane tension.

The actin regulating proteins drebrin and IQGAP1 were included in the localisation and depletion screens to assess the importance of signalling and regulation through these proteins at the cortex.

First, I observed that GFP-tagged drebrin (Fig. 5.8B) and IQGAP1 (Fig. 5.8C) both localised to the cell cortex in M2 cells. Drebrin and IQGAP1 both localised strongly to the cell cortex and were present in retracting but not in expanding blebs (Fig. 5.8B and C respectively, white arrowhead for growing bleb and red arrowhead for retracting bleb). Interestingly IQGAP1 seemed to get recruited earlier than drebrin to the bleb cortex. To verify this observation I visualised the recruitment of drebrin, IQGAP1, and LifeAct on two colour kymographs, where LifeAct appears red, drebrin or IQGAP1 in green, and co-localisation in yellow (Fig. 5.9B and C). Indeed, drebrin was recruited to the bleb after actin (Fig. 5.9B, red arrowhead) late during retraction (Fig. 5.9B, yellow arrowhead), whereas IQGAP1 got recruited to the bleb (Fig. 5.9C, yellow arrowhead) very shortly after actin (Fig. 5.9C, red arrowhead).

These results suggest that actin may be needed for the localisation of drebrin and IQGAP1 and could be confirmed by following their recruitment to the blebs upon treatment of transfected cells with actin sequestering drugs.

Because drebrin inhibits myosin binding to actin (Hayashi et al., 1996; Ishikawa et al., 2007) and tropomyosin activity (Ishikawa et al., 1994) I expected to observe increased contractility and thus either more blebs or larger blebs upon drebrin depletion. I also expected to observe large blebs upon IQGAP1 depletion, because of its role in localising Diaph1 in other cell types and organelles (Brandt et al., 2007). Alternatively, small blebs could have occurred, if IQGAP1 was needed for stimulating the Arp2/3 complex (Le Clainche et al., 2007).

However, when I depleted drebrin or IQGAP1 with shRNAs, I could observe no abnormal phenotypes compared to control, suggesting that neither drebrin nor IQGAP1 are essential for cortex maintenance. The role of IQGAP1 at cortex nucleation could further be studied by measuring the cortex accumulation rate in blebs induced in IQGAP1 depleted cells (see chapter 4.6.2) to assess if IQGAP1 has any role in the nucleation of the cortex.

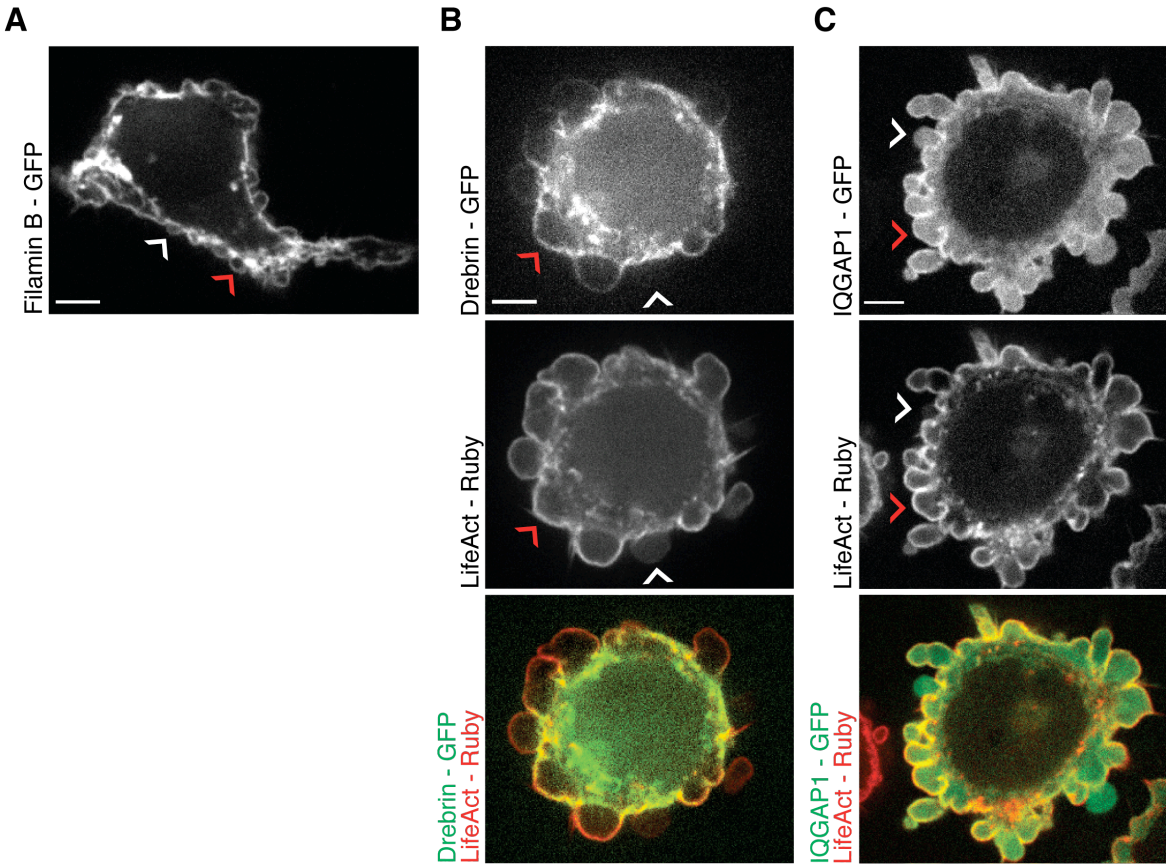

Figure 5.8: Filamin B, drebrin, and IQGAP1 localise to the cell cortex.

In all images, white arrowheads indicate a growing bleb and red arrowheads a retracting bleb. All images are single confocal section of live cells. Filamin B-GFP (A) localises to the cell cortex in M2 cells. Cells overexpressing filamin B are elongated and form small blebs. The localisation of drebrin-GFP (B) and IQGAP1-GFP (C), both in green, were studied in M2 cells stably expressing LifeAct-Ruby, in red. Drebrin-GFP appears to accumulate in blebs late during retraction (red arrowhead). IQGAP1-GFP is recruited to the retracting blebs (red arrowhead). All images were acquired with 100x magnification. Scale bars 5µm.

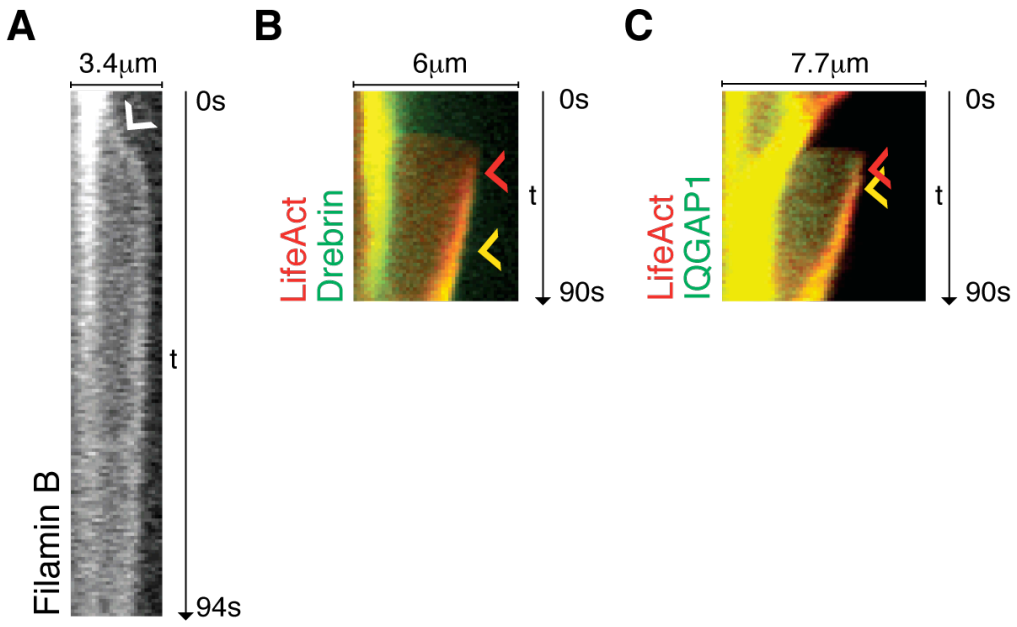

Figure 5.9: Recruitment of filamin B, drebrin, and IQGAP1 to the bleb.

In all kymographs bleb expansion is shown in the horizontal axis and time on the vertical axis. Filamin B (A) localises to the bleb membrane throughout the bleb lifetime (arrowhead). The recruitment of drebrin and IQGAP1 are shown in two colour kymographs, where drebrin or IQGAP1 are in green and LifeAct in red. F-actin (B, red arrowhead) appears under the bleb membrane shortly after expansion slows, but drebrin (B, green) appears only late during retraction (yellow arrowhead) as the trace turns yellow due to co-localisation with LifeAct. IQGAP1 (C, yellow arrowhead) appears in the bleb shortly after F-actin (red, red arrowhead).

5.5.3 The RhoA regulator p115RhoGEF is needed for cortical integrity

To assess the importance of RhoA regulators in the cortex homeostasis I depleted p115RhoGEF and p50RhoGAP in M2 cells.

I envisaged two possible phenotypes upon p115RhoGEF depletion. First, because microinjection of RhoA inhibitors described previously led to decreased number of blebbing cells, I expected to see less blebbing. Second, as RhoA activates formins (Higashida et al., 2004) and in particular Diaph1 (Watanabe et al., 1997), it is likely that p115RhoGEF depletion could lead to impaired Diaph1 activation and thus to formation of large blebs. Third, another downstream effector of RhoA is ROCK1 needed for contractility, thus if contractility was compromised in the p115RhoGEF depleted cells, instead of large blebs, small blebs or less blebs could be expected to form or the cells could stop blebbing.

Interestingly, p115RhoGEF depletion led to formation of larger blebs (Fig. 5.10A) than in cells transfected with non-silencing shRNA (Fig. 5.10B). This phenotype was observed with all three shRNAs targeting p115RhoGEF. Interestingly, it appears that p115RhoGEF only affects the Diaph1 pathway of RhoA and raises a few interesting questions. First, would expression of CA-Diaph1 rescue the large bleb phenotype caused by p115RhoGEF depletion? Second, does p115RhoGEF depletion have any effect on the ROCK pathway downstream of RhoA and if not, why does p115RhoGEF depletion only affect formin activation? Finally, does p115RhoGEF regulate other proteins than RhoA, which could regulate the cell cortex?

Finally, RhoGAPs promote the GTPase activity of RhoA and therefore inactivate RhoA signalling (Moon and Zheng, 2003). It has been reported previously that overexpression of p50RhoGAP leads to RhoA inhibition and to a decreased number of blebbing cells (Charras et al., 2006). Thus, when p50RhoGAP is silenced, RhoA-GTP should accumulate in the cells possibly

leading to increased contractility through myosin activation, which could result in the formation of large blebs. In addition an increase in the filament mass might be observed through formin activation.

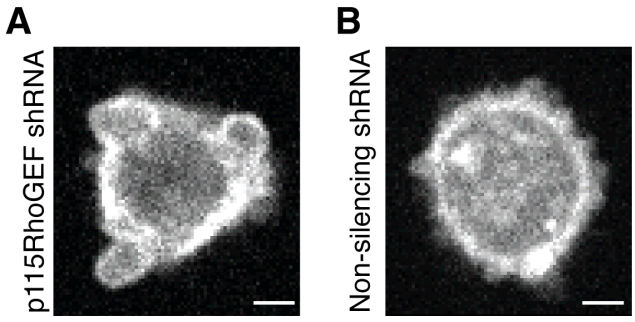

Figure 5.10: Depletion of p115RhoGEF leads to formation of large blebs.

Both images are live confocal microscopy images of M2 cells stably expressing LifeAct-Ruby and transfected with either shRNA targeting p115RhoGEF (A) or non-silencing shRNA (B). Cells transfected with p115RhoGEF shRNA formed significantly larger blebs than cells transfected with non-silencing shRNA. Both images were acquired with 40x magnification. Scale bars 5µm.

In contrast to p115RhoGEF depletion, silencing p50RhoGAP did not cause cortical defects in blebbing M2 cells *per se*, but the cells appeared to have problems in attachment to the glass coverslip, suggesting problems in forming adhesions. The inability of the cells to adhere (in 4h) to the glass coverslips was observed with all three shRNAs targeting p50RhoGAP. I was first surprised by this result, but interestingly, it has been shown, that efficient spreading of Rat1 fibroblasts is dependent on RhoA inhibition by p190RhoGAP (Arthur and Burridge, 2001). Indeed p190RhoGAP depletion in Rat1 cells led to attachment problems, which were suggested to be caused by increased contractility (Arthur and Burridge, 2001). Consistent with these studies, silencing of p50RhoGAP led to attachment problems in M2 cells suggesting, that RhoA inhibition by p50RhoGAP is necessary for efficient spreading and adhesion to the substrate of contractile blebbing M2 cells.

5.5.4 Flightless-I is a potential regulator of Diaph1 at the cell cortex

Flightless-I (Fli-I) has been reported to activate Diaph1 *in vitro* through helping RhoA release the autoinhibitory interaction of Diaph1 as well as enhancing actin polymerisation activity by recruiting actin monomers to the FH1-FH2 domains of Diaph1 (Higashi et al., 2010). Thus, given the importance of Diaph1 in actin nucleation at the cortex, I wanted to study if Fli-I is one of the main regulators of the cortex nucleation.

First, I observed that upon transfection GFP-tagged Fli-I displayed mostly cytoplasmic localisation and only weak cortical enrichment could be detected. I decided to perform a simultaneous permeabilisation-fixation to remove the unbound fraction of Fli-I-GFP and indeed observed that the bound fraction of Fli-I localised to the cell cortex (Fig. 5.11A). Interestingly in the bleb cortex the localisation of Fli-I was weaker than in the cell body (Fig. 5.11A, arrowheads).

The role of Fli-I has been studied in *D. melanogaster*. It was shown that in the cells of Fli-I mutant embryos cortical actin was unevenly distributed leading to cortical defects (Straub et al., 1996). Thus and because Fli-I has been suggested to activate Diaph1 (Higashi et al., 2010), I expected to observe cortical defects upon Fli-I depletion. Indeed, if Fli-I is needed for Diaph1 activation, a phenotype similar to Diaph1 depletion should be detected upon Fli-I depletion. Interestingly when I silenced Fli-I with shRNAs I observed cells with large blebs (Fig. 5.11B), a phenotype similar to Diaph1 silencing. The phenotype was observed with all three shRNAs targeting Fli-I.

Together, the cortical localisation and the large bleb phenotype upon Fli-I depletion suggest that Fli-I is a potential regulator of Diaph1 and the cell cortex. However, further characterization is required for showing how Fli-I functions in cells. Indeed flightless-I is a gelsolin family protein (Campbell et al., 1993) and *C. elegans* flightless-I homolog was shown to sever F-actin (Goshima et al., 1999). Thus, its possible capping or severing activities remain to be elucidated in mammalian cells. Most importantly it has to be assessed whether or not Fli-I binds to and regulates Diaph1 in mammalian cells as suggested by *in vitro* studies (Higashi et al., 2010). This could be studied by pulldown assays, using Fli-I as a bait to reveal its binding partners from M2 cell lysates. Indeed this experiment would not only reveal if Fli-I binds Diaph1, but also other potential binding partners including its regulators such as leucine rich repeat (in Fli-I) interacting protein 1 and 2 (LLRFIP1 and -2) found in our proteomic list. Further true interaction of Diaph1 and Fli-I in cells could be studied by fluorescence resonance energy transfer (FRET) microscopy, which could reveal if Diaph1 and Fli-I are in a close proximity to one another and thus bind to one another in cells. In addition, intracellular interaction could also be studied by following if Diaph1 and Fli-I speckles co-localise. However, both imaging approaches are technically challenging. Finally, if Fli-I indeed regulates Diaph1 at the cell cortex, upstream regulators of Fli-I remain to be elucidated.

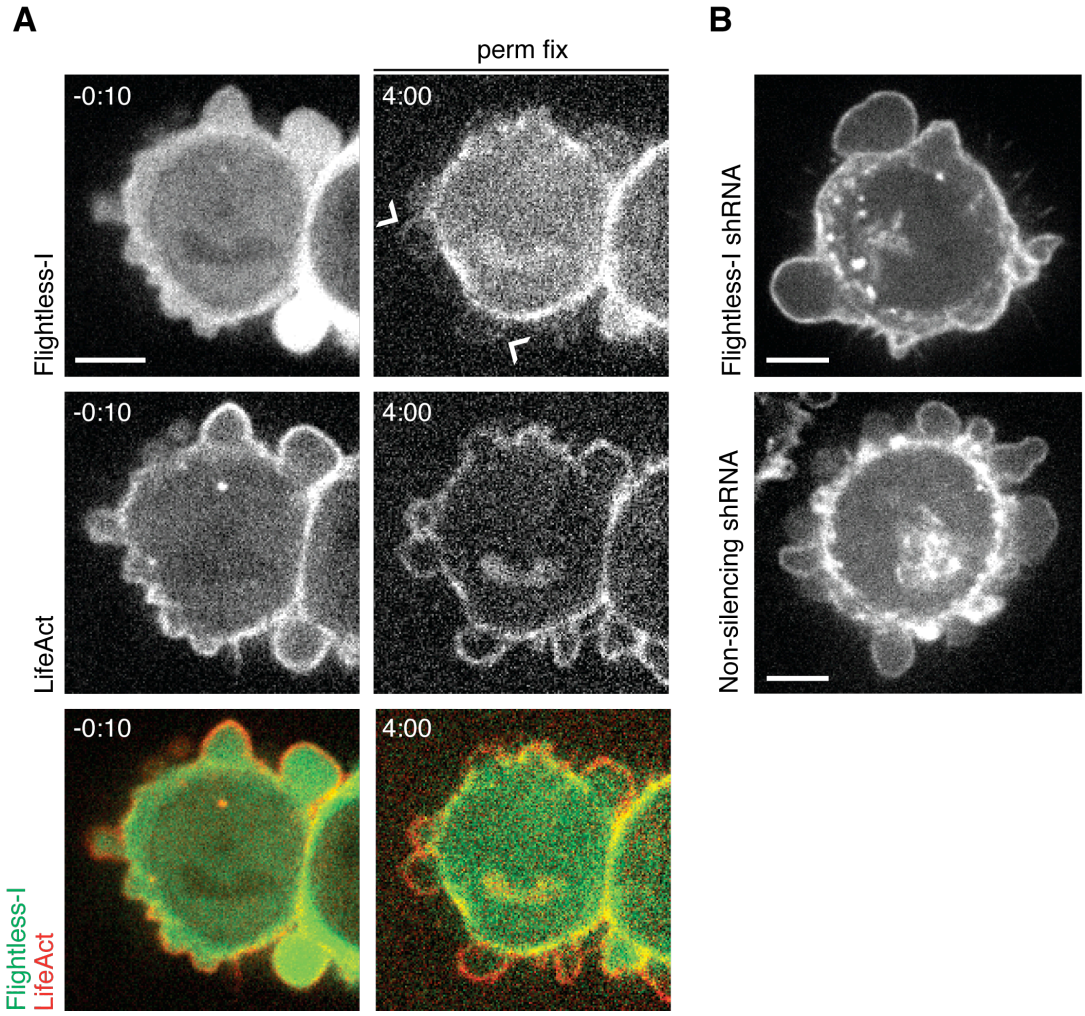

Figure 5.11: Flightless-I is a potential regulator of the cell cortex.

All images are confocal microscopy images of M2 cells stably expressing LifeAct-Ruby. After (A) simultaneous permeabisation-fixation (performed at timepoint 0.00) flightless-I-GFP localises to the cell cortex in M2 cells. Strong localisation at the cortex was observed in the cell body and weaker in blebs (arrowheads). Time is given as min:sec. Live microscopy images of M2 cells (B), where one cell is transfected with shRNA targeting flightless-I and the other with non-silencing shRNA. Cells expressing flightless-I shRNA form large blebs. All images were acquired with 100x magnification. Scale bars 5µm.

5.6 Conclusions

We showed previously that blebs separated from M2 cells retain dynamic cortices (chapter 4, Fig, 4.11), which appeared similar to whole cell cortices at their ultrastructural level. First, by examining regions of enrichment in bleb fraction compared to whole cells using immunoblotting and mass spectrometry analysis, we showed that purified bleb fractions were enriched in actin and thus a suitable model to study the actin cortex. However, the purified bleb fractions were also enriched in Golgi complex and ER, and because both of these structures bind F-actin (di Campli et al., 1999; Kachar and Reese, 1988), the detergent insoluble pellet contains not only cortical actin, but presumably also Golgi complex and ER bound actin. Although visually the majority of the F-actin in the blebs appears cortical, a careful analysis whether or not a protein found in the mass spectrometry has a role at the cortex has to be carried out.

In chapter 4, we used proteomic analysis of the detergent insoluble pellet to study which actin nucleators were associated with the cortex. The analysis did not only verify the cortical association of Diaph1 and the Arp2/3 complex, but also revealed the whole protein composition of the cortex. The purified bleb fractions contained multiple proteins from different cell organelles, but most importantly were enriched in cytoskeletal proteins, which could be categorised into actin and actin binding proteins, tubulin and microtubule binding proteins, and others like spectrins and septins. Of these categories, actin and actin binding proteins were the most abundant in the pellet of the bleb fraction. The actin group of proteins was further categorised into actin nucleators, actin isoforms, capping proteins, regulatory proteins, crosslinking proteins, turnover proteins, membrane linking proteins, motors, other actin binding proteins, and focal adhesion proteins resulting in many proteins in each category.

We were particularly interested in revealing which small GTPases participate in the regulation of the cell cortex. We found that many Rab GTPases were associated with the pellet, but most interestingly Rac1, RhoA, RhoC, and RhoG together with two RhoA specific regulators, p115RhoGEF and p50RhoGAP, were present at the pellet.

To study which proteins in the pellet of the bleb fraction were strongly bound to actin, we treated the bleb fraction with the barbed end binding drug cytochalasin D, which resulted in an overall loss of actin regulating proteins from the pellet consistent with the decreased number of filaments. The pellet association of capping proteins, α-actinins, cortex-membrane linkers, and myosins were most dramatically decreased by the cytochalasin D treament, suggesting of strong actin association.

Taken together the localisation and depletion studies presented in this chapter yield many new insights into actin regulation. First, barbed end capping by heterodimeric capping protein, but not by gelsolin, is important for the cortex homeostasis (Table 5.4). Indeed, depletion of CapZ led to formation of large blebs while gelsolin depletion did not. Second, although cofilin-1 only displayed cytoplasmic localisation and no abnormal phenotype upon its depletion was observed, silencing Aip1 revealed that either effective depolymerisation of F-actin or barbed end capping by Aip1 is needed for cortical stability (Table 5.4). Third, silencing Myo1C, filamin B, drebrin, or IQGAP1 did not have a phenotype, although they all localised to the cortex in M2 cells suggesting a more subtle or no role in cortex homeostasis or contractility (Table 5.4). Finally, silencing p115RhoGEF and flightless-I, but not p50RhoGAP, led to overall changes in cellular phenotype, suggesting they could be key regulators of the cell cortex (Table 5.4), however more in depth studies are needed for confirmation.

Protein	Abundance	Pellet association	Localisation	Silencing phenotype
Heterodimeric capping protein	+++	+++	cytoplasmic	large blebs
Gelsolin	+	+++	cytoplasmic	no phenotype
Cofilin-1	+++	*	cytoplasmic	no phenotype
Profilin-I	++	*	cytoplasmic	no phenotype
Aip1	+++	+++	cytoplasmic	large blebs
Flightless-I	+	+	cortical	large blebs
p115RhoGEF	++	no data	no data	large blebs
p50RhoGAP	+	no data	no data	attachment problem
Filamin B	+++	+++	cortical	no phenotype
Myo1C	+++	+++	cortical	no phenotype
Drebrin	+++	+++	cortical	no phenotype
IQGAP1	+++	*	cortical	no phenotype

Table 5.4: Many actin regulating proteins were abundant and strongly bound to the pellet of the bleb fraction, but only few of them have a potential role at the cortex.

In the table the second column represents the abundance of the protein in the pellet of the bleb fraction according to the mass spectrometry analysis and third column its association to the pellet studied by following changes upon cytochalasin D treatment. In both + means low abundance/association, +++ high abundance/association, and * represents no change upon cytochalasin D treatment. The localisation of the protein is presented in the fourth column and the phenotype upon silencing with shRNA in the fifth column.

6 DISCUSSION

6.1 Introduction

The aims of this thesis were to determine how the actin cortex assembles in cells and to study aspects of the protein composition of the cortex. In particular, we hoped to learn which actin nucleators or nucleation independent mechanisms were needed for cortex assembly and which F-actin associated proteins were needed for cortex homeostasis. I used membrane blebs as my model system for cortex assembly and maintenance, as blebs are first devoid of actin but reconstitute a cortex when expansion slows and therefore bleb size can be used as a reporter of cortical defects.

I envisaged four models of how the actin cortex could reassemble in membrane blebs (Fig. 6.1). First, the cell cortex existing at the base of the bleb could elongate and reassemble into the bleb starting from the sides of the bleb (Fig. 6.1A). Second, small cortex fragments could persist at the bleb membrane during expansion and elongate to regenerate the submembranous cortex (Fig. 6.1B). Third, actin seeds could enter into the bleb along with the cytosol during expansion, be captured by cortex-membrane linker proteins at the bleb membrane, and elongate (Fig. 6.1C). Finally, active actin nucleation might be needed for cortex reconstitution (Fig. 6.1D).

To understand how the cortex reassembles in membrane blebs, I first investigated the nucleation independent models of cortex reassembly. Rapid timelapse imaging of the F-actin reporter LifeAct in live blebbing M2 cells revealed that the cell cortex was not just elongated from existing cortex at the sides of the bleb neck, rather F-actin appeared at the bleb perimeter at random locations, thus invalidating the invasion model of cortex reassembly. Second, quantum dot-phalloidin microinjection studies revealed that actin seeds do not stay bound to the bleb membrane during expansion, and that F-actin only appears under the bleb membrane when expansion slows. Third, microinjected small, fluorescent, stabilised actin seeds did not localise to

cortical actin structures in blebbing cells consistent with studies by others in other cell lines (Sanders and Wang, 1990) and thus membrane-actin linker proteins do not appear to capture pre-polymerised actin filaments invalidating the flow of actin seeds model.

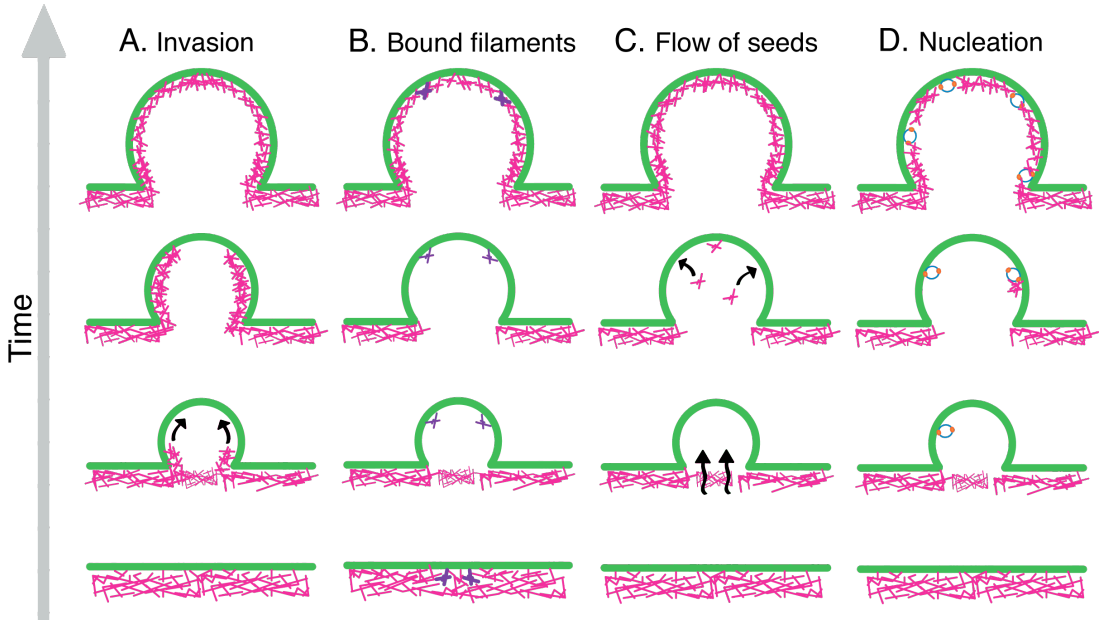

Figure 6.1: Potential mechanisms of how the actin cortex could reassemble in blebs.

A. Elongation of existing cell cortex could invade the bleb by growing sequentially from the sides of the bleb.
B. Cortex fragments bound to actin-membrane linker proteins could persist under the bleb membrane during expansion.
C. Actin seeds could flow along with the cytosol into the bleb during expansion and be captured by the membrane linker proteins at the membrane during late expansion.
D. Active F-actin nucleation by actin nucleators could be needed for cortex reassembly.

After having shown that no nucleation independent mechanisms of cortex regrowth participated in cortex reassembly in blebs, I investigated which actin nucleators are needed for *de novo* cortex reassembly. Using localisation studies combined with qPCR, I showed cortical presence of many actin nucleators, however only formin Diaph1 and the Arp2/3 complex were functional in the cortex. Indeed depletion studies showed that when Diaph1 is silenced, the cells form large blebs. In contrast, small blebs formed when the Arp2/3 complex was inhibited, both suggestive of perturbations to the cortex. Disruption of both nucleators simultaneously led to loss of cortical actin suggesting Diaph1 and the Arp2/3 complex are needed for cortex nucleation and maintenance (Fig. 6.2). Several evidence presented next suggest that Diaph1 and the Arp2/3 complex act independently. First, two separate phenotypes were seen upon Diaph1 or Arp2/3 complex depletion. Second, phalloidin stainings of total F-actin mass revealed that when both nucleators were depleted simultaneously the decrease in F-actin mass was not very different from the addition of their individual effects. Finally, the cortex accumulation rate measurements revealed that accumulation of Diaph1 nucleated and elongated F-actin in the metaphase cortex was ~4-fold faster than that nucleated by the Arp2/3 complex and in controls the accumulation rate was intermediate between Diaph1 and Arp2/3 complex nucleated actin. Further, both were associated with the cortex in mass spectrometry analyses of the isolated blebs.

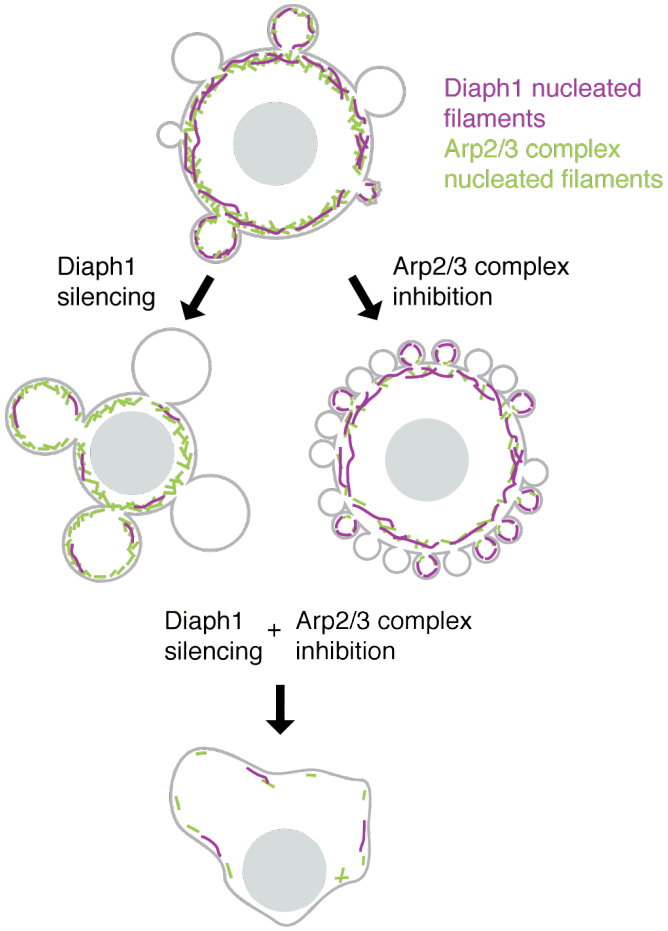

Figure 6.2: Schematic model of cortical actin nucleation by Diaph1 and the Arp2/3 complex.

Top, in normal conditions the cortex is nucleated and maintained by Diaph1, which nucleates and elongates long linear filaments, and the Arp2/3 complex, which produces shorter branched filaments. Left, when Diaph1 is silenced cells form large blebs, cortex formation relies only on the Arp2/3 complex (green filaments). Arp2/3 complex nucleated filaments polymerise by spontaneous monomer addition to their free barbed ends leading to slower elongation compared to filaments, elongated by Diaph1. Thus, in Diaph1 depleted cells stalling the bleb growth by reassembly of a new cortex is slower leading to formation of large blebs. Right, when the Arp2/3 complex is inhibited, cells form small blebs, because the cortex is nucleated and elongated fast by Diaph1 (purple filaments). Bottom, when both are depleted simultaneously, the cells lose most of their actin cortex and display large shape changes.

Finally we studied the protein composition of the cortex by mass spectrometry analysis of the bleb fraction. We observed, that the detergent insoluble fraction of the separated blebs was enriched in actin compared to whole cells but contained some nuclear material and intracellular membrane organelles, including Golgi complex and ER. More detailed analysis of the pellet of the bleb fraction revealed the presence of different actin isoforms, capping proteins, regulatory proteins, crosslinking proteins, turnover proteins, membrane linker proteins, motor proteins, scaffold proteins, and focal adhesion proteins in addition to actin nucleators. Proteins belonging to the capping, turnover, membrane linking, motor, and scaffold protein categories and potential cortex regulators were chosen for further analysis. Interestingly although cortical localisation of heterodimeric capping protein and Aip1 could not be observed by using GFP-tagging, depletion studies revealed, that both were needed for cortex maintenance. In contrast, GFP-tagged filamin B, drebrin, and IQGAP1 localised to the cell cortex, but their depletion did not lead to cortical defects suggesting more subtle or no role in the cell cortex. Interestingly overexpression of filamin B in filamin A-deficient blebbing M2 cells (Cunningham et al., 1992), did not fully rescue blebbing, suggesting filamins perhaps have less important role in membrane-cortex adhesion than generally thought. Studies of the cortex regulators revealed, that depletion of the cortex associated RhoA activator p115RhoGEF led to cortical defects, but depletion of the cortex-associated inactivator p50RhoGAP had no effect on the blebbing phenotype. Finally a potential Diaph1 activator, flightless-I, localised to the cell cortex and its depletion led to large bleb phenotype reminiscent of the one observed in Diaph1 depletion studies, suggesting that flightless-I could be one of the main regulators of actin nucleation via Diaph1 at the cortex.

These findings have expanded our understanding of the actin cortex. First, active actin nucleation by Diaph1 and the Arp2/3 complex are needed for cortex reassembly. Second, the cortex consists, in addition to actin and actin nucleators, of filament capping proteins, regulatory proteins, actin

crosslinking proteins, actin turnover proteins, cortex-membrane linker proteins, motor proteins, and scaffold proteins. Further localisation and depletion studies revealed that from these functional groups at least F-actin nucleation, filament barbed end capping, possibly severing and/or depolymerisation, and regulation of the cortex are essential for cortical actin homeostasis.

6.2 The Arp2/3 complex and formins are necessary for actin nucleation in lamellipodia, filopodia, stress fibers and the cell cortex

It was long believed that the Arp2/3 complex and formins were needed in exclusion from one another to generate different actin structures in cells. Indeed, the Arp2/3 complex alone was thought to be needed for lamellipodia formation at the leading edge of the cell, whereas formins were thought to be exclusively needed for filopodia and stress fiber formation. However, recent reports and my studies presented in this thesis have revealed that the Arp2/3 complex and formins appear to act together to generate many different cellular actin structures, including lamellipodia (Gupton et al., 2007; Sarmiento et al., 2008; Yang et al., 2007), filopodia (Svitkina et al., 2003), stress fibers (Hotulainen and Lappalainen, 2006), and the actin cortex.

In the late 1990s, it was discovered that the Arp2/3 complex induced formation of a branched actin network in the lamellipodium at the leading edge of cells (Mullins et al., 1998; Svitkina and Borisy, 1999). Further it was proposed that the short stiff branches generated by the Arp2/3 complex were necessary to push the cell membrane forward, and that long linear filaments generated by formins were not suited for generating pushing forces (Pollard et al., 2000).

Formins, especially Diaph family formins, were first identified in stress fibers (Watanabe et al., 1999) and later in filopodia (Pellegrin and Mellor, 2005; Peng et al., 2003). Because stress fiber assembly is induced by Diaph1

(Watanabe et al., 1999) and filopodia formation by Diaph3 overexpression (Peng et al., 2003), formins were though to be exclusively responsible for the assembly of these structures. In addition, the cell cortex was suggested to be nucleated by a formin, as the Arp2/3 complex displayed only cytoplasmic localisation in blebbing cells upon GFP-tagging, whereas RhoA, upstream of formins, localised to the cell membrane (Charras et al., 2006).

Such partitioning of the role of formins and the Arp2/3 complex started to appear incorrect with the identification of formins in the leading edge of migrating cells (Gupton et al., 2007; Sarmiento et al., 2008; Yang et al., 2007). Recently the Arp2/3 complex and formins have been found acting either together or independently from one another, in most of the cell's actin structures. First, it was revealed that although the Arp2/3 complex is necessary for actin assembly in lamellipodia, formins, in particular Diaph3, also participate in lamellipodia formation (Fig. 6.3 lamellipodium) (Gupton et al., 2007; Sarmiento et al., 2008; Yang et al., 2007). Interestingly lamellipodia in Diaph3 depleted cells contained only unusually short branched filaments (Yang et al., 2007). Thus, it was proposed that in lamellipodia Diaph3 is needed for elongation of Arp2/3 complex nucleated filaments (Yang et al., 2007).

Second, it was shown, that stress fibers are not only assembled by formins, but also that the Arp2/3 complex participates in their formation (Fig. 6.3 stress fiber). Indeed, dorsal stress fibers, which are acto-myosin bundles attached to focal adhesions, were shown to be generated by formin Diaph1 (Hotulainen and Lappalainen, 2006). In contrast, transverse arcs, which are curved acto-myosin bundles free from focal adhesions, form from Arp2/3 complex nucleated filaments that mature into bundled acto-myosin structures (Hotulainen and Lappalainen, 2006).

Third, it was shown that, at the leading edge of cells, filopodia arise from the branched network of actin (Fig. 6.3 filopodium) (Svitkina et al., 2003). It

appears that formins, in particular Diaph3, elongate some branches nucleated by the Arp2/3 complex leading to filopodial growth (Svitkina et al., 2003).

Finally, I have shown that Diaph1 and the Arp2/3 complex also nucleate and maintain the actin cortex (Fig. 6.3 cell cortex) and act there independently from one another suggestive of two populations of filaments. One population consist of long linear filaments that elongate fast, whereas the other comprises of branched actin filaments that grow slower by spontaneous polymerisation.

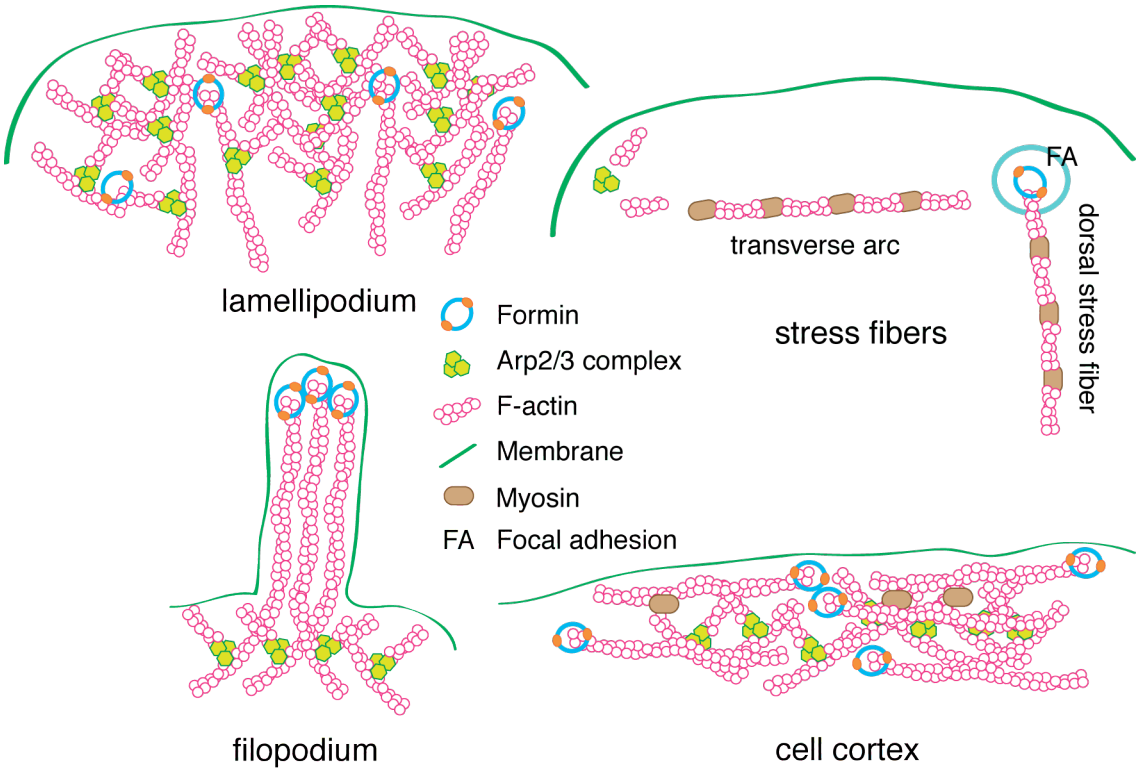

Figure 6.3: Arp2/3 complex and formin organisation in lamellipodium, filopodium, stress fibers, and the cell cortex.

In the lamellipodium (top left), the barbed ends of actin filaments are oriented towards the cell front and push the membrane forward. The majority of the filaments in the lamellipodium are nucleated by the Arp2/3 complex, forming a branched actin network. Formins nucleate and elongate single linear filaments, but can also elongate Arp2/3 complex nucleated branches in the lamellipodium (Yang et al., 2007). Filopodia (bottom left), often emerging from the lamellipodium, are elongated by formins positioned at the tip of the filopodium (Pellegrin and Mellor, 2005). Transverse arcs (top right) form from the Arp2/3 complex nucleated filaments, which mature into short filament bundles and actin filaments of dorsal stress fibers (top right) are elongated by formins from the focal adhesion (Hotulainen and Lappalainen, 2006). In the cell cortex (bottom right) formin Diaph1 and the Arp2/3 complex act independently in generating the actin cortex. Both stress fibers and the cell cortex are contractile structures.

In the first instance it appears logical that Diaph3 and the Arp2/3 complex act together in the lamellipodium as Diaph3 could produce mother filaments for the Arp2/3 complex to bind to and nucleate new branches as speculated previously by Sally Zigmond (Zigmond, 2004). Another possibility supported by experimental data is that Diaph3 could elongate single branches nucleated by the Arp2/3 complex (Yang et al., 2007). Such a co-operative actin assembly would mean that Diaph3 would need to be tightly regulated to prevent unwanted filopodial formation. Indeed, it was shown that filopodial formation is controlled by a WAVE-Arp2/3 complex that binds to Diaph3 and inhibit its activity at the leading edge of the cell (Beli et al., 2008).

Interestingly such co-operative nucleation/elongation does not appear to occur in the cell cortex. Indeed, disruption of Diaph1 or the Arp2/3 complex led to different phenotypes in blebbing cells. Diaph1 depletion caused the formation of large blebs and, in contrast, inhibition of the Arp2/3 complex led to formation of small blebs. In addition, measurements of total F-actin mass in blebbing M2 cells, where the majority of the F-actin is cortical, support this. We showed that when Diaph1 or the Arp2/3 complex is depleted, the total F-actin content decreases, but when both nucleators are depleted simultaneously no significant additive effect was observed. Further, cortex regrowth rate measurements in induced blebs in HeLa cells revealed that, when Diaph1 was silenced (Arp2/3 complex mediated nucleation, spontaneous elongation), the cortex regrowth rate slowed, and when Arp2/3 complex was inhibited (Diaph1 mediated nucleation and elongation), the cortex regrowth rate was accelerated. These data suggest that cortex regrowth results from the combined, but independent, action of Diaph1 and the Arp2/3 complex.

That Diaph1 and the Arp2/3 complex should act independently in the cortex is intriguing. Indeed, if Diaph3 elongates Arp2/3 complex nucleated filaments in lamellipodia (Yang et al., 2007), why this does not occur in the cortex with the Arp2/3 complex and Diaph1 and what does this mean for the structural

integrity and contractility of the cortex? Maybe short branches are needed in the cortex to create the dense meshwork of filaments, that we observed in scanning electron micrographs (Fig. 4.11), which coats the whole inner surface of the plasma membrane to maintain the shape of the cell. It was proposed that short branches are stiff and thus able to push the cell membrane (Pollard et al., 2000). Indeed, maybe filament length in the dense meshwork is critical for the ability to resist mechanical forces, which is one of the most important functions of the cellular cortex as the cell membrane is unable to exert extracellular forces or resist shear stresses (Hamill and Martinac, 2001).

Then if short filaments are needed in the cortex to create a dense and stiff meshwork, why is Diaph1 needed? It is possible that Diaph1 is essential especially for cortex reassembly. Indeed we showed, that Diaph1 accelerates the cortex regrowth rate ~4-fold compared to Arp2/3 complex nucleated filaments. This is consistent with *in vitro* studies, where mDia1 bound filaments were shown to elongate ~7-fold faster than filaments with free barbed ends (Romero et al., 2004). It is likely that, when the cell membrane lacks cortex, speed is of the essence as maintenance of shape, resistance to external mechanical stresses, spindle positioning, cytokinesis, or migration are at risk. Thus, in the case of cortex rupture or membrane delamination, Diaph1 is needed to nucleate and elongate a new cortex fast.

If the cortex is composed of short, branched filaments and long linear filaments, how does this affect the contractility, which is one of the most important properties of the cortex. The best-characterized contractile structure is the muscle sarcomere, consisting of thin, long, parallel actin bundles and thick myosin filaments, which slide past another during contraction (Alberts, 2002). Another well-studied contractile structure are stress fibers, which are composed of relatively short crosslinked actin filaments and myosin bundles, which display a periodic distribution along the length of the stress fiber (Cramer et al., 1997).

Both of these structures give us clues of how the two filament populations might behave in the cortex. Indeed long linear Diaph1 assembled filaments could form into parallel bundles with the help of actin crosslinkers and act like the thin filaments in the sarcomere. Another possibility is that long Diaph1 assembled filaments could become severed into short filaments by ADF/cofilin, which is present at the cortex. These short filaments could then bundle and bind to myosins and form stress fiber like structures.

Interestingly transverse arcs have been suggested to form from Arp2/3 complex nucleated filaments, which mature into short filament bundles and bind to myosins to become a contractile stress fiber (Hotulainen and Lappalainen, 2006). Such branch dissociation and maturation could occur in the cortex through coronin. Indeed, coronin dissociates the Arp2/3 complex from the sides of mother filaments (Cai et al., 2008), it was found to localise to the cell cortex (Charras et al., 2006), and associates with the cortex in the cortical fraction of separated blebs.

However, unlike in stress fibers (Cramer et al., 1997) no periodic localisation of myosin, actin, or α-actinin has been observed in the cortex (Charras et al., 2006). Thus, more studies are needed to reveal how Diaph1 or the Arp2/3 complex nucleated filaments organise themselves with myosins at the cortex, something that could be studied for example by immuno scanning electron microscopy.

6.3 Regulation of cortical actin nucleation

The Arp2/3 complex is regulated through a number of nucleation promoting factors (NPFs), which are needed for complex activation. One of the best-characterized NPFs, N-WASP, has been suggested to activate the Arp2/3 complex at the cell membrane at sites of endocytosis (Benesch et al., 2005; Bu et al., 2009; Innocenti et al., 2005; Tsujita et al., 2006) (Fig. 6.4). The more recently discovered NPF WHAMM possibly recruits the Arp2/3 complex

to the *cis*-Golgi network (Campellone et al., 2008). A well-characterized NPF, the WAVE complex, was shown to activate the Arp2/3 complex in the lamellipodium (Innocenti et al., 2005; Suetsugu et al., 2003; Yamazaki et al., 2003; Yan et al., 2003) and cell-cell adhesions (Yamazaki et al., 2007) (Fig. 6.4). We suggest that the WAVE complex may also activate the Arp2/3 complex at the cell cortex (Fig. 6.4) because Nap1 and Sra1 subunits of the WAVE complex were associated with the cortical fraction of isolated blebs. In addition, the NPF cortactin was associated with the cortex, where it possibly stabilises Arp2/3 branch points (Ammer and Weed, 2008).

The Arp2/3 complex can also be negatively regulated. It was shown that the Arp2/3 complex dissociates from branch points when ATP is hydrolysed in Arp2 (Le Clainche et al., 2003), but several proteins specifically catalysing debranching have also been characterized. In particular, coronin was found to dissociate Arp2/3 complex from the sides of mother filaments (Cai et al., 2008) and the ADF homology protein GMF was shown to induce de-branching of daughter filaments nucleated by the Arp2/3 complex in *S. cerevisiae* (Gandhi et al., 2010). No mammalian GMF homologs (GMF β and γ) were found in the mass spectrometry analysis of the isolated blebs, but interestingly coronin was associated with the cortex suggesting that it might participate in branch remodeling, which might be essential for contractility as discussed in the previous section.

In summary, in the cortex, our evidence suggests that the Arp2/3 complex is regulated by the WAVE complex, cortactin, and coronin. But further experiments will be needed to ascertain that WAVE indeed activates the Arp2/3 complex in the cortex. In addition further experiments are needed to understand the balance between branch stabilisation by cortactin and branch dissociation by coronin in the cortex.

In contrast to Arp2/3 complex regulation, Diaph1 regulation in the cell appears more complex, perhaps because Diaph1 has multiple roles in cells.

RhoA can activate actin polymerisation through formins (Higashida et al., 2004) by releasing the intramolecular DID-DAD domain interaction by binding to the GBD-DID (Lammers et al., 2005; Otomo et al., 2005). Consistent with this RhoA has been found to localise together with Diaph1 in multiple structures of the cell.

First, Diaph1 and RhoA have been shown to participate in stress fiber formation by inducing actin polymerisation starting from focal adhesions (Hotulainen and Lappalainen, 2006) (Fig. 6.4). To date interaction of Diaph1 with focal adhesion proteins have not been reported, but RhoA appears to get recruited to focal adhesion through syndecan-4 (Dovas et al., 2006) (Fig. 6.4). Second, Diaph1 and RhoA are involved in the formation of phagocytic cup, and Diaph1 function at the cell membrane at the site of the phagocytic cup formation was shown to be dependent on IQGAP1 (Brandt et al., 2007) and CLIP170 (Lewkowicz et al., 2008) (Fig. 6.4), which were both identified in our mass spectrometry data. Third, Diaph1 and RhoA interactions were described at adherens junctions (Carramusa et al., 2007; Ryu et al., 2009), where RhoA is recruited by p120 catenin (Cozzolino et al., 2003) (Fig. 6.4). Fourth, regulation of Golgi complex structure has been linked to Diaph1 and RhoA (Zilberman et al., 2011) (Fig. 6.4), though Diaph1 and RhoA upstream regulators in Golgi have not been characterized. Fifth, Diaph1 is involved in filopodia formation, but appears to be regulated and recruited there by Rif instead of RhoA (Goh et al., 2011) (Fig. 6.4). Finally, I showed that Diaph1 is involved in cell cortex nucleation (Fig. 6.4) and RhoA (Fig. 6.4) localises to bleb membranes in M2 cells (Charras et al., 2006) and in the cortex of metaphase HeLa cells (Nishimura and Yonemura, 2006). Domain analysis of Diaph1 revealed that Diaph1 GBD+FH3 was sufficient to target the formin to the cell membrane and depletion of p115RhoGEF, an activator of RhoA (Snyder et al., 2002), led to formation of large blebs, a phenotype similar to Diaph1 depletion, further suggesting that RhoA is needed for Diaph1 activity in the cortex.

Taken together RhoA appears to regulate Diaph1 in many structures of the cell including the cell cortex. Thus, to understand how RhoA and Diaph1 are regulated in and recruited to the cell cortex, their cortical upstream regulators need to be identified.

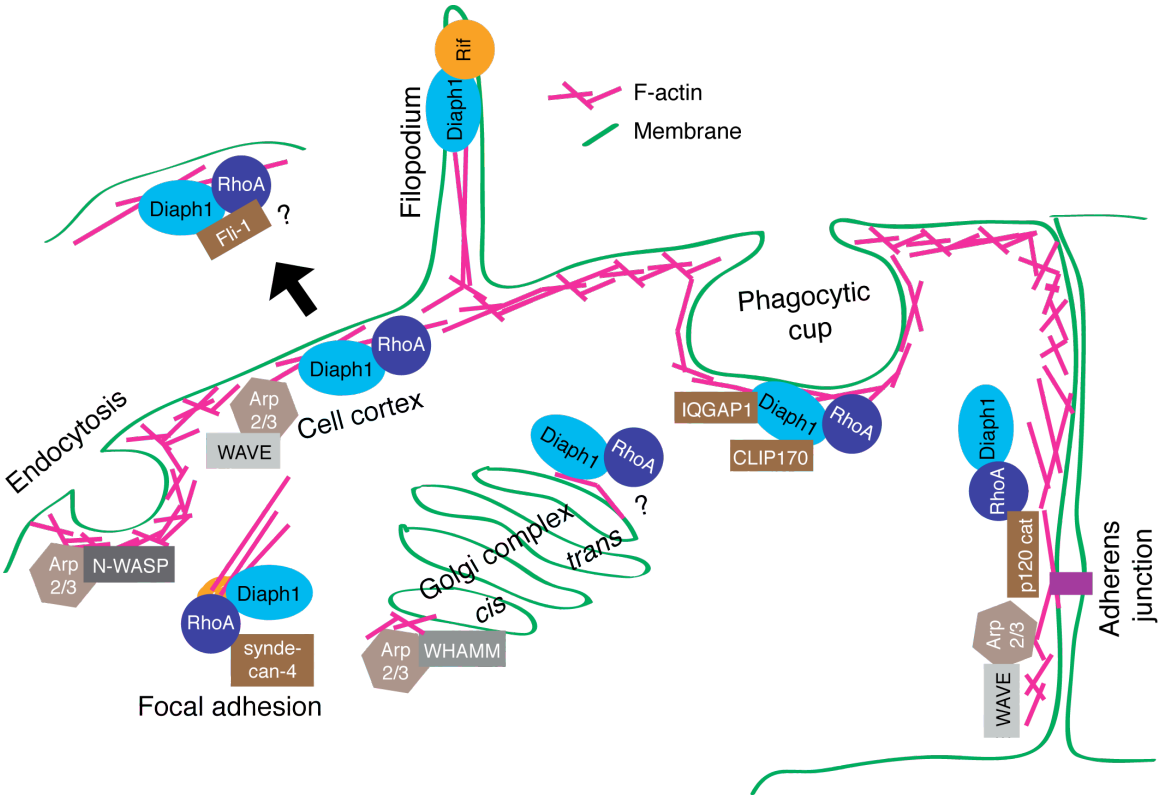

Figure 6.4: The Arp2/3 complex and Diaph1 are recruited to many different cell structures associated with membranous actin.

The Arp2/3 complex and Diaph1 with its activator RhoA are present in multiple structures in the cell. Known recruitment partners are presented in the cartoon. The Arp2/3 complex is recruited to sites of endocytosis by N-WASP, to *cis*-Golgi by WHAMM, and to cell-cell adhesions and the cortex by the WAVE complex. Diaph1 and RhoA can be recruited to focal adhesions by syndecan-4, to phagocytic cups by IQGAP1 and CLIP170, and to adherens junctions by p120 catenin. Diaph1 is recruited to filopodia by Rif. Diaph1 and RhoA are also present in the Golgi complex, where their upstream regulators are unknown. Finally, Diaph1 and RhoA are also present in the cell cortex together with Arp2/3-WAVE. A potential upstream regulator of Diaph1 with RhoA at the cortex is flightless-I (Fli-1). See main text for details and references.

Interestingly, multiple possibilities exist of how Diaph1 alone or both RhoA and Diaph1 together could be regulated and recruited to the cortex. First, as IQGAP1 and CLIP170 were both identified in the cortex, they could recruit Diaph1 to the cell membrane. Indeed, IQGAP1 did localise to the cell cortex in blebbing cells, however no phenotype was observed upon IQGAP1 depletion, suggesting a minor role in cortex assembly. However, further studies are needed to assess if IQGAP1 is needed for Diaph1 localisation in blebbing cells and if CLIP170 participates in Diaph1 recruitment.

Second, RhoC has been shown to bind Diaph1 (Rose et al., 2005). Indeed, in addition to RhoA, RhoC was also found to be associated with the cortex. Thus RhoC might participate in Diaph1 activation and recruitment at the cell membrane, however the localisation and function of RhoC in the cortex remains to be studied.

Third, Memo was shown to recruit RhoA and Diaph1 to the cell membrane at leading edge of migrating cells (Zaoui et al., 2008). We did not find Memo associated with the cortex, suggesting that in blebbing cells it is likely not required for the recruitment of RhoA and Diaph1.

Fourth, IRSp53, a protein deforming membranes, has been shown directly to interact with Diaph1 in filopodia (Goh et al., 2011a). Indeed we found that BAIAP2 (5 peptides, PAI 8.8), a human homolog of IRSp53, associated with the cortex. Further studies of this possible regulator of Diaph1 at the cell cortex are needed.

Finally, flightless-I has been suggested to activate Diaph1 *in vitro* through helping RhoA in releasing the autoinhibitory interaction of formins (Higashi et al., 2010). I found that Fli-I is associated with and localised to the cortex in M2 cells, suggesting that it might be involved in Diaph1 regulation. In addition, depletion of Fli-I led to formation of large blebs, similar to the Diaph1 silencing phenotype, suggesting that Fli-I might indeed be needed for

Diaph1 activation at the cortex. Further studies are needed to show if Fli-I interacts with Diaph1 in blebbing cells as discussed in chapter 5.5.4.

If Fli-I does interact with and regulate Diaph1 in the cortex it would be interesting to show how Fli-I itself is regulated. Interestingly the protein interaction database String reveals seven Fli-I interactors (Fig. 6.5). From these LRRFIP1 and -2 were present in the cortical fraction of the separated blebs (LRRFIP1 3 peptides PAI 3.5 and LRRFIP2 5 peptides PAI 6.1), suggesting that they are potential regulators of Fli-I at the cortex. Indeed, first their localisation in blebbing cells needs to be revealed as well as whether their depletion leads to a large bleb phenotype like Diaph1 or Fli-I silencing. In addition, their binding to Fli-I could be studied by pulldown assays. Surprisingly the String database did not suggest that Fli-I binds to Diaph1 despite of published papers. Finally Fli-I may also associate with Arp3.

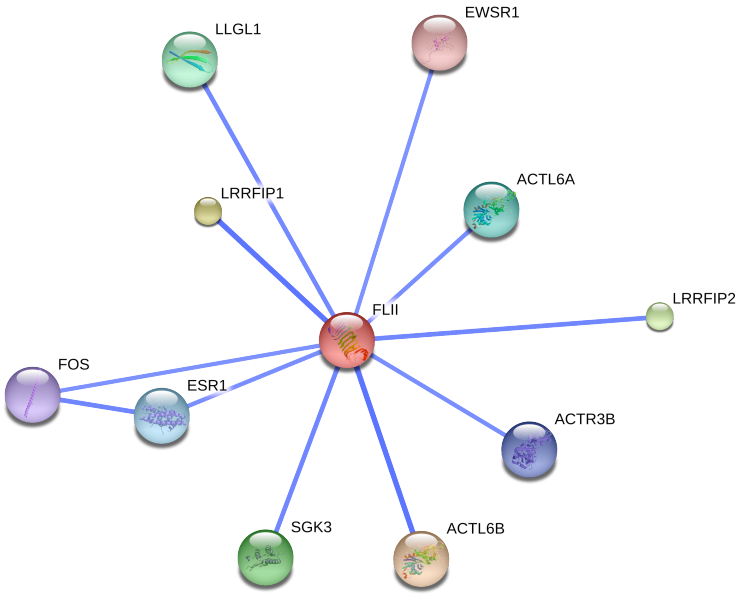

Figure 6.5: Flightless-I interacting proteins.

String database searches suggest that seven proteins are associated with Fli-I (red). Associations are represented with blue lines. LRRFIP1 and -2 were both detected in the cortical fraction of the separated blebs. Fli-I also appears to interact with ACTR3 (Arp3).

Indeed, could the regulation of the Arp2/3 complex and Diaph1 be coordinated somehow at the cell cortex? It has been shown, that a fine balance of RhoA and WAVE activities at the leading edge of migrating cells is necessary for correct assembly of a lamellipodial structure (Sarmiento et al., 2008). It was shown that expectedly WAVE silencing inhibited lamellipodia formation, but surprisingly induced filopodia formation. Further, it was observed that RhoA signalling was upregulated when WAVE and N-WASP were simultaneously silenced, and that this enhanced RhoA signalling was needed for filopodia formation. Finally it was concluded, that the balance between lamellipodial and filopodial protrusions depended on the regulation between WAVE/N-WASP and RhoA (Sarmiento et al., 2008), suggestive of a feedback loop, which can be used to trigger either filopodia or lamellipodia formation at the leading edge of the cell. Interestingly another study also concluded that filopodia formation at the leading edge of motile cells is regulated by WAVE-Arp2/3 complex as this complex can bind to and inhibit Diaph3 activity (Beli et al., 2008).

These are interesting observations that could apply to regulation of the cell cortex. Indeed as Diaph1 has been shown to localise to the tips of filopodia (Goh et al., 2011), it may promote filopodia formation and thus its activity at the cortex would need to be tightly regulated. Further, even if Diaph1 did not induce filopodia formation, its activity at the cortex would likely need to negatively controlled somehow as Diaph1 is a very efficient nucleator (Li and Higgs, 2003). It is possible that the WAVE complex has an inhibitory effect on RhoA at the cortex, leading to RhoA being able to maintain moderate Diaph1 activity at the cortex, without inducting filopodia formation. However active WAVE complex would not only inhibit RhoA but also promote Arp2/3 complex nucleation leading to questions of how lamellipodia formation is then inhibited. Interactions of the WAVE complex with RhoA or Diaph1 remain to be investigated in blebbing cells, but interestingly the String database predicts that Nap1 (NCKAP1) and Sra1 (CYFIP2) both interact with Diaph1 (Fig. 6.6). However, String did not suggest a direct link between Nap1/Sra1

and RhoA. Nonetheless, clues exist that the Arp2/3 complex and Diaph1 regulation could be coordinated and thus should be investigated. In particular, pulldown assays using Diaph1 as a bait might reveal an interaction with the WAVE complex.

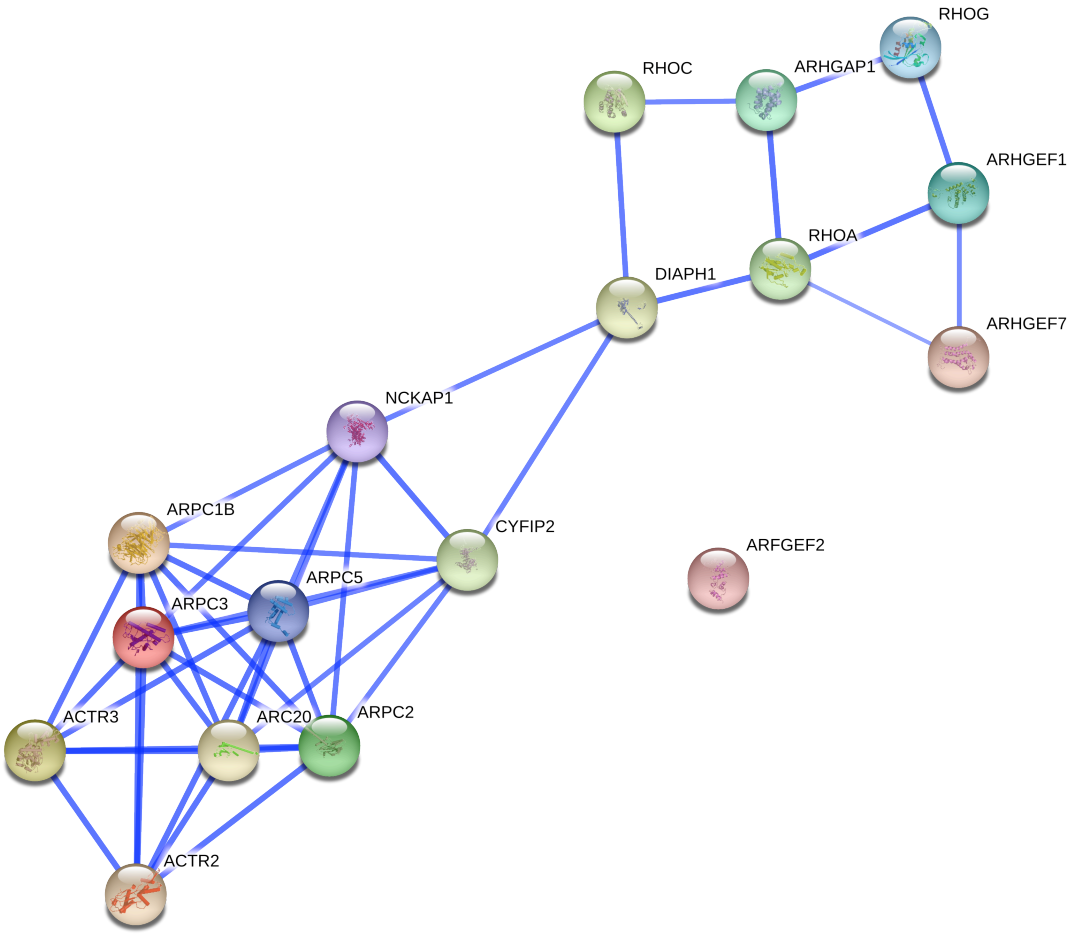

Figure 6.6: The String database predicts a link between the WAVE complex and Diaph1.

A String medium confidence interaction map was generated by inputting the subunits of the Arp2/3 complex, cortex associated WAVE complex subunits, Diaph1, and cortex associated Rho GTPases and their potential regulators. The Arp2/3 complex with its subunits are at the bottom left corner and Diaph1 with RhoA, RhoC, RhoG, and potential Rho GTPase regulators are on the upper right corner. Associations are represented with blue lines. The String database search predicts that Nap1 (NCKAP1) and Sra1 (CYFIP2) interact with Diaph1, suggesting that Diaph1 and Arp2/3 regulation might be linked in the cell cortex.

6.4 What is the minimal set of proteins needed for cortical actin homeostasis?

Membrane-F-actin interactions followed by liposome-cortex interactions have been of great interest in recent years especially among the biophysicists, who are interested in understanding cortical mechanics (Limozin and Sackmann, 2002; Pontani et al., 2009; Sengupta et al., 2006). But understanding *in vitro* the actin turnover dynamics of the cell cortex is also interesting for biologists as our understanding of the turnover dynamics of the actin cortex lag far behind that of lamellipodia or filopodia. Indeed, actin based motility has been studied in great detail using *in vitro* assays to answer questions on velocity of the movement compared to the number of actin filaments, how is the Arp2/3 complex involved in motility, and how dense the branched network of F-actin must be for movement to occur (Wiesner et al., 2003). Carrying out these studies was only possible once the main components needed for actin based motility, G-actin, ADF/cofilin, profilin, gelsolin, N-WASP, and the Arp2/3 complex, had been characterised (Pantaloni et al., 2001). In contrast, the main constituents of the cell cortex have remained elusive. In spite of this, Pontani *et al.* investigated whether or not the minimal set of proteins needed for motility (G-actin, ADF/cofilin, profilin, gelsolin, N-WASP, and the Arp2/3 complex) would be able to form an actin cortex in the inner leaflet of liposomes (Pontani et al., 2009). In response to activation of actin polymerisation by a change to F-buffer, an actin 'cortex' formed and the authors concluded that in such a liposome assay the cortex thickness and F-actin mesh size were similar to those of whole cells (Pontani et al., 2009), though neither of these values has really been well characterized in cells.

During the course of this thesis, I studied the actin cortex composition by identifying proteins from the cortical fraction of isolated blebs using mass spectrometry analysis, which was done in collaboration with Dr. Romeo and Dr. Roux. The mass spectrometry analysis revealed that many actin binding proteins associate with the cortex. Some of the proteins we identified had

already been shown to play a role in the cell cortex (ezrin, myosin II, RhoA (Charras et al., 2006)), whereas the role of others remained to be investigated.

I showed that Diaph1 and the Arp2/3 complex are needed for cortex nucleation. In addition, I revealed that capping and severing/depolymerisation appear crucial for maintenance of an actin cortex as depletion of heterodimeric capping protein or Aip1 led to cortical defects in blebbing cells. Interestingly, the minimal set of components utilised by Pontani *et al.* was close to the most abundant proteins we identified in the cortex (Pontani et al., 2009). However, certain aspects of their study did not truly reflect cortical composition. Indeed, they did not include membrane linking by ERM-proteins in the system, nor Diaph1-mediated polymerisation and myosin II contractility. Thus, performing the liposome assay with G-actin, the Arp2/3 complex, Diaph1, heterodimeric capping protein, ADF/cofilin, profilin, myosin II, and ezrin (Fig. 6.7) would be of great interest to study if these proteins are the minimal set of constituents needed for cortex formation, maintenance, and functionality. Indeed, we could compare cortex meshsize between cells and the liposomes in detail using scanning electron micrographs. In addition we could try to compare the actin turnover rate between cells and liposomes by fluorescence recovery after photobleaching studies (FRAP). Further, we could compare the adhesion force of cell membrane to the cortex by measuring tether forces using optical tweezers (Raucher, 2008).

We know that membrane linking, nucleation, capping, and depolymerisation /severing are important for cortical dynamics, but the role of actin crosslinking remains to be studied. Indeed, α-actinin-1 and -4 were present in the cortical fraction of separated blebs, but their role in the cortex has not yet been studied thoroughly. Interestingly, Pontani *et al.* did not have α-actinin or any other actin crosslinkers in their liposome assay, nonetheless the actin cortex thickness appeared comparable to that of whole cells (Pontani et al., 2009). In their assay, the Arp2/3 complex induced branching might have been

sufficient to crosslinking filaments, however in more physiological systems (i.e. in the cell) crosslinking of the cortical filaments (Fig. 6.7) by actin crosslinking proteins might be needed to regulate cortical thickness or cortical integrity, and this remains to be assessed especially in the view of possible debranching by coronin. In addition, it was showed that, at the rear of lamellipodium, myosin clusters are able to orient actin filaments into bundles (Yam et al., 2007). Thus, as the cell cortex is a contractile structure such myosin II mediated filament re-alignment is also likely to occur in the cell cortex.

In this thesis I have revealed that F-actin nucleation by Diaph1 and the Arp2/3 complex are essential for cortex assembly (Fig. 6.7). Further I identified, that many proteins involved in actin turnover are potentially bound to the cortex and essential for cortical integrity (Fig. 6.7). Indeed, silencing studies suggest that severing and depolymerisation of the cortex together with barbed end capping are essential for cortex homeostasis. In addition it has been previously shown that membrane-cortex linking and myosin induced contractility are needed for the functionality of the cortex (Charras et al., 2006; Straight et al., 2003). Finally, actin crosslinking and profilin mediated actin monomer recycling are certainly important for cortex maintenance, although not thoroughly studied in this thesis.

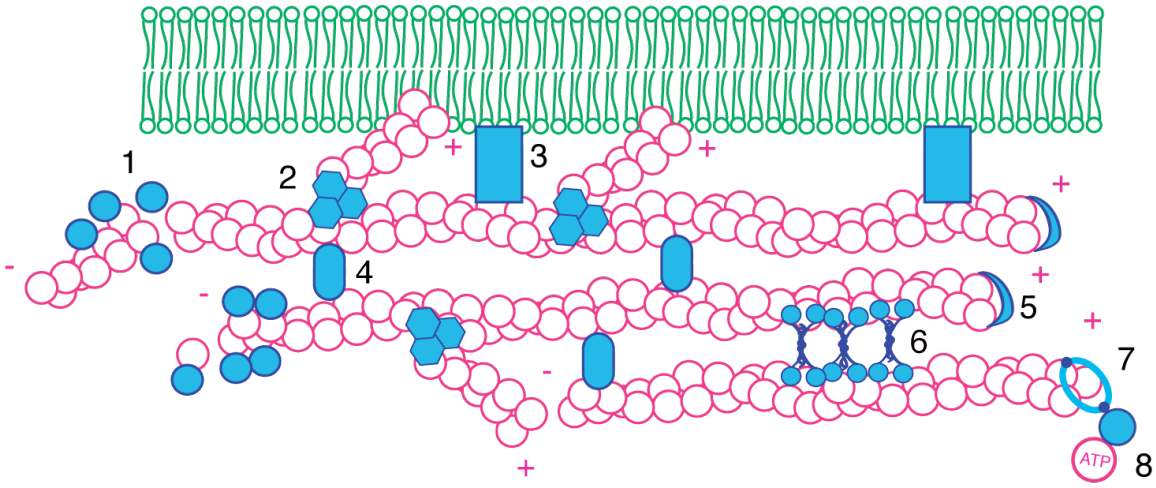

Figure 6.7: Are these the minimal set of proteins needed for cortex nucleation, maintenance, and functionality?

A schematic picture of the potential minimal set of proteins needed for cortex nucleation, maintenance, and functionality. Cell membrane (green), F-actin (pink), and cortex-associated actin-binding proteins are presented (blue). (1) Severing and depolymerisation by ADF/cofilin is possibly needed for cortex maintenance. (2) F-actin nucleation by the Arp2/3 complex is essential for cortex assembly. (3) Ezrin (or other ERM-proteins) are needed to link the cortex to the membrane as inhibition of ezrin caused defects in bleb retraction in blebbing cells (Charras et al., 2006). (4) Actin crosslinking with α-actinin could be needed to maintain cortex homeostasis, structure, and mechanical properties. (5) Depletion of heterodimeric capping protein led to cortical defects indicating capping is essential for governing the length of filaments within the cortex. (6) Contractility produced by myosin is an important property of the cortex. (7) F-actin nucleation by Diaph1 is essential for cortex assembly. (8) Profilin recycles ADP-actin into ATP-actin monomers for polymerisation.

7 REFERENCES

Ahuja, R., R. Pinyol, N. Reichenbach, L. Custer, J. Klingensmith, M.M. Kessels, and B. Qualmann. 2007. Cordon-bleu is an actin nucleation factor and controls neuronal morphology. *Cell*. 131:337-50.

Aizawa, H., M. Katadae, M. Maruya, M. Sameshima, K. Murakami-Murofushi, and I. Yahara. 1999. Hyperosmotic stress-induced reorganization of actin bundles in Dictyostelium cells over-expressing cofilin. *Genes Cells*. 4:311-24.

Alberts, B. 2008. Molecular Biology of the Cell. Garland Science, NY.

Alberts, B. 2002. Molecular Biology of the Cell. Garland Science, NY.

Albrecht-Buehler, G. 1980. Autonomous movements of cytoplasmic fragments. *Proc Natl Acad Sci U S A*. 77:6639-43.

Amann, K.J., and T.D. Pollard. 2001a. Direct real-time observation of actin filament branching mediated by Arp2/3 complex using total internal reflection fluorescence microscopy. *Proc Natl Acad Sci U S A*. 98:15009-13.

Amann, K.J., and T.D. Pollard. 2001b. The Arp2/3 complex nucleates actin filament branches from the sides of pre-existing filaments. *Nat Cell Biol*. 3:306-10.

Amano, M., M. Ito, K. Kimura, Y. Fukata, K. Chihara, T. Nakano, Y. Matsuura, and K. Kaibuchi. 1996. Phosphorylation and activation of myosin by Rho-associated kinase (Rho-kinase). *J Biol Chem*. 271:20246-9.

Ammer, A.G., and S.A. Weed. 2008. Cortactin branches out: roles in regulating protrusive actin dynamics. *Cell Motil Cytoskeleton*. 65:687-707.

Ang, S.F., Z.S. Zhao, L. Lim, and E. Manser. 2010. DAAM1 is a formin required for centrosome re-orientation during cell migration. *PLoS One*. 5.

Arthur, W.T., and K. Burridge. 2001. RhoA inactivation by p190RhoGAP regulates cell spreading and migration by promoting membrane protrusion and polarity. *Mol Biol Cell*. 12:2711-20.

Afshar, K., B. Stuart, and S.A. Wasserman. 2000. Functional analysis of the Drosophila diaphanous FH protein in early embryonic development. *Development*. 127:1887-97.

Azoury, J., K.W. Lee, V. Georget, P. Rassinier, B. Leader, and M.H. Verlhac. 2008. Spindle positioning in mouse oocytes relies on a dynamic meshwork of actin filaments. *Curr Biol*. 18:1514-9.

Bae, Y.H., Z. Ding, L. Zou, A. Wells, F. Gertler, and P. Roy. 2009. Loss of profilin-1 expression enhances breast cancer cell motility by Ena/VASP proteins. *J Cell Physiol*. 219:354-64.

Bagshaw, C.R., and D.R. Trentham. 1974. The characterization of myosin-product complexes and of product-release steps during the magnesium ion-dependent adenosine triphosphatase reaction. *Biochem J*. 141:331-49.

Baldassarre, M., Z. Razinia, C.F. Burande, I. Lamsoul, P.G. Lutz, and D.A. Calderwood. 2009. Filamins regulate cell spreading and initiation of cell migration. *PLoS One*. 4:e7830.

Bartolini, F., J.B. Moseley, J. Schmoranzer, L. Cassimeris, B.L. Goode, and G.G. Gundersen. 2008. The formin mDia2 stabilizes microtubules independently of its actin nucleation activity. *J Cell Biol*. 181:523-36.

Barylko, B., D.D. Binns, and J.P. Albanesi. 2000. Regulation of the enzymatic and motor activities of myosin I. *Biochim Biophys Acta*. 1496:23-35.

Bashour, A.M., A.T. Fullerton, M.J. Hart, and G.S. Bloom. 1997. IQGAP1, a Rac- and Cdc42-binding protein, directly binds and cross-links microfilaments. *J Cell Biol*. 137:1555-66.

Bazellieres, E., D. Massey-Harroche, M. Barthelemy-Requin, F. Richard, J.P. Arsanto, and A. Le Bivic. 2012. Apico-basal elongation requires a drebrin-E-EB3 complex in columnar human epithelial cells. *J Cell Sci*. 125:919-31.

Bear, J.E., T.M. Svitkina, M. Krause, D.A. Schafer, J.J. Loureiro, G.A. Strasser, I.V. Maly, O.Y. Chaga, J.A. Cooper, G.G. Borisy, and F.B. Gertler. 2002. Antagonism between Ena/VASP proteins and actin filament capping regulates fibroblast motility. *Cell*. 109:509-21.

Beggs, A.H., T.J. Byers, J.H. Knoll, F.M. Boyce, G.A. Bruns, and L.M. Kunkel. 1992. Cloning and characterization of two human skeletal muscle alpha-actinin genes located on chromosomes 1 and 11. *J Biol Chem*. 267:9281-8.

Beli, P., D. Mascheroni, D. Xu, and M. Innocenti. 2008. WAVE and Arp2/3 jointly inhibit filopodium formation by entering into a complex with mDia2. *Nat Cell Biol*. 10:849-57.

Bellanger, J.M., J.B. Lazaro, S. Diriong, A. Fernandez, N. Lamb, and A. Debant. 1998. The two guanine nucleotide exchange factor domains of Trio link the Rac1 and the RhoA pathways in vivo. *Oncogene*. 16:147-52.

Benesch, S., S. Polo, F.P. Lai, K.I. Anderson, T.E. Stradal, J. Wehland, and K. Rottner. 2005. N-WASP deficiency impairs EGF internalization and actin assembly at clathrin-coated pits. *J Cell Sci*. 118:3103-15.

Bensenor, L.B., H.M. Kan, N. Wang, H. Wallrabe, L.A. Davidson, Y. Cai, D.A. Schafer, and G.S. Bloom. 2007. IQGAP1 regulates cell motility by linking growth factor signaling to actin assembly. *J Cell Sci*. 120:658-69.

Bereiter-Hahn, J., M. Luck, T. Miebach, H.K. Stelzer, and M. Voth. 1990. Spreading of trypsinized cells: cytoskeletal dynamics and energy requirements. *J Cell Sci*. 96 (Pt 1):171-88.

Bernstein, B.W., and J.R. Bamburg. 1982. Tropomyosin binding to F-actin protects the F-actin from disassembly by brain actin-depolymerizing factor (ADF). *Cell Motil*. 2:1-8.

Berryman, M., and A. Bretscher. 2000. Identification of a novel member of the chloride intracellular channel gene family (CLIC5) that associates with the actin cytoskeleton of placental microvilli. *Mol Biol Cell*. 11:1509-21.

Biro, M., S. Kroschwald, Y. Romeo, M. Bovellan, A. Boden, P.P. Roux, G. Charras, and E. Paluch. 2012. Cellular blebs as tools for dissecting actin cortex composition and homeostasis. *Manuscript under review.*

Blanchoin, L., and T.D. Pollard. 1999. Mechanism of interaction of Acanthamoeba actophorin (ADF/Cofilin) with actin filaments. *J Biol Chem*. 274:15538-46.

Blanchoin, L., T.D. Pollard, and S.E. Hitchcock-DeGregori. 2001. Inhibition of the Arp2/3 complex-nucleated actin polymerization and branch formation by tropomyosin. *Curr Biol*. 11:1300-4.

Blaser, H., M. Reichman-Fried, I. Castanon, K. Dumstrei, F.L. Marlow, K. Kawakami, L. Solnica-Krezel, C.P. Heisenberg, and E. Raz. 2006. Migration of zebrafish primordial germ cells: a role for myosin contraction and cytoplasmic flow. *Dev Cell*. 11:613-27.

Block, J., T.E. Stradal, J. Hanisch, R. Geffers, S.A. Kostler, E. Urban, J.V. Small, K. Rottner, and J. Faix. 2008. Filopodia formation induced by active mDia2/Drf3. *J Microsc*. 231:506-17.

Boal, D.H. 2002. Mechanics of the cell. Cambridge University Press.

Bobkov, A.A., A. Muhlrad, D.A. Pavlov, K. Kokabi, A. Yilmaz, and E. Reisler. 2006. Cooperative effects of cofilin (ADF) on actin structure suggest allosteric mechanism of cofilin function. *J Mol Biol*. 356:325-34.

Boguski, M.S., and F. McCormick. 1993. Proteins regulating Ras and its relatives. *Nature*. 366:643-54.

Boone, C.W., L.E. Ford, H.E. Bond, D.C. Stuart, and D. Lorenz. 1969. Isolation of plasma membrane fragments from HeLa cells. *J Cell Biol*. 41:378-92.

Bosch, M., K.H. Le, B. Bugyi, J.J. Correia, L. Renault, and M.F. Carlier. 2007. Analysis of the function of Spire in actin assembly and its synergy with formin and profilin. *Mol Cell*. 28:555-68.

Bose, A., A. Guilherme, S.I. Robida, S.M. Nicoloro, Q.L. Zhou, Z.Y. Jiang, D.P. Pomerleau, and M.P. Czech. 2002. Glucose transporter recycling in response to insulin is facilitated by myosin Myo1c. *Nature*. 420:821-4.

Boucrot, E., and T. Kirchhausen. 2007. Endosomal recycling controls plasma membrane area during mitosis. *Proc Natl Acad Sci U S A*. 104:7939-44.

Bovellan, M., M. Fritzsche, C. Stevens, and G. Charras. 2010. Death-associated protein kinase (DAPK) and signal transduction: blebbing in programmed cell death. *FEBS J*. 277:58-65.

Brandt, D.T., S. Marion, G. Griffiths, T. Watanabe, K. Kaibuchi, and R. Grosse. 2007. Dia1 and IQGAP1 interact in cell migration and phagocytic cup formation. *J Cell Biol*. 178:193-200.

Bravo-Cordero, J.J., M. Oser, X. Chen, R. Eddy, L. Hodgson, and J. Condeelis. 2011. A novel spatiotemporal RhoC activation pathway locally regulates cofilin activity at invadopodia. *Curr Biol*. 21:635-44.

Bray, D. 2001. Cell Movements from Molecules to Motility. Garland Publishing, NY.

Bray, D., and J.G. White. 1988. Cortical flow in animal cells. *Science*. 239:883-8.

Breitsprecher, D., S.A. Koestler, I. Chizhov, M. Nemethova, J. Mueller, B.L. Goode, J.V. Small, K. Rottner, and J. Faix. 2011. Cofilin cooperates with fascin to disassemble filopodial actin filaments. *J Cell Sci*. 124:3305-18.

Bretscher, A., K. Edwards, and R.G. Fehon. 2002. ERM proteins and merlin: integrators at the cell cortex. *Nat Rev Mol Cell Biol*. 3:586-99.

Bu, W., A.M. Chou, K.B. Lim, T. Sudhaharan, and S. Ahmed. 2009. The Toca-1-N-WASP complex links filopodial formation to endocytosis. *J Biol Chem*. 284:11622-36.

Burgess, D.R., K.O. Broschat, and J.M. Hayden. 1987. Tropomyosin distinguishes between the two actin-binding sites of villin and affects actin-binding properties of other brush border proteins. *J Cell Biol*. 104:29-40.

Burridge, K., and L. Connell. 1983. Talin: a cytoskeletal component concentrated in adhesion plaques and other sites of actin-membrane interaction. *Cell Motil*. 3:405-17.

Burton, K., and D.L. Taylor. 1997. Traction forces of cytokinesis measured with optically modified elastic substrata. *Nature*. 385:450-4.

Buss, F., C. Temm-Grove, S. Henning, and B.M. Jockusch. 1992. Distribution of profilin in fibroblasts correlates with the presence of highly dynamic actin filaments. *Cell Motil Cytoskeleton*. 22:51-61.

Butkevich, E., S. Hulsmann, D. Wenzel, T. Shirao, R. Duden, and I. Majoul. 2004. Drebrin is a novel connexin-43 binding partner that links gap junctions to the submembrane cytoskeleton. *Curr Biol*. 14:650-8.

Cai, L., A.M. Makhov, D.A. Schafer, and J.E. Bear. 2008. Coronin 1B antagonizes cortactin and remodels Arp2/3-containing actin branches in lamellipodia. *Cell*. 134:828-42.

Cai, L., T.W. Marshall, A.C. Uetrecht, D.A. Schafer, and J.E. Bear. 2007. Coronin 1B coordinates Arp2/3 complex and cofilin activities at the leading edge. *Cell*. 128:915-29.

Campbell, H.D., T. Schimansky, C. Claudianos, N. Ozsarac, A.B. Kasprzak, J.N. Cotsell, I.G. Young, H.G. de Couet, and G.L. Miklos. 1993. The Drosophila melanogaster flightless-I gene involved in gastrulation and muscle degeneration encodes gelsolin-like and leucine-rich repeat domains and is conserved in Caenorhabditis elegans and humans. *Proc Natl Acad Sci U S A*. 90:11386-90.

Campellone, K.G., and M.D. Welch. 2010. A nucleator arms race: cellular control of actin assembly. *Nat Rev Mol Cell Biol*. 11:237-51.

Campellone, K.G., N.J. Webb, E.A. Znameroski, and M.D. Welch. 2008. WHAMM is an Arp2/3 complex activator that binds microtubules and functions in ER to Golgi transport. *Cell*. 134:148-61.

Cant, K., and L. Cooley. 1996. Single amino acid mutations in Drosophila fascin disrupt actin bundling function in vivo. *Genetics*. 143:249-58.

Carlier, M.F., V. Laurent, J. Santolini, R. Melki, D. Didry, G.X. Xia, Y. Hong, N.H. Chua, and D. Pantaloni. 1997. Actin depolymerizing factor (ADF/cofilin) enhances the rate of filament turnover: implication in actin-based motility. *J Cell Biol*. 136:1307-22.

Carramusa, L., C. Ballestrem, Y. Zilberman, and A.D. Bershadsky. 2007. Mammalian diaphanous-related formin Dia1 controls the organization of E-cadherin-mediated cell-cell junctions. *J Cell Sci*. 120:3870-82.

Carroll, E.A., D. Gerrelli, S. Gasca, E. Berg, D.R. Beier, A.J. Copp, and J. Klingensmith. 2003. Cordon-bleu is a conserved gene involved in neural tube formation. *Dev Biol*. 262:16-31.

Castrillon, D.H., and S.A. Wasserman. 1994. Diaphanous is required for cytokinesis in Drosophila and shares domains of similarity with the products of the limb deformity gene. *Development*. 120:3367-77.

Chan, A.Y., M. Bailly, N. Zebda, J.E. Segall, and J.S. Condeelis. 2000. Role of cofilin in epidermal growth factor-stimulated actin polymerization and lamellipod protrusion. *J Cell Biol*. 148:531-42.

Chan, M.W., T.Y. El Sayegh, P.D. Arora, C.A. Laschinger, C.M. Overall, C. Morrison, and C.A. McCulloch. 2004. Regulation of intercellular adhesion strength in fibroblasts. *J Biol Chem*. 279:41047-57.

Chang, F., D. Drubin, and P. Nurse. 1997. cdc12p, a protein required for cytokinesis in fission yeast, is a component of the cell division ring and interacts with profilin. *J Cell Biol*. 137:169-82.

Charras, G.T. 2008. A short history of blebbing. *J Microsc*. 231:466-78.

Charras, G.T., M. Coughlin, T.J. Mitchison, and L. Mahadevan. 2008. Life and times of a cellular bleb. *Biophys J*. 94:1836-53.

Charras, G.T., C.K. Hu, M. Coughlin, and T.J. Mitchison. 2006. Reassembly of contractile actin cortex in cell blebs. *J Cell Biol*. 175:477-90.

Charras, G., and E. Paluch. 2008. Blebs lead the way: how to migrate without lamellipodia. *Nat Rev Mol Cell Biol*. 9:730-6.

Charras, G.T., J.C. Yarrow, M.A. Horton, L. Mahadevan, and T.J. Mitchison. 2005. Non-equilibration of hydrostatic pressure in blebbing cells. *Nature*. 435:365-9.

Chen, J.L., L. Lacomis, H. Erdjument-Bromage, P. Tempst, and M. Stamnes. 2004. Cytosol-derived proteins are sufficient for Arp2/3 recruitment and ARF/coatomer-dependent actin polymerization on Golgi membranes. *FEBS Lett*. 566:281-6.

Cheng, L., and Y. Mao. 2011. mDia3-EB1-APC: A connection between kinetochores and microtubule plus ends. *Commun Integr Biol*. 4:480-2.

Chereau, D., M. Boczkowska, A. Skwarek-Maruszewska, I. Fujiwara, D.B. Hayes, G. Rebowski, P. Lappalainen, T.D. Pollard, and R. Dominguez. 2008. Leiomodin is an actin filament nucleator in muscle cells. *Science*. 320:239-43.

Chereau, D., F. Kerff, P. Graceffa, Z. Grabarek, K. Langsetmo, and R. Dominguez. 2005. Actin-bound structures of Wiskott-Aldrich syndrome protein (WASP)-homology domain 2 and the implications for filament assembly. *Proc Natl Acad Sci U S A*. 102:16644-9.

Chesarone, M.A., A.G. DuPage, and B.L. Goode. 2010. Unleashing formins to remodel the actin and microtubule cytoskeletons. *Nat Rev Mol Cell Biol*. 11:62-74.

Cheung, A., J.A. Dantzig, S. Hollingworth, S.M. Baylor, Y.E. Goldman, T.J. Mitchison, and A.F. Straight. 2002. A small-molecule inhibitor of skeletal muscle myosin II. *Nat Cell Biol*. 4:83-8.

Chhabra, E.S., and H.N. Higgs. 2006. INF2 Is a WASP homology 2 motif-containing formin that severs actin filaments and accelerates both polymerization and depolymerization. *J Biol Chem*. 281:26754-67.

Chhabra, E.S., V. Ramabhadran, S.A. Gerber, and H.N. Higgs. 2009. INF2 is an endoplasmic reticulum-associated formin protein. *J Cell Sci*. 122:1430-40.

Coleman, M.L., E.A. Sahai, M. Yeo, M. Bosch, A. Dewar, and M.F. Olson. 2001. Membrane blebbing during apoptosis results from caspase-mediated activation of ROCK I. *Nat Cell Biol*. 3:339-45.

Colon-Franco, J.M., T.S. Gomez, and D.D. Billadeau. 2010. Dynamic remodeling of the actin cytoskeleton by FMNL1gamma is required for structural maintenance of the Golgi complex. *J Cell Sci*. 124:3118-26.

Conley, C.A., K.L. Fritz-Six, A. Almenar-Queralt, and V.M. Fowler. 2001. Leiomodins: larger members of the tropomodulin (Tmod) gene family. *Genomics*. 73:127-39.

Cooper, J.A., J.D. Blum, and T.D. Pollard. 1984. Acanthamoeba castellanii capping protein: properties, mechanism of action, immunologic cross-reactivity, and localization. *J Cell Biol*. 99:217-25.

Copeland, S.J., B.J. Green, S. Burchat, G.A. Papalia, D. Banner, and J.W. Copeland. 2007. The diaphanous inhibitory domain/diaphanous autoregulatory domain interaction is able to mediate heterodimerization between mDia1 and mDia2. *J Biol Chem*. 282:30120-30.

Coue, M., S.L. Brenner, I. Spector, and E.D. Korn. 1987. Inhibition of actin polymerization by latrunculin A. *FEBS Lett*. 213:316-8.

Cox, P.R., and H.Y. Zoghbi. 2000. Sequencing, expression analysis, and mapping of three unique human tropomodulin genes and their mouse orthologs. *Genomics*. 63:97-107.

Cozzolino, M., V. Stagni, L. Spinardi, N. Campioni, C. Fiorentini, E. Salvati, S. Alema, and A.M. Salvatore. 2003. p120 Catenin is required for growth factor-dependent cell motility and scattering in epithelial cells. *Mol Biol Cell*. 14:1964-77.

Craig, R., L.E. Greene, and E. Eisenberg. 1985. Structure of the actin-myosin complex in the presence of ATP. *Proc Natl Acad Sci U S A*. 82:3247-51.

Cramer, L.P., M. Siebert, and T.J. Mitchison. 1997. Identification of novel graded polarity actin filament bundles in locomoting heart fibroblasts: implications for the generation of motile force. *J Cell Biol*. 136:1287-305.

Creed, S.J., N. Bryce, P. Naumanen, R. Weinberger, P. Lappalainen, J. Stehn, and P. Gunning. 2008. Tropomyosin isoforms define distinct microfilament populations with different drug susceptibility. *Eur J Cell Biol*. 87:709-20.

Cunningham, C.C. 1995. Actin polymerization and intracellular solvent flow in cell surface blebbing. *J Cell Biol*. 129:1589-99.

Cunningham, C.C., J.B. Gorlin, D.J. Kwiatkowski, J.H. Hartwig, P.A. Janmey, H.R. Byers, and T.P. Stossel. 1992. Actin-binding protein requirement for cortical stability and efficient locomotion. *Science*. 255:325-7.

Cunningham, C.C., T.P. Stossel, and D.J. Kwiatkowski. 1991. Enhanced motility in NIH 3T3 fibroblasts that overexpress gelsolin. *Science*. 251:1233-6.

Dai, J., and M.P. Sheetz. 1999. Membrane tether formation from blebbing cells. *Biophys J*. 77:3363-70.

Davy, D.A., H.D. Campbell, S. Fountain, D. de Jong, and M.F. Crouch. 2001. The flightless I protein colocalizes with actin- and microtubule-based structures in motile Swiss 3T3 fibroblasts: evidence for the involvement of PI 3-kinase and Ras-related small GTPases. *J Cell Sci*. 114:549-62.

Debant, A., C. Serra-Pages, K. Seipel, S. O'Brien, M. Tang, S.H. Park, and M. Streuli. 1996. The multidomain protein Trio binds the LAR transmembrane tyrosine phosphatase, contains a protein kinase domain, and has separate rac-specific and rho-specific guanine nucleotide exchange factor domains. *Proc Natl Acad Sci U S A*. 93:5466-71.

De La Cruz, E.M., A.L. Wells, S.S. Rosenfeld, E.M. Ostap, and H.L. Sweeney. 1999. The kinetic mechanism of myosin V. *Proc Natl Acad Sci U S A*. 96:13726-31.

DeMali, K.A., C.A. Barlow, and K. Burridge. 2002. Recruitment of the Arp2/3 complex to vinculin: coupling membrane protrusion to matrix adhesion. *J Cell Biol*. 159:881-91.

Dentler, W.L., and C. Adams. 1992. Flagellar microtubule dynamics in Chlamydomonas: cytochalasin D induces periods of microtubule shortening and elongation; and colchicine induces disassembly of the distal, but not proximal, half of the flagellum. *J Cell Biol*. 117:1289-98.

Derivery, E., J. Fink, D. Martin, A. Houdusse, M. Piel, T.E. Stradal, D. Louvard, and A. Gautreau. 2008. Free Brick1 is a trimeric precursor in the assembly of a functional wave complex. *PLoS One*. 3:e2462.

DeRosier, D.J., and K.T. Edds. 1980. Evidence for fascin cross-links between the actin filaments in coelomocyte filopodia. *Exp Cell Res*. 126:490-4.

DesMarais, V., I. Ichetovkin, J. Condeelis, and S.E. Hitchcock-DeGregori. 2002. Spatial regulation of actin dynamics: a tropomyosin-free, actin-rich compartment at the leading edge. *J Cell Sci*. 115:4649-60.

Dettenhofer, M., F. Zhou, and P. Leder. 2008. Formin 1-isoform IV deficient cells exhibit defects in cell spreading and focal adhesion formation. *PLoS One*. 3:e2497.

Dharmalingam, E., A. Haeckel, R. Pinyol, L. Schwintzer, D. Koch, M.M. Kessels, and B. Qualmann. 2009. F-BAR proteins of the syndapin family shape the plasma membrane and are crucial for neuromorphogenesis. *J Neurosci*. 29:13315-27.

Ding, Z., D. Gau, B. Deasy, A. Wells, and P. Roy. 2009. Both actin and polyproline interactions of profilin-1 are required for migration, invasion and capillary morphogenesis of vascular endothelial cells. *Exp Cell Res*. 315:2963-73.

di Campli, A., F. Valderrama, T. Babia, M.A. De Matteis, A. Luini, and G. Egea. 1999. Morphological changes in the Golgi complex correlate with actin cytoskeleton rearrangements. *Cell Motil Cytoskeleton*. 43:334-48.

Dissmann, E., and H. Hinssen. 1994. Immunocytochemical localization of gelsolin in fibroblasts, myogenic cells, and isolated myofibrils. *Eur J Cell Biol*. 63:336-44.

Djinovic-Carugo, K., P. Young, M. Gautel, and M. Saraste. 1999. Structure of the alpha-actinin rod: molecular basis for cross-linking of actin filaments. *Cell*. 98:537-46.

Doi, Y. 1992. Interaction of gelsolin with covalently cross-linked actin dimer. *Biochemistry*. 31:10061-9.

Dovas, A., A. Yoneda, and J.R. Couchman. 2006. PKCbeta-dependent activation of RhoA by syndecan-4 during focal adhesion formation. *J Cell Sci*. 119:2837-46.

Dugina, V., I. Zwaenepoel, G. Gabbiani, S. Clement, and C. Chaponnier. 2009. Beta and gamma-cytoplasmic actins display distinct distribution and functional diversity. *J Cell Sci*. 122:2980-8

Dumont, J., K. Million, K. Sunderland, P. Rassinier, H. Lim, B. Leader, and M.H. Verlhac. 2007. Formin-2 is required for spindle migration and for the late steps of cytokinesis in mouse oocytes. *Dev Biol*. 301:254-65.

Echarri, A., O. Muriel, D.M. Pavon, H. Azegrouz, F. Escolar, M.C. Terron, F. Sanchez-Cabo, F. Martinez, M.C. Montoya, O. Llorca, and M.A. Del Pozo. 2012. Caveolar domain organization and trafficking is regulated by Abl kinases and mDia1. *J Cell Sci*. advance online publication March 27

Eden, S., R. Rohatgi, A.V. Podtelejnikov, M. Mann, and M.W. Kirschner. 2002. Mechanism of regulation of WAVE1-induced actin nucleation by Rac1 and Nck. *Nature*. 418:790-3.

Edwards, D.C., and G.N. Gill. 1999. Structural features of LIM kinase that control effects on the actin cytoskeleton. *J Biol Chem*. 274:11352-61.

Eisenmann, K.M., E.S. Harris, S.M. Kitchen, H.A. Holman, H.N. Higgs, and A.S. Alberts. 2007. Dia-interacting protein modulates formin-mediated actin assembly at the cell cortex. *Curr Biol*. 17:579-91.

Eisenmann, K.M., R.A. West, D. Hildebrand, S.M. Kitchen, J. Peng, R. Sigler, J. Zhang, K.A. Siminovitch, and A.S. Alberts. 2007. T cell responses in mammalian diaphanous-related formin mDia1 knock-out mice. *J Biol Chem*. 282:25152-8.

Etienne-Manneville, S., and A. Hall. 2002. Rho GTPases in cell biology. *Nature*. 420:629-35.

Evangelista, M., D. Pruyne, D.C. Amberg, C. Boone, and A. Bretscher. 2002. Formins direct Arp2/3-independent actin filament assembly to polarize cell growth in yeast. *Nat Cell Biol*. 4:260-9.

Fackler, O.T., and R. Grosse. 2008. Cell motility through plasma membrane blebbing. *J Cell Biol*. 181:879-84.

Faix, J., and K. Rottner. 2006. The making of filopodia. *Curr Opin Cell Biol*. 18:18-25.

Falck, S., V.O. Paavilainen, M.A. Wear, J.G. Grossmann, J.A. Cooper, and P. Lappalainen. 2004. Biological role and structural mechanism of twinfilin-capping protein interaction. *EMBO J*. 23:3010-9.

Falet, H., K.M. Hoffmeister, R. Neujahr, and J.H. Hartwig. 2002. Normal Arp2/3 complex activation in platelets lacking WASp. *Blood*. 100:2113-22.

Fath, K.R., C.J. Edgell, and K. Burridge. 1989. The distribution of distinct integrins in focal contacts is determined by the substratum composition. *J Cell Sci*. 92 (Pt 1):67-75.

Feng, Y., M.H. Chen, I.P. Moskowitz, A.M. Mendonza, L. Vidali, F. Nakamura, D.J. Kwiatkowski, and C.A. Walsh. 2006. Filamin A (FLNA) is required for cell-cell contact in vascular development and cardiac morphogenesis. *Proc Natl Acad Sci U S A*. 103:19836-41.

Feng, Y., and C.A. Walsh. 2004. The many faces of filamin: a versatile molecular scaffold for cell motility and signalling. *Nat Cell Biol*. 6:1034-8.

Fernandez-Borja, M., L. Janssen, D. Verwoerd, P. Hordijk, and J. Neefjes. 2005. RhoB regulates endosome transport by promoting actin assembly on endosomal membranes through Dia1. *J Cell Sci*. 118:2661-70.

Filipenko, N.R., and D.M. Waisman. 2001. The C terminus of annexin II mediates binding to F-actin. *J Biol Chem*. 276:5310-5.

Fishkind, D.J., L.G. Cao, and Y.L. Wang. 1991. Microinjection of the catalytic fragment of myosin light chain kinase into dividing cells: effects on mitosis and cytokinesis. *J Cell Biol*. 114:967-75.

Flanagan, M.D., and S. Lin. 1980. Cytochalasins block actin filament elongation by binding to high affinity sites associated with F-actin. *J Biol Chem*. 255:835-8.

Fowler, V.M. 1996. Regulation of actin filament length in erythrocytes and striated muscle. *Curr Opin Cell Biol*. 8:86-96.

Fowler, V.M. 1997. Capping actin filament growth: tropomodulin in muscle and nonmuscle cells. *Soc Gen Physiol Ser*. 52:79-89.

Fowler, V.M., N.J. Greenfield, and J. Moyer. 2003. Tropomodulin contains two actin filament pointed end-capping domains. *J Biol Chem*. 278:40000-9.

Friedl, P., S. Borgmann, and E.B. Brocker. 2001. Amoeboid leukocyte crawling through extracellular matrix: lessons from the Dictyostelium paradigm of cell movement. *J Leukoc Biol*. 70:491-509.

Friedl, P., and E.B. Brocker. 2000. The biology of cell locomotion within three-dimensional extracellular matrix. *Cell Mol Life Sci*. 57:41-64.

Fucini, R.V., J.L. Chen, C. Sharma, M.M. Kessels, and M. Stamnes. 2002. Golgi vesicle proteins are linked to the assembly of an actin complex defined by mAbp1. *Mol Biol Cell*. 13:621-31.

Fujiki, Y., A.L. Hubbard, S. Fowler, and P.B. Lazarow. 1982. Isolation of intracellular membranes by means of sodium carbonate treatment: application to endoplasmic reticulum. *J Cell Biol*. 93:97-102.

Fukata, M., T. Watanabe, J. Noritake, M. Nakagawa, M. Yamaga, S. Kuroda, Y. Matsuura, A. Iwamatsu, F. Perez, and K. Kaibuchi. 2002. Rac1 and Cdc42 capture microtubules through IQGAP1 and CLIP-170. *Cell*. 109:873-85.

Furusawa, T., S. Ikawa, N. Yanai, and M. Obinata. 2000. Isolation of a novel PDZ-containing myosin from hematopoietic supportive bone marrow stromal cell lines. *Biochem Biophys Res Commun*. 270:67-75.

Galkin, V.E., A. Orlova, N. Lukoyanova, W. Wriggers, and E.H. Egelman. 2001. Actin depolymerizing factor stabilizes an existing state of F-actin and can change the tilt of F-actin subunits. *J Cell Biol*. 153:75-86.

Gandhi, M., B.A. Smith, M. Bovellan, V. Paavilainen, K. Daugherty-Clarke, J. Gelles, P. Lappalainen, and B.L. Goode. 2010. GMF is a cofilin homolog that binds Arp2/3 complex to stimulate filament debranching and inhibit actin nucleation. *Curr Biol*. 20:861-7.

Gasca, S., D.P. Hill, J. Klingensmith, and J. Rossant. 1995. Characterization of a gene trap insertion into a novel gene, cordon-bleu, expressed in axial structures of the gastrulating mouse embryo. *Dev Genet*. 17:141-54.

Gasman, S., S. Chasserot-Golaz, M. Malacombe, M. Way, and M.F. Bader. 2004. Regulated exocytosis in neuroendocrine cells: a role for subplasmalemmal Cdc42/N-WASP-induced actin filaments. *Mol Biol Cell*. 15:520-31.

Gasman, S., Y. Kalaidzidis, and M. Zerial. 2003. RhoD regulates endosome dynamics through Diaphanous-related Formin and Src tyrosine kinase. *Nat Cell Biol*. 5:195-204.

Gasteier, J.E., S. Schroeder, W. Muranyi, R. Madrid, S. Benichou, and O.T. Fackler. 2005. FHOD1 coordinates actin filament and microtubule alignment to mediate cell elongation. *Exp Cell Res*. 306:192-202.

Gates, J., J.P. Mahaffey, S.L. Rogers, M. Emerson, E.M. Rogers, S.L. Sottile, D. Van Vactor, F.B. Gertler, and M. Peifer. 2007. Enabled plays key roles in embryonic epithelial morphogenesis in Drosophila. *Development*. 134:2027-39.

Gautreau, A., H.Y. Ho, J. Li, H. Steen, S.P. Gygi, and M.W. Kirschner. 2004. Purification and architecture of the ubiquitous Wave complex. *Proc Natl Acad Sci U S A*. 101:4379-83.

Geiger, B. 1983. Membrane-cytoskeleton interaction. *Biochim Biophys Acta*. 737:305-41.

Geiger, B., K.T. Tokuyasu, A.H. Dutton, and S.J. Singer. 1980. Vinculin, an intracellular protein localized at specialized sites where microfilament bundles terminate at cell membranes. *Proc Natl Acad Sci U S A*. 77:4127-31.

Gerke, V., and S.E. Moss. 2002. Annexins: from structure to function. *Physiol Rev*. 82:331-71.

Gerke, V., and K. Weber. 1984. Identity of p36K phosphorylated upon Rous sarcoma virus transformation with a protein purified from brush borders; calcium-dependent binding to non-erythroid spectrin and F-actin. *EMBO J*. 3:227-33.

Giansanti, M.G., S. Bonaccorsi, B. Williams, E.V. Williams, C. Santolamazza, M.L. Goldberg, and M. Gatti. 1998. Cooperative interactions between the central spindle and the contractile ring during Drosophila cytokinesis. *Genes Dev*. 12:396-410.

Gilbert, H.R., and C. Frieden. 1983. Preparation, purification and properties of a crosslinked trimer of G-actin. *Biochem Biophys Res Commun*. 111:404-8.

Gimona, M., J.A. Kazzaz, and D.M. Helfman. 1996. Forced expression of tropomyosin 2 or 3 in v-Ki-ras-transformed fibroblasts results in distinct phenotypic effects. *Proc Natl Acad Sci U S A*. 93:9618-23.

Glenney, J.R., Jr., B. Tack, and M.A. Powell. 1987. Calpactins: two distinct Ca++-regulated phospholipid- and actin-binding proteins isolated from lung and placenta. *J Cell Biol*. 104:503-11.

Goebeler, V., D. Ruhe, V. Gerke, and U. Rescher. 2006. Annexin A8 displays unique phospholipid and F-actin binding properties. *FEBS Lett*. 580:2430-4.

Goh, W.I., K.B. Lim, T. Sudhaharan, K.P. Sem, W. Bu, A.M. Chou, and S. Ahmed. 2011a. mDia1 and WAVE2 proteins interact directly with IRSp53 in filopodia and are involved in filopodium formation. *J Biol Chem*. 287:4702-14.

Goh, W.I., T. Sudhaharan, K.B. Lim, K.P. Sem, C.L. Lau, and S. Ahmed. 2011. Rif-mDia1 interaction is involved in filopodium formation independent of Cdc42 and Rac effectors. *J Biol Chem*. 286:13681-94.

Goley, E.D., and M.D. Welch. 2006. The ARP2/3 complex: an actin nucleator comes of age. *Nat Rev Mol Cell Biol*. 7:713-26.

Gomez, T.S., K. Kumar, R.B. Medeiros, Y. Shimizu, P.J. Leibson, and D.D. Billadeau. 2007. Formins regulate the actin-related protein 2/3 complex-independent polarization of the centrosome to the immunological synapse. *Immunity*. 26:177-90.

Goode, B.L., D.G. Drubin, and P. Lappalainen. 1998. Regulation of the cortical actin cytoskeleton in budding yeast by twinfilin, a ubiquitous actin monomer-sequestering protein. *J Cell Biol*. 142:723-33.

Goshima, M., K. Kariya, Y. Yamawaki-Kataoka, T. Okada, M. Shibatohge, F. Shima, E. Fujimoto, and T. Kataoka. 1999. Characterization of a novel Ras-binding protein Ce-FLI-1 comprising leucine-rich repeats and gelsolin-like domains. *Biochem Biophys Res Commun*. 257:111-6.

Gregorio, C.C., A. Weber, M. Bondad, C.R. Pennise, and V.M. Fowler. 1995. Requirement of pointed-end capping by tropomodulin to maintain actin filament length in embryonic chick cardiac myocytes. *Nature*. 377:83-6.

Guo, Y., L. Cheng, S. Ahmad, and Y. Mao. 2011. Formin mDia3: A novel target for Aurora B kinase. *Bioarchitecture*. 1:88-90.

Gupton, S.L., K.L. Anderson, T.P. Kole, R.S. Fischer, A. Ponti, S.E. Hitchcock-DeGregori, G. Danuser, V.M. Fowler, D. Wirtz, D. Hanein, and C.M. Waterman-Storer. 2005. Cell migration without a lamellipodium: translation of actin dynamics into cell movement mediated by tropomyosin. *J Cell Biol*. 168:619-31.

Gupton, S.L., K. Eisenmann, A.S. Alberts, and C.M. Waterman-Storer. 2007. mDia2 regulates actin and focal adhesion dynamics and organization in the lamella for efficient epithelial cell migration. *J Cell Sci*. 120:3475-87.

Habas, R., Y. Kato, and X. He. 2001. Wnt/Frizzled activation of Rho regulates vertebrate gastrulation and requires a novel Formin homology protein Daam1. *Cell*. 107:843-54.

Hamill, O.P., and B. Martinac. 2001. Molecular basis of mechanotransduction in living cells. *Physiol Rev*. 81:685-740.

Han, Y., E. Eppinger, I.G. Schuster, L.U. Weigand, X. Liang, E. Kremmer, C. Peschel, and A.M. Krackhardt. 2009. Formin-like 1 (FMNL1) is regulated by N-terminal myristoylation and induces polarized membrane blebbing. *J Biol Chem*. 284:33409-17.

Hannemann, S., R. Madrid, J. Stastna, T. Kitzing, J. Gasteier, A. Schonichen, J. Bouchet, A. Jimenez, M. Geyer, R. Grosse, S. Benichou, and O.T. Fackler. 2008. The Diaphanous-related Formin FHOD1 associates with ROCK1 and promotes Src-dependent plasma membrane blebbing. *J Biol Chem*. 283:27891-903.

Harborth, J., S.M. Elbashir, K. Bechert, T. Tuschl, and K. Weber. 2001. Identification of essential genes in cultured mammalian cells using small interfering RNAs. *J Cell Sci*. 114:4557-65.

Harder, T., R. Kellner, R.G. Parton, and J. Gruenberg. 1997. Specific release of membrane-bound annexin II and cortical cytoskeletal elements by sequestration of membrane cholesterol. *Mol Biol Cell*. 8:533-45.

Harris, E.S., T.J. Gauvin, E.G. Heimsath, and H.N. Higgs. 2010. Assembly of filopodia by the formin FRL2 (FMNL3). *Cytoskeleton (Hoboken)*. 67:755-72.

Harris, E.S., and H.N. Higgs. 2006. Biochemical analysis of mammalian formin effects on actin dynamics. *Methods Enzymol*. 406:190-214.

Harris, E.S., F. Li, and H.N. Higgs. 2004. The mouse formin, FRLalpha, slows actin filament barbed end elongation, competes with capping protein, accelerates polymerization from monomers, and severs filaments. *J Biol Chem*. 279:20076-87.

Hart, A.W., J.E. Morgan, J. Schneider, K. West, L. McKie, S. Bhattacharya, I.J. Jackson, and S.H. Cross. 2006. Cardiac malformations and midline skeletal defects in mice lacking filamin A. *Hum Mol Genet*. 15:2457-67.

Hart, M.J., M.G. Callow, B. Souza, and P. Polakis. 1996. IQGAP1, a calmodulin-binding protein with a rasGAP-related domain, is a potential effector for cdc42Hs. *EMBO J*. 15:2997-3005.

Hart, M.J., X. Jiang, T. Kozasa, W. Roscoe, W.D. Singer, A.G. Gilman, P.C. Sternweis, and G. Bollag. 1998. Direct stimulation of the guanine nucleotide exchange activity of p115 RhoGEF by Galpha13. *Science*. 280:2112-4

Hartwig, J.H., K.A. Chambers, K.L. Hopcia, and D.J. Kwiatkowski. 1989. Association of profilin with filament-free regions of human leukocyte and platelet membranes and reversible membrane binding during platelet activation. *J Cell Biol*. 109:1571-9.

Haston, W.S., and J.M. Shields. 1984. Contraction waves in lymphocyte locomotion. *J Cell Sci*. 68:227-41.

Hawkins, M., B. Pope, S.K. Maciver, and A.G. Weeds. 1993. Human actin depolymerizing factor mediates a pH-sensitive destruction of actin filaments. *Biochemistry*. 32:9985-93.

Hayashi, K., R. Ishikawa, L.H. Ye, X.L. He, K. Takata, K. Kohama, and T. Shirao. 1996. Modulatory role of drebrin on the cytoskeleton within dendritic spines in the rat cerebral cortex. *J Neurosci*. 16:7161-70.

Hayden, S.M., P.S. Miller, A. Brauweiler, and J.R. Bamburg. 1993. Analysis of the interactions of actin depolymerizing factor with G- and F-actin. *Biochemistry*. 32:9994-10004.

Hayes, M.J., C.J. Merrifield, D. Shao, J. Ayala-Sanmartin, C.D. Schorey, T.P. Levine, J. Proust, J. Curran, M. Bailly, and S.E. Moss. 2004. Annexin 2 binding to phosphatidylinositol 4,5-bisphosphate on endocytic vesicles is regulated by the stress response pathway. *J Biol Chem*. 279:14157-64.

Hayes, M.J., D. Shao, M. Bailly, and S.E. Moss. 2006. Regulation of actin dynamics by annexin 2. *EMBO J*. 25:1816-26.

Hegmann, T.E., J.L. Lin, and J.J. Lin. 1989. Probing the role of nonmuscle tropomyosin isoforms in intracellular granule movement by microinjection of monoclonal antibodies. *J Cell Biol*. 109:1141-52.

Heiska, L., K. Alfthan, M. Gronholm, P. Vilja, A. Vaheri, and O. Carpen. 1998. Association of ezrin with intercellular adhesion molecule-1 and -2 (ICAM-1 and ICAM-2). Regulation by phosphatidylinositol 4, 5-bisphosphate. *J Biol Chem*. 273:21893-900.

Heiss, S.G., and J.A. Cooper. 1991. Regulation of CapZ, an actin capping protein of chicken muscle, by anionic phospholipids. *Biochemistry*. 30:8753-8.

Helfer, E., E.M. Nevalainen, P. Naumanen, S. Romero, D. Didry, D. Pantaloni, P. Lappalainen, and M.F. Carlier. 2006. Mammalian twinfilin sequesters ADP-G-actin and caps filament barbed ends: implications in motility. *EMBO J*. 25:1184-95.

Higashi, T., T. Ikeda, T. Murakami, R. Shirakawa, M. Kawato, K. Okawa, M. Furuse, T. Kimura, T. Kita, and H. Horiuchi. 2010. Flightless-I (Fli-I) regulates the actin assembly activity of diaphanous-related formins (DRFs) Daam1 and mDia1 in cooperation with active Rho GTPase. *J Biol Chem*. 285:16231-8.

Higashida, C., T. Miyoshi, A. Fujita, F. Oceguera-Yanez, J. Monypenny, Y. Andou, S. Narumiya, and N. Watanabe. 2004. Actin polymerization-driven molecular movement of mDia1 in living cells. *Science*. 303:2007-10.

Higgs, H.N. 2005. Formin proteins: a domain-based approach. *Trends Biochem Sci*. 30:342-53.

Higgs, H.N., and K.J. Peterson. 2005. Phylogenetic analysis of the formin homology 2 domain. *Mol Biol Cell*. 16:1-13.

Hillberg, L., L.S. Zhao Rathje, M. Nyakern-Meazza, B. Helfand, R.D. Goldman, C.E. Schutt, and U. Lindberg. 2006. Tropomyosins are present in lamellipodia of motile cells. *Eur J Cell Biol*. 85:399-409.

Hirao, M., N. Sato, T. Kondo, S. Yonemura, M. Monden, T. Sasaki, Y. Takai, and S. Tsukita. 1996. Regulation mechanism of ERM (ezrin/radixin/moesin) protein/plasma membrane association: possible involvement of phosphatidylinositol turnover and Rho-dependent signaling pathway. *J Cell Biol*. 135:37-51.

Hochmuth, R.M., and W.D. Marcus. 2002. Membrane tethers formed from blood cells with available area and determination of their adhesion energy. *Biophys J*. 82:2964-9.

Hokanson, D.E., and E.M. Ostap. 2006. Myo1c binds tightly and specifically to phosphatidylinositol 4,5-bisphosphate and inositol 1,4,5-trisphosphate. *Proc Natl Acad Sci U S A*. 103:3118-23.

Holaska, J.M., A.K. Kowalski, and K.L. Wilson. 2004. Emerin caps the pointed end of actin filaments: evidence for an actin cortical network at the nuclear inner membrane. *PLoS Biol*. 2:E231.

Holmes, K.C., I. Angert, F.J. Kull, W. Jahn, and R.R. Schroder. 2003. Electron cryo-microscopy shows how strong binding of myosin to actin releases nucleotide. *Nature*. 425:423-7.

Hotulainen, P., and P. Lappalainen. 2006. Stress fibers are generated by two distinct actin assembly mechanisms in motile cells. *J Cell Biol*. 173:383-94.

Hsu, Y.H., W.L. Lin, Y.T. Hou, Y.S. Pu, C.T. Shun, C.L. Chen, Y.Y. Wu, J.Y. Chen, T.H. Chen, and T.S. Jou. 2010. Podocalyxin EBP50 ezrin molecular complex enhances the metastatic potential of renal cell carcinoma through recruiting Rac1 guanine nucleotide exchange factor ARHGEF7. *Am J Pathol*. 176:3050-61.

Hudson, A.M., and L. Cooley. 2002. A subset of dynamic actin rearrangements in Drosophila requires the Arp2/3 complex. *J Cell Biol*. 156:677-87.

Hug, C., P.Y. Jay, I. Reddy, J.G. McNally, P.C. Bridgman, E.L. Elson, and J.A. Cooper. 1995. Capping protein levels influence actin assembly and cell motility in dictyostelium. *Cell*. 81:591-600.

Innocenti, M., S. Gerboth, K. Rottner, F.P. Lai, M. Hertzog, T.E. Stradal, E. Frittoli, D. Didry, S. Polo, A. Disanza, S. Benesch, P.P. Di Fiore, M.F. Carlier, and G. Scita. 2005. Abi1 regulates the activity of N-WASP and WAVE in distinct actin-based processes. *Nat Cell Biol*. 7:969-76.

Innocenti, M., A. Zucconi, A. Disanza, E. Frittoli, L.B. Areces, A. Steffen, T.E. Stradal, P.P. Di Fiore, M.F. Carlier, and G. Scita. 2004. Abi1 is essential for the formation and activation of a WAVE2 signalling complex. *Nat Cell Biol*. 6:319-27.

Isenberg, G., U. Aebi, and T.D. Pollard. 1980. An actin-binding protein from Acanthamoeba regulates actin filament polymerization and interactions. *Nature*. 288:455-9.

Ishikawa, R., K. Hayashi, T. Shirao, Y. Xue, T. Takagi, Y. Sasaki, and K. Kohama. 1994. Drebrin, a development-associated brain protein from rat embryo, causes the dissociation of tropomyosin from actin filaments. *J Biol Chem*. 269:29928-33.

Ishikawa, R., K. Katoh, A. Takahashi, C. Xie, K. Oseki, M. Watanabe, M. Igarashi, A. Nakamura, and K. Kohama. 2007. Drebrin attenuates the interaction between actin and myosin-V. *Biochem Biophys Res Commun*. 359:398-401.

Ishizaki, T., M. Maekawa, K. Fujisawa, K. Okawa, A. Iwamatsu, A. Fujita, N. Watanabe, Y. Saito, A. Kakizuka, N. Morii, and S. Narumiya. 1996. The small GTP-binding protein Rho binds to and activates a 160 kDa Ser/Thr protein kinase homologous to myotonic dystrophy kinase. *EMBO J*. 15:1885-93.

Ismail, A.M., S.B. Padrick, B. Chen, J. Umetani, and M.K. Rosen. 2009. The WAVE regulatory complex is inhibited. *Nat Struct Mol Biol*. 16:561-3.

Iwasa, J.H., and R.D. Mullins. 2007. Spatial and temporal relationships between actin-filament nucleation, capping, and disassembly. *Curr Biol*. 17:395-406.

Janke, J., K. Schluter, B. Jandrig, M. Theile, K. Kolble, W. Arnold, E. Grinstein, A. Schwartz, L. Estevez-Schwarz, P.M. Schlag, B.M. Jockusch, and S. Scherneck. 2000. Suppression of tumorigenicity in breast cancer cells by the microfilament protein profilin 1. *J Exp Med*. 191:1675-86.

Johnson, K.E. 1976. Circus movements and blebbing locomotion in dissociated embryonic cells of an amphibian, Xenopus laevis. *J Cell Sci*. 22:575-83.

Johnston, S.A., J.P. Bramble, C.L. Yeung, P.M. Mendes, and L.M. Machesky. 2008. Arp2/3 complex activity in filopodia of spreading cells. *BMC Cell Biol*. 9:65.

Jones, P.G., G.J. Moore, and D.M. Waisman. 1992. A nonapeptide to the putative F-actin binding site of annexin-II tetramer inhibits its calcium-dependent activation of actin filament bundling. *J Biol Chem*. 267:13993-7.

Ju, R., P. Cirone, S. Lin, H. Griesbach, D.C. Slusarski, and C.M. Crews. 2010. Activation of the planar cell polarity formin DAAM1 leads to inhibition of endothelial cell proliferation, migration, and angiogenesis. *Proc Natl Acad Sci U S A*. 107:6906-11.

Kabsch, W., and K.C. Holmes. 1995. The actin fold. *FASEB J*. 9:167-74.

Kachar, B., and T.S. Reese. 1988. The mechanism of cytoplasmic streaming in characean algal cells: sliding of endoplasmic reticulum along actin filaments. *J Cell Biol*. 106:1545-52.

Kaksonen, M., Y. Sun, and D.G. Drubin. 2003. A pathway for association of receptors, adaptors, and actin during endocytic internalization. *Cell*. 115:475-87.

Kaksonen, M., C.P. Toret, and D.G. Drubin. 2005. A modular design for the clathrin- and actin-mediated endocytosis machinery. *Cell*. 123:305-20.

Kanters, E., J. van Rijssel, P.J. Hensbergen, D. Hondius, F.P. Mul, A.M. Deelder, A. Sonnenberg, J.D. van Buul, and P.L. Hordijk. 2008. Filamin B mediates ICAM-1-driven leukocyte transendothelial migration. *J Biol Chem*. 283:31830-9.

Kato, A., S. Kurita, A. Hayashi, N. Kaji, K. Ohashi, and K. Mizuno. 2008. Critical roles of actin-interacting protein 1 in cytokinesis and chemotactic migration of mammalian cells. *Biochem J*. 414:261-70.

Katoh, M. 2004. Identification and characterization of human FHDC1, mouse Fhdc1 and zebrafish fhdc1 genes in silico. *Int J Mol Med*. 13:929-34.

Keller, H., and P. Eggli. 1998. Actin accumulation in pseudopods or in the tail of polarized walker carcinosarcoma cells quantitatively correlates with local folding of the cell surface membrane. *Cell Motil Cytoskeleton*. 40:342-53.

Keller, H.U. 2000. Redundancy of lamellipodia in locomoting Walker carcinosarcoma cells. *Cell Motil Cytoskeleton*. 46:247-56.

Keon, B.H., P.T. Jedrzejewski, D.L. Paul, and D.A. Goodenough. 2000. Isoform specific expression of the neuronal F-actin binding protein, drebrin, in specialized cells of stomach and kidney epithelia. *J Cell Sci*. 113 Pt 2:325-36.

Kerkhoff, E., J.C. Simpson, C.B. Leberfinger, I.M. Otto, T. Doerks, P. Bork, U.R. Rapp, T. Raabe, and R. Pepperkok. 2001. The Spir actin organizers are involved in vesicle transport processes. *Curr Biol*. 11:1963-8.

Kida, Y., T. Shiraishi, and T. Ogura. 2004. Identification of chick and mouse Daam1 and Daam2 genes and their expression patterns in the central nervous system. *Brain Res Dev Brain Res*. 153:143-50.

Kida, Y.S., T. Sato, K.Y. Miyasaka, A. Suto, and T. Ogura. 2007. Daam1 regulates the endocytosis of EphB during the convergent extension of the zebrafish notochord. *Proc Natl Acad Sci U S A*. 104:6708-13.

Kiema, T., Y. Lad, P. Jiang, C.L. Oxley, M. Baldassarre, K.L. Wegener, I.D. Campbell, J. Ylanne, and D.A. Calderwood. 2006. The molecular basis of filamin binding to integrins and competition with talin. *Mol Cell*. 21:337-47.

Kim, E., E. Bobkova, G. Hegyi, A. Muhlrad, and E. Reisler. 2002. Actin cross-linking and inhibition of the actomyosin motor. *Biochemistry*. 41:86-93.

Kimura, K., M. Ito, M. Amano, K. Chihara, Y. Fukata, M. Nakafuku, B. Yamamori, J. Feng, T. Nakano, K. Okawa, A. Iwamatsu, and K. Kaibuchi. 1996. Regulation of myosin phosphatase by Rho and Rho-associated kinase (Rho-kinase). *Science*. 273:245-8.

Kitzing, T.M., A.S. Sahadevan, D.T. Brandt, H. Knieling, S. Hannemann, O.T. Fackler, J. Grosshans, and R. Grosse. 2007. Positive feedback between Dia1, LARG, and RhoA regulates cell morphology and invasion. *Genes Dev*. 21:1478-83.

Kitzing, T.M., Y. Wang, O. Pertz, J.W. Copeland, and R. Grosse. 2010. Formin-like 2 drives amoeboid invasive cell motility downstream of RhoC. *Oncogene*. 29:2441-8.

Knight, P., and G. Offer. 1978. p-NN'-phenylenebismaleimide, a specific cross-linking agent for F-actin. *Biochem J*. 175:1023-32.

Knight, P., and G. Offer. 1980. Investigation, by cross-linking, of conformational changes in F-actin during its interactions with myosin. *Biochemistry*. 19:4682-7.

Korobova, F., and T. Svitkina. 2008. Arp2/3 complex is important for filopodia formation, growth cone motility, and neuritogenesis in neuronal cells. *Mol Biol Cell*. 19:1561-74.

Kotani, H., K. Takaishi, T. Sasaki, and Y. Takai. 1997. Rho regulates association of both the ERM family and vinculin with the plasma membrane in MDCK cells. *Oncogene*. 14:1705-13.

Kovac, E.M., M. Goodwin, R.G. Ali, A.D. Paterson, and A.S. Yap. 2002. Cadherin-directed actin assembly: E-cadherin physically associates with the Arp2/3 complex to direct actin assembly in nascent adhesive contacts. *Curr Biol*. 12:379-82.

Kovar, D.R. 2006. Molecular details of formin-mediated actin assembly. *Curr Opin Cell Biol*. 18:11-7.

Kovar, D.R., J.R. Kuhn, A.L. Tichy, and T.D. Pollard. 2003. The fission yeast cytokinesis formin Cdc12p is a barbed end actin filament capping protein gated by profilin. *J Cell Biol*. 161:875-87.

Kovar, D.R., J.Q. Wu, and T.D. Pollard. 2005. Profilin-mediated competition between capping protein and formin Cdc12p during cytokinesis in fission yeast. *Mol Biol Cell*. 16:2313-24.

Kowalski, J.R., C. Egile, S. Gil, S.B. Snapper, R. Li, and S.M. Thomas. 2005. Cortactin regulates cell migration through activation of N-WASP. *J Cell Sci*. 118:79-87.

Kubota, H.Y. 1981. Creeping locomotion of the endodermal cells dissociated from gastrulae of the Japanese newt, Cynops pyrrhogaster. *Exp Cell Res*. 133:137-48.

Kueh, H.Y., G.T. Charras, T.J. Mitchison, and W.M. Brieher. 2008. Actin disassembly by cofilin, coronin, and Aip1 occurs in bursts and is inhibited by barbed-end cappers. *J Cell Biol*. 182:341-53.

Kumar, N., J. Robidoux, K.W. Daniel, G. Guzman, L.M. Floering, and S. Collins. 2007. Requirement of vimentin filament assembly for beta3-adrenergic receptor activation of ERK MAP kinase and lipolysis. *J Biol Chem*. 282:9244-50.

Kunda, P., A.E. Pelling, T. Liu, and B. Baum. 2008. Moesin controls cortical rigidity, cell rounding, and spindle morphogenesis during mitosis. *Curr Biol*. 18:91-101.

Kuo, J.C., X. Han, C.T. Hsiao, J.R. Yates, 3rd, and C.M. Waterman. 2011. Analysis of the myosin-II-responsive focal adhesion proteome reveals a role for beta-Pix in negative regulation of focal adhesion maturation. *Nat Cell Biol*. 13:383-93.

Kureishy, N., V. Sapountzi, S. Prag, N. Anilkumar, and J.C. Adams. 2002. Fascins, and their roles in cell structure and function. *Bioessays*. 24:350-61.

Kuroda, S., M. Fukata, K. Kobayashi, M. Nakafuku, N. Nomura, A. Iwamatsu, and K. Kaibuchi. 1996. Identification of IQGAP as a putative target for the small GTPases, Cdc42 and Rac1. *J Biol Chem*. 271:23363-7.

Kuroda, S., M. Fukata, M. Nakagawa, K. Fujii, T. Nakamura, T. Ookubo, I. Izawa, T. Nagase, N. Nomura, H. Tani, I. Shoji, Y. Matsuura, S. Yonehara, and K. Kaibuchi. 1998. Role of IQGAP1, a target of the small GTPases Cdc42 and Rac1, in regulation of E-cadherin-mediated cell-cell adhesion. *Science*. 281:832-5.

Lammermann, T., B.L. Bader, S.J. Monkley, T. Worbs, R. Wedlich-Soldner, K. Hirsch, M. Keller, R. Forster, D.R. Critchley, R. Fassler, and M. Sixt. 2008. Rapid leukocyte migration by integrin-independent flowing and squeezing. *Nature*. 453:51-5.

Lammers, M., R. Rose, A. Scrima, and A. Wittinghofer. 2005. The regulation of mDia1 by autoinhibition and its release by Rho*GTP. *EMBO J*. 24:4176-87.

Lancaster, C.A., P.M. Taylor-Harris, A.J. Self, S. Brill, H.E. van Erp, and A. Hall. 1994. Characterization of rhoGAP. A GTPase-activating protein for rho-related small GTPases. *J Biol Chem*. 269:1137-42.

Langridge, P.D., and R.R. Kay. 2006. Blebbing of Dictyostelium cells in response to chemoattractant. *Exp Cell Res*. 312:2009-17.

Lansbergen, G., I. Grigoriev, Y. Mimori-Kiyosue, T. Ohtsuka, S. Higa, I. Kitajima, J. Demmers, N. Galjart, A.B. Houtsmuller, F. Grosveld, and A. Akhmanova. 2006. CLASPs attach microtubule plus ends to the cell cortex through a complex with LL5beta. *Dev Cell*. 11:21-32.

Lappalainen, P., and D.G. Drubin. 1997. Cofilin promotes rapid actin filament turnover in vivo. *Nature*. 388:78-82.

Lassing, I., and U. Lindberg. 1985. Specific interaction between phosphatidylinositol 4,5-bisphosphate and profilactin. *Nature*. 314:472-4.

Le Clainche, C., D. Schlaepfer, A. Ferrari, M. Klingauf, K. Grohmanova, A. Veligodskiy, D. Didry, D. Le, C. Egile, M.F. Carlier, and R. Kroschewski. 2007. IQGAP1 stimulates actin assembly through the N-WASP-Arp2/3 pathway. *J Biol Chem*. 282:426-35.

Leader, B., H. Lim, M.J. Carabatsos, A. Harrington, J. Ecsedy, D. Pellman, R. Maas, and P. Leder. 2002. Formin-2, polyploidy, hypofertility and positioning of the meiotic spindle in mouse oocytes. *Nat Cell Biol*. 4:921-8.

Lee, K., J.L. Gallop, K. Rambani, and M.W. Kirschner. 2010. Self-assembly of filopodia-like structures on supported lipid bilayers. *Science*. 329:1341-5.

Lehrer, S.S., and E.P. Morris. 1982. Dual effects of tropomyosin and troponin-tropomyosin on actomyosin subfragment 1 ATPase. *J Biol Chem*. 257:8073-80.

Leung, T., E. Manser, L. Tan, and L. Lim. 1995. A novel serine/threonine kinase binding the Ras-related RhoA GTPase which translocates the kinase to peripheral membranes. *J Biol Chem*. 270:29051-4.

Lewis, A.K., and P.C. Bridgman. 1992. Nerve growth cone lamellipodia contain two populations of actin filaments that differ in organization and polarity. *J Cell Biol*. 119:1219-43.

Lewkowicz, E., F. Herit, C. Le Clainche, P. Bourdoncle, F. Perez, and F. Niedergang. 2008. The microtubule-binding protein CLIP-170 coordinates mDia1 and actin reorganization during CR3-mediated phagocytosis. *J Cell Biol*. 183:1287-98.

Li, D., M.A. Hallett, W. Zhu, M. Rubart, Y. Liu, Z. Yang, H. Chen, L.S. Haneline, R.J. Chan, R.J. Schwartz, L.J. Field, S.J. Atkinson, and W. Shou. 2011. Dishevelled-associated activator of morphogenesis 1 (Daam1) is required for heart morphogenesis. *Development*. 138:303-15.

Li, F., and H.N. Higgs. 2003. The mouse Formin mDia1 is a potent actin nucleation factor regulated by autoinhibition. *Curr Biol*. 13:1335-40.

Li, H., F. Guo, B. Rubinstein, and R. Li. 2008. Actin-driven chromosomal motility leads to symmetry breaking in mammalian meiotic oocytes. *Nat Cell Biol*. 10:1301-8.

Limozin, L., and E. Sackmann. 2002. Polymorphism of cross-linked actin networks in giant vesicles. *Phys Rev Lett*. 89:168103.

Linardopoulou, E.V., S.S. Parghi, C. Friedman, G.E. Osborn, S.M. Parkhurst, and B.J. Trask. 2007. Human subtelomeric WASH genes encode a new subclass of the WASP family. *PLoS Genet*. 3:e237.

Littlefield, R., and V.M. Fowler. 1998. Defining actin filament length in striated muscle: rulers and caps or dynamic stability? *Annu Rev Cell Dev Biol*. 14:487-525.

Liu, R., M.T. Abreu-Blanco, K.C. Barry, E.V. Linardopoulou, G.E. Osborn, and S.M. Parkhurst. 2009. Wash functions downstream of Rho and links linear and branched actin nucleation factors. *Development*. 136:2849-60.

Liu, W., A. Sato, D. Khadka, R. Bharti, H. Diaz, L.W. Runnels, and R. Habas. 2008. Mechanism of activation of the Formin protein Daam1. *Proc Natl Acad Sci U S A*. 105:210-5.

Liu, Z., L.A. van Grunsven, E. Van Rossen, B. Schroyen, J.P. Timmermans, A. Geerts, and H. Reynaert. 2010. Blebbistatin inhibits contraction and accelerates migration in mouse hepatic stellate cells. *Br J Pharmacol*. 159:304-15.

Lu, J., W. Meng, F. Poy, S. Maiti, B.L. Goode, and M.J. Eck. 2007. Structure of the FH2 domain of Daam1: implications for formin regulation of actin assembly. *J Mol Biol*. 369:1258-69.

Luna, A., O.B. Matas, J.A. Martinez-Menarguez, E. Mato, J.M. Duran, J. Ballesta, M. Way, and G. Egea. 2002. Regulation of protein transport from the Golgi complex to the endoplasmic reticulum by CDC42 and N-WASP. *Mol Biol Cell*. 13:866-79.

Lund, R., R. Leth-Larsen, O.N. Jensen, and H.J. Ditzel. 2009. Efficient isolation and quantitative proteomic analysis of cancer cell plasma membrane proteins for identification of metastasis-associated cell surface markers. *J Proteome Res*. 8:3078-90.

Lymn, R.W., and E.W. Taylor. 1971. Mechanism of adenosine triphosphate hydrolysis by actomyosin. *Biochemistry*. 10:4617-24.

Machaidze, G., A. Sokoll, A. Shimada, A. Lustig, A. Mazur, A. Wittinghofer, U. Aebi, and H.G. Mannherz. 2010. Actin filament bundling and different nucleating effects of mouse Diaphanous-related formin FH2 domains on actin/ADF and actin/cofilin complexes. *J Mol Biol*. 403:529-45.

Machesky, L.M., S.J. Atkinson, C. Ampe, J. Vandekerckhove, and T.D. Pollard. 1994. Purification of a cortical complex containing two unconventional actins from Acanthamoeba by affinity chromatography on profilin-agarose. *J Cell Biol*. 127:107-15.

Maciver, S.K., H.G. Zot, and T.D. Pollard. 1991. Characterization of actin filament severing by actophorin from Acanthamoeba castellanii. *J Cell Biol*. 115:1611-20.

Maddox, A.S., and K. Burridge. 2003. RhoA is required for cortical retraction and rigidity during mitotic cell rounding. *J Cell Biol*. 160:255-65.

Maekawa, M., T. Ishizaki, S. Boku, N. Watanabe, A. Fujita, A. Iwamatsu, T. Obinata, K. Ohashi, K. Mizuno, and S. Narumiya. 1999. Signaling from Rho to the actin cytoskeleton through protein kinases ROCK and LIM-kinase. *Science*. 285:895-8.

Maekawa, S., S. Endo, and H. Sakai. 1982. A protein in starfish sperm head which bundles actin filaments in vitro: purification and characterization. *J Biochem*. 92:1959-72.

Mahoney, N.M., D.A. Rozwarski, E. Fedorov, A.A. Fedorov, and S.C. Almo. 1999. Profilin binds proline-rich ligands in two distinct amide backbone orientations. *Nat Struct Biol*. 6:666-71.

Mallavarapu, A., and T. Mitchison. 1999. Regulated actin cytoskeleton assembly at filopodium tips controls their extension and retraction. *J Cell Biol*. 146:1097-106.

Mangeat, P., and K. Burridge. 1984. Actin-membrane interaction in fibroblasts: what proteins are involved in this association? *J Cell Biol*. 99:95s-103s.

Marchand, J.B., D.A. Kaiser, T.D. Pollard, and H.N. Higgs. 2001. Interaction of WASP/Scar proteins with actin and vertebrate Arp2/3 complex. *Nat Cell Biol*. 3:76-82.

Martinez-Quiles, N., H.Y. Ho, M.W. Kirschner, N. Ramesh, and R.S. Geha. 2004. Erk/Src phosphorylation of cortactin acts as a switch on-switch off mechanism that controls its ability to activate N-WASP. *Mol Cell Biol*. 24:5269-80.

Maruyama, K., and S. Ebashi. 1965. Alpha-actinin, a new structural protein from striated muscle. II. Action on actin. *J Biochem*. 58:13-9.

Mass, R.L., R. Zeller, R.P. Woychik, T.F. Vogt, and P. Leder. 1990. Disruption of formin-encoding transcripts in two mutant limb deformity alleles. *Nature*. 346:853-5.

Matas, O.B., J.A. Martinez-Menarguez, and G. Egea. 2004. Association of Cdc42/N-WASP/Arp2/3 signaling pathway with Golgi membranes. *Traffic*. 5:838-46.

Matsuda, K., S. Matsuda, C.M. Gladding, and M. Yuzaki. 2006. Characterization of the delta2 glutamate receptor-binding protein delphilin: Splicing variants with differential palmitoylation and an additional PDZ domain. *J Biol Chem*. 281:25577-87.

Matsudaira, P. 1991. Modular organization of actin crosslinking proteins. *Trends Biochem Sci*. 16:87-92.

Matsui, T., M. Amano, T. Yamamoto, K. Chihara, M. Nakafuku, M. Ito, T. Nakano, K. Okawa, A. Iwamatsu, and K. Kaibuchi. 1996. Rho-associated kinase, a novel serine/threonine kinase, as a putative target for small GTP binding protein Rho. *EMBO J*. 15:2208-16.

Matsui, T., M. Maeda, Y. Doi, S. Yonemura, M. Amano, K. Kaibuchi, and S. Tsukita. 1998. Rho-kinase phosphorylates COOH-terminal threonines of ezrin/radixin/moesin (ERM) proteins and regulates their head-to-tail association. *J Cell Biol*. 140:647-57.

Matsui, T., S. Yonemura, and S. Tsukita. 1999. Activation of ERM proteins in vivo by Rho involves phosphatidyl-inositol 4-phosphate 5-kinase and not ROCK kinases. *Curr Biol*. 9:1259-62.

Matusek, T., A. Djiane, F. Jankovics, D. Brunner, M. Mlodzik, and J. Mihaly. 2006. The Drosophila formin DAAM regulates the tracheal cuticle pattern through organizing the actin cytoskeleton. *Development*. 133:957-66.

Matusek, T., R. Gombos, A. Szecsenyi, N. Sanchez-Soriano, A. Czibula, C. Pataki, A. Gedai, A. Prokop, I. Rasko, and J. Mihaly. 2008. Formin proteins of the DAAM subfamily play a role during axon growth. *J Neurosci*. 28:13310-9.

May, R.C., E. Caron, A. Hall, and L.M. Machesky. 2000. Involvement of the Arp2/3 complex in phagocytosis mediated by FcgammaR or CR3. *Nat Cell Biol*. 2:246-8.

McGough, A., and W. Chiu. 1999. ADF/cofilin weakens lateral contacts in the actin filament. *J Mol Biol*. 291:513-9.

McGough, A., B. Pope, W. Chiu, and A. Weeds. 1997. Cofilin changes the twist of F-actin: implications for actin filament dynamics and cellular function. *J Cell Biol*. 138:771-81.

McGough, A.M., C.J. Staiger, J.K. Min, and K.D. Simonetti. 2003. The gelsolin family of actin regulatory proteins: modular structures, versatile functions. *FEBS Lett*. 552:75-81.

McKenna, N.M., Y.L. Wang, and M.E. Konkel. 1989. Formation and movement of myosin-containing structures in living fibroblasts. *J Cell Biol*. 109:1163-72.

Mejillano, M.R., S. Kojima, D.A. Applewhite, F.B. Gertler, T.M. Svitkina, and G.G. Borisy. 2004. Lamellipodial versus filopodial mode of the actin nanomachinery: pivotal role of the filament barbed end. *Cell*. 118:363-73.

Melki, R., S. Fievez, and M.F. Carlier. 1996. Continuous monitoring of Pi release following nucleotide hydrolysis in actin or tubulin assembly using 2-amino-6-mercapto-7-methylpurine ribonucleoside and purine-nucleoside phosphorylase as an enzyme-linked assay. *Biochemistry*. 35:12038-45.

Mercer, J., and A. Helenius. 2008. Vaccinia virus uses macropinocytosis and apoptotic mimicry to enter host cells. *Science*. 320:531-5.

Mermall, V., P.L. Post, and M.S. Mooseker. 1998. Unconventional myosins in cell movement, membrane traffic, and signal transduction. *Science*. 279:527-33.

Merrifield, C.J. 2004. Seeing is believing: imaging actin dynamics at single sites of endocytosis. *Trends Cell Biol*. 14:352-8.

Merrifield, C.J., D. Perrais, and D. Zenisek. 2005. Coupling between clathrin-coated-pit invagination, cortactin recruitment, and membrane scission observed in live cells. *Cell*. 121:593-606.

Mersich, A.T., M.R. Miller, H. Chkourko, and S.D. Blystone. 2010. The formin FRL1 (FMNL1) is an essential component of macrophage podosomes. *Cytoskeleton (Hoboken)*. 67:573-85.

Miki, H., K. Miura, and T. Takenawa. 1996. N-WASP, a novel actin-depolymerizing protein, regulates the cortical cytoskeletal rearrangement in a PIP2-dependent manner downstream of tyrosine kinases. *EMBO J*. 15:5326-35.

Mills, J.C., N.L. Stone, J. Erhardt, and R.N. Pittman. 1998. Apoptotic membrane blebbing is regulated by myosin light chain phosphorylation. *J Cell Biol*. 140:627-36.

Mimura, N., and A. Asano. 1978. Actin-related gelation of Ehrlich tumour cell extracts is reversibly inhibited by low concentrations of Ca2+. *Nature*. 272:273-6.

Michelot, A., and D.G. Drubin. 2011. Building distinct actin filament networks in a common cytoplasm. *Curr Biol*. 21:R560-9

Mitchison, T.J., G.T. Charras, and L. Mahadevan. 2008. Implications of a poroelastic cytoplasm for the dynamics of animal cell shape. *Semin Cell Dev Biol*. 19:215-23.

Miyagi, Y., T. Yamashita, M. Fukaya, T. Sonoda, T. Okuno, K. Yamada, M. Watanabe, Y. Nagashima, I. Aoki, K. Okuda, M. Mishina, and S. Kawamoto. 2002. Delphilin: a novel PDZ and formin homology domain-containing protein that synaptically colocalizes and interacts with glutamate receptor delta 2 subunit. *J Neurosci*. 22:803-14.

Mizuno, H., C. Higashida, Y. Yuan, T. Ishizaki, S. Narumiya, and N. Watanabe. 2011. Rotational movement of the formin mDia1 along the double helical strand of an actin filament. *Science*. 331:80-3.

Mockrin, S.C., and E.D. Korn. 1980. Acanthamoeba profilin interacts with G-actin to increase the rate of exchange of actin-bound adenosine 5'-triphosphate. *Biochemistry*. 19:5359-62.

Mogilner, A., and G. Oster. 1996. Cell motility driven by actin polymerization. *Biophys J*. 71:3030-45.

Moon, S.Y., and Y. Zheng. 2003. Rho GTPase-activating proteins in cell regulation. *Trends Cell Biol*. 13:13-22.

Moriyama, K., H. Aizawa, K. Iida, and I. Yahara. 1999. [Molecular functions of cofilin which regulates reorganization of actin cytoskeleton]. *Seikagaku*. 71:101-14.

Morrell, J.L., M. Morphew, and K.L. Gould. 1999. A mutant of Arp2p causes partial disassembly of the Arp2/3 complex and loss of cortical actin function in fission yeast. *Mol Biol Cell*. 10:4201-15.

Moulding, D.A., M.P. Blundell, D.G. Spiller, M.R. White, G.O. Cory, Y. Calle, H. Kempski, J. Sinclair, P.J. Ancliff, C. Kinnon, G.E. Jones, and A.J. Thrasher. 2007. Unregulated actin polymerization by WASp causes defects of mitosis and cytokinesis in X-linked neutropenia. *J Exp Med*. 204:2213-24

Mullins, R.D., J.A. Heuser, and T.D. Pollard. 1998a. The interaction of Arp2/3 complex with actin: nucleation, high affinity pointed end capping, and formation of branching networks of filaments. *Proc Natl Acad Sci U S A*. 95:6181-6.

Mullins, R.D., J.F. Kelleher, J. Xu, and T.D. Pollard. 1998b. Arp2/3 complex from Acanthamoeba binds profilin and cross-links actin filaments. *Mol Biol Cell*. 9:841-52.

Ng, T., M. Parsons, W.E. Hughes, J. Monypenny, D. Zicha, A. Gautreau, M. Arpin, S. Gschmeissner, P.J. Verveer, P.I. Bastiaens, and P.J. Parker. 2001. Ezrin is a downstream effector of trafficking PKC-integrin complexes involved in the control of cell motility. *EMBO J*. 20:2723-41.

Nicotera, P., M. Leist, and E. Ferrando-May. 1999. Apoptosis and necrosis: different execution of the same death. *Biochem Soc Symp*. 66:69-73.

Niederman, R., and T.D. Pollard. 1975. Human platelet myosin. II. In vitro assembly and structure of myosin filaments. *J Cell Biol*. 67:72-92.

Nishida, E. 1985. Opposite effects of cofilin and profilin from porcine brain on rate of exchange of actin-bound adenosine 5'-triphosphate. *Biochemistry*. 24:1160-4.

Nishikawa, S., K. Homma, Y. Komori, M. Iwaki, T. Wazawa, A. Hikikoshi Iwane, J. Saito, R. Ikebe, E. Katayama, T. Yanagida, and M. Ikebe. 2002. Class VI myosin moves processively along actin filaments backward with large steps. *Biochem Biophys Res Commun*. 290:311-7.

Nishimura, T., H. Honda, and M. Takeichi. 2012. Planar cell polarity links axes of spatial dynamics in neural-tube closure. *Cell*. 149:1084-97.

Nishimura, Y., and S. Yonemura. 2006. Centralspindlin regulates ECT2 and RhoA accumulation at the equatorial cortex during cytokinesis. *J Cell Sci*. 119:104-14.

Nobes, C.D., and A. Hall. 1995. Rho, rac, and cdc42 GTPases regulate the assembly of multimolecular focal complexes associated with actin stress fibers, lamellipodia, and filopodia. *Cell*. 81:53-62.

Nolen, B.J., N. Tomasevic, A. Russell, D.W. Pierce, Z. Jia, C.D. McCormick, J. Hartman, R. Sakowicz, and T.D. Pollard. 2009. Characterization of two classes of small molecule inhibitors of Arp2/3 complex. *Nature*. 460:1031-4

Noritake, J., M. Fukata, K. Sato, M. Nakagawa, T. Watanabe, N. Izumi, S. Wang, Y. Fukata, and K. Kaibuchi. 2004. Positive role of IQGAP1, an effector of Rac1, in actin-meshwork formation at sites of cell-cell contact. *Mol Biol Cell*. 15:1065-76.

Novick, P., and M. Zerial. 1997. The diversity of Rab proteins in vesicle transport. *Curr Opin Cell Biol*. 9:496-504.

Nyman, T., R. Page, C.E. Schutt, R. Karlsson, and U. Lindberg. 2002. A cross-linked profilin-actin heterodimer interferes with elongation at the fast-growing end of F-actin. *J Biol Chem*. 277:15828-33.

O'Connell, C.B., A.K. Warner, and Y.L. Wang. 2001. Distinct roles of the equatorial and polar cortices in the cleavage of adherent cells. *Curr Biol*. 11:702-7.

Ohta, Y., N. Suzuki, S. Nakamura, J.H. Hartwig, and T.P. Stossel. 1999. The small GTPase RalA targets filamin to induce filopodia. *Proc Natl Acad Sci U S A*. 96:2122-8.

Okada, K., L. Blanchoin, H. Abe, H. Chen, T.D. Pollard, and J.R. Bamburg. 2002. Xenopus actin-interacting protein 1 (XAip1) enhances cofilin fragmentation of filaments by capping filament ends. *J Biol Chem*. 277:43011-6.

Okada, K., T. Obinata, and H. Abe. 1999. XAIP1: a Xenopus homologue of yeast actin interacting protein 1 (AIP1), which induces disassembly of actin filaments cooperatively with ADF/cofilin family proteins. *J Cell Sci*. 112 (Pt 10):1553-65.

Oliferenko, S., K. Paiha, T. Harder, V. Gerke, C. Schwarzler, H. Schwarz, H. Beug, U. Gunthert, and L.A. Huber. 1999. Analysis of CD44-containing lipid rafts: Recruitment of annexin II and stabilization by the actin cytoskeleton. *J Cell Biol*. 146:843-54.

Olofsson, B. 1999. Rho guanine dissociation inhibitors: pivotal molecules in cellular signalling. *Cell Signal*. 11:545-54.

Olson, E.C. 1996. Onset of electrical excitability during a period of circus plasma membrane movements in differentiating Xenopus neurons. *J Neurosci*. 16:5117-29.

Otomo, T., C. Otomo, D.R. Tomchick, M. Machius, and M.K. Rosen. 2005. Structural basis of Rho GTPase-mediated activation of the formin mDia1. *Mol Cell*. 18:273-81.

Otey, C.A., and O. Carpen. 2004. Alpha-actinin revisited: a fresh look at an old player. *Cell Motil Cytoskeleton*. 58:104-11.

Palmgren, S., P.J. Ojala, M.A. Wear, J.A. Cooper, and P. Lappalainen. 2001. Interactions with PIP2, ADP-actin monomers, and capping protein regulate the activity and localization of yeast twinfilin. *J Cell Biol*. 155:251-60.

Palmgren, S., M. Vartiainen, and P. Lappalainen. 2002. Twinfilin, a molecular mailman for actin monomers. *J Cell Sci*. 115:881-6.

Paluch, E., M. Piel, J. Prost, M. Bornens, and C. Sykes. 2005. Cortical actomyosin breakage triggers shape oscillations in cells and cell fragments. *Biophys J*. 89:724-33.

Pantaloni, D., C. Le Clainche, and M.F. Carlier. 2001. Mechanism of actin-based motility. *Science*. 292:1502-6.

Paul, A.S., and T.D. Pollard. 2008. The role of the FH1 domain and profilin in formin-mediated actin-filament elongation and nucleation. *Curr Biol*. 18:9-19.

Pechlivanis, M., A. Samol, and E. Kerkhoff. 2009. Identification of a short Spir interaction sequence at the C-terminal end of formin subgroup proteins. *J Biol Chem*. 284:25324-33.

Peitsch, W.K., C. Grund, C. Kuhn, M. Schnolzer, H. Spring, M. Schmelz, and W.W. Franke. 1999. Drebrin is a widespread actin-associating protein enriched at junctional plaques, defining a specific microfilament anchorage system in polar epithelial cells. *Eur J Cell Biol*. 78:767-78.

Pelham, R.J., Jr., J.J. Lin, and Y.L. Wang. 1996. A high molecular mass non-muscle tropomyosin isoform stimulates retrograde organelle transport. *J Cell Sci*. 109 (Pt 5):981-9.

Pellegrin, S., and H. Mellor. 2005. The Rho family GTPase Rif induces filopodia through mDia2. *Curr Biol*. 15:129-33.

Peng, J., S.M. Kitchen, R.A. West, R. Sigler, K.M. Eisenmann, and A.S. Alberts. 2007. Myeloproliferative defects following targeting of the Drf1 gene encoding the mammalian diaphanous related formin mDia1. *Cancer Res*. 67:7565-71.

Peng, J., B.J. Wallar, A. Flanders, P.J. Swiatek, and A.S. Alberts. 2003. Disruption of the Diaphanous-related formin Drf1 gene encoding mDia1 reveals a role for Drf3 as an effector for Cdc42. *Curr Biol*. 13:534-45.

Pietromonaco, S.F., P.C. Simons, A. Altman, and L. Elias. 1998. Protein kinase C-theta phosphorylation of moesin in the actin-binding sequence. *J Biol Chem*. 273:7594-603.

Pinner, S., and E. Sahai. 2008. PDK1 regulates cancer cell motility by antagonising inhibition of ROCK1 by RhoE. *Nat Cell Biol*. 10:127-37.

Pletjushkina, O.J., Z. Rajfur, P. Pomorski, T.N. Oliver, J.M. Vasiliev, and K.A. Jacobson. 2001. Induction of cortical oscillations in spreading cells by depolymerization of microtubules. *Cell Motil Cytoskeleton*. 48:235-44.

Pollard, T.D. 1986. Rate constants for the reactions of ATP- and ADP-actin with the ends of actin filaments. *J Cell Biol*. 103:2747-54.

Pollard, T.D. 2007. Regulation of actin filament assembly by Arp2/3 complex and formins. *Annu Rev Biophys Biomol Struct*. 36:451-77.

Pollard, T.D., L. Blanchoin, and R.D. Mullins. 2000. Molecular mechanisms controlling actin filament dynamics in nonmuscle cells. *Annu Rev Biophys Biomol Struct*. 29:545-76.

Pollard, T.D., and G.G. Borisy. 2003. Cellular motility driven by assembly and disassembly of actin filaments. *Cell*. 112:453-65.

Pomorski, P., P. Krzeminski, A. Wasik, K. Wierzbicka, J. Baranska, and W. Klopocka. 2007. Actin dynamics in Amoeba proteus motility. *Protoplasma*. 231:31-41.

Pontani, L.L., J. van der Gucht, G. Salbreux, J. Heuvingh, J.F. Joanny, and C. Sykes. 2009. Reconstitution of an actin cortex inside a liposome. *Biophys J*. 96:192-8.

Ponti, A., M. Machacek, S.L. Gupton, C.M. Waterman-Storer, and G. Danuser. 2004. Two distinct actin networks drive the protrusion of migrating cells. *Science*. 305:1782-6.

Ponting, C.P., and R.B. Russell. 2000. Identification of distant homologues of fibroblast growth factors suggests a common ancestor for all beta-trefoil proteins. *J Mol Biol*. 302:1041-7.

Popowicz, G.M., M. Schleicher, A.A. Noegel, and T.A. Holak. 2006. Filamins: promiscuous organizers of the cytoskeleton. *Trends Biochem Sci*. 31:411-9.

Pring, M., M. Evangelista, C. Boone, C. Yang, and S.H. Zigmond. 2003. Mechanism of formin-induced nucleation of actin filaments. *Biochemistry*. 42:486-96.

Pruyne, D., M. Evangelista, C. Yang, E. Bi, S. Zigmond, A. Bretscher, and C. Boone. 2002. Role of formins in actin assembly: nucleation and barbed-end association. *Science*. 297:612-5.

Quinlan, M.E., J.E. Heuser, E. Kerkhoff, and R.D. Mullins. 2005. Drosophila Spire is an actin nucleation factor. *Nature*. 433:382-8.

Quinlan, M.E., S. Hilgert, A. Bedrossian, R.D. Mullins, and E. Kerkhoff. 2007. Regulatory interactions between two actin nucleators, Spire and Cappuccino. *J Cell Biol*. 179:117-28.

Ramalingam, N., H. Zhao, D. Breitsprecher, P. Lappalainen, J. Faix, and M. Schleicher. 2010. Phospholipids regulate localization and activity of mDia1 formin. *Eur J Cell Biol*. 89:723-32.

Rankin, K.E., and L. Wordeman. 2010. Long astral microtubules uncouple mitotic spindles from the cytokinetic furrow. *J Cell Biol*. 190:35-43.

Rappsilber, J., U. Ryder, A.I. Lamond, and M. Mann. 2002. Large-scale proteomic analysis of the human spliceosome. *Genome Res*. 12:1231-45

Raucher, D. 2008. Chapter 17: Application of laser tweezers to studies of membrane-cytoskeleton adhesion. *Methods Cell Biol*. 89:451-66.

Rebowski, G., M. Boczkowska, D.B. Hayes, L. Guo, T.C. Irving, and R. Dominguez. 2008. X-ray scattering study of actin polymerization nuclei assembled by tandem W domains. *Proc Natl Acad Sci U S A*. 105:10785-90.

Reczek, D., and A. Bretscher. 1998. The carboxyl-terminal region of EBP50 binds to a site in the amino-terminal domain of ezrin that is masked in the dormant molecule. *J Biol Chem*. 273:18452-8

Reinhard, M., K. Jouvenal, D. Tripier, and U. Walter. 1995. Identification, purification, and characterization of a zyxin-related protein that binds the focal adhesion and microfilament protein VASP (vasodilator-stimulated phosphoprotein). *Proc Natl Acad Sci U S A*. 92:7956-60.

Ren, J.G., Z. Li, and D.B. Sacks. 2007. IQGAP1 modulates activation of B-Raf. *Proc Natl Acad Sci U S A*. 104:10465-9.

Rescher, U., D. Ruhe, C. Ludwig, N. Zobiack, and V. Gerke. 2004. Annexin 2 is a phosphatidylinositol (4,5)-bisphosphate binding protein recruited to actin assembly sites at cellular membranes. *J Cell Sci*. 117:3473-80.

Ridley, A.J. 2011. Life at the leading edge. *Cell*. 145:1012-22.

Riedl, J., A.H. Crevenna, K. Kessenbrock, J.H. Yu, D. Neukirchen, M. Bista, F. Bradke, D. Jenne, T.A. Holak, Z. Werb, M. Sixt, and R. Wedlich-Soldner. 2008. Lifeact: a versatile marker to visualize F-actin. *Nat Methods*. 5:605-7

Rittmeyer, E.N., S. Daniel, S.C. Hsu, and M.A. Osman. 2008. A dual role for IQGAP1 in regulating exocytosis. *J Cell Sci*. 121:391-403.

Roadcap, D.W., and J.E. Bear. 2009. Double JMY: making actin fast. *Nat Cell Biol*. 11:375-6.

Rodal, A.A., J.W. Tetreault, P. Lappalainen, D.G. Drubin, and D.C. Amberg. 1999. Aip1p interacts with cofilin to disassemble actin filaments. *J Cell Biol*. 145:1251-64.

Rogers, S.L., U. Wiedemann, N. Stuurman, and R.D. Vale. 2003. Molecular requirements for actin-based lamella formation in Drosophila S2 cells. *J Cell Biol*. 162:1079-88.

Romero, S., C. Le Clainche, D. Didry, C. Egile, D. Pantaloni, and M.F. Carlier. 2004. Formin is a processive motor that requires profilin to accelerate actin assembly and associated ATP hydrolysis. *Cell*. 119:419-29.

Rosales-Nieves, A.E., J.E. Johndrow, L.C. Keller, C.R. Magie, D.M. Pinto-Santini, and S.M. Parkhurst. 2006. Coordination of microtubule and microfilament dynamics by Drosophila Rho1, Spire and Cappuccino. *Nat Cell Biol*. 8:367-76.

Rose, R., A. Wittinghofer, and M. Weyand. 2005. The purification and crystallization of mDia1 in complex with RhoC. *Acta Crystallogr Sect F Struct Biol Cryst Commun*. 61:225-7.

Roy, C., M. Martin, and P. Mangeat. 1997. A dual involvement of the amino-terminal domain of ezrin in F- and G-actin binding. *J Biol Chem*. 272:20088-95.

Roy, M., Z. Li, and D.B. Sacks. 2005. IQGAP1 is a scaffold for mitogen-activated protein kinase signaling. *Mol Cell Biol*. 25:7940-52.

Rubenstein, P.A. 1990. The functional importance of multiple actin isoforms. *Bioessays*. 12:309-15.

Ruppert, C., J. Godel, R.T. Muller, R. Kroschewski, J. Reinhard, and M. Bahler. 1995. Localization of the rat myosin I molecules myr 1 and myr 2 and in vivo targeting of their tail domains. *J Cell Sci*. 108 (Pt 12):3775-86.

Ryu, J.K., L.W. Zhang, H.R. Jin, S. Piao, M.J. Choi, B. Tuvshintur, M. Tumurbaatar, S.H. Shin, J.Y. Han, W.J. Kim, and J.K. Suh. 2009. Derangements in endothelial cell-to-cell junctions involved in the pathogenesis of hypercholesterolemia-induced erectile dysfunction. *J Sex Med*. 6:1893-907.

Sagot, I., A.A. Rodal, J. Moseley, B.L. Goode, and D. Pellman. 2002. An actin nucleation mechanism mediated by Bni1 and profilin. *Nat Cell Biol*. 4:626-31.

Sahai, E., and C.J. Marshall. 2003. Differing modes of tumour cell invasion have distinct requirements for Rho/ROCK signalling and extracellular proteolysis. *Nat Cell Biol*. 5:711-9.

Sanders, M.C., and Y.L. Wang. 1990. Exogenous nucleation sites fail to induce detectable polymerization of actin in living cells. *J Cell Biol*. 110:359-65.

Sarmiento, C., W. Wang, A. Dovas, H. Yamaguchi, M. Sidani, M. El-Sibai, V. Desmarais, H.A. Holman, S. Kitchen, J.M. Backer, A. Alberts, and J. Condeelis. 2008. WASP family members and formin proteins coordinate regulation of cell protrusions in carcinoma cells. *J Cell Biol*. 180:1245-60.

Sato, N., N. Funayama, A. Nagafuchi, S. Yonemura, and S. Tsukita. 1992. A gene family consisting of ezrin, radixin and moesin. Its specific localization at actin filament/plasma membrane association sites. *J Cell Sci*. 103 (Pt 1):131-43.

Sawa, M., S. Suetsugu, A. Sugimoto, H. Miki, M. Yamamoto, and T. Takenawa. 2003. Essential role of the C. elegans Arp2/3 complex in cell migration during ventral enclosure. *J Cell Sci*. 116:1505-18.

Sawyer, G.M., A.R. Clark, S.P. Robertson, and A.J. Sutherland-Smith. 2009. Disease-associated substitutions in the filamin B actin binding domain confer enhanced actin binding affinity in the absence of major structural disturbance: Insights from the crystal structures of filamin B actin binding domains. *J Mol Biol*. 390:1030-47.

Schafer, D.A., P.B. Jennings, and J.A. Cooper. 1996. Dynamics of capping protein and actin assembly in vitro: uncapping barbed ends by polyphosphoinositides. *J Cell Biol*. 135:169-79.

Scherer, W.F., J.T. Syverton, and G.O. Gey. 1953. Studies on the propagation in vitro of poliomyelitis viruses. IV. Viral multiplication in a stable strain of human malignant epithelial cells (strain HeLa) derived from an epidermoid carcinoma of the cervix. *J Exp Med*. 97:695-710.

Schevzov, G., N.S. Bryce, R. Almonte-Baldonado, J. Joya, J.J. Lin, E. Hardeman, R. Weinberger, and P. Gunning. 2005. Specific features of neuronal size and shape are regulated by tropomyosin isoforms. *Mol Biol Cell*. 16:3425-37.

Schirenbeck, A., T. Bretschneider, R. Arasada, M. Schleicher, and J. Faix. 2005. The Diaphanous-related formin dDia2 is required for the formation and maintenance of filopodia. *Nat Cell Biol*. 7:619-25.

Schlaepfer, D.D., and H.T. Haigler. 1987. Characterization of Ca2+-dependent phospholipid binding and phosphorylation of lipocortin I. *J Biol Chem*. 262:6931-7.

Schmidt, A., and A. Hall. 2002. Guanine nucleotide exchange factors for Rho GTPases: turning on the switch. *Genes Dev*. 16:1587-609.

Schmidt, V.A., L. Scudder, C.E. Devoe, A. Bernards, L.D. Cupit, and W.F. Bahou. 2003. IQGAP2 functions as a GTP-dependent effector protein in thrombin-induced platelet cytoskeletal reorganization. *Blood*. 101:3021-8.

Schott, D., J. Ho, D. Pruyne, and A. Bretscher. 1999. The COOH-terminal domain of Myo2p, a yeast myosin V, has a direct role in secretory vesicle targeting. *J Cell Biol*. 147:791-808.

Schuh, M., and J. Ellenberg. 2008. A new model for asymmetric spindle positioning in mouse oocytes. *Curr Biol*. 18:1986-92.

Schwintzer, L., N. Koch, R. Ahuja, J. Grimm, M.M. Kessels, and B. Qualmann. 2011. The functions of the actin nucleator Cobl in cellular morphogenesis critically depend on syndapin I. *EMBO J*. 30:3147-59.

Sedeh, R.S., A.A. Fedorov, E.V. Fedorov, S. Ono, F. Matsumura, S.C. Almo, and M. Bathe. 2010. Structure, evolutionary conservation, and conformational dynamics of Homo sapiens fascin-1, an F-actin crosslinking protein. *J Mol Biol*. 400:589-604.

Sedzinski, J., M. Biro, A. Oswald, J.Y. Tinevez, G. Salbreux, and E. Paluch. 2011. Polar actomyosin contractility destabilizes the position of the cytokinetic furrow. *Nature*. 476:462-6.

Segundo, C., F. Medina, C. Rodriguez, R. Martinez-Palencia, F. Leyva-Cobian, and J.A. Brieva. 1999. Surface molecule loss and bleb formation by human germinal center B cells undergoing apoptosis: role of apoptotic blebs in monocyte chemotaxis. *Blood*. 94:1012-20.

Selden, L.A., H.J. Kinosian, J. Newman, B. Lincoln, C. Hurwitz, L.C. Gershman, and J.E. Estes. 1998. Severing of F-actin by the amino-terminal half of gelsolin suggests internal cooperativity in gelsolin. *Biophys J*. 75:3092-100.

Sellers, J.R. 2000. Myosins: a diverse superfamily. *Biochim Biophys Acta*. 1496:3-22.

Sengupta, K., L. Limozin, M. Tristl, I. Haase, M. Fischer, and E. Sackmann. 2006. Coupling artificial actin cortices to biofunctionalized lipid monolayers. *Langmuir*. 22:5776-85.

Seth, A., C. Otomo, and M.K. Rosen. 2006. Autoinhibition regulates cellular localization and actin assembly activity of the diaphanous-related formins FRLalpha and mDia1. *J Cell Biol*. 174:701-13.

Sharma, C.P., R.M. Ezzell, and M.A. Arnaout. 1995. Direct interaction of filamin (ABP-280) with the beta 2-integrin subunit CD18. *J Immunol*. 154:3461-70.

Shaw, R.J., M. Henry, F. Solomon, and T. Jacks. 1998. RhoA-dependent phosphorylation and relocalization of ERM proteins into apical membrane/actin protrusions in fibroblasts. *Mol Biol Cell*. 9:403-19.

Sheen, V.L., Y. Feng, D. Graham, T. Takafuta, S.S. Shapiro, and C.A. Walsh. 2002. Filamin A and Filamin B are co-expressed within neurons during periods of neuronal migration and can physically interact. *Hum Mol Genet*. 11:2845-54.

Sheetz, M.P., J.E. Sable, and H.G. Dobereiner. 2006. Continuous membrane-cytoskeleton adhesion requires continuous accommodation to lipid and cytoskeleton dynamics. *Annu Rev Biophys Biomol Struct*. 35:417-34.

Sheterline, P.a.S., J. 1994. Actin.

Shikama, N., C.W. Lee, S. France, L. Delavaine, J. Lyon, M. Krstic-Demonacos, and N.B. La Thangue. 1999. A novel cofactor for p300 that regulates the p53 response. *Mol Cell*. 4:365-76.

Shimada, A., M. Nyitrai, I.R. Vetter, D. Kuhlmann, B. Bugyi, S. Narumiya, M.A. Geeves, and A. Wittinghofer. 2004. The core FH2 domain of diaphanous-related formins is an elongated actin binding protein that inhibits polymerization. *Mol Cell*. 13:511-22.

Silacci, P., L. Mazzolai, C. Gauci, N. Stergiopulos, H.L. Yin, and D. Hayoz. 2004. Gelsolin superfamily proteins: key regulators of cellular functions. *Cell Mol Life Sci*. 61:2614-23.

Simons, P.C., S.F. Pietromonaco, D. Reczek, A. Bretscher, and L. Elias. 1998. C-terminal threonine phosphorylation activates ERM proteins to link the cell's cortical lipid bilayer to the cytoskeleton. *Biochem Biophys Res Commun*. 253:561-5.

Sleep, J.A., and R.L. Hutton. 1980. Exchange between inorganic phosphate and adenosine 5'-triphosphate in the medium by actomyosin subfragment 1. *Biochemistry*. 19:1276-83.

Small, J.V., and J.E. Celis. 1978. Filament arrangements in negatively stained cultured cells: the organization of actin. *Cytobiologie*. 16:308-25.

Small, J.V., M. Herzog, M. Haner, and U. Abei. 1994. Visualization of actin filaments in keratocyte lamellipodia: negative staining compared with freeze-drying. *J Struct Biol*. 113:135-41.

Snyder, J.T., D.K. Worthylake, K.L. Rossman, L. Betts, W.M. Pruitt, D.P. Siderovski, C.J. Der, and J. Sondek. 2002. Structural basis for the selective activation of Rho GTPases by Dbl exchange factors. *Nat Struct Biol*. 9:468-75.

Sperry, R.B., N.H. Bishop, J.J. Bramwell, M.N. Brodeur, M.J. Carter, B.T. Fowler, Z.B. Lewis, S.D. Maxfield, D.M. Staley, R.M. Vellinga, and M.D. Hansen. 2010. Zyxin controls migration in epithelial-mesenchymal transition by mediating actin-membrane linkages at cell-cell junctions. *J Cell Physiol*. 222:612-24.

Spudich, J.A., and S. Watt. 1971. The regulation of rabbit skeletal muscle contraction. I. Biochemical studies of the interaction of the tropomyosin-troponin complex with actin and the proteolytic fragments of myosin. *J Biol Chem*. 246:4866-71.

Sroka, J., M. von Gunten, G.A. Dunn, and H.U. Keller. 2002. Phenotype modulation in non-adherent and adherent sublines of Walker carcinosarcoma cells: the role of cell-substratum contacts and microtubules in controlling cell shape, locomotion and cytoskeletal structure. *Int J Biochem Cell Biol*. 34:882-99.

Stastna, J., X. Pan, H. Wang, A. Kollmannsperger, S. Kutscheidt, V. Lohmann, R. Grosse, and O.T. Fackler. 2011. Differing and isoform-specific roles for the formin DIAPH3 in plasma membrane blebbing and filopodia formation. *Cell Res*. 22:728-45.

Steffen, A., J. Faix, G.P. Resch, J. Linkner, J. Wehland, J.V. Small, K. Rottner, and T.E. Stradal. 2006. Filopodia formation in the absence of functional WAVE- and Arp2/3-complexes. *Mol Biol Cell*. 17:2581-91.

Stewart, D.M., S. Treiber-Held, C.C. Kurman, F. Facchetti, L.D. Notarangelo, and D.L. Nelson. 1996. Studies of the expression of the Wiskott-Aldrich syndrome protein. *J Clin Invest*. 97:2627-34.

Stossel, T.P., J. Condeelis, L. Cooley, J.H. Hartwig, A. Noegel, M. Schleicher, and S.S. Shapiro. 2001. Filamins as integrators of cell mechanics and signalling. *Nat Rev Mol Cell Biol*. 2:138-45.

Stovold, C.F., T.H. Millard, and L.M. Machesky. 2005. Inclusion of Scar/WAVE3 in a similar complex to Scar/WAVE1 and 2. *BMC Cell Biol*. 6:11.

Stradal, T., W. Kranewitter, S.J. Winder, and M. Gimona. 1998. CH domains revisited. *FEBS Lett*. 431:134-7.

Straight, A.F., A. Cheung, J. Limouze, I. Chen, N.J. Westwood, J.R. Sellers, and T.J. Mitchison. 2003. Dissecting temporal and spatial control of cytokinesis with a myosin II Inhibitor. *Science*. 299:1743-7.

Straub, K.L., M.C. Stella, and M. Leptin. 1996. The gelsolin-related flightless I protein is required for actin distribution during cellularisation in Drosophila. *J Cell Sci*. 109 (Pt 1):263-70.

Suetsugu, S., D. Yamazaki, S. Kurisu, and T. Takenawa. 2003. Differential roles of WAVE1 and WAVE2 in dorsal and peripheral ruffle formation for fibroblast cell migration. *Dev Cell*. 5:595-609.

Sun, C.X., M.A. Magalhaes, and M. Glogauer. 2007. Rac1 and Rac2 differentially regulate actin free barbed end formation downstream of the fMLP receptor. *J Cell Biol*. 179:239-45.

Sun, H.Q., M. Yamamoto, M. Mejillano, and H.L. Yin. 1999. Gelsolin, a multifunctional actin regulatory protein. *J Biol Chem*. 274:33179-82.

Sun, S.C., Q.Y. Sun, and N.H. Kim. 2011a. JMY is required for asymmetric division and cytokinesis in mouse oocytes. *Mol Hum Reprod*.

Sun, S.C., Z.B. Wang, Y.N. Xu, S.E. Lee, X.S. Cui, and N.H. Kim. 2011b. Arp2/3 complex regulates asymmetric division and cytokinesis in mouse oocytes. *PLoS One*. 6:e18392.

Sung, L.A., V.M. Fowler, K. Lambert, M.A. Sussman, D. Karr, and S. Chien. 1992. Molecular cloning and characterization of human fetal liver tropomodulin. A tropomyosin-binding protein. *J Biol Chem*. 267:2616-21.

Sung, L.A., and J.J. Lin. 1994. Erythrocyte tropomodulin binds to the N-terminus of hTM5, a tropomyosin isoform encoded by the gamma-tropomyosin gene. *Biochem Biophys Res Commun*. 201:627-34.

Svitkina, T.M., and G.G. Borisy. 1998. Correlative light and electron microscopy of the cytoskeleton of cultured cells. *Methods Enzymol*. 298:570-92.

Svitkina, T.M., and G.G. Borisy. 1999. Arp2/3 complex and actin depolymerizing factor/cofilin in dendritic organization and treadmilling of actin filament array in lamellipodia. *J Cell Biol*. 145:1009-26.

Svitkina, T.M., E.A. Bulanova, O.Y. Chaga, D.M. Vignjevic, S. Kojima, J.M. Vasiliev, and G.G. Borisy. 2003. Mechanism of filopodia initiation by reorganization of a dendritic network. *J Cell Biol*. 160:409-21.

Svitkina, T.M., A.B. Verkhovsky, and G.G. Borisy. 1995. Improved procedures for electron microscopic visualization of the cytoskeleton of cultured cells. *J Struct Biol*. 115:290-303.

Szklarczyk, D., A. Franceschini, M. Kuhn, M. Simonovic, A. Roth, P. Minguez, T. Doerks, M. Stark, J. Muller, P. Bork, L.J. Jensen, and C. von Mering. 2011. The STRING database in 2011: functional interaction networks of proteins, globally integrated and scored. *Nucleic Acids Res*. 39:D561-8.

Takahashi, K., and A. Hattori. 1989. Alpha-actinin is a component of the Z-filament, a structural backbone of skeletal muscle Z-disks. *J Biochem*. 105:529-36.

Takahashi, K., T. Sasaki, A. Mammoto, K. Takaishi, T. Kameyama, S. Tsukita, and Y. Takai. 1997. Direct interaction of the Rho GDP dissociation inhibitor with ezrin/radixin/moesin initiates the activation of the Rho small G protein. *J Biol Chem*. 272:23371-5.

Takenawa, T., and S. Suetsugu. 2007. The WASP-WAVE protein network: connecting the membrane to the cytoskeleton. *Nat Rev Mol Cell Biol*. 8:37-48.

Takeya, R., K. Taniguchi, S. Narumiya, and H. Sumimoto. 2008. The mammalian formin FHOD1 is activated through phosphorylation by ROCK and mediates thrombin-induced stress fibre formation in endothelial cells. *EMBO J*. 27:618-28.

Tanaka, H., R. Shirkoohi, K. Nakagawa, H. Qiao, H. Fujita, F. Okada, J. Hamada, S. Kuzumaki, M. Takimoto, and N. Kuzumaki. 2006. siRNA gelsolin knockdown induces epithelial-mesenchymal transition with a cadherin switch in human mammary epithelial cells. *Int J Cancer*. 118:1680-91.

Tehrani, S., N. Tomasevic, S. Weed, R. Sakowicz, and J.A. Cooper. 2007. Src phosphorylation of cortactin enhances actin assembly. *Proc Natl Acad Sci U S A*. 104:11933-8.

Tinevez, J.Y., U. Schulze, G. Salbreux, J. Roensch, J.F. Joanny, and E. Paluch. 2009. Role of cortical tension in bleb growth. *Proc Natl Acad Sci U S A*. 106:18581-6.

Tojkander, S., G. Gateva, and P. Lappalainen. 2012. Actin stress fibers - assembly, dynamics and biological roles. *J Cell Sci*. 125:1855-64.

Totsukawa, G., Y. Yamakita, S. Yamashiro, D.J. Hartshorne, Y. Sasaki, and F. Matsumura. 2000. Distinct roles of ROCK (Rho-kinase) and MLCK in spatial regulation of MLC phosphorylation for assembly of stress fibers and focal adhesions in 3T3 fibroblasts. *J Cell Biol*. 150:797-806.

Toure, A., O. Dorseuil, L. Morin, P. Timmons, B. Jegou, L. Reibel, and G. Gacon. 1998. MgcRacGAP, a new human GTPase-activating protein for Rac and Cdc42 similar to Drosophila rotundRacGAP gene product, is expressed in male germ cells. *J Biol Chem*. 273:6019-23.

Tran Quang, C., A. Gautreau, M. Arpin, and R. Treisman. 2000. Ezrin function is required for ROCK-mediated fibroblast transformation by the Net and Dbl oncogenes. *EMBO J*. 19:4565-76.

Traynor, D., and R.R. Kay. 2007. Possible roles of the endocytic cycle in cell motility. *J Cell Sci*. 120:2318-27.

Trinkaus, J.P. 1973. Surface activity and locomotion of Fundulus deep cells during blastula and gastrula stages. *Dev Biol*. 30:69-103.

Tseng, Y., K.M. An, O. Esue, and D. Wirtz. 2004. The bimodal role of filamin in controlling the architecture and mechanics of F-actin networks. *J Biol Chem*. 279:1819-26.

Tseng, Y., B.W. Schafer, S.C. Almo, and D. Wirtz. 2002. Functional synergy of actin filament cross-linking proteins. *J Biol Chem*. 277:25609-16.

Tsuji, T., T. Miyoshi, C. Higashida, S. Narumiya, and N. Watanabe. 2009. An order of magnitude faster AIP1-associated actin disruption than nucleation by the Arp2/3 complex in lamellipodia. *PLoS One*. 4:e4921.

Tsujita, K., S. Suetsugu, N. Sasaki, M. Furutani, T. Oikawa, and T. Takenawa. 2006. Coordination between the actin cytoskeleton and membrane deformation by a novel membrane tubulation domain of PCH proteins is involved in endocytosis. *J Cell Biol*. 172:269-79.

Tsukita, S., K. Oishi, N. Sato, J. Sagara, and A. Kawai. 1994. ERM family members as molecular linkers between the cell surface glycoprotein CD44 and actin-based cytoskeletons. *J Cell Biol*. 126:391-401.

Turner, C.E., J.R. Glenney, Jr., and K. Burridge. 1990. Paxillin: a new vinculin-binding protein present in focal adhesions. *J Cell Biol*. 111:1059-68.

Turunen, O., T. Wahlstrom, and A. Vaheri. 1994. Ezrin has a COOH-terminal actin-binding site that is conserved in the ezrin protein family. *J Cell Biol*. 126:1445-53.

Tyler, J.M., J.M. Anderson, and D. Branton. 1980. Structural comparison of several actin-binding macromolecules. *J Cell Biol*. 85:489-95.

Ueda, H., R. Nagae, M. Kozawa, R. Morishita, S. Kimura, T. Nagase, O. Ohara, S. Yoshida, and T. Asano. 2008. Heterotrimeric G protein betagamma subunits stimulate FLJ00018, a guanine nucleotide exchange factor for Rac1 and Cdc42. *J Biol Chem*. 283:1946-53.

Uehata, M., T. Ishizaki, H. Satoh, T. Ono, T. Kawahara, T. Morishita, H. Tamakawa, K. Yamagami, J. Inui, M. Maekawa, and S. Narumiya. 1997. Calcium sensitization of smooth muscle mediated by a Rho-associated protein kinase in hypertension. *Nature*. 389:990-4.

Uruno, T., J. Liu, P. Zhang, Y. Fan, C. Egile, R. Li, S.C. Mueller, and X. Zhan. 2001. Activation of Arp2/3 complex-mediated actin polymerization by cortactin. *Nat Cell Biol*. 3:259-66.

Vaillant, D.C., S.J. Copeland, C. Davis, S.F. Thurston, N. Abdennur, and J.W. Copeland. 2008. Interaction of the N- and C-terminal autoregulatory domains of FRL2 does not inhibit FRL2 activity. *J Biol Chem*. 283:33750-62.

van der Flier, A., and A. Sonnenberg. 2001. Structural and functional aspects of filamins. *Biochim Biophys Acta*. 1538:99-117.

Vartiainen, M., P.J. Ojala, P. Auvinen, J. Peranen, and P. Lappalainen. 2000. Mouse A6/twinfilin is an actin monomer-binding protein that localizes to the regions of rapid actin dynamics. *Mol Cell Biol*. 20:1772-83.

Verkhovsky, A.B., T.M. Svitkina, and G.G. Borisy. 1995. Myosin II filament assemblies in the active lamella of fibroblasts: their morphogenesis and role in the formation of actin filament bundles. *J Cell Biol*. 131:989-1002.

Wakatsuki, T., B. Schwab, N.C. Thompson, and E.L. Elson. 2001. Effects of cytochalasin D and latrunculin B on mechanical properties of cells. *J Cell Sci*. 114:1025-36.

Wang, Y.L., J.D. Silverman, and L.G. Cao. 1994. Single particle tracking of surface receptor movement during cell division. *J Cell Biol*. 127:963-71.

Watanabe, N., T. Kato, A. Fujita, T. Ishizaki, and S. Narumiya. 1999. Cooperation between mDia1 and ROCK in Rho-induced actin reorganization. *Nat Cell Biol*. 1:136-43.

Watanabe, N., P. Madaule, T. Reid, T. Ishizaki, G. Watanabe, A. Kakizuka, Y. Saito, K. Nakao, B.M. Jockusch, and S. Narumiya. 1997. p140mDia, a mammalian homolog of Drosophila diaphanous, is a target protein for Rho small GTPase and is a ligand for profilin. *EMBO J*. 16:3044-56.

Watanabe, N., and T.J. Mitchison. 2002. Single-molecule speckle analysis of actin filament turnover in lamellipodia. *Science*. 295:1083-6.

Watanabe, S., Y. Ando, S. Yasuda, H. Hosoya, N. Watanabe, T. Ishizaki, and S. Narumiya. 2008. mDia2 induces the actin scaffold for the contractile ring and stabilizes its position during cytokinesis in NIH 3T3 cells. *Mol Biol Cell*. 19:2328-38.

Watanabe, S., K. Okawa, T. Miki, S. Sakamoto, T. Morinaga, K. Segawa, T. Arakawa, M. Kinoshita, T. Ishizaki, and S. Narumiya. 2010. Rho and anillin-dependent control of mDia2 localization and function in cytokinesis. *Mol Biol Cell*. 21:3193-204.

Watanabe, T., M. Inui, B.Y. Chen, M. Iga, and K. Sobue. 1994. Annexin VI-binding proteins in brain. Interaction of annexin VI with a membrane skeletal protein, calspectin (brain spectrin or fodrin). *J Biol Chem*. 269:17656-62.

Watanabe, T., S. Wang, J. Noritake, K. Sato, M. Fukata, M. Takefuji, M. Nakagawa, N. Izumi, T. Akiyama, and K. Kaibuchi. 2004. Interaction with IQGAP1 links APC to Rac1, Cdc42, and actin filaments during cell polarization and migration. *Dev Cell*. 7:871-83.

Wear, M.A., and J.A. Cooper. 2004. Capping protein: new insights into mechanism and regulation. *Trends Biochem Sci*. 29:418-28.

Wear, M.A., A. Yamashita, K. Kim, Y. Maeda, and J.A. Cooper. 2003. How capping protein binds the barbed end of the actin filament. *Curr Biol*. 13:1531-7.

Weaver, A.M., A.V. Karginov, A.W. Kinley, S.A. Weed, Y. Li, J.T. Parsons, and J.A. Cooper. 2001. Cortactin promotes and stabilizes Arp2/3-induced actin filament network formation. *Curr Biol*. 11:370-4.

Weber, A., C.R. Pennise, G.G. Babcock, and V.M. Fowler. 1994. Tropomodulin caps the pointed ends of actin filaments. *J Cell Biol*. 127:1627-35.

Weber, A., C.R. Pennise, and V.M. Fowler. 1999. Tropomodulin increases the critical concentration of barbed end-capped actin filaments by converting ADP.P(i)-actin to ADP-actin at all pointed filament ends. *J Biol Chem*. 274:34637-45.

Weed, S.A., A.V. Karginov, D.A. Schafer, A.M. Weaver, A.W. Kinley, J.A. Cooper, and J.T. Parsons. 2000. Cortactin localization to sites of actin assembly in lamellipodia requires interactions with F-actin and the Arp2/3 complex. *J Cell Biol*. 151:29-40.

Welch, M.D., A.H. DePace, S. Verma, A. Iwamatsu, and T.J. Mitchison. 1997. The human Arp2/3 complex is composed of evolutionarily conserved subunits and is localized to cellular regions of dynamic actin filament assembly. *J Cell Biol*. 138:375-84.

Welch, M.D., and R.D. Mullins. 2002. Cellular control of actin nucleation. *Annu Rev Cell Dev Biol*. 18:247-88.

Wells, A.L., A.W. Lin, L.Q. Chen, D. Safer, S.M. Cain, T. Hasson, B.O. Carragher, R.A. Milligan, and H.L. Sweeney. 1999. Myosin VI is an actin-based motor that moves backwards. *Nature*. 401:505-8.

Wen, Y., C.H. Eng, J. Schmoranzer, N. Cabrera-Poch, E.J. Morris, M. Chen, B.J. Wallar, A.S. Alberts, and G.G. Gundersen. 2004. EB1 and APC bind to mDia to stabilize microtubules downstream of Rho and promote cell migration. *Nat Cell Biol*. 6:820-30.

Westendorf, J.J. 2001. The formin/diaphanous-related protein, FHOS, interacts with Rac1 and activates transcription from the serum response element. *J Biol Chem*. 276:46453-9.

Whittaker, M., E.M. Wilson-Kubalek, J.E. Smith, L. Faust, R.A. Milligan, and H.L. Sweeney. 1995. A 35-A movement of smooth muscle myosin on ADP release. *Nature*. 378:748-51.

Wiesner, S., E. Helfer, D. Didry, G. Ducouret, F. Lafuma, M.F. Carlier, and D. Pantaloni. 2003. A biomimetic motility assay provides insight into the mechanism of actin-based motility. *J Cell Biol*. 160:387-98.

Winter, D., A.V. Podtelejnikov, M. Mann, and R. Li. 1997. The complex containing actin-related proteins Arp2 and Arp3 is required for the motility and integrity of yeast actin patches. *Curr Biol*. 7:519-29.

Wolf, K., I. Mazo, H. Leung, K. Engelke, U.H. von Andrian, E.I. Deryugina, A.Y. Strongin, E.B. Brocker, and P. Friedl. 2003. Compensation mechanism in tumor cell migration: mesenchymal-amoeboid transition after blocking of pericellular proteolysis. *J Cell Biol*. 160:267-77.

Woychik, R.P., R.L. Maas, R. Zeller, T.F. Vogt, and P. Leder. 1990. 'Formins': proteins deduced from the alternative transcripts of the limb deformity gene. *Nature*. 346:850-3.

Xu, Y., J.B. Moseley, I. Sagot, F. Poy, D. Pellman, B.L. Goode, and M.J. Eck. 2004. Crystal structures of a Formin Homology-2 domain reveal a tethered dimer architecture. *Cell*. 116:711-23.

Yam, P.T., C.A. Wilson, L. Ji, B. Hebert, E.L. Barnhart, N.A. Dye, P.W. Wiseman, G. Danuser, and J.A. Theriot. 2007. Actin-myosin network reorganization breaks symmetry at the cell rear to spontaneously initiate polarized cell motility. *J Cell Biol*. 178:1207-21.

Yamashiro, S., K.D. Speicher, D.W. Speicher, and V.M. Fowler. 2010. Mammalian tropomodulins nucleate actin polymerization via their actin monomer binding and filament pointed end-capping activities. *J Biol Chem*. 285:33265-80.

Yamashita, A., K. Maeda, and Y. Maeda. 2003. Crystal structure of CapZ: structural basis for actin filament barbed end capping. *EMBO J*. 22:1529-38.

Yamauchi, J., Y. Miyamoto, J.R. Chan, and A. Tanoue. 2008. ErbB2 directly activates the exchange factor Dock7 to promote Schwann cell migration. *J Cell Biol*. 181:351-65.

Yamazaki, D., T. Oikawa, and T. Takenawa. 2007. Rac-WAVE-mediated actin reorganization is required for organization and maintenance of cell-cell adhesion. *J Cell Sci*. 120:86-100.

Yamazaki, D., S. Suetsugu, H. Miki, Y. Kataoka, S. Nishikawa, T. Fujiwara, N. Yoshida, and T. Takenawa. 2003. WAVE2 is required for directed cell migration and cardiovascular development. *Nature*. 424:452-6.

Yan, C., N. Martinez-Quiles, S. Eden, T. Shibata, F. Takeshima, R. Shinkura, Y. Fujiwara, R. Bronson, S.B. Snapper, M.W. Kirschner, R. Geha, F.S. Rosen, and F.W. Alt. 2003. WAVE2 deficiency reveals distinct roles in embryogenesis and Rac-mediated actin-based motility. *EMBO J*. 22:3602-12.

Yang, C., L. Czech, S. Gerboth, S. Kojima, G. Scita, and T. Svitkina. 2007. Novel roles of formin mDia2 in lamellipodia and filopodia formation in motile cells. *PLoS Biol*. 5:e317.

Yayoshi-Yamamoto, S., I. Taniuchi, and T. Watanabe. 2000. FRL, a novel formin-related protein, binds to Rac and regulates cell motility and survival of macrophages. *Mol Cell Biol*. 20:6872-81.

Yi, K., J.R. Unruh, M. Deng, B.D. Slaughter, B. Rubinstein, and R. Li. 2011. Dynamic maintenance of asymmetric meiotic spindle position through Arp2/3-complex-driven cytoplasmic streaming in mouse oocytes. *Nat Cell Biol*. 13:1252-8.

Yin, H.L., and T.P. Stossel. 1979. Control of cytoplasmic actin gel-sol transformation by gelsolin, a calcium-dependent regulatory protein. *Nature*. 281:583-6.

Yonemura, S., M. Hirao, Y. Doi, N. Takahashi, T. Kondo, and S. Tsukita. 1998. Ezrin/radixin/moesin (ERM) proteins bind to a positively charged amino acid cluster in the juxta-membrane cytoplasmic domain of CD44, CD43, and ICAM-2. *J Cell Biol*. 140:885-95.

Yoshida, M., N. Sakuragi, K. Kondo, and E. Tanesaka. 2006. Cleavage with phospholipase of the lipid anchor in the cell adhesion molecule, csA, from Dictyostelium discoideum. *Comp Biochem Physiol B Biochem Mol Biol*. 143:138-44.

Young, K.G., and J.W. Copeland. 2008. Formins in cell signaling. *Biochim Biophys Acta*. 1803:183-90.

Young, K.G., S.F. Thurston, S. Copeland, C. Smallwood, and J.W. Copeland. 2008. INF1 is a novel microtubule-associated formin. *Mol Biol Cell*. 19:5168-80.

Zallen, J.A., Y. Cohen, A.M. Hudson, L. Cooley, E. Wieschaus, and E.D. Schejter. 2002. SCAR is a primary regulator of Arp2/3-dependent morphological events in Drosophila. *J Cell Biol*. 156:689-701.

Zaoui, K., S. Honore, D. Isnardon, D. Braguer, and A. Badache. 2008. Memo-RhoA-mDia1 signaling controls microtubules, the actin network, and adhesion site formation in migrating cells. *J Cell Biol*. 183:401-8.

Zhou, F., P. Leder, and S.S. Martin. 2006. Formin-1 protein associates with microtubules through a peptide domain encoded by exon-2. *Exp Cell Res*. 312:1119-26.

Zhu, X.L., L. Liang, and Y.Q. Ding. 2008. Overexpression of FMNL2 is closely related to metastasis of colorectal cancer. *Int J Colorectal Dis*. 23:1041-7.

Zigmond, S.H. 2004. Formin-induced nucleation of actin filaments. *Curr Opin Cell Biol*. 16:99-105.

Zilberman, Y., N.O. Alieva, S. Miserey-Lenkei, A. Lichtenstein, Z. Kam, H. Sabanay, and A. Bershadsky. 2011. Involvement of the Rho-mDia1 pathway in the regulation of Golgi complex architecture and dynamics. *Mol Biol Cell*. 22:2900-11.

Zuchero, J.B., A.S. Coutts, M.E. Quinlan, N.B. Thangue, and R.D. Mullins. 2009. p53-cofactor JMY is a multifunctional actin nucleation factor. *Nat Cell Biol*. 11:451-9.

8 APPENDIX

8.1 Abbreviations

ACTR2	Arp2, actin related protein 2
ACTR3	Arp3, actin related protein 3
ADF	actin depolymerising factor
ADF-H	actin depolymerising factor homology
ADP	adenosine diphosphate
Aip1	actin interacting protein 1
Arp	actin related protein
ARPC	actin related protein complex
ATP	adenosine triphosphate
BFP	blue fluorescent protein
CA	constitutively active
CAAX	cysteine, aliphatic amino acid, aliphatic amino acid, variable
CapZ	capping protein from the Z-disc
CC	coiled coil
CMV	cytomegalovirus
COBL	Cordon Bleu
Daam	Dishevelled-associated activator of morphogenesis
DAD	diaphanous auto-regulatory domain
DD	dimerisation domain
Diaph	Diaphanous
DID	diaphanous inhibitory domain
DIP	diaphanous-interacting protein
DMSO	dimethyl sulfoxide
DRF	Diaphanous related formin
ER	endoplasmic reticulum

ERM	ezrin-radixin-moesin
F-actin	filamentous actin
FH1	formin homology 1
FH2	formin homology 2
Fhod	FH1 and FH2 domain containing protein
Fli-I	Flightless-I
fMLP	formylmethionine – leucine – proline
Fmn	formin
Fmnl	formin-like protein
FRAP	fluorescence recovery after photobleaching
FSI	formin-spire interaction domain
G-actin	globular actin
GADPH	glyceraldehyde 3-phosphate dehydrogenase
GAP	GTPase-activating protein
GBD	GTPase binding domain
GDI	Rho GDP-dissociation inhibitor
GDP	guanosine diphosphate
GEF	guanine nucleotide-exchange factor
GFP	green fluorescent protein
GMF	glia maturation factor
GTP	guanosine triphosphate
ICAM-1	intercellular adhesion molecule-1
INF	inverted formin
LMOD	leiomodin
LPA	lysophosphatidic acid
MRLC	myosin regulatory light chain
mRNA	messenger RNA
MTBD	microtubule binding domain
MYH	myosin heavy chain
Myo1C	myosin-IC
NPF	nucleation promoting factor
N-WASP	neural Wiscott-Aldrich syndrome protein

PAI	protein abundance index
PCR	polymerase chain reaction
PDZ	postsynaptic density protein disc large zona occludens 1 domain
PIP_2	phosphatidyl-inositol 4,5-bisphosphate
RNAi	RNA interference
ROCK	Rho-associated protein kinase
SD	standard deviation
SEM	scanning electron microscopy
SH3	Scr homology 3
shRNA	short hairpin RNA
VASP	vasodilator-stimulated phosphoprotein
VCA	WH2 or verprolin, central, acidic
VDAC	voltage-dependent anion channel
WASH	Wiscott-Aldrich syndrome protein and Scar homolog
WASP	Wiscott-Aldrich syndrome protein
WH2	Wasp homology 2 domain
WHAMM	WASP homolog associated with actin, membranes, and microtubules
WAVE	WASP family verprolin homologous protein
2D	two-dimensional
3D	three-dimensional

8.2 List of figures

8.3 List of tables

8.4 List of movies

All movies are on the attached CD.

Movie 1: Single molecule imaging of Diaph1 during the bleb life-cycle.
M2 blebbing cells stably expressing the F-actin reporter protein LifeAct-Ruby (red) were transfected with GFP-Diaph1 (green). Speckles of GFP-Diaph1 fluorescence appeared under the bleb membrane during retraction (indicated by arrowheads). Scale bar 3μm. Total duration 95s.

Movie 2: Representative blebbing cell transfected with non-silencing shRNA.
M2 blebbing cells stably expressing GFP-Actin were transfected with non-silencing shRNA. Transfected cells were identified based on the expression of a BFP marker present on the shRNA vector. Scale bar 5μm. Total duration 230s.

Movie 3: Representative blebbing cell transfected with shRNA targeting Diaph1.
M2 blebbing cells stably expressing GFP-Actin were transfected with shRNA targeting Diaph1. Depletion of Diaph1 led to the formation of very large blebs compared to control cells (**Movie 2**) but the cells still retained a well-defined actin cortex. Transfected cells were identified based on the expression of a BFP marker present on the shRNA vector. Scale bar 5μm. Total duration 230s.

Movie 4: Localisation of CA-Diaph1 in blebbing cells.
M2 blebbing cells were transfected with constitutively active (CA) Diaph1 tagged with GFP. CA-Diaph1 localised to the cell membrane at all times during the bleb life-cycle and showed marked enrichment during retraction. Scale bar 3μm. Total duration 51s.

Movie 5: Neutrophil treated with the Arp2/3 complex inhibitor CK666.

A differentiated HL60 neutrophil-like cell stably expressing GFP-actin was treated with 100μM CK666 at time t=90s. After the onset of treatment, the lamellipodium was rapidly lost due to inhibition of incorporation of new Arp2/3 complex at the tip of the lamellipodium. Scale bar 5μm. Total duration 260s.

Movie 6: Blebbing cell treated with CK666 presenting a 'small bleb' phenotype.

M2 blebbing cells stably expressing GFP-Actin were treated with 100μM CK666 at time t=0s. After the onset of treatment, 50% of cells presented a phenotype with smaller blebs, loss of cortical actin fluorescence, and an increase in cytoplasmic actin fluorescence. The intensity scales are kept constant between images in this video. Scale bar 5μm. Duration 230s before treatment and 640s after treatment (including 300s incubation with CK666).

Movie 7: Blebbing cell treated with CK666 presenting a 'broad bleb' phenotype.

M2 blebbing cells stably expressing GFP-Actin were treated with 100μM CK666 at time t=0s. After the onset of treatment, 25% of cells presented a phenotype with broad blebs, loss of cortical actin fluorescence, and an increase in cytoplasmic actin fluorescence. The intensity scales are kept constant between images in this video. Scale bar 5μm. Duration 230s before treatment and 640s after treatment (including 300s incubation with CK666).

Movie 8: Representative blebbing cell transfected with shRNA targeting Diaph1.

M2 blebbing cells stably expressing GFP-Actin were transfected with shRNA targeting Diaph1. Transfected cells were identified based on the expression of a BFP marker present on the shRNA vector. Scale bar 5μm. Total duration 230s.

Movie 9: Blebbing cell depleted in Diaph1 treated with Arp2/3 complex inhibitor.

The Diaph1-depleted cell shown in **Movie 8** was treated with 100μM CK666 at time t=0s (in this movie). Prior to treatment, the cell formed large blebs and retained a clear actin cortex. After treatment, the cell rapidly lost its shape and the majority of its cortical actin. The cell only retained a few discernible foci of cortical actin and the nucleus was expelled from the cell body into a large bulge. Scale bar 5μm. Total duration 340 s (timing in the movie includes 300s incubation time with CK666).